NRC·CNRC

NRC Publications Archive
Archives des publications du CNRC

Performance-based unified procedure for determination of seismic force modification factors Rd, R_o in NBC

Fazileh, Farrokh; Fathi-Fazl, Reza; Huang, Xu

For the publisher's version, please access the DOI link below./ Pour consulter la version de l'éditeur, utilisez le lien DOI ci-dessous.

Publisher's version / Version de l'éditeur:
https://doi.org/10.4224/40003049
Client Report (National Research Council of Canada. Construction Research Centre); no. A1-018030, 2023-03

NRC Publications Archive Record / Notice des Archives des publications du CNRC :
https://nrc-publications.canada.ca/eng/view/object/?id=888962b7-83a8-408e-ab27-3f842559e7af
https://publications-cnrc.canada.ca/fra/voir/objet/?id=888962b7-83a8-408e-ab27-3f842559e7af

Access and use of this website and the material on it are subject to the Terms and Conditions set forth at
https://nrc-publications.canada.ca/eng/copyright
READ THESE TERMS AND CONDITIONS CAREFULLY BEFORE USING THIS WEBSITE.

L'accès à ce site Web et l'utilisation de son contenu sont assujettis aux conditions présentées dans le site
https://publications-cnrc.canada.ca/fra/droits
LISEZ CES CONDITIONS ATTENTIVEMENT AVANT D'UTILISER CE SITE WEB.

Questions? Contact the NRC Publications Archive team at PublicationsArchive-ArchivesPublications@nrc-cnrc.gc.ca. If you wish to email the authors directly, please see the first page of the publication for their contact information.

Vous avez des questions? Nous pouvons vous aider. Pour communiquer directement avec un auteur, consultez la première page de la revue dans laquelle son article a été publié afin de trouver ses coordonnées. Si vous n'arrivez pas à les repérer, communiquez avec nous à PublicationsArchive-ArchivesPublications@nrc-cnrc.gc.ca.

National Research Council Canada | Conseil national de recherches Canada

Canada

NRC·CNRC

Performance-based Unified Procedure for Determination of Seismic Force Modification Factors R_d, R_o in NBC

Version 1.0

Farrokh Fazileh, Reza Fathi-Fazl, Xu Huang

Sustainable Resilient Infrastructures and Communities
Construction Research Centre
March 2023

National Research Council Canada | Conseil national de recherches Canada

Canada

This page is intentionally left blank.

Performance-based Unified (PBU) Procedure for Determination of *Seismic Force Modification Factors* R_d, R_o in the NBC

Prepared by:
Sustainable Resilient Infrastructures and Communities Unit
Construction Research Centre
National Research Council Canada
Ottawa, Canada

Funded by:
Codes Canada R&D Program
Construction Research Centre
National Research Council Canada

March 2023
Report No. A1-018030

© 2023 His Majesty the King in Right of Canada, as represented by the National Research Council Canada

All rights reserved. No part of this publication may be reproduced, stored in a retrieval system, or transmitted in any form or by any means, electronic, mechanical, photocopying, recording or otherwise, without the prior written permission of the National Research Council Canada.

This page is intentionally left blank.

TABLE OF CONTENTS

Acknowledgement xiii

Foreword to the PBU Procedure xv

Executive Summary xvii

1 Intent and Scope 1

2 Notice 3

3 Definitions 4

4 Background 6

4.1 Seismic Force Modification Factors in the NBC 2005 to 2020 7

4.2 Structural System Dependent Factors Prior to NBC 2005 9

4.3 *Life Safety* Objective in the NBC 9

5 *Performance-Based Unified (PBU) Procedure* for Determining *Seismic Force Modification Factors* in the NBC 12

5.1 Introduction 12

5.2 Required System Information (Step 1) 15

5.2.1 Intended Applications of System 16

5.2.2 Establishment of Design Requirements 16

5.2.3 Data from Experimental Investigation 20

5.3 *Archetype* Development (Step 2) 23

5.3.1 *Archetype* Configurations and Behavioural Effects 24

5.3.2 *PG* Identification 28

5.3.3 *Archetype* Design 30

5.4 *Archetype* Nonlinear Modelling (Step 3) 34

5.4.1 *Archetype* Model Idealization 35

5.4.2 Modelling of Deteriorations 42

5.4.3 Modelling Software 46

5.5 Nonlinear Analysis (Steps 4 to 6) 47

5.5.1 Nonlinear Static Analysis (*Archetype* Preliminary Screening) 47
5.5.2 Input Ground Motions 50
5.5.3 *Archetype* Detailed Screening 52
5.5.4 *Incremental Dynamic Analysis* 54
5.6 Uncertainty (Step 7) 58
5.6.1 Design Requirement Uncertainty 58
5.6.2 Test Data Uncertainty 61
5.6.3 Modelling Uncertainty 63
5.6.4 *Record-to-Record Uncertainty* 65
5.6.5 Total Uncertainty 66
5.7 Performance Evaluation (Step 8) 67
5.7.1 Performance Evaluation Using Target *Performance Levels* 68
5.7.2 *Performance Margin Ratio* for Evaluation of Performance Groups 71
5.7.3 *Adjusted Performance Margin Ratio* 71
5.7.4 Acceptable *Adjusted Performance Margin Ratio* 72
5.8 Documentation and Peer Review (Step 9) 73
5.8.1 Recommended Qualifications, Expertise and Responsibilities for Development Team 73
5.8.2 Documentation of Development and Results 74
5.8.3 Peer Review Panel 75
5.8.4 Submittal 76
6 Example Applications 77
6.1 Reinforced Concrete Moment Resisting Systems 77
6.1.1 *Archetype* Development 78
6.1.2 *Archetype* Modelling 83
6.1.3 Nonlinear Analysis 85
6.1.4 Performance Evaluation 90
6.1.5 Iteration: Adjustment of Rd 93

6.1.6 Influence of Ground Motion Set 96
6.1.7 Summary Observations 102
6.2 Light Framed Wood Shear Wall System 103
6.2.1 *Archetype* Development 103
6.2.2 *Archetype* Modelling 105
6.2.3 Nonlinear Analysis 109
6.2.4 Performance Evaluation 113
6.2.5 Summary Observations 115
6.3 Conventional Construction Reinforced Concrete Shear Wall System 116
6.3.1 Archetype Development 116
6.3.2 *Archetype* Modelling 121
6.3.3 Nonlinear Analysis 126
6.3.4 Performance Evaluation 134
6.3.5 Summary Observations 136
6.4 Moderately Ductile Steel Concentrically Braced Frame System 137
6.4.1 *Archetype* Development 137
6.4.2 *Archetype* Modelling 145
6.4.3 Nonlinear Analysis 149
6.4.4 Performance Evaluation 156
6.4.5 Summary Observations 159
7 References 161
Appendix A: Seismic Modification Factors in NBC 168
A.1 NBC 2005 to 2020 168
A.2 NBC 1990 to 1995 171
A.3 NBC 1970 to 1985 174
A.4 NBC 1965 176
Appendix B: Scale Factor for Nonlinear Analysis in Detailed Screening Process 177
Appendix C: Ground Motions for Nonlinear Timehistory Analysis and *IDA* 181

LIST OF TABLES

Table 4-1 Interstorey drift limits in NBC 2020 for buildings of different *importance categories* (NRC 2022) 10

Table 5-1 Comparison between FEMA P695 and *PBU procedure* methodologies 15

Table 5-2 Irregularity and related design requirements suggested by the NBC 2020 26

Table 5-3 Definitions of seismic categories in the NBC 2020 28

Table 5-4 Generic *performance group* matrix (inspired by FEMA P695) 29

Table 5-5 Coefficients for fundamental period calculation in the NBC 2020 33

Table 5-6 Quality rating of the design requirements (ATC 2009) 59

Table 5-7 Quality rating of test data from an experimental investigation program (ATC 2009) . 61

Table 5-8 Quality rating of *archetype* models (ATC 2009) 64

Table 5-9 *Performance levels* for different *importance categories* in the NBC 2020 70

Table 5-10 Acceptable values of *adjusted performance margin ratios* 73

Table 6-1 CC-CMF and D-CMF *archetypes* developed for performance evaluation 80

Table 6-2 Overstrength factors and period-based ductility factors for *LS* 87

Table 6-3 Detailed *archetype* screening results for *LS* 88

Table 6-4 Performance evaluation results for *LS* 89

Table 6-5 *IDA* results for CC-CMF *archetypes* 92

Table 6-6 *IDA* results for D-CMF *archetypes* 93

Table 6-7 Pushover analysis results for $Rd = 2.0$ 94

Table 6-8 Screening results for *PG* 4 designed with $Rd = 2.0$ 95

Table 6-9 Performance evaluation results for *PG* 4 designed with $Rd = 2.0$ 95

Table 6-10 βRTR values for ground motion Set-1 and Set-2 (*CP*) 99

Table 6-11 Screening results of CC-CMF and D-CMF *archetypes* 100

Table 6-12 *IDA* results of CC-CMF *archetypes* for *LS* 101

Table 6-13 *IDA* results of D-CMF *archetypes* for *CP* 102

Table 6-14 *Performance groups* and building *archetypes* information 105
Table 6-15 Overstrength-related factor values for all *PG*s 110
Table 6-16 Period-based ductility values of the *archetypes* 111
Table 6-17 Results of detailed *archetype* screening 112
Table 6-18 *Performance margin ratios* of all *archetypes* 113
Table 6-19 *Archetype* performance evaluation 114
Table 6-20 *SSF* values 115
Table 6-21 Proposed *archetypes* and *performance groups* 118
Table 6-22 Pushover analysis results 129
Table 6-23 *PMR* of *archetype*s A4, A8, and A12 (*PG* 4) 133
Table 6-24 *SSF* of *archetypes* in PG 2 and PG 4 135
Table 6-25 *PMR* of *archetypes* in PG 2 and PG 4 136
Table 6-26 *Performance groups* 137
Table 6-27 Number and configuration of the braced frames in the low-rise office buildings 141
Table 6-28 Layout of braced frames in mid-rise office buildings 143
Table 6-29 Layout of braced frames in storage buildings 145
Table 6-30 Global and local performance criteria 150
Table 6-31 Pushover analysis results 151
Table 6-32 Screening results 154
Table 6-33 Performance evaluation 157

LIST OF FIGURES

Figure 4-1 Determination of design base shear, *V*, from Mitchel et al. (2003) 9

Figure 5-1 Flowchart for evaluating *seismic force modification factors* (Fazileh et al. 2023a)... 13

Figure 5-2 Sub-process for obtaining required system information 16

Figure 5-3 Flowchart for *archetype* development 23

Figure 5-4: Plot of CLE level spectral acceleration spectrum defined by the NBC 2020 31

Figure 5-5 Process for developing nonlinear *archetype* models..... 34

Figure 5-6 Range of nonlinear elements used for *archetype* models (Deierlein et al. 2010) 37

Figure 5-7 Leaning columns in moment frame and shear wall systems (ATC 2009) 40

Figure 5-8 Regulation of concrete and steel rebar constitutive properties (ATC 2017a)..... 43

Figure 5-9 Backbone curve defined in concentrated hinge models (ATC 2009) 44

Figure 5-10 Monotonic versus cyclic backbone curve models (ATC 2017a) 44

Figure 5-11 *Incremental dynamic analysis* curve showing Simulated Collapse (SC) and Non-Simulate Collapse (NSC) points (FEMA, 2009) 46

Figure 5-12 Flowchart for pushover analysis and calculating R_o and μ_T 48

Figure 5-13 Pushover behaviour idealized by a bilinear curve (FEMA, 2009)..... 49

Figure 5-14 Flowchart for *archetype* detailed screening process 53

Figure 5-15 Flowchart for performing *IDA* (modified from FEMA P695) 55

Figure 5-16 *IDA* curves resulted for a single *archetype* model (reproduced from Figure 6-6 of FEMA P695, 2009)..... 56

Figure 5-17 Flowchart to consider all sources of uncertainty..... 58

Figure 5-18 Fragility curve resulted from performance data points (reproduced from Figure 6-7 of FEMA P695, 2009)..... 66

Figure 5-19 Two system fragility curves with the same median value but different total uncertainty values (ATC 2009)..... 67

Figure 5-20 Flowchart for performance evaluation procedure 68

Figure 5-21 General scheme for seismic performance evaluation of systems using *IDA* results in *PBU procedure*; a) *performance level* spectral intensities obtained from *IDA*, b) fragility curve developed for an *archetype* (Fazileh, et al., 2023) 69

Figure 5-22 Performance evaluation of a system; a) performance-based approach in the *PBU procedure*, b) risk-based approach in NIST GCR 12-917-20 (NIST 2012) 70

Figure 6-1 Three-dimensional and plan views of the reference building 79

Figure 6-2 High and low gravity levels considered using different framing layouts 81

Figure 6-3 Different bay lengths considered in the study 82

Figure 6-4 Different number of storeys considered in the study 82

Figure 6-5 Vertical geometric irregularity in two-, four-, and six-storey frames 83

Figure 6-6 Nonlinear frame model in OpenSees 84

Figure 6-7 Verification examples: a) specimen BG-6, b) specimen U3, and c) specimen U4 85

Figure 6-8 Spectral accelerations of the scaled (a) Set-1 (b) Set-2 ground motions at the structural period of *archetype* C-2S4H 98

Figure 6-9 OpenSees model of a light-frame wood shear wall 106

Figure 6-10 Pinching4 F-D curve used in the OpenSees model for nonlinear static and dynamic analyses (McKenna 2011) 106

Figure 6-11 Coordinate of a F-D curve 107

Figure 6-12 Calibration of the Pinching4 material against a tested shear wall (Specimen E1, (Line et al. 2008)) 108

Figure 6-13 Elastic material used for modelling rod tie-downs 109

Figure 6-14 Roof displacements corresponding to different *performance levels* 109

Figure 6-15 3D view of the five-storey building 117

Figure 6-16 Plan view of the five-story building 117

Figure 6-17 Seismic categories used in this study 119

Figure 6-18 3D view of regular *archetypes* 120

Figure 6-19 3D view of *archetypes* 1 and 3 121

Figure 6-20 *Archetypes* with GILD irregularity: (left): 3D view, (right): plan view 121

Figure 6-21 2D modelling of shear wall and leaning column in OpenSeesPy (Zhu et al. 2018) 122

Figure 6-22 Tributary area of the shear wall and leaning column 123

Figure 6-23 Wall section configuration implemented in OpenSeesPy 124

Figure 6-24 Section aggregator command in OpenSees (McKenna 2011) 125

Figure 6-25 Section analysis of A12 at the base: Left) Moment-curvature, Right) Boundary steel fibre in tension 125

Figure 6-26 Verification and calibration: left) The analytical and experimental hysteresis of the specimen, right) Specimen RW-A15-P10-S78 tested by Tran and Wallace (Tran and Wallace 2015) 126

Figure 6-27 Pushover curves for all *archetypes*; a) *PG*1. b) *PG*2, c) *PG*3, d) *PG*4, e) *PG*5, f) *PG*7 128

Figure 6-28 *Archetype* screening for A4: a) Maximum inter-storey drift under the first scale factor, b) Maximum inter-storey drift under the second scale factor, c) Maximum rebar tensile strain under the first scale factor, d) Maximum rebar tensile strain under the second scale factor 131

Figure 6-29 *Archetype* screening for A8: a) Maximum inter-storey drift under the first scale factor, b) Maximum inter-storey drift under the second scale factor, c) Maximum rebar tensile strain under the first scale factor, d) Maximum rebar tensile strain under the second scale factor 132

Figure 6-30 *Archetype* screening for A12: a) Maximum inter-storey drift under the first scale factor, b) Maximum inter-storey drift under the second scale factor 133

Figure 6-31 *IDA* curves for a) A4, b) A8, and c) A12 134

Figure 6-32 Target epsilon values for Vancouver and Montreal 135

Figure 6-33 Inverted V-bracing (IV), two-storey X-bracing (2X), and one-storey X-bracing (1X) configurations for a 4-storey building 138

Figure 6-34 Low-rise office buildings in Montreal (SC3) 140

Figure 6-35 Plan view of the mid-rise office buildings 142

Figure 6-36 Structure plan views and braced frame elevations for the mid-rise storage buildings 144

Figure 6-37 Discretization of the cross-section of the bracing members and gusset plate assemblies 147

Figure 6-38 Simulation of the cyclic inelastic response of Specimen HSS1-1 from (Fell et al. 2009) 148

ACKNOWLEDGEMENTS

Authors:

Farrokh Fazileh, Ph.D., P.Eng.

Reza Fathi-Fazil, Ph.D., P.Eng.

Xu Huang, Ph.D.

The authors would like to acknowledge Codes Canada for providing financial support for this project, and Mr. Jitender Singh for coordinating with the Task Group on R_d & R_o of the Standing Committee on Earthquake Design (SC-ED).

The following research teams are acknowledged for their contributions and valuable feedback provided during the project's technical meetings and application of this procedure on selected systems in the National Building Code of Canada:

University of British Columbia:

Dr. Carlos E. Ventura

Dr. Tony Yang

Ms. Mahsa Hosseini

Dr. Armin Bebamzadeh

University of Ottawa:

Dr. Murat Saatcioglu

Dr. Ghasan Doudak

Mr. Sadegh Khosravi

Mr. Esmaeil Morshedi

Dr. Abouzar Dolati

Carleton University:

Dr. David T. Lau

Dr. Vahid Sadeghian

Dr. Jeffery Erochko

Mr. Mohammadreza Salek

Polytechnique Montréal:

Dr. Robert Tremblay

Dr. Hiro Inamasu

McMaster University:

Dr. Lydell Wiebe

The authors acknowledge the efforts by Dr. Tremblay, Dr. Bebamzadeh, Dr. Sadegian, and Mr. Salek in the selecting and scaling of ground motions for eastern and western Canada locations, which are employed in application of this procedure on selected systems in the NBC.

The authors would also like to acknowledge the comments and feedback received during this research project and the technical review of this document performed by Dr. Zhen Cai from the Seismic Resilience Team (SRT) of NRC's Construction Research Centre.

Last but not least, the authors also acknowledge the continuous support from the management team at Codes Canada, including Mr. André Laroche, Ms. Fiona Hill, and Ms. Amanda Robbins, as well as the R&D directors Dr. Ahmed Kashef and Mr. Thomas Ferguson.

This page is intentionally left blank.

FOREWORD TO THE PBU PROCEDURE

The current National Building Code of Canada (NBC) includes more than forty (40) *Seismic Force Resisting Systems* (*SFRSs*), each with individual *seismic force modification factors* (i.e., ductility-related factor, R_d, and an overstrength-related factor, R_o). These modification factors, however, are largely based on engineering judgment and qualitative comparisons of seismic response characteristics of different *SFRSs*. The potential response characteristics and ability of the designed structural systems based on the corresponding factors to meet the performance objectives in the NBC are unknown. Therefore, a unified procedure and methodology is required to quantify the inelastic response characteristics and performance of structures designed to the NBC and to assess the adequacy of the structural system provisions to meet the performance objectives.

The objective of this document is to present a *performance-based unified* (*PBU*) *procedure* for systematic quantification of R_d and R_o factors for different *SFRSs* in the NBC. The *PBU procedure* was primarily developed based on FEMA P-695 "Quantification of Building Seismic Performance Factors" (ATC 2009) with regard to its statistical nature and the use of *Incremental Dynamic Analysis* (*IDA*). However, it has been improved and heavily modified to suit the Canadian context, especially for the performance objective, *seismic hazard level*, and seismic design requirements. In addition, the *PBU procedure* incorporates a number of new features, including the introduction of 1) a new multi-level screening procedure using a nonlinear pushover and time history analysis before proceeding with labourious *IDA*; 2) a different approach for selection of ground motions; 3) a different approach for calculating *record-to-record uncertainty*; and 4) a new performance-based approach (instead of a risk-based approach in FEMA P-695). Key differences between the *PBU* and FEMA P-695 methodologies are highlighted below:

- *Screening procedure*. This unique feature of the *PBU procedure* is designed to minimize the number of required *IDA*s.
- *Overstrength factor*. The overstrength factor Ω in FEMA P-695 is determined based on maximum values. The overstrength factor R_o in the *PBU* is based on the minimum values to be consistent with the NBC's intent of minimum dependable overstrength factor.
- *IDA requirement*. This is required for all *archetypes* in FEMA P-695, but only required for *archetypes* not passing the *screening procedure* as part of the *PBU procedure (i.e., critical archetypes)*.
- *Ground motions*. A fixed set of far-field ground motions is used for *IDA* in FEMA P-695. Two different approaches are proposed in the *PBU procedure* for ground motion selection.

- *Record-to-record uncertainty*. The record-to-record uncertainty is fixed for the set of ground motions provided in FEMA P-695. However, it varies based on the ground motion selection in the *PBU procedure*.
- *Spectral shape factor*. *Spectral shape factor* is used in FEMA P-695 to account for *spectral shape effects*. This factor is only required for one of the ground motion selection approaches in the *PBU procedure*.
- *Acceptance criteria*. FEMA P-695 only focuses on building collapse, while the *PBU procedure* is capable of accounting for various performance objectives, such as *Immediate Occupancy* (*IO*), *Life Safety* (*LS*), and *Collapse Prevention* (*CP*).
- *Performance evaluation*. Unlike the risk-based methodology suggested by FEMA P-695, the *PBU procedure* is based on a performance-based approach using a constant acceptable *performance margin ratio* against different *performance levels* not met for different *importance categories*.

More technical details about the development of the *PBU procedure* in this document are provided in the Final Project Report (No. A1-018030) for the development of the *PBU procedure*.

The authors of the *PBU procedure* would appreciate specific suggestions for further improvement.

EXECUTIVE SUMMARY

One of the main objectives of the National Building Code of Canada (NBC) is to ensure life safety, which is described as Structural Safety objective.. To achieve this objective, the current NBC requires designers to carry out dynamic analysis of buildings; however, because of the complexity and time-consuming nature of dynamic analysis procedures, structures meeting certain limits and restrictions are permitted to be designed using an alternative analysis approach known as *equivalent static force procedure*. This procedure approximates the complex nonlinear dynamic response of structures by the linear response of an equivalent single-degree-of-freedom system. Because of its simplicity and effectiveness, the *equivalent static force procedure* has become a fundamental part of seismic design provisions of many building codes, including the NBC, and has been commonly used for the design of buildings to resist earthquakes.

Ductility-related *seismic force modification factor*, R_d, and overstrength-related *seismic force modification factor*, R_o, are key inputs for the seismic design of buildings using the *equivalent static force procedure*. The NBC 2020 provides values for R_d and R_o factors for more than 40 different *SFRSs* . The earthquake force on a building and the performance of the building is a function of the R_d and R_o values for the *SFRSs* used in the building.

The *seismic force modification factors* (R_d and R_o) were originally determined based on engineering judgment and a qualitative approach that involved comparing the performance of several *SFRSs* observed during past earthquakes; however, because of the lack of a standardized approach for the determination of these factors, it is not clear whether this approach provides uniform performance between various types of *SFRSs*. Additionally, a large number of new *SFRSs* and high-performance structural systems (e.g., energy dissipation devices) have been developed in recent years and are increasingly becoming available for designers to be used in buildings to resist earthquakes. To properly address these new and innovative systems in the NBC, there is a need to thoroughly investigate and quantify their ability to meet the intended performance objectives, including structural safety. The aforementioned, highlighted the need for the development of a unified procedure for determining *seismic force modification factors* that is consistent with the performance objectives and definitions in the current NBC.

The Seismic Resilience Team (SRT) in the Sustainable Resilient Infrastructures and Communities (SRIC) unit of the Construction Research Centre (CRC) at NRC, jointly with Codes Canada, proposed a multi-year R&D project to address this issue. The outcome of this project is a *performance-based unified (PBU) procedure* to systematically quantify the *seismic force modification factors* for different *SFRSs* in the NBC. The procedure is also applicable to evaluating the seismic design requirements of new *SFRSs* to be introduced into future editions of the NBC.

The *PBU procedure* is developed upon the FEMA P-695 methodology, but has been extensively modified given the inconsistencies in the seismic hazards, performance objectives, building design requirements, and construction practices between the U.S. and Canada. In addition, the *PBU procedure* features a unique two-level *screening procedure* to minimize the number of *archetypes* requiring *IDA* using nonlinear pushover and time history analyses.

The *PBU procedure* is presented in this document along with several example applications to illustrate the procedure for evaluating the code-specified R_d and R_o. The applications include the development of over 120 different *archetypes* for five selected *SFRSs* in the NBC: reinforced concrete (RC) moment-resisting frame systems (conventional construction and ductile), conventional construction RC shear wall systems, moderately ductile steel concentrically braced frame systems, and light-framed wood shear wall systems. The seismic performance of the *SFRSs* in the NBC based on current seismic requirements in the CSA standards is found to range from systems meeting the *Life Safety performance level* to some systems that do not meet *CP performance level*. These findings should be considered generally representative, but not necessarily indicative of all *SFRSs* in the NBC due to the limited number of evaluated *SFRSs*.

.

1 Intent and Scope

In the current edition of the National Building Code (NBC) of Canada (NRC 2022), ductility-related *seismic force modification factor*, R_d, and overstrength-related *seismic force modification factor*, R_o, are key inputs for seismic design of new buildings in NBC provisions. The NBC provides values for R_d and R_o factors for more than 40 different *SFRSs*. The earthquake force on a building and the performance of the building are a function of the R_d and R_o values for the *SFRSs* used in the building.

The current R_d and R_o values in the NBC were developed qualitatively over the last 20 years without using a unified procedure to quantify the values. For example, the approach used in the determination of R_d and R_o values for a timber *SFRS* may be different from the approach used for a concrete *SFRS*. The lack of a unified approach leads to inconsistent *performance level*s between structures built with different materials. The current values were expected to meet the *structural safety* objective required as per the NBC, but the lack of a unified procedure poses the following potential issues:

- Current R_d and R_o values may be overly optimistic (less conservative) for some *SFRSs* and unduly low (overly conservative) for others. This could result in a design that might not provide adequate safety force in the former case and uneconomical in the latter;
- Performance objectives of post-disaster and high-importance buildings, which are critical for disaster preparedness and public safety, may not be warranted; and
- Introducing new and innovative solutions for *SFRSs* in the NBC is somewhat difficult. For example, the introduction of one specific *SFRS* took close to two code cycles and required significant effort and time to reach consensus in absence of a unified procedure.

This document presents the *performance-based unified (PBU) procedure* that provides a systematic approach for determining the *seismic force modification factors* (R_d and R_o) for buildings with different *SFRSs* in order to achieve the intended *performance levels* in the NBC. It can also be used to evaluate the ability of the NBC-approved systems to achieve the intended *performance levels*. The scope of the proposed procedure is summarized as follows:

- *Compatible with the NBC*. The procedure is based on and intended for use with applicable design criteria and requirements of the current NBC (i.e., NBC 2020). For newly proposed *SFRSs*, the proposed procedure requires identification and use of applicable structural design and detailing requirements in the NBC and applicable CSA structural design standards.

- *Applicable to new SFRSs*. The proposed procedure is applicable to the determination of *seismic force modification factors* appropriate for the design of new *SFRSs*. However, it is not intended to be applied to the design of non-structural systems.
- *Concepts consistent with current seismic modification factor definitions*. The proposed procedure is consistent with the definitions of *seismic force modification factors* (R_d and R_o) in the NBC.
- *Performance expressed in terms of performance margin ratio*. *Performance Margin Ratio (PMR)* is defined as the ratio of median performance spectral intensity to Design Ground Motion (DGM) spectral intensity. After adjusting for *spectral shape effects*, *PMR* becomes *Adjusted Performance Margin Ratio (APMR)*, which should be more than the *acceptable APMR*. The *acceptable APMR* represents the system safety factor accounting for both uncertainty and level of confidence and indicates the acceptable margin between the DGM spectral intensity and the median spectral intensity. The calculation of median performance spectral intensity depends on the *performance levels* considered for *SFRSs* with different *importance categories* defined in the NBC 2020.

The proposed procedure has incorporated certain assumptions deemed appropriate for simplified and reliable evaluation of the seismic performance of *SFRSs*. Key assumptions and potential limitations of the procedure are summarized as follows:

- *Influence of secondary systems on seismic performance*. The seismic performance evaluation of an *SFRS* based on the proposed procedure ignores the influence of secondary systems, such as gravity system and non-structural components, which are not included in the designation of the *SFRS*. These secondary systems can either improve or diminish the seismic performance of the *SFRS*.
- Nonlinear modelling parameters and *acceptance criteria*. In the absence of systematic guidelines for defining nonlinear modelling parameters and *acceptance criteria* for different structural *performance levels* in Canada, the *PBU procedure* adopts the recommendations in ASCE/SEI 41 (ASCE 2017a). These parameters and ac in most cases are found to be conservative for new *SFRSs* in Canada.
- *Not system-specific irregularities.* Irregularities that are not system-specific, such as torsional stiffness and non-orthogonal system irregularities, are not explicitly considered in the *PBU procedure* for evaluating the *performance margin ratios* and related *seismic force modification factors* for generic *SFRSs*.

2 Notice

The *PBU procedure* presented herein is intended as a systematic approach to quantifying *seismic force modification factors* (R_d and R_o) for different *SFRSs* in the NBC. It is also applicable to evaluating seismic design requirements of new *SFRSs* to be included in future editions of the NBC.

3 Definitions

Words and terms used in the *PBU procedure* that are not included in the following list of definitions have the meanings that are commonly assigned to them in the context in which they are used, including the specialized use of terms by the various trades and professions to which the terminology applies.

The words and terms in italics used throughout the *PBU procedure* have the following meanings:

Acceptance criteria mean limiting values of properties, such as drift, strength demand, and inelastic deformation, used to determine the acceptability of a component at a given *performance level*.

Adjusted performance margin ratio (APMR) means the *performance margin ratio* adjusted by the *spectral shape factor*.

Archetype means a structure that captures the essence and variability of the performance characteristics of the *seismic force resisting system* of interest.

Collapse Prevention (CP) performance level means the post-earthquake damage state in which a structure has damaged components and continues to support gravity loads, but retains no margin against collapse.

Equivalent static force (ESF) procedure means the procedure described in Article 4.1.8.11 in the NBC 2020 that may be used for structures that meet the limits and restrictions as described in Article 4.1.8.7 in the NBC 2020.

Immediate occupancy (IO) performance level means the post-earthquake damage state in which a structure remains safe to occupy and essentially retains its pre-earthquake strength and stiffness.

Importance category means the classification of buildings based on intended use and occupancy in accordance with Table 4.1.2.1 of the NBC 2020.

Incremental dynamic analysis (IDA) means a series of nonlinear response history analyses using an input ground motion that is incrementally scaled to increasing intensities until certain *acceptance criteria* are not met anymore.

Life Safety (LS) performance level means the post-earthquake damage state in which a structure has damaged components, but retains a margin of safety against the onset of partial or total collapse.

Performance group (PG) means the assembly of structural system *archetypes* that reflect major divisions, or changes in behaviour, within the *archetype* design space.

Performance level means the structural *performance level* of a structural system to meet *Immediate Occupancy*, *Life Safety*, or *Collapse Prevention* requirements.

Performance margin ratio (PMR) means the ratio of median 5%-damped spectral acceleration of the target *performance level* ground motion, $\hat{S}_{PT}$, to the 5%-damped spectral acceleration of the code-level earthquake, S_{DT}.

Performance objective means the combination of the requirements for use of different hazard levels and different *performance levels*.

Performance-based unified (PBU) procedure means a performance-based procedure that systematically quantifies *seismic force modification factors* (R_d and R_o) and other seismic design requirements of an *SFRS* using local and global performance *acceptance criteria*.

Record-to-record uncertainty means variability in the response of index *archetypes* to different ground motion records.

Seismic force modification factors refer to the ductility-related factor R_d in the NBC 2020 that reflects the capability of a structure to dissipate energy through reversed cyclic inelastic behaviour and to the overstrength-related factor R_o in the NBC 2020 that accounts for the dependable portion of reserve strength in a structural system designed according to the provisions in Article 4.1.8.9 of the NBC 2020.

Seismic force resisting system (SFRS) means a structural system that has been considered in the design to provide the required resistance to the earthquake forces and effects defined in Subsection 4.1.8 of the NBC 2020.

Seismic hazard level means ground-shaking demands of specified severity, developed on either a probabilistic or deterministic basis.

Spectral shape effect means the effect of spectral ordinates at periods other than the fundamental period of a structure on its dynamic response.

Spectral shape factor (SSF) means the factor used to adjust the *performance margin ratio* to account for the *spectral shape effect.*

Structural Safety means limiting the probability that, as a result of the design or construction of the building, a person in or adjacent to the building will be exposed to an unacceptable risk of injury due to structural failure.

4 Background

Strong ground motions around the world are a major cause of many casualties and significant economic losses every year. Even developed countries such as Japan, New Zealand, and the US have suffered billions of dollars in earthquake-induced losses in the past decade. The Insurance Bureau of Canada in 2015 (IBC 2015) estimated the economic losses due to potential earthquakes in eastern Canada and western Canada to be in the range of 60 and 75 billion dollars, respectively. These losses mainly result from building damage and collapse and from business interruption due to the loss of functionality.

Earthquake engineering is a relatively young branch of civil engineering compared to other disciplines in civil engineering. Although many historic buildings around the world have performed well for centuries, their seismic resistance has been a by-product of good conceptual design rather than analysis. Early design provisions related to earthquakes were first introduced after the devastating earthquake of 1699 in Lima, Peru and 1755 in Lisbon, Portugal. These provisions were restricted to construction rules and height limitations. The first engineering recommendations for seismic analysis were made in 1909 in Italy where, in the first storey, the horizontal force was equal to 1/12 of the weight above, and in the second and third storeys, 1/8 of the weight above. The first seismic code in Japan specified buildings to be designed for 10% of their weight in 1924, and the first edition of the Uniform Building Code (ICBO 1927) had requirements of 7.5% to 10% of the total dead load plus the live load of the building depending on the soil conditions (Fajfar 2017).

Designing a building structure for a lateral seismic force that is proportionate to the total weight of the building is based on the assumption that the main features of the dynamic response of the structure can be represented by an *equivalent static force*. This approach has been implemented in most building codes around the world as a balanced method between the required accuracy and complexity of analysis for typical regular buildings.

Building codes since the mid-twentieth century have provided some provisions to structural designers for the seismic design of new buildings. These provisions have been evolving with new lessons learned over the past few decades with the *life safety* objective in mind. The NBC prescribes minimum requirements that need to be considered for the design of new buildings.

In the current edition of the National Building Code of Canada, ductility-related *seismic force modification factor* and overstrength-related *seismic force modification factor* are key inputs for seismic design of new buildings in NBC provisions. The NBC provides values for and factors for

more than 40 different *SFRSs*. The earthquake force on a building and the performance of the building are a function of the R_d and R_o values for the *SFRSs* used in the building.

This chapter provides a brief overview of the evolution of coefficients and factors accounting for the effect of overstrength and ductility capacity of structural systems in the NBC with a focus on the *equivalent static force procedure*, which has been the default seismic analysis procedure for the design of new buildings for decades. Although the default analysis procedure has been replaced with the dynamic analysis procedure since the NBC 2005 (NRC 2005), it is permitted to be used for designing buildings satisfying certain seismic restrictions and limitations as described in Article 4.1.8.7 of the NBC 2020 (NRC 2022). The review starts with the *seismic force modification factors* (i.e., a ductility-related factor, R_d and an overstrength-related factor, R_o), which have been used in the NBC since 2005 (NRC 2005). Their relationship to the single *seismic force modification factor R* used in the NBC 1990 (NRC 1990) to NBC 1995 (NRC 1995), and the coefficient *K* introduced and retained in the NBC 1970 (NRC 1970) throughout the NBC 1985 (NRC 1985) are discussed. More details about these factors/coefficients and their background are provided in final report #A1-018030 (Fazileh et al. 2023b). The *structural safety* objective in the NBC is also presented.

4.1 Seismic Force Modification Factors in the NBC 2005 to 2020

Since the NBC 2005, although the dynamic analysis approach became the default analysis method and was enforced to be used for structures with certain irregularities, the *equivalent static force procedure* was still permitted to be used for certain conditions. Except for the changes made for the seismic hazards and the upper and lower bounds of the design base shear for specific *SFRSs*, the equation developed in the NBC 2005 is consistently used in the NBC 2005 to the current NBC (i.e., NBC 2020) to calculate the minimum design base shear (V):

$$V = S(T_a)M_v I_E W/(R_d R_o) \tag{4.1}$$

where,

$S(T_a)$ = 5%-damped design spectral response acceleration, expressed as a ratio to gravitational acceleration, for a period of T_a; T_a is the fundamental lateral period of vibration of the building in the direction under consideration;
M_v = factor to account for higher mode effects on base shear, as defined in Sentence 4.1.8.11.(6) in the NBC 2020;
I_E = earthquake importance factor of the structure, as described in Sentence 4.1.8.5.(1) in the NBC 2020;

W = building weight equal to the summation of the dead load, except that the minimum partition load need not exceed 0.5 kPa, 25% of the design snow load, 60% of the storage load for areas used for storage, and the full contents of any tanks as described in the NBC 2020;
R_d = ductility-related *seismic force modification factor*;
R_o = overstrength-related *seismic force modification factor*.

The overstrength-related *seismic force modification factor*, R_o, in the NBC 2020 that ranges from 1.0 to 1.7, is intended to represent the minimum level of overstrength that can be counted on for each particular *SFRS*. As provided in Mitchel et al. (2003), R_o includes the contribution of size (R_{size} restricted choices of sizes of members and elements including rounding of sizes and dimensions), the difference between nominal and factored resistances R_{φ}, the ratio of actual yield strength to minimum specified yield strength R_{yield}, the effect of strain hardening R_{sh}, and the effect of mobilizing the full capacity of a structural system by the formation of a collapse mechanism R_{mech}, as expressed below.

$$R_o = R_{size} R_{\varphi} R_{yield} R_{sh} R_{mech} \tag{4.2}$$

The ductility-related *seismic force modification factor*, R_d, in the NBC 2020 ranges from 1.0 for structural systems that exhibit little or no ductility to 5.0 for the most ductile structural systems. The R_d values are intended to reflect the degree of ductility provided by each particular *SFRS*. The concept of R_d is illustrated in Figure 4-1, where Δ is the roof displacement; Δ_e is roof displacement corresponding to the equivalent lateral force V_e at the base of the structure representing elastic response, and Δ_y is the equivalent yield displacement for elasto-plastic idealized curve, which is shown in red. From Figure 4-1 it appears that V_y, the lateral force at yielding, is intended to be the lateral force capacity of the system at the point where a complete mechanism is formed in the *SFRS*. This interpretation seems in agreement with the *performance objective* of the structural system (near collapse) when it is subjected to rare seismic events with a 2% probability of exceedance in 50 years, as prescribed by the NBC 2005. The corresponding roof displacement (Δ_e) to V_e, as shown in Figure 4-1, can also be interpreted as the ultimate displacement for the code-compliant *performance level*. Then the ductility-related *seismic force modification factor* can be presented by:

$$R_d = \frac{\Delta_e}{\Delta_y} \tag{4.3}$$

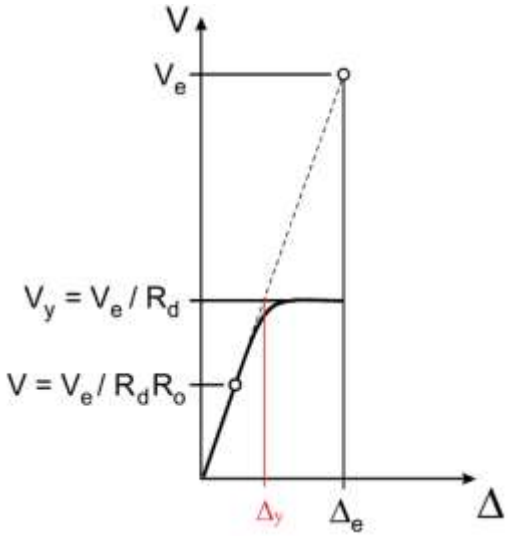

Figure 4-1 Determination of design base shear, *V*, from Mitchel et al. (2003)

4.2 Structural System Dependent Factors prior to the NBC 2005

In the NBC 1953 and 1960, no specific factor was used to account for structural system behaviour in the minimum requirements of the building code. In the NBC 1965, for the first time a C factor was introduced to account for construction type of the building, as observation of damages in several major earthquakes hinted that different building construction results in different structural responses. In the NBC 1970 to 1985, K factors were used to represent type of construction, damping, ductility, and energy absorption. K factors were used to account for the ability of different structural systems (e.g., moment-resisting frames, shear walls, etc.) to dissipate seismic demands on structural elements. In the NBC 1990 and 1995, the K factor was reformulated to derive the force reduction factors (R-factors). R-factors in the NBC 1990 and 1995 were different for different materials (e.g., steel, concrete) and different structural systems (shear walls, moment-resisting frames, etc.). Details of the different structural system-dependent factors in different editions of the NBC are provided in Appendix A.

4.3 *Structural Safety* Objective in the NBC

The NBC is an objective-based national model building code. OS2 *Structural Safety* which is an objective of the NBC, is to limit the probability that, as a result of the design or construction of the building, a person in or adjacent to the building will be exposed to an unacceptable risk of injury due to structural failure. The risks of injury due to structural failure addressed in this Code are those caused by:

OS2.1 – loads bearing on the building elements that exceed their loadbearing capacity

OS2.2 – loads bearing on the building that exceed the loadbearing properties of the supporting medium

OS2.3 – damage to or deterioration of building elements

OS2.4 – vibration or deflection of building elements

OS2.5 – instability of the building or part thereof

OS2.6 – collapse of the excavation

The structural commentary of the NBC 2020 describes undesirable situations and their consequences, the occurrence of which the Code intends to prevent in buildings. The definitions of the objectives include two key phrases: "*limit the probability of failure*" and "*unacceptable risk*". "*Limit the probability*" acknowledges that the NBC cannot entirely prevent those undesirable situations from happening, and "*unacceptable risk*" acknowledges that the NBC 2020 cannot eliminate all risks. The latter implies that the "a*cceptable risk*" is the risk remaining once compliance with the NBC 2020 has been achieved. The objectives are entirely qualitative and are not intended to be used on their own in the design and approval processes.

For seismic design of buildings, the *structural safety* objective aims to provide an acceptable level of safety for building occupants and the general public as the building responds to strong ground motion; in other words, to minimize loss of life. This implies that, although there may be extensive structural and non-structural damage during the design ground motion, there is a reasonable degree of confidence that the building will not collapse, nor will its attachments break off and fall on people near the building. This *performance level* is termed "*extensive damage*" because, although the structure may have lost a substantial amount of its initial strength and stiffness, it retains a margin of resistance against collapse (NRC, 2015).

Table 4-1 Interstorey drift limits in the NBC 2020 for buildings of different *importance categories* (NRC 2022)

Importance Category	Interstorey drift limit
Post-disaster	0.01 h_s[1]
High importance	0.02 h_s
All other *importance categories*	0.025 h_s
[1]h_s is the interstorey height	

Damage to non-structural components can be minimized by limiting their deflections, limiting the interstorey drift in the structure, paying careful attention to detailing, providing adequate clearances from the adjacent structures, and protecting elements tied rigidly to the structure from

deformations. As shown in the table, the NBC 2020 indicates that, for a very rare event (i.e., probability of exceedance of 2% in 50 years), the building could be in a state of near collapse (Devall 2003). A much more stringent limit is applied to post-disaster buildings because these buildings are expected to remain operational immediately following an earthquake. It should be noted that the interstorey drift limits in the NBC 2020 are independent of the type of *SFRS* and capacity of ductility. Therefore, different levels of damage and performance are expected for different *SFRSs* when subjected to code-level earthquake shaking.

It is important to recognize that the wide range of possible building characteristics, site conditions, and earthquake characteristics will contribute to a very wide range of actual seismic *performance levels* during any future earthquake. Although the NBC seismic provisions are intended to provide an acceptable level of protection, experience and observations during past earthquakes elsewhere in the world have shown that a wide variation in the extent of damage can be expected during any future earthquake event. Irregular structures and those with poor detailing can be expected to perform poorly, while regular, well-designed, and well-detailed structures can be expected to perform considerably better. This implies that buildings satisfying the *structural safety* objective may demonstrate substantially different seismic performance and thus sustain various levels of building damage.

In summary, the *structural safety* objective is the primary consideration of the seismic design of new buildings as per the NBC 2020. *Structural safety* does not mean that there will be no risk to human lives, but the risk is acceptably low. *Structural safety* is achieved through the seismic design of buildings in accordance with the NBC 2020 seismic provisions for the near collapse basic objective. The *structural safety* objective does not ensure the consistent seismic performance of buildings designed. Conversely, buildings satisfying the *structural safety* objective in the NBC may experience significantly different levels of building damage when subjected to strong earthquakes.

Performance-based seismic design is a promising solution to tackle the inconsistent seismic performance in buildings and has been implemented in standards and guidelines such as the ASCE/SEI 41-17 Seismic Evaluation and Retrofit of Existing Buildings (ASCE 2017b) and the PEER Guidelines for Performance-Based Seismic Design of Tall Buildings (PEER 2017). Although the NBC has been moving in the direction of performance-based seismic design, it is expected to take a number of NBC cycles to complete this transition.

5 *Performance-based Unified (PBU) Procedure* for Determining *Seismic Force Modification Factors* in the NBC

5.1 Introduction

The *PBU procedure* for determining *seismic force modification factors* (R_d, R_o) in the NBC is provided in this chapter. The *PBU procedure* is developed benefitting from several research works done in the U.S. including: FEMA P-695 *Quantification of Building Seismic Performance Factors* (ATC 2009), NIST GCR 10-917-8 (NIST 2010), NIST GCR 12-917-20 (NIST 2012), and FEMA P-2012 (ATC 2012). The methodology of the *PBU procedure* suits the Canadian context, specifically for the performance objective, *seismic hazard level*, and seismic design requirements. In addition, the *PBU procedure* methodology incorporates several new features, including: 1) the introduction of a new multi-level screening procedure using a nonlinear pushover and time history analyses before going into laborious *IDA*; 2) a different approach for selection of ground motions; 3) a different approach for calculating *record-to-record uncertainty*; and 4) a new performance-based approach (instead of risk-based approach).

Figure 5-1 shows a flowchart that illustrates the step-by-step process for implementing the *PBU procedure*. In this flowchart, the process starts with obtaining required system information (step 1), which includes detailed design requirements and results from material, component, and system testing. Initial trial values of R_d and R_o, as well as desired performance objectives of the system are set at this step. Moreover, the design requirements are either specified in the applicable CSA standards or for new systems to be developed and approved by the applicable CSA standards.

In step 2, the system behaviour is characterized using structural system *archetypes* representing the whole range of intended applications by considering different effects, including configuration issues, structural design parameters, application height limits, and system lateral behaviour. These *archetypes* are then binned into different *performance groups* in terms of key design variables affecting the seismic response of the *SFRSs* to provide a basis for statistical assessment within the performance evaluation procedure. The *archetypes* need to be designed using the detailed design requirements as defined in step 1. Later in step 3, *archetype* nonlinear models are developed for performance evaluation, using nonlinear elements to simulate all significant failure modes.

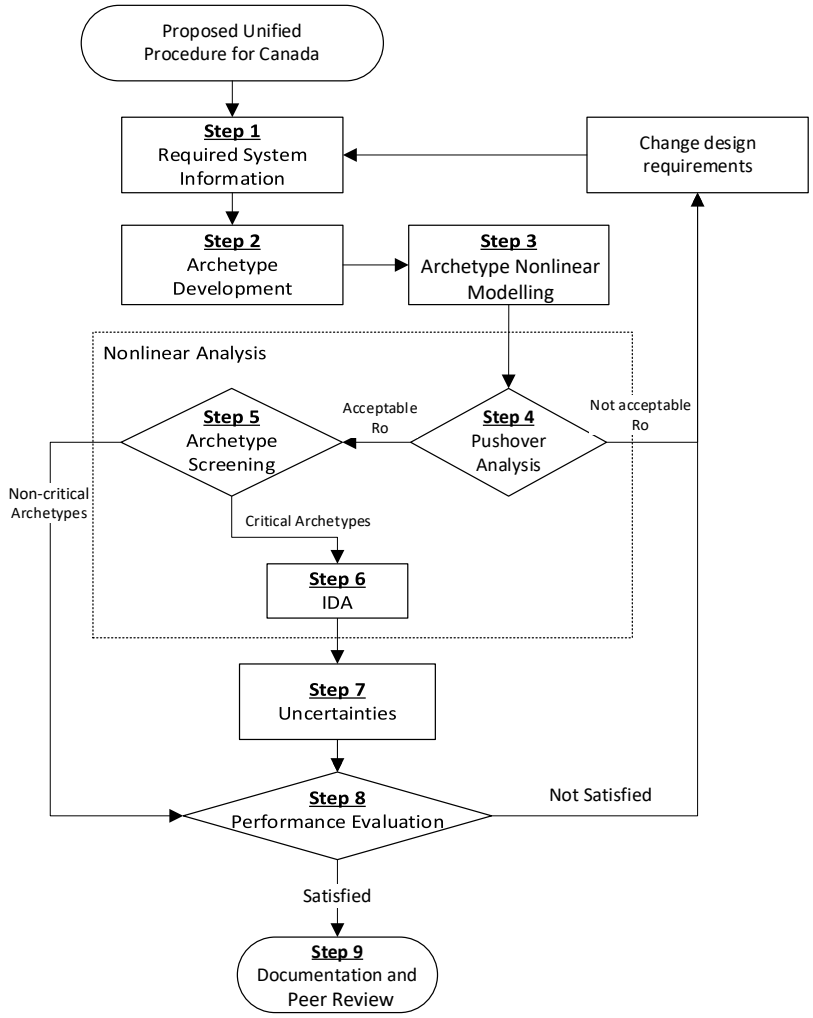

Figure 5-1 Flowchart for evaluating *seismic force modification factors* (Fazileh et al. 2023a)

Nonlinear static analysis (pushover analysis) is used in step 4 to obtain the pushover curve in order to calculate the lower-bound value of the overstrength (R_o) and period-based ductility (μ_T) factors. The pushover analysis is also used as an initial step in a preliminary screening process to check the values of R_o prior to getting into detailed Nonlinear Time History Analysis (NLTHA) in step 5. This preliminary screening process is further discussed in Section 5.5.1.

In step 5, the *archetypes* passing the preliminary screening process are consequently subjected to the detailed screening process, where they are evaluated using several target-level ground motions to separate critical *archetypes* from non-critical ones. The non-critical *archetypes* are directly sent to the performance evaluation (step 8). The critical *archetypes*, on the other hand, are the ones that need to be evaluated further using *IDA* (step 6) to calculate their *PMRs*. Details of the detailed screening process for calculating *PMR* values are provided in Section 5.5.3. A suitable set of ground motions consistent with the different regions of Canadian seismicity (i.e., West and East)

are required for both the detailed screening and the *IDA*. The selection of ground motion records is recommended in the *PBU procedure* and further discussed in Section 5.5.2.

In step 7, different sources of uncertainty are accounted for based on the *IDA* results and the details considered within the procedure. Section 5.6 provides details of the uncertainty estimations in the *PBU procedure*.

In the performance evaluation (step 8), the calculated *PMR* values are adjusted for *spectral shape effects* to obtain *APMR* values. The seismic response of the system is then evaluated by comparing the *APMR* values with *acceptable APMR* values, defined based on acceptable conditional collapse probabilities. If the seismic response is not satisfactory (i.e., *APMR* < *acceptable APMR*), steps 1 to 8 should be repeated with adjusted R_d and R_o and design requirements until the desired response is obtained. Finally, when a satisfactory response is achieved (*APMR* ≥ *acceptable APMR*), the results need to be documented and approved by an independent peer review panel (step 9).

In comparison with the FEMA P-695, the *PBU procedure* contains major changes to the nonlinear analysis steps (steps 4 to 6), as well as the performance evaluation step (step 8), while minor changes are proposed in step 7, where uncertainties are estimated. In the nonlinear analysis steps, the multi-level screening process is intended to reduce the required number of models for which *IDA* should be conducted. Moreover, both local and global performance criteria are used, which are defined based on the desired performance objectives of the system in different *importance categories* of the NBC, in the performance evaluation step to make the *PBU* performance-based procedure. The *PBU procedure* replaced the risk-based approach used in the FEMA P-695 and the NIST GCR 12-917-20 (NIST 2012) to cover buildings with different *importance categories* in the NBC. The differences between the *PBU procedure* methodology and the FEMA P-695 methodology are highlighted in Figure 5-1.

Table 5-1 Comparison of the FEMA P-695 and *PBU procedure* methodologies

	FEMA P-695	***PBU Procedure***
Preliminary screening	No	Yes
Detailed screening	No	Yes
Overstrength factor	Ω based on maximum values	R_o based on minimum values
***IDA* requirement**	Required for all *archetypes*	Required for *archetypes* not passing screening
Ground motions	Fixed set (far field)	Two different approaches for ground motion selection
Record-to-record uncertainty	Fixed for the set of ground motions	Varies based on the ground motion selection
Spectral shape factor	Yes	Only needed for one of the ground motion selection approaches
Acceptance criteria	Collapse	*Collapse Prevention*, *Life Safety*, *Immediate Occupancy*
Performance evaluation	Risk-based using different acceptable ACMR against collapse for different risk categories as suggested by NIST GCR 12-917-20	Performance-based using constant acceptable *APMR* against different *performance levels* not met for different *importance categories*

The above steps are described in more detail in the following sections.

5.2 Required System Information (Step 1)

System information is required for establishing R_d and R_o as part of the development, documentation, and review of the proposed *SFRS*. As outlined in Figure 5-2, the system information includes 1) a comprehensive description of the proposed *SFRS*, 2) clear and complete design requirements and specifications, and 3) test data and other supporting evidence from experimental investigations. In the design requirements, trial values of R_d and R_o are provided. The trial values and other design requirements are required to be modified if the seismic response is not satisfactory. In the following sections, the required system information is discussed in detail.

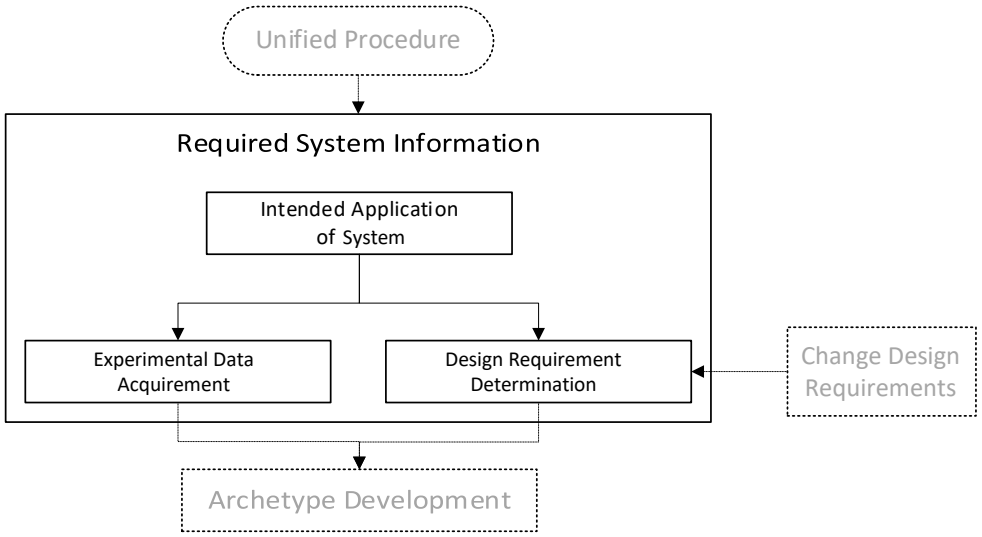

Figure 5-2 Sub-process for obtaining required system information

5.2.1 Intended Applications of the System

Before conducting any evaluation on a newly proposed *SFRS*, the intended applications and expected performance of the system need to be defined. The following information could be used as a guide for determining the intended applications;

1) Any similarities or differences between the proposed *SFRS* and the current code-conforming *SFRSs*,
2) Anticipated function and occupancy of the structure constructed by the proposed *SFRS*,
3) Typical geometric configurations (e.g., framing layout, spans, story height, overall heights),
4) Expected nonlinear behaviour of the proposed *SFRS* under seismic loading,
5) Structural gravity system to be used in combination with the proposed *SFRS*,
6) Methods of construction.

5.2.2 Establishment of the Design Requirements

The design requirements provide the fundamental information used to design the structure using the proposed *SFRS*. It should include restrictions and limitations on the application of the proposed system and also the methodology to proportion and detail all components, analyze the predicted response, and confirm the behaviour of the proposed system.

5.2.2.1 Basis of the Design Requirements

The design requirements are based on the applicable criteria specified in the NBC and applicable material design standards (e.g., CSA Standards) and other related standards as referred to in Table

1.3.1.2 of the NBC 2020. Additionally, if applicable, the proposed design requirements may include additional system-specific requirements other than the existing requirements.

As a basis of the design requirements, structures using the proposed *SFRS* need to have components capable of providing adequate strength, stiffness, and energy dissipation to withstand the design ground motions applied in any direction within the prescribed deformation and strength limits. The load path should be complete and continuous to transfer all vertical and lateral forces to the beams, columns, and foundations properly. Foundations should be designed to accommodate forces and deformations coming from the structure by ground motions considering their dynamic nature. Additionally, the design of a structure should consider potential adverse effects on the stability of the structure due to the failure of the members, connections, or foundations of the *SFRS*.

5.2.2.2 *Seismic Force Modification Factors* and Requirements

According to the NBC, the nonlinear behaviour of an *SFRS* is accounted for by R_d and R_o factors. Moreover, the lateral deflection is multiplied by $R_d R_o / I_E$, where I_E is the earthquake importance factor of the structure, based on the equal displacement rule.

In developing the design requirements for the proposed *SFRS*, the trial values of R_o and R_d need to be provided. If available, the trial values should be the values of R_o and R_d provided in the NBC 2020. In addition to R_o and R_d, drift limits representing different *performance levels*, minimum seismic design base shear, and other requirements for determining the design seismic demands of the proposed *SFRS*, should also be provided in the design requirements. It is worth noting that the *performance level* considered in this document only refers to structural *performance level*. The trial modification factors and other design requirements need to be modified if the seismic response is not satisfactory.

5.2.2.3 Limits on Application and Strength Limit States

The design requirements should comprehensively address all expected system configurations, specifically irregular configurations where non-ductile failure modes and unintended concentration of inelastic actions are likely to occur. To prevent any unfavourable seismic response in all configurations, design restrictions should be clearly defined. These restrictions may include certain limitations (e.g., height limits), restrictions to certain seismicity levels, minimum design forces, required analysis methods, required minimum detailing, and specific drift limits. In cases of an *SFRS* with different behaviour than the current *SFRS*s in the NBC, the structural response should consider the effects on other elements of the building not considered as part of the *SFRS*, including the gravity-load-carrying system and non-structural components.

Additionally, the design requirements should include acceptable material properties, components, connections, assemblies, and overall seismic behaviour of the proposed *SFRS*, with sufficient details so that analytical models of each component behaviour can be developed. Information necessary to quantify all pertinent strength limit states, including internal forces, yield and rupture points, and local and global instabilities, should also be included in the design requirements.

5.2.2.4 Design Criteria for Components to Remain Elastic

Most *SFRSs* are designed to be ductile and to dissipate energy through inelastic behaviour. This inelastic behaviour is only guaranteed when components remain elastic (or force-controlled components, which have small inelastic deformation capacity with a sharp deterioration in strength) supporting the ductile components, and having adequate capacity to withstand the increased seismic force resulted from the inelastic behaviour. This is especially important if these components are also an integral part of the gravity load-resisting system.

According to the NBC 2020, the components to remain elastic (capacity-protected non-yielding components) need to be designed to resist the design force associated with the lateral load capacity of the *SFRS*. However, the capacity design force does not need to exceed the elastic forces determined using $R_d R_o$ equal to 1.0 or 1.3 (in the case proven that the non-yielding elements may possess some overstrength and ductility) as per different CSA standards. The design requirements should be written in a manner that all such components and the methodology for determining the increased design force are clearly identified.

5.2.2.5 Material Properties

All material properties that serve as reference values for the design of components, as well as criteria for determining and measuring these properties, should be documented in the design requirements. Note that the documentation is not required for materials that are already prescribed in the NBC or material design standards referenced by the NBC. The material properties should be obtained by performing experimental tests based on existing applicable ASTM standards. The material properties include, but are not limited to, tensile, compressive, and shear stress and strain properties, friction properties between parts that might slide, bond properties at the interface of two materials, and other properties on which component behaviour depends strongly. Based on the type of loading that components may experience, materials testing should consider various conditions, including low-cycle fatigue and fracture properties, bi-axial and tri-axial stress conditions, evaluation of variability in material properties, ageing effect, effects of environmental conditions, etc.

5.2.2.6 Strength and Stiffness Requirements

The design requirements should contain guidance on the determination of effective elastic stiffness of structural components. The elastic stiffness is defined as the stiffness that is used in analytical models to provide a good estimate of the storey-drift demand at the design level. In addition to the stiffness, the nominal strength of the structural member should be defined in terms of the material properties and component detailing required for ductile behaviour, and also should account for loads and load combinations resulting from code-level ground motions. Uncertainty in component strength, as well as the seriousness of the consequences of failure, should be reflected in the resistance factor associated with the design strength equation. It is suggested to use the resistance factors calibrated for use with common gravity load combinations provided in the material design standards. If applicable, interaction with other components and the nature of loads should be considered in determining the strength capacity. Where the strength of a component is sensitive to the level of the gravity load, both the upper and lower bounds of the gravity loads are considered.

The design requirements should also include the design procedure for ductile and non-ductile connections. If the proposed system uses a ductile connection, then the requirements should be provided to ensure adequate deformation capacity of connections and to prevent any significant premature losses of capacity.

5.2.2.7 Approximate Fundamental Period, T_a

The formulations provided in Article 4.1.8.11 of the NBC 2020 could be used for determining the approximate fundamental period (T_a) of the proposed system. Where the NBC formulations are not applicable, a new approximate fundamental period formulation and an upper bound coefficient should be defined in the design requirements. The newly suggested formula(s) for T_a needs to provide an estimate of the mean minus one standard deviation of the fundamental period of the proposed system.

5.2.2.8 Gravity–load-resisting Systems

The gravity loads of the structure could be carried by either the proposed *SFRS* or a gravity-load-carrying system. In the first case, where the gravity-load-carrying system is also part of the *SFRS*, requirements related to the gravity-load-carrying system should be included in the proposed seismic design requirements. In the second case, where a gravity-load-carrying system is provided for transmitting gravity loads to the base, the gravity-related requirements (e.g., potential failure modes of the system, floor diaphragm design, collector design) need not be included in the seismic design requirements. Instead, code requirements that are common to many *SFRSs* could be prepared for these gravity-load-carrying systems. However, if the lateral behaviour of the proposed *SFRS* affects the gravity-load-carrying system significantly, it should be reflected in the design

requirements. As an example, if the deformation demands of a proposed *SFRS* exceed the capacity of the gravity-load-carrying system, an additional drift limit or other restricting measures should be defined in the design requirements.

5.2.3 Data from Experimental Investigation

Experimental data is required to establish material properties, develop design criteria, calibrate and validate component models, and confirm behaviour for a proposed *SFRS*. To achieve these objectives, a system-testing program needs to be provided and include the information on 1) material test data, 2) component and connection test data, and 3) assembly and system test data.

The test data preferably should be based on the specimens designed and detailed according to the design requirements. However, experimental results from other testing programs may be used to supplement an experimental investigation program, but those results must be obtained from reliable sources, and their applicability to the system under consideration should be evaluated. Where a Canadian experimental database is not available, an available U.S. database can be of great help, but the experimental data should be adjusted based on the existing design requirements in Canada.

There are practical limitations on how comprehensive an experimental testing program could be. Generally, the testing program should consider the effects of cumulative damage, strain rate, boundary condition of the specimen, interaction between structural components, direction and type of loading, gravity load effects, environmental condition, and quality level of field construction. The experimental loads should be applied to specimens in a manner that replicates the actual loads transferred from the system. The number of tests should be sufficient so that important statistical values can be obtained from the data directly. The configuration and number of components and assembly test specimens should be sufficient so that all common failure modes that could occur in typical system configurations are observed and evaluated. Finally, the testing program should be documented in detail and cover all required information, such as important details of specimen and test setup, instrumentations, important issues and observations prior to and during the testing.

5.2.3.1 Material Testing Program

Only with a reliable material stress-strain relationship could the strength, stiffness, and deformation characteristics of a system and its components can be accurately predicted. The material tests should be conducted based on the applicable ASTM standards, as listed in Table 1.3.1.2 of the NBC 2020. In addition to general testing requirements, the material tests should consider low-cycle fatigue and fracture properties, bi-axial and tri-axial stress conditions, variability in material properties, ageing effect, and effects of environmental conditions.

5.2.3.2 Component and Connection Testing Programs

The test data are required to develop, calibrate, and validate the design criteria and analytical models of different structural components and connections in linear and nonlinear deformation ranges. In idealized models, components are characterized using hysteresis curves, and therefore, cyclic tests are required to identify and quantify the hysteresis parameters affecting the seismic response of the proposed system. It is important to note that the specimen tests are required to continue until severe ductile or brittle strength deteriorations are captured and all the important characteristics needed in design equations and analytical models are verified. Moreover, all seismic and gravity-load applications and loading histories should be representative of what the component experiences during an earthquake. Therefore, the gravity loads should be applied to the specimens, unless it is proven that their effects are negligible. To capture all important values and make the calculations of relevant stiffness and strength feasible, the specimen should also be instrumented sufficiently.

As recommended by FEMA P-695, it is suggested that a minimum of two tests are required for each set of primary variables in the test configuration of the component testing program. If brittle behaviour with rapid deterioration is observed, the minimum number of tests should be increased to three. If the brittle behaviour is not of concern, it is suggested that one of the tests be conducted by a monotonic loading test to facilitate the analytical investigations.

A connection is a medium that transfers forces and deformations between adjacent components. Similar to components, connections should be tested under both gravity and seismic loadings, unless it is proven that the gravity load results in more favourable connection behaviour. In connection tests, all required information to develop the connection design criteria and simulate its analytical behaviour should be measured through proper loading history and instrumentation.

5.2.3.3 Assembly- and System-testing Program

An assembly is an arrangement of structural components whose seismic behaviour can be described in terms of a single response quantity, such as storey drift. The assembly tests are required where important interactions between different parts of a system (e.g., between components and connections) exist and cannot be reliably predicted by the analytical investigations. In cases where the strain rate effects are not important, the assembly tests could be conducted using a quasi-static loading history.

As a type of assembly test, a complete structural system test may be performed for validation purposes. The system test is not used as a tool for developing the analytical models, and therefore, it should not be used to replace any other tests at the material, component, connection, and assembly levels. Usually, a system test is conducted using either dynamic or quasi-static testing

procedures. A dynamic test should be used where the system behaviour and the collapse response are rate dependent or when it is more important to investigate system behaviour under a real earthquake. This test should be performed on an earthquake simulator (shake table) using realistic code-level ground motions. Where dynamic testing is not required, the quasi-static cyclic test is conducted by means of hydraulic actuators and using a proper cyclic loading history representative of the code-level earthquake (CLE) demand, and a loading pattern to distribute the lateral forces along the height of the system (building).

5.2.3.4 Loading History

The performance evaluation of an *SRFS* strongly depends on its strength and deformation capacities. These capacities, in turn, are a function of cumulative damage, which implies that the loading history is important in determining the characteristics of a system. The loading history should be representative of the force transmitted to the specimen during the earthquake. Since earthquakes are unpredictable and different specimens may experience different loading during an earthquake, there is no unique loading history to be used in testing.

There are different quasi-static loading protocols developed to study the seismic response of structural components, such as the loading histories used widely in multi-institutional testing programs (e.g., ATC-24 (ATC, 1992); SAC loading protocols (Krawinkler et al. 2000), CUREE-Caltech loading protocols (Krawinkler et al. 2001), etc.), and code-based loading protocols (e.g., AISC 341 (ANSI/AISC 2016a), ASTM E2126 (ASTM E2126-19 2019), FEMA 461 (ATC 2007), AC130-ICC (ICC 2009)). All these load histories follow the same concept, but are different in detail. Usually, these loading histories are not representative of cyclic response approaching collapse; however, they do serve the purpose of quantifying deterioration properties for analytical modelling, particularly if a cyclic test is complemented with a monotonic loading test that provides information on the force-displacement capacity boundary. Examples of typical quasi-static loading protocols presented in different reference manuals and used widely in experimental and analytical evaluations are presented below.

- ATC-24 protocol for steel elements (ATC, 1992)
- SAC protocol for steel elements (Krawinkler et al. 2000)
- SPD protocol for wood and masonry elements (Porter 1987)
- CUREE-Caltech protocol for wood elements (Krawinkler et al. 2001)
- ISO 21581 and 16670 protocol for wood elements (Technical Committee : ISO/TC 165 Timber structures 2003, Technical Committee ISO/TC 165 2010)
- FEMA 461 for drift-sensitive non-structural and structural components (ATC 2007)

- AISC 341 standard loading protocols (ANSI/AISC 2016a)
- ASTM E2126 for shear resistance of vertical elements of *SFRS* (ASTM E2126-19 2019)
- AC130-ICC for wood shear panels (ICC 2009)
- Near-fault SAC protocol for steel elements (Krawinkler et al. 2000)
- Near-fault CUREE protocol for wood elements (Krawinkler et al. 2001)

Generally, the deformation-controlled loading history should be used for all cases, except for small deflections in which components remain elastic, or for the components that are an essential part of the load path and are fully force-controlled, not experiencing any inelastic deformation. For the latter case, the force-controlled loading history is suggested to be used. Criteria for a force-controlled loading history are suggested to be used as presented in FEMA 461, *Interim Testing Protocols for Determining the Seismic Performance Characteristics of Structural and Nonstructural Components,* (ATC 2007).

5.3 *Archetype* Development (Step 2)

An *archetype* is a prototypical representation of the proposed *SFRS* that provides a systematic means for characterizing its key features and behaviour related to the seismic performance when the system is subjected to earthquake ground motions. A proper set of *archetypes* should be developed to cover a reasonably broad range of permitted buildings based on the design requirements considering different effects, including configuration issues, structural design parameters, application limitations, and system lateral behaviour. Development of the structural system *archetypes* follows the process outlined in Figure 5-3. As shown in the figure, the required *archetypes* are developed using configurational and behavioural criteria. Then, for performance evaluation, the *archetypes* are binned into different *performance groups* and are designed using the proposed design requirements.

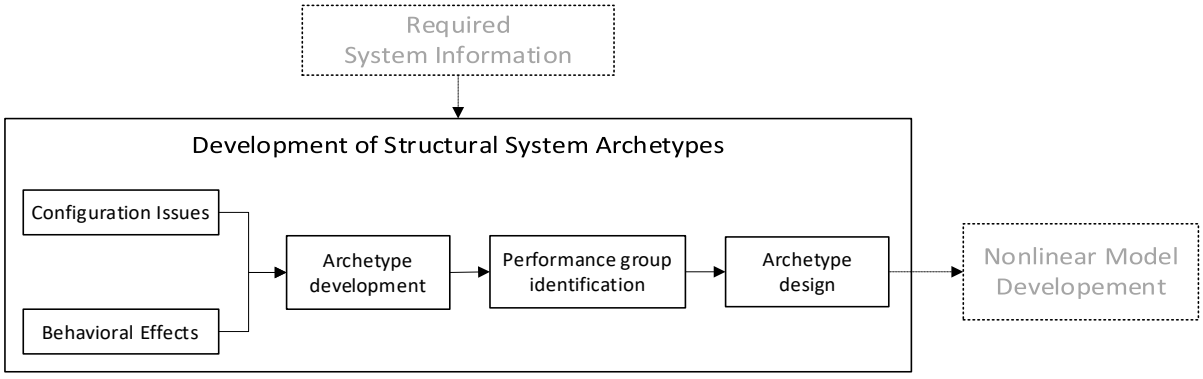

Figure 5-3 Flowchart for *archetype* development

5.3.1 *Archetype* Configurations and Behavioural Effects

Different *archetype* configurations should be developed by considering the structural configuration issues and behavioural effects. In this regard, design variables and related physical properties, which affect the seismic performance of the system, are defined. Then, the design space is established by considering bounds on the design variables using the seismic design requirements and existing practical constraints. The *archetype* configurations are finally defined based on the design variables and their design spaces. Note that dominant deterioration and possible collapse mechanisms should also be considered carefully in determining the *archetype* configurations. These parameters, which are involved in behavioural effects, are often influenced by configurational decisions.

The *archetype* configurations should be sufficiently broad to capture the feasible configurations under the design requirements, but are not supposed to cover every possible combination of design parameters. They should be limited to critical configurations to make the performance evaluation practical. To this end, the *PBU procedure* suggests that a set of *archetype* configurations will generally include about 20 to 30 specific structural configurations, though the specific number will depend on the characteristics of the *SFRS* and the limits of the *archetype* design space.

In defining the *archetype* configurations, complete lateral and vertical load paths of the *SFRS* should be considered. Moreover, the *archetypes* should have all of the components specified in the design codes having a significant effect on the seismic performance of the system. Portions of the structure that comprise the gravity-load-resisting system, but are not specifically designed to resist the seismic forces, need not be included in the *archetype* configurations; however, their effects should be included in the seismic mass, P-Δ calculations, as well as applying the *acceptance criteria* for different *performance levels* of the structure in the nonlinear models.

As a guide on establishing *archetype* configurations, the factors related to the structural configuration issues and seismic behavioural effects are discussed in detail in the following subsections. Note that the criteria discussed in the following sections are general and mostly applicable to the existing *SFRSs* in the NBC. For a newly proposed *SFRS*, additional criteria may be required.

5.3.1.1 Geometric Variations

Different framing layouts, span lengths, and number of bays should be considered in defining the *archetypes*. The variables should be chosen within the code-permitted range considering the effects of occupancy and use of the building, type of gravity system, and practical limitations. In terms of occupancy and use, the geometry of the systems intended for residential occupancies may be quite different from office occupancies or industrial uses.

In terms of height variation, the *archetype* should include the range of storey heights and number of storeys permitted by the code. The height variation in *archetypes* is required to represent the effect of the structural period and the localization of inelastic deformations. Short-period, long-period and, in some cases, intermediate-period buildings need to be considered in the *archetype* configurations. Due to significant differences in the response characteristics of very tall buildings, and limited low-frequency content in the ground motions specified for collapse assessment, the *PBU procedure* limits the methodology of performance evaluations to buildings with a fundamental period of $T_a \leq 4.0$ seconds.

The *archetypes* may include alternative configurations of the *SFRS*, which should be taken into account for determining *archetype* configurations. For instance, steel bracing systems could use different types of bracing, such as chevron and X braces. Concrete shear wall systems could have variations in aspect ratio that result in flexural-, shear-, or flexural-shear-dominant behaviours. Moreover, shear wall systems could have different cross sections in plan and opening layout in height, which affect the system response significantly. Additionally, variations in the structural component types should be reflected in the *archetype* configurations. For example, framed systems could have different types of connection details (e.g., welded, bolted, or reduced beam section), different beam and column members (e.g., box, wide flange, built-up), different brace members (e.g., HSS, pipe, C-shape, W-shape), and light-frame wood shear wall sheathing, framing, and fasteners.

5.3.1.2 System Irregularity

The *archetypes* should include the irregular configurations affecting the seismic performance of structures by disrupting the distribution of nonlinearity throughout the system (i.e., localizing the nonlinearity in an irregular portion of the system) and/or changing the lateral seismic force distribution over the height and plan of buildings. The irregularities should be considered to the extent that it would influence the dynamic response of the *SFRS* under assessment specifically. Therefore, the *archetypes* should be carefully defined based on the irregular configurations that are permitted by the system design requirements, but significantly decrease the *PMR* values.

To define the irregular *archetypes*, the irregularity set suggested by the NBC 2020 could be used as a guide. The NBC provides some general structural irregularities and defines their triggering criteria and also design restrictions. The design restrictions include: imposing analysis restrictions (e.g., *Equivalent Static Force Procedure*, Dynamic Procedure, and 3D analysis considering orthogonal directions), limiting system application (e.g., limiting the application of the system in high seismicity level and for post-disaster buildings), and suggesting some other requirements (e.g., using amplified seismic force and amplified lateral displacement for calculating the seismic demands). The irregularities, related design restrictions, as well as irregularity consequences are

provided in Table 5-2 (ATC 2012). As recommended by FEMA P2012 (ATC 2012), it is suggested that *archetypes* with more than 75% of strength on one side of the centre of mass be considered, rather than *archetypes* with vertical mass irregularity. It should be noted that some of the irregular configurations are not system-specific (e.g., torsional stiffness, non-orthogonal systems) and need not be considered for evaluation of the newly proposed systems.

In addition to the general irregularities suggested by the NBC 2020, some system-specific irregular configurations may be addressed in the proposed design requirements. For example, concrete and steel design standards (CSA 23.3:19 2019, CSA S16:19 2019) require Strong Column/Weak Beam (SCWB) in some moment-resisting frame systems, while wall discontinuity is prohibited in some shear wall systems. These system-specific irregular configurations should be taken into account in the *archetype* development as well.

Table 5-2 Irregularity and related design requirements suggested by the NBC 2020

Irregular type		Design restrictions			Irregularity consequences	
		Analysis	Application	Others	Disrupting nonlinearity distribution	Disrupting lateral force distribution
Torsional stiffness	Horizontal	✓	✓	✓		✓
Non-orthogonal systems	Horizontal	✓				✓
Out-of-plane offset	Horizontal	✓	✓	✓	✓	✓
Soft storey (stiffness)	Vertical	✓	✓		✓	✓
Weak storey (strength)	Vertical	✓	✓	✓	✓	✓
Weight (mass)	Vertical	✓				✓
Vertical geometric	Vertical	✓	✓	✓	✓	✓
In-plane discontinuity	Vertical	✓	✓	✓	✓	✓
Gravity-induced lateral demand	Vertical	✓	✓	✓	✓	✓
Sloped column	Vertical	✓	✓	✓	✓	✓

5.3.1.3 Gravity Load Levels

Various gravity load levels (self-weight and superimposed dead and live loads) should be considered in determining the *archetype* configurations. In this regard, occupancy and use of the buildings, which define the superimposed dead and live loads and also the framing layout (which affects the tributary gravity load transmitted to the system), should be carefully defined. Large gravity demands result in a higher overstrength factor value, lower inelastic deformation capacity, and higher lateral demand resulted by P-Δ effects. The *PBU procedure* suggests that considering two levels of the gravity load, i.e., high and low, is sufficient for most *SFRSs*.

5.3.1.4 Strength and Stiffness

The *archetype* configurations must include the variation of differences between design strength and calculated seismic demands. The design strength is a function of design earthquake intensity, component detailing requirements, capacity design requirements, and also the overstrength factor. The overstrength factor is, in turn, results from gravity loads, wind loads, minimum seismic load and other loading requirements. On the other hand, the demands are a function of structural configuration and gravity load intensity. It is noted that the *archetype* configurations need not incorporate standard practice for designing that exceeds minimum design requirements and results in excessive R_o, but not used in all design cases (e.g., using one member size at multiple locations to meet the construction practice expectations). Moreover, increased design strength resulting from non-seismic requirements that are not applied universally to all structures in all locations (e.g., non-frequent strong wind and some specific non-seismic forces) need not be considered in defining the *archetype* configurations.

The elastic lateral stiffness of the system affects its dynamic behaviour, sensitivity to P-Δ effects, and also induced deformation demands on critical components. The *archetype* configurations should take into account all sources of the flexibility or stiffness (e.g., the flexibility of the floor and roof diaphragms in a low-rise industrial structure with a large floor plan and stiff seismic-force-resisting elements), which increase or decrease the lateral stiffness and are likely to influence the *SFRS* behaviour. In addition, the *archetype* should include system configurations that are more sensitive to the drift limits and require satisfying additional minimum stiffness. This requirement increases R_o and probably increases the strength capacity of the system, as well.

5.3.1.5 Inelastic Deformation Capacity

The inelastic deformation capacity of a component is a function of design requirements (including detailing rules and capacity design provisions), member geometric proportions, and calculated member forces that can vary with the structural configuration. The *archetype* configuration should include the variations affecting the inelastic deformation capacity of the *SFRS*. Note that the impact of structural redundancy on the redistribution of internal forces and distribution of inelastic deformations should also be reflected in the *archetype* configurations.

5.3.1.6 Seismicity Levels

The *archetypes* should be representative of buildings located in the different seismicity levels permitted by the design requirements. In this regard, the NBC 2020 divides the country into four seismic categories as provided in Table 5-3. For each seismic category, *archetype* configurations should include the maximum and minimum intensity values, associated design and detailing requirements, and any other restrictions related to that level. To consider limited scenarios for

seismicity levels and make the performance evaluation more practical, the *PBU procedure* suggests that it is sufficient to evaluate the *SFRS* for the highest (most severe) seismicity levels permitted, and then verify for lower seismicity levels.

Table 5-3 Definitions of seismic categories in the NBC 2020

Seismicity Category	$I_E S(0.2)$		$I_E S(1.0)$	
	Minimum	Maximum	Minimum	Maximum
SC1		0.2		0.1
SC2	0.2	0.35	0.1	0.2
SC3	0.35	0.75	0.2	0.3
SC4	0.75		0.3	

where: $S(T)$ is the design spectral acceleration, expressed as a ratio to gravitational acceleration, at period T, as defined in Sentence 4.1.8.4.(6) of the NBC 2020.

5.3.1.7 Building *Importance Categories*

The *importance categories* suggested by the NBC should also be reflected in the *archetype* configurations. The NBC divides buildings into four different *importance categories*; Low, Normal, High and Post-disaster, based on their intended use and occupancy. In each category, different levels of seismic load and some additional design requirements are prescribed in order to meet a specific seismic performance objective. However, most of the design requirements are common among different *importance categories*. For performance evaluation purposes, the *archetypes* must be representative of the design requirements applicable to the *importance category* of interest. Because the proposed systems are usually used in multiple *importance categories*, developing the *archetypes* for each *importance category* would be time-consuming. Alternatively, it is suggested that the *archetypes* be prepared for the Normal *importance category* with common design requirements, and then additional *archetype* configuration should be added, if required, when the system is evaluated for higher or lower *importance categories*.

5.3.2 *PG* Identification

Archetype configurations are divided into different *performance groups*, in terms of key design variables that significantly affect the seismic performance of the proposed system, to provide the basis for statistical assessment within the performance evaluation process. The *performance groups* should contain multiple *archetype* configurations that reflect the possible variations defined by the design space of the key variables. However, they should not be made larger than necessary, biased towards certain configurations, or influence the average *PMRs* within a *performance group*.

A generic *performance group* matrix is developed for the *PBU procedure*, as shown in Table 5-4. According to the table, the *archetypes* could be divided as follows: basic structural configuration,

gravity load level, *importance category*, seismicity level, and period domain. However, the number of basic structural configurations and other key variables are system-dependent and could vary in different systems. As a minimum, it is suggested that all systems should have at least two seismicity levels and two period domains in each basic structural configuration. In addition, it is suggested that each *performance group* include at least three *archetype* configurations, without any limits for maximum number. It is expected that each *performance group* would typically have three to six *archetype* configurations. The minimum of three *archetypes* could be waived if it is not feasible to have three alternative designs within a specific *performance group*.

Table 5-4 Generic *performance group* matrix (inspired by FEMA P-695)

Group No.	Grouping criteria				Number of *archetypes*
	Basic configuration	Design load level		Period domain	
		Gravity	Seismic		
PG-1	Type 1	High	Max	Short	≥3
PG-2				Long	≥3
PG-3			Min	Short	≥3
PG-4				Long	≥3
PG-5		Low	Max	Short	≥3
PG-6				Long	≥3
PG-7			Min	Short	≥3
PG-8				Long	≥3
PG-9	Type 2	High	Max	Short	≥3
PG-10				Long	≥3
PG-11			Min	Short	≥3
PG-12				Long	≥3
PG-13		Low	Max	Short	≥3
PG-14				Long	≥3
PG-15			Min	Short	≥3
PG-16				Long	≥3

Basic structural configuration: The basic structural configurations are intended to capture the major variations in *SFRSs* permissible within the design requirements. Examples of the major alternative configurations could be: 1) variations in bracing configurations (e.g., X-bracing versus chevron bracing) in steel concentrically braced frames; 2) variations in framing spans and storey heights in moment frames; and 3) variations in shear wall aspect ratios that may influence its shear- or flexural-dominant behaviour.

Gravity load level: If the gravity load variations significantly affect the seismic behaviour of the system, they should be involved in the *performance group* matrix. As discussed, the gravity load variations are related to the intensity of dead and live loads and also the framing layout. For

example, in residential buildings including the moment-resisting frames, high gravity load level is defined in the case of the space frame, where the *SFRS* is designed for carrying gravity and lateral loads simultaneously, and low gravity level is defined in the case of the perimeter frame, where the gravity and lateral loads are carried separately using additional gravity load systems. In wall systems, the differences can be distinguished through the use of load-bearing walls (where most of the gravity loads are directly supported by the walls) versus non-load-bearing walls (where gravity loads are supported by other means, such as frames).

Seismicity levels: The proposed system should be evaluated for all seismicity levels by the design requirements. But considering all seismicity levels makes the procedure almost impractical. In this regard, it is suggested that it is sufficient to check the *SFRS* for the highest permitted seismicity level considering its maximum and minimum intensities at that level. If the maximum intensity at the highest seismicity level controls the performance of the system, evaluating the system at lower seismicity levels is not required. Otherwise, if the minimum of the highest seismicity level results in higher collapse probability of performance not met, the system should be assessed for the minimum intensity of the next seismicity level as well.

Period domain: Since the behaviour of an *SRFS* is strongly influenced by its fundamental period, variations in the period range should be reflected in determining the *performance groups*. It is suggested that a minimum of two period domains be considered for binning the *archetypes*; short-period *archetypes* including limited number of storeys and storey height (where the fundamental period is in the constant acceleration region of the design spectrum), and long-period *archetypes* including medium to tallest practical *archetypes* (where the fundamental period is in the constant velocity region of the design spectrum). The transition period for short-period and long-period systems is defined in Section 5.3.3.3.

5.3.3 *Archetype* Design

Each *archetype* configuration should be designed by applying the proposed design requirements, substantiated by test data. The design process should include all significant design features that are likely to affect structural response and collapse behaviour, including all component and connection designs. The following sections describe related seismic design requirements, all based on the requirements contained within the NBC 2020, to highlight specific aspects of the design procedure relevant to the performance evaluation of the system. As discussed in Section 5.2.2, the *archetype* configurations are designed based on the trial values of R_d and R_o and other proposed design requirements. Therefore, in the iterative performance evaluation process, the *archetypes* may need to be redesigned based on the revised values of R_d and R_o and also new design requirements if the desired response is not achieved.

5.3.3.1 Method of Analysis for Design

The *equivalent Static Force procedure* could be used for lateral seismic force calculations, except for cases where this procedure is not allowed by Article 4.1.8.7 of the NBC 2020. This method is based on the assumption that the main features of the dynamic response of the structure are represented by a single mode response at the fundamental lateral period, T. The NBC indicates that the *ESF* procedure could be used for all buildings located in low (i.e., SC1 in Table 5-3) and moderate (i.e., SC2 in Table 5-3) seismicity levels, for regular buildings less than 60 m in height and have T<2.0 sec, or for buildings with some structural irregularity types that are less than 20 m in height and have T<0.5. Other than these cases, the buildings should be analyzed by the Linear Dynamic Analysis procedure, using either Modal Response Spectrum (MRS) or Numerical Integration Linear Time History (NILTH) methods. Alternatively, Nonlinear Dynamic Analysis may be used where a special study is required.

5.3.3.2 Seismic Design Intensity

The NBC 2020 prescribes the use of a multi-period CLE design spectrum, which has a 2% probability of being exceeded in 50 years. In this regard, 5%-damped CLE spectral accelerations, S_a, for periods of 0.2, 0.5, 1.0, 2.0, 5.0, and 10.0 seconds are provided in the 2020 National Building Code of Canada Seismic Hazard Tool (https://doi.org/10.23687/b1bd3cf0-0672-47f4-8bfa-290ae75fde9b) for selected locations across Canada. Considering a site designation, X, the CLE design spectrum is obtained (see Figure 5-4). For the purpose of performance assessment across all possible site classifications, it is suggested that the soil coefficient values, based on the default Site Class D, be used uniformly for all *archetype* designs.

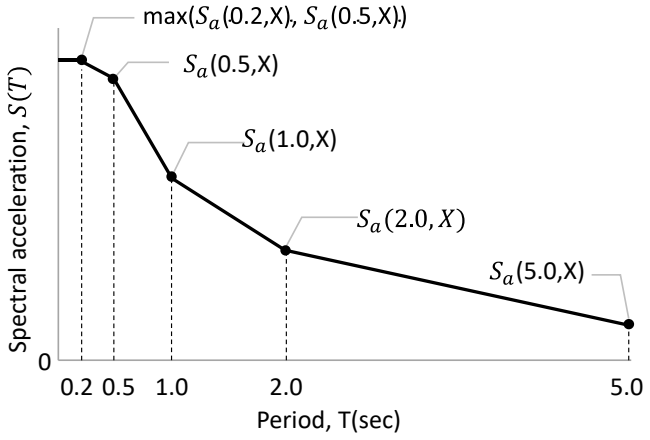

Figure 5-4: Plot of CLE-level spectral acceleration spectrum defined by the NBC 2020

Additionally, the NBC 2020 defines different seismic categories by considering lower and upper bounds on the CLE design spectrum values at periods of 0.2 sec and 1.0 sec multiplied by the

importance factor (I_E). The suggested seismic categories are provided in Table 5-3. As discussed in Sections 5.3.1.6 and 5.3.2, each *archetype* should be carefully designed for the upper and lower bounds of the maximum seismicity level for which the proposed system is applicable. In the next steps, the same design intensities are used for the seismic performance evaluation of the system.

5.3.3.3 Transition Period

The methodology presented in this section requires statistical evaluation of the short-period *archetypes* separately from the long-period *archetypes*, distinguished by the transition period. Commentary J of the NBC 2015 (NRC, 2015b) defines the transition period as equal to 0.5 sec, in which the design base shear for short-period and long-period structures is separated. As discussed in Section 5.3.2, this value should be used as one of the criteria for binning the *archetypes* into different *performance groups*.

5.3.3.4 Seismic Base Shear, V

According to the NBC 2020, the *archetypes* are designed using the seismic base shear, V, as defined by Eq. (5.1), where $S(T)$ is design spectral acceleration at the fundamental period of T, M_v is a factor to account for the higher mode effect, I_E is importance factor, W is effective seismic weight, and R_dR_o is production of trial values of the ductility-related (R_d) and overstrength-related (R_o) *seismic force modification factors*.

$$V = S(T)M_vI_EW/(R_dR_o) \tag{5.1}$$

This base shear equation is used as the basis for the applied forces when the *ESF procedure* is used for design, and to scale design values in accordance with Article 4.1.8.12 of the NBC 2020, when the modal response spectrum method is used. As suggested by the NBC, for buildings located on a site designated as other than X_F and having an *SFRS* with an R_d equal to or greater than 1.5, the base shear need not be greater than the larger of 2/3V (T=0.2 sec) and V (T=0.5 sec). Moreover, for walls, coupled walls, and frame systems, the design base shear should not be less than V (T=4.0 sec), and for moment-resisting frames, braced frames, and other systems, the base shear should not be less than V (T=2.0 sec).

5.3.3.5 Fundamental Period, T

The fundamental period is used within the methodology for establishing the design base shear and also defining the ground motion spectral intensity for performance evaluation of the system. In both cases, the methodology uses the fundamental period suggested by the NBC 2020 according to Eq. (5.2), where, h_n is the building height (in metres), and C_u, C_t and x are system-dependent coefficients provided in Table 5-5.

$$T = C_u T_a = C_u C_t h_n^x \quad (5.2)$$

The approximate fundamental period, T_a, represents the lower bound values of the building's period, and using coefficient C_u, the resultant fundamental period, T, approximates the average value of the building's period. Alternative formulas for the approximate fundamental period of the proposed *SFRSs* with different dynamic characteristics should be specified as part of the design requirements for such systems.

Table 5-5 Coefficients for fundamental period calculation in the NBC 2020

System	C_u	C_t	x
a) for moment-resisting frames that resist 100% of the required lateral forces and where the frame is not enclosed by or adjoined by more rigid elements that would tend to prevent the frame from resisting lateral forces,			
i) Steel	1.5	0.085	3/4
ii) Concrete	1.5	0.075	3/4
iii) Other moment frames	1.5	T_a=0.1N	
b) Braced frames	2.0	0.025	1.0
c) Shear wall	2.0	0.050	3/4
d) Other structures	1.0	0.050	3/4

5.3.3.6 Loads and Load Combinations

The *archetypes* should be designed for gravity and seismic load effects using related load combinations suggested by the NBC 2020. Basic seismic load combinations for strength design calculations are presented in Eq. (5.3) and (5.4), where D includes the structural self-weight and superimposed dead loads, L is the live load (including appropriate live load reduction factors), and E is the effect of horizontal seismic forces resulting from the base shear, V.

$$1.0D + 1.0E + 0.5L + 0.25\text{S} \quad (5.3)$$

$$1.0D + 1.0E \quad (5.4)$$

FEMA P-695 suggests that snow load, S, soil and superimposed earth pressure are not required for the *archetype* design. The snow load is an environmental load that varies independently of seismic intensity and is not considered to be a primary factor affecting seismic performance. In the *PBU*

procedure, however, it is suggested that the snow load portion be included both in the seismic weight of the building and in the companion load action with live loads.

Soil and superimposed earth pressure are not typical and, when present, generally apply to design of structural components that do not affect the performance of the *SFRS* significantly. Wind load is also not required for the *archetype* design, except where the wind load governs the design. In that case, minimum wind load values should be used based on the lowest basic wind speed for all regions of Canada, and consider building (plan) configurations that minimize lateral forces due to wind load.

5.4 *Archetype* Nonlinear Modelling (Step 3)

Archetype models represent mathematical idealization of the *archetype* configurations and are used to simulate the linear and nonlinear behaviour of components from yielding up to the total collapse point of the system. The models are defined based on the component properties and limit state criteria and should be accurately calibrated and validated with a predefined set of material-, component-, and system-level test data. Later, in the performance assessment of the proposed *SFRS*, the developed models are used for conducting nonlinear static and dynamic analyses.

The procedure for developing the nonlinear *archetype* models is outlined in a flowchart presented in Figure 5-5. According to the flowchart, the existing modelling methodologies are used to develop nonlinear models. Then, simulated and non-simulated deteriorations (see Section 5.4.2) are defined in the models. The accuracy of the modelling technique and the deterioration modes used should be validated against experimental studies. In the following sections, different modelling methodologies and some general considerations in developing the nonlinear models and determining the performance points of the system are presented in detail.

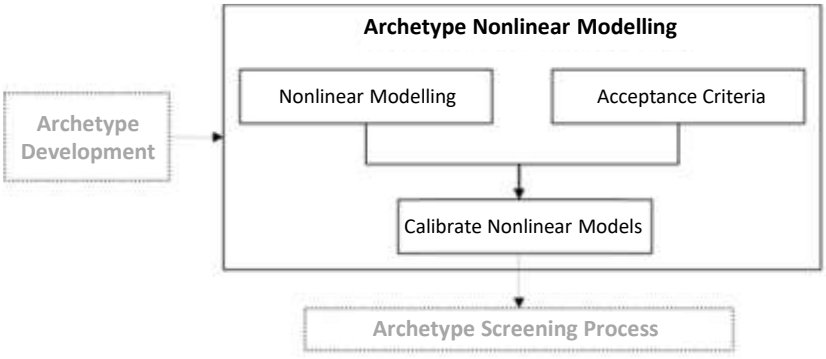

Figure 5-5 Process for developing nonlinear *archetype* models

5.4.1 *Archetype* Model Idealization

Due to the complexity of the structural systems, it is not always possible or necessary to simulate all linear and nonlinear effects in the *archetype* models. Simplified assumptions should be used to idealize the *archetype* models and make them unbiased, transparent, and practical to achieve the desired results. However, the idealized *archetype* models should still be capable of distinguishing between significant response modes and key design features of the proposed *SFRS* and also should capture all significant nonlinear effects related to the seismic response of the system. Some general considerations are presented here as a guide for the nonlinear model development of the performance evaluation.

5.4.1.1 Elevation and Plan Configuration

Elevation and plan configurations of the *archetypes* should be idealized by considering components that are critical for structural system response. Excluding some components is reasonable provided that it does not lead to (1) a non-conservative assessment, and (2) unacceptable bias in the calculated response. In most cases, two-dimensional frames, including the main structural elements, are sufficient to represent the typical response of the system. Examples are regular and vertically irregular configurations of moment frame, shear wall, and braced frame systems. Where the horizontal irregularities are considered in the *archetype* configurations, three-dimensional models may be required to capture the plan configuration and the interactions of spatially distributed systems, except where the important effects could be properly included in the two-dimensional models. Torsional irregularity, out-of-plane offset irregularity, and flexibility of diaphragms fall into this category. In cases where the three-dimensional models are used, they need to include the code requirements for accidental torsion as well as inherent torsion. The inherent torsion is considered through the appropriate distribution of mass and assignment of element properties. However, for accidental torsion, the seismic codes suggest that the centre of mass be offset from its actual location to achieve the prescribed eccentricity.

5.4.1.2 Elastic and Inelastic Component Actions

In a system, component actions are classified into two categories based on their inelastic response:

1. Deformation-controlled actions: defined where a reliable inelastic deformation capacity with gradual strength decay exists. This category is represented by inelastic elements in the *archetype* models. Examples of the deformation-controlled action include the flexural response of beams or walls, axial deformations of buckling-restrained braces, shear and/or flexural yielding of coupling beams between walls, or links of eccentrically braced frames.

2. Force-controlled actions: defined where the actions are intended to remain elastic due to concerns for sudden failure modes. Elastic elements are used for actions, such as: connections, shear in reinforced concrete shear walls, axial forces in columns, and shear and flexure in floor diaphragms. However, if a more detailed response is desired, some force-controlled components having limited ductility may be represented by a proper nonlinear behaviour. Examples of these components are joint panel zones in concrete and steel special moment frames, ductile wood, or steel diaphragms, etc.

5.4.1.3 Modelling Approaches for Inelastic Components

For modelling the inelastic components, the nonlinear elements can range from uniaxial spring hinge models (also referred to as macro models) to detailed continuum Finite Element (FE) models (also referred to as micro models), as depicted in Figure 5-6. The concentrated models (Figure 5-6 (a) and (b)) are highly phenomenological, where functions describing the structural response are based on the calibration of the overall component response. These models have the advantage of being computationally efficient due to using few degrees of freedom and concentrated nonlinear behaviour. However, the fibre and continuum finite element models (Figure 5-6 (c) to (d)) are more detailed at the material level and, therefore, are less computationally efficient. The choice of model type for a given application depends on different factors such as reliability and practicality of models for the proposed structural system and material, *archetype* configurations and governing modes of behaviour, level of detail available for input data and analysis objectives, computational efficiency, as well as available software and computational resources.

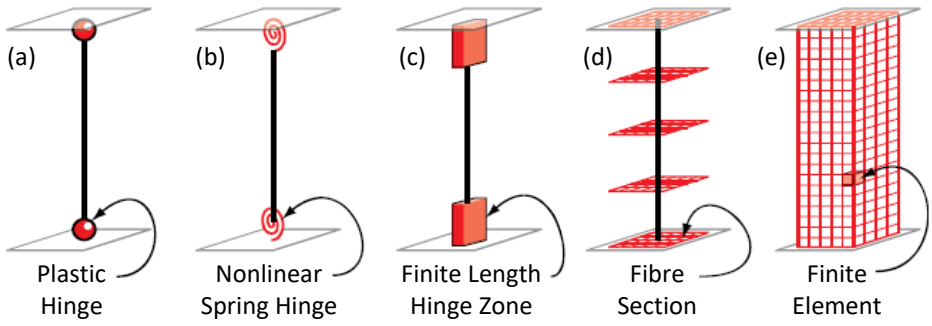

Figure 5-6 Range of nonlinear elements used for *archetype* models (Deierlein et al. 2010)

Generally, the concentrated spring and hinge models (Figure 5-6(a) and (b)) capture complicated behaviour by highly idealized nonlinear behaviour in localized regions of the structure. The models are typically implemented to simulate the single degree of freedom response (e.g., moment-rotation), but they can include multi-axial response through yield surfaces (e.g., P-M_x-M_y interaction surface, where P is the axial force, M_x and M_y are moments with respect to the x- and y-axis of the section surface, respectively). Although these macro models are computationally efficient, they are empirical and limited to the ranges of components and behaviour modes for which they have been calibrated. Therefore, in cases where the behaviour of the components is unknown due to a lack of experimental data, the application of these models is not suggested. On the other hand, where the component behaviour is well studied using a set of reliable experimental data, these models would be more reliable than the micro modelling approaches, especially where high nonlinearity and significant deteriorations exist. Most of the important response parameters in moment frame, shear wall, and braced frames could be accurately captured by these modelling approaches, from the yielding up to the significant degradations. However, the effects such as interactions among axial, flexure, and shear in concrete members, and interaction of local and torsional-flexural buckling in steel members, are difficult to capture using these concentrated plasticity models.

As one of the refined modelling techniques, fibre models (Figure 5-6(d)) capture the section response by numerical integration of the material response through the member cross-section employing the kinematic assumptions, such as the Euler-Bernoulli (plane sections remain plane). This model can be used either in conjunction with a finite-length hinge zone (Figure 5-6(c)) or with model formulations that simulate distributed inelasticity along the member length (Figure 5-6(d)). Contrary to the spring and hinge models, the interaction of axial and flexural behaviours (i.e., P-Mx-My) is properly considered by the fibre models. However, cross-section warping or distortion cannot be captured due to using the Euler-Bernoulli formulation, and therefore, shear

and flexure interaction in concrete members, local buckling of reinforcing bars or steel web and flanges, slip between components of the section, material cracking and crashing, cannot be properly modelled in this method. This modelling technique is commonly used for modelling the flexural and axial interactions in beams, columns, braces, and flexural-dominant shear walls from the yielding point to the collapse point by considering strength and stiffness degradations. However, due to its considerable computational costs, the fibre modelling technique is preferred to be used in member configurations for which limited empirical data is available to accurately formulate the concentrated plasticity (e.g., reinforced concrete core walls).

Continuum finite element models (Figure 5-6(e)) represent the element behaviour at the most fundamental level and provide the ability to model the complete interaction of three-dimensional response, including complex geometries and multi-axial stress and strain states. This modelling technique is significantly time-consuming and, therefore, its application is limited to simulating portions of the overall system for verification purposes. Examples of finite element application includes: shell elements for core walls, web and flanges of thin-walled members, gusset and other plate-like connections.

5.4.1.4 2D versus 3D Component Response

The need to simulate the three-dimensional (3D) response of the components depends on the expected impact of three-dimensional effects on the overall structural response. For most cases, the two-dimensional (2D) response is likely to be sufficient, such as beams and columns in moment-resisting frames, planar RC shear walls, wooden shear walls, and bracing elements in different braced frame systems. However, there may be cases where 3D response (e.g., out-of-plane torsional-flexural instability of laterally unbraced beam-columns or braces) or 3D geometry (e.g., reinforced-concrete C-shaped core walls) are important to be captured. Alternatively, in cases where a 3D response is required, strength and deformation capacities of the 2D elements could be modified to represent the accurate response.

5.4.1.5 Material Properties

Nonlinear models should represent the median response of the structural system. Typically, this is achieved by using probable (expected) properties of materials and components. The probable material properties should be obtained based on the median of material test data, or by taking average in the cases of limited data and modest levels of uncertainty. Alternatively, if code-specified materials are used, the probable material behaviour could be calculated using existing requirements in the material standards. In this regard, CSA S16-14 (CSA 2014a) suggests that the probable yield stress factor (R_y) for steel elements shall be taken as 1.1 and the product $R_y F_y$ as no less than 460 MPa for hollow structural sections (HSS) and 385 MPa for other section types.

For reinforced concrete elements, CSA A23.3-14 (CSA 2014b) suggests that the probable strength be calculated using $1.25f_y$ as the stress in the tension reinforcement and the specified values of f_c' in the compression concrete. These probable material properties should be used for determining the probable stiffness, strength, and inelastic response of structural components.

5.4.1.6 Gravity Loads and Seismic Mass

Expected gravity loads using a proper load combination should be applied to the models before conducting any seismic analysis. According to the NBC 2020 design load combinations, the expected gravity load combination should be taken as $1.0D + 0.5L + 0.25S$, where D is permanent loads due to the weight of building components as specified in Article 4.1.4 of the NBC 2020, L is structural live load due to intended use and occupancy as specified in Article 4.1.5 of the NBC 2020, and S is the snow loads as specified in Article 4.1.6 of the NBC 2020.

All masses physically tied to the structure, including dead loads and portion of live loads as well as snow loads, should be included in the seismic mass calculations as per the requirements of the NBC 2020. The dead load includes structural weight and superimposed dead loads as specified in Article 4.1.4.1 of the NBC, except that the minimum partition load need not exceed 0.5 kPa. The live load includes 60% of the storage load for areas used for storage, except that storage garages need not be considered storage areas. Note that the assumed live load effects in the gravity load combination are different from that in the seismic mass determination since the two effects are related but involve different phenomena (vertical forces versus horizontal motions). In this regard, loose furniture and human occupants that are included in the gravity live load are not included in the seismic mass.

5.4.1.7 Gravity System Modelling

The model should accurately include all the gravity loads affecting the lateral seismic response of the system. Where the *SFRSs* are well distributed, the gravity mass tributary to the frame and the seismic mass that must be resisted for lateral seismic excitation are usually the same. However, where gravity systems other than the *SFRSs* are used, the additional gravity loads should be incorporated into the *archetype* models. Traditionally, the additional loads are applied through leaning columns as shown in Figure 5-7. According to the figure, each leaning column includes a single vertical truss element that is connected to the main model using rigid links with frictionless hinges to exclude its contribution to the lateral resistance of the system. In cases where 3D models are used, the special distribution of leaning columns should be modelled as described in FEMA P2012 (ATC 2012).

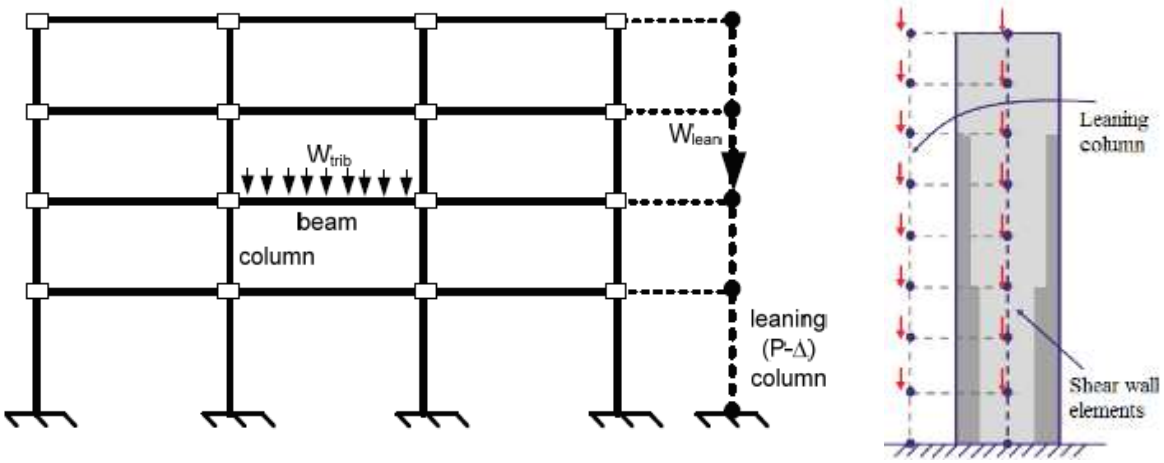

Figure 5-7 Leaning columns in moment frame and shear wall systems (ATC 2009)

5.4.1.8 Geometric Nonlinearity in Structural Analysis

Nonlinear geometry should be considered for computing the stiffness matrix during the nonlinear static and dynamic analyses. In particular, nonlinear geometry includes P-delta effects (P-Δ and P-δ), which are defined as a destabilizing force (or moment) exerted by gravity loads on vertical load-carrying members due to lateral side sway and can have a significant effect on the strength and deformation capacities of the system. The first effect, the P-Δ effect which consists of the increase in the overturning moment on a full frame or storey due to storey deformation, could be captured by either linear P-Δ transformation or large deformation (co-rotational) transformation rules within the structural analysis software. However, in the cases of sway-sensitive *archetypes* (e.g., *archetypes* with gravity-induced lateral demand (GILD) irregularity), the large deformation transformation rule should be used to accurately capture the P-Δ effect. Conversely, the P-δ effect, which causes a magnification of moments due to deformations within the element, is rarely supported by the structural analysis software. Therefore, when the P-δ effects are deemed to be important and should be explicitly included in the models (e.g., when the member is sensitive to buckling), they could be simulated by breaking up the member into multiple elements (two to six elements, depending on the desired accuracy).

5.4.1.9 Modelling of Damping

The inherent damping of the structure, which is not associated with the response of nonlinear elements such as friction, should be considered through viscous damping (velocity-dependent force), in addition to the hysteretic energy dissipation capacity of the nonlinear elements. Typically, viscous damping is modelled using Rayleigh damping, modal damping, or a combination of the two. In Rayleigh damping, the velocity-dependent force (C) is mass (M) and stiffness (K) proportional, i.e., $C = \alpha M + \beta K$. Mass-proportional damping (αM) and stiffness-proportional

damping (βK) tend to over-damp the low-frequency and high-frequency responses, respectively. The α and β constants in this equation are typically calculated based on the percentage of critical damping in the first mode period (T) and third or higher mode period ($\approx 0.1T$). Alternatively, the modal damping technique could be used, in which the value of critical damping in each desired elastic vibration mode is specified directly in the analysis. This type of damping tends to over-damp the high-frequency modes only.

In both techniques, it is critical to determine the proper value of the inherent damping. As suggested in Commentary J of the NBC 2015 (NRC 2015a), the inherent damping of the structure in the nonlinear dynamic analysis should not exceed 3% of the critical damping in the modes dominating the seismic response of the structure, unless a higher value can be justified.

5.4.1.10 Soil Structure Interaction

Soil structure interaction (SSI) could be included in the *archetype* models where the interaction significantly changes the seismic demand on the system. Generally, the SSI includes kinematic and inertial effects. The kinematic effect pertains to the spatial variability of input ground motions over the building plan area and through the soil/foundation depth (embedment effects) of basements. This effect is not system-dependent and need not be included in the *archetype* models. However, the inertial effect contributes to the stiffness of the system and tends to increase the fundamental period of the system. In flexible (long-period) systems, this effect is assumed to be conservative and could be ignored. However, for stiff (short-period) systems, considering the inertial effects could be of significant importance to accurately capture the ductility demand for the performance evaluation. The NIST GCR 12-917-21 report, *Soil-Structure Interaction for Building Structures*, (NEHRP Consultants Joint Venture 2012), suggests Eq. (5.5) for determining whether the SSI needs to be considered, where h is the building height, V_s is the shear-wave velocity of the soil, and T is the fixed-based fundamental period of the system.

$$R = \frac{h}{V_s T} \tag{5.5}$$

In this equation, h/T quantifies the stiffness of the superstructure and shear-wave velocity, V_s, is closely related to the soil shear modulus. According to the NIST report, the inertial effect is negligible for $R < 0.1$, which occurs in flexible systems and is significant when $R > 0.1$, as in the case of stiff systems. If the contribution of the inertial effects is significant, the SSI needs to be considered through either distributed or concentrated springs, as described in the NIST GCR 12-917-21 report.

5.4.1.11 Floor Diaphragm Flexibility

Diaphragms and their components, including chords and collectors, are categorized as force-controlled components. In most cases, the diaphragms are stiff enough to be modelled as perfectly rigid using kinematic constraints. However, where the flexibility of the diaphragm and its components significantly affect the seismic response, they should be included with a finite amount of stiffness. *Archetypes* with irregular configurations including torsional sensitivity, re-entrant corner, diaphragm discontinuity, vertical geometry, in-plane offset and weak story irregularities, may require explicit modelling of the in-plane and out-of-plane diaphragm stiffness to accurately capture the distribution of forces among different *SFRSs*. In these cases, to reduce the computation time, diaphragms away from irregular levels may be analyzed as rigid if the lateral distribution of forces in gravity-load-resisting elements is not significantly changed when compared to a baseline model with semi-rigid diaphragms. In addition to the irregular configurations, diaphragm flexibility may be required for very short-period systems having a fundamental period of T<0.5 sec. In this case, similar to soil structure interaction, considering the diaphragm flexibility would be of significant importance to accurately capture the ductility demand.

For concrete slabs and concrete over metal deck slabs, as suggested by the NIST GCR 17-917-46v1 report; *Guidelines for Nonlinear Structural Analysis for Design of Buildings* (ATC 2017a), the in-plane and out-of-plane effective stiffness would vary between 5% to 30% and 25% to 35%, respectively. The upper and lower bounds could be used to capture the upper and lower bounds of the response. Moreover, the NIST report suggests that the chord and collector element effective stiffness should be matched with the stiffness assumed for similar beam-column elements. For other slabs, such as metal decks without concrete topping and wood-sheathed floors, the effective stiffness should be obtained from related reference standards and guidelines, e.g., (SDI 2015, AWC 2016). In terms of diaphragm flexibility, the Canadian concrete material standard, CSA A23.3-14 (CSA 2014b), suggests that the effective out-of-plane stiffness (I_e) of slab frame elements should be considered as 20% of their gross sections (I_g), i.e., $I_e = 0.2I_g$.

5.4.2 Modelling of Deteriorations

For evaluating the seismic performance of the proposed system, the *archetype* models should capture all significant nonlinear effects up to the performance point of the system, including all failure modes. Generally, it can be done through explicit simulation of deteriorations in the nonlinear analyses and/or considering non-simulated failure criteria by employing alternative limit state checks on demand quantities. These two failure modes are discussed in detail in the following sections.

5.4.2.1 Simulated Deteriorations

To the extent possible, the *archetype* models should include significant deterioration modes affecting the seismic performance of the system. Typically, this is achieved by proper modelling of stiffness, strength, and inelastic deformation under cyclic loading, as well as considering accurate cyclic deterioration modes in the hysteresis response of components. In the fibre and finite element models, where element behaviour is obtained by introducing accurate stress-strain relationships, the hysteresis response and cyclic deteriorations are defined by material constitutive models. In other words, different deteriorations and failures including stiffness degradation, concrete cracking and crushing, and rebar and steel element fractures, are directly simulated in the material behaviour, and then are integrated through the sections and elements to obtain the global behaviour of the system. As an example, Figure 5-8 shows the regularization of concrete and steel rebar material response by defining the strain capacities as a function of a mesh-dependent characteristic length and also the concrete-crushing/steel-yielding energy. In cases where the local failures are hard to capture directly (e.g., rebar buckling of the reinforced concrete elements and local buckling of the steel components), some proper modifications in the softening portion of the stress-strain behaviour could be introduced to incorporate these effects. Note that in these modelling strategies (fibre and finite element models), the failure points and degradation modes should be carefully validated with a set of experimental data, at both the component and system levels.

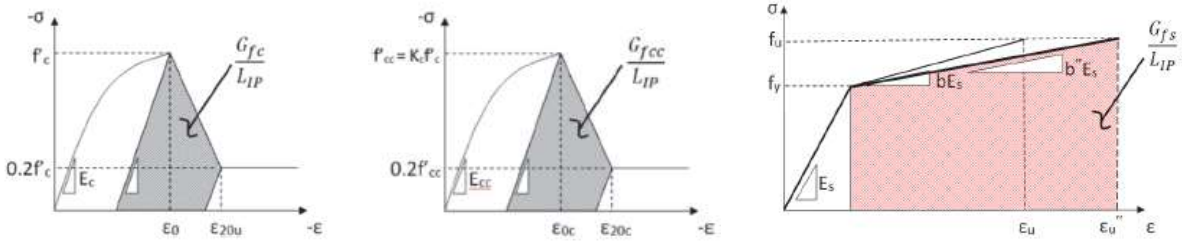

Unconfined concrete for compression | Confined concrete for compression | Reinforcing steel for tension and compression

Figure 5-8 Regulation of concrete and steel rebar constitutive properties (ATC 2017a)

As shown in Figure 5-9, the most significant factors affecting the inelastic response of a structural element are the strength at yield, F_y, the maximum strength, F_c, the plastic deformation capacity, δ_p, the post-capping tangent stiffness, K_{pc}, and the residual strength, F_r. These factors are used for developing the backbone curves employed in the concentric plastic hinge modelling methodologies. Using the backbone curves, most of the deterioration modes (e.g., concrete

crushing, confinement tie yielding and rupture, longitudinal bar buckling and rupture in concrete components, steel fracture in tension, local buckling and lateral torsional buckling in steel components) are simulated through the negative slope region of the backbone curve. In addition to these failures, cyclic deteriorations including both stiffness and strength degradations should also be simulated in this method (see Figure 5-10(a)). Although the failure points and different deteriorations are case-specific, it is suggested that for many cases of reinforced concrete, steel, and wood components, the deterioration model proposed by Ibarra et al. (2005) satisfactorily matches experimental results and analytical predictions (ATC 2009).

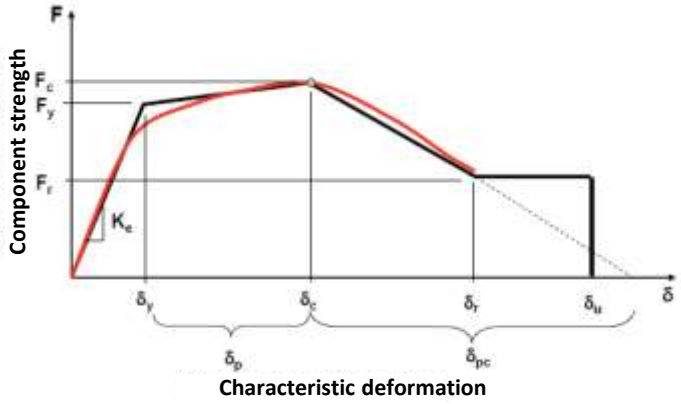

Figure 5-9 Backbone curve defined in concentrated hinge models (ATC 2009)

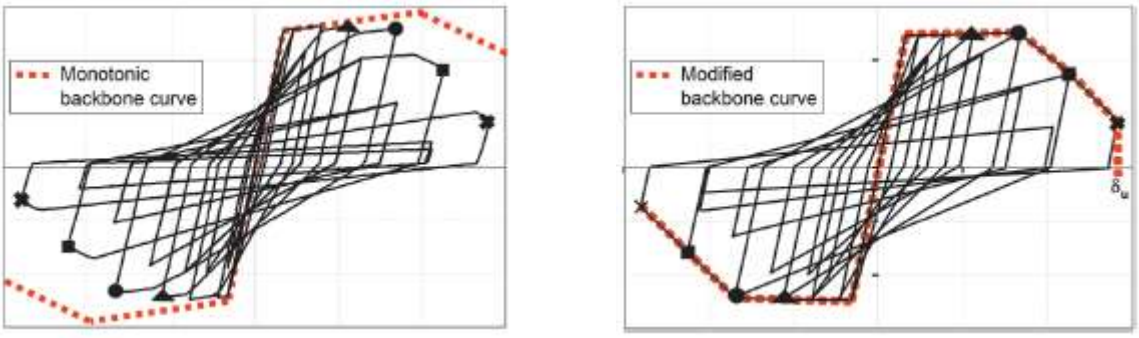

a) model with monotonic backbone curve and direct simulation of cyclic deteriorations

b) model with degraded backbone curve (cyclic backbone curve)

Figure 5-10 Monotonic versus cyclic backbone curve models (ATC 2017a)

Conventionally, the backbone curves used in the concentrated hinge models should be defined and calibrated based on the median monotonic test data, and then, the cyclic strength and stiffness degradations are added to the models. In this way, the statistical variations of the component response are explicitly accounted for in the collapse risk assessment. However, the backbone curves provided by the seismic evaluation manuals (e.g., ASCE/SEI 41-17) are defined based on the cyclic test data (generalized cyclic envelope), and therefore, some degrees of the cyclic

deterioration are incorporated into the backbone curve (see Figure 5-10(b)). Using the cyclic envelope backbone curves in dynamic analyses results in a conservative estimate of median response (ATC 2009, 2017b). According to FEMA P-695, it is suggested that, in cases where monotonic test data are not available, the cyclic envelope may be used as a conservative estimation of the monotonic backbone curve. The accuracy of the models in terms of initial stiffness, maximum strength, deformation corresponding to different *performance levels*, and cyclic deteriorations should be validated against a set of experimental data.

Using a direct simulation of the deterioration modes in different modelling strategies (i.e., concentric plastic hinges, fibre and FE models) provides the opportunity to redistribute forces within the system model, and therefore, the performance point of the system could be determined based on its global behaviour, rather than the local limit state of a single component.

5.4.2.2 Non-simulated Deteriorations

Where it is not possible to directly simulate all significant deteriorations, non-simulated deterioration modes are used using alternative limit state checks on structural response. In this methodology, it is assumed that the first occurrence of a failure in an element results in total failure of the system, and the force redistribution to other components within the system is ignored. Therefore, this approach estimates the lower bound of the median performance point of the system in a conservative manner. In addition, it increases the uncertainty of modelling in the performance evaluation process. Examples of possible non-simulated performance modes in structural components are force-controlled actions (actions with low ductility or unpredictable inelastic behaviour), such as shear failure and subsequent axial failure in reinforced concrete columns, fracture in the connections or hinge regions of steel moment frame components, failure of tie-downs in light-frame wood shear walls. In these cases, the assessment approach of the non-simulated limit state is proposed to be similar to the ASCE/SEI 41-17 procedure (ASCE 2017b) for force-controlled actions, where the maximum force demand developed is compared to the capacity of the element. Additionally, the non-simulated performance point could be based on any other structural response parameter measured in the analysis, such as inter-storey drift limit. If needed, proper inter-storey drift limits representing performance points of the non-structural components and gravity frame systems should be defined.

5.4.2.3 System *Acceptance Criteria*

The system *acceptance criteria* are defined based on the target *performance level* in the design requirements. Using the simulated and non-simulated deteriorations described above, the performance of each *archetype* is obtained and compared against the *acceptance criteria*. For example, if the target *performance level* of a system is *CP*, the collapse of the system should occur

in both nonlinear static and dynamic analyses, when the seismic demands exceed the *acceptance criteria* for *CP*. Figure 5-11 illustrates the simulated (SC) and non-simulated (NSC) collapses of a system in an *IDA* curve with the *CP* target *performance level*. Using a direct simulation of the deteriorations provides the opportunity to redistribute forces within the system model, and therefore, the performance of the system could be determined based on its global response, rather than the local limit state of a single component.

Note that limit state checks for the non-simulated modes should be established based on test data and other supporting evidence and should represent the median value of the governing response parameter. Moreover, when establishing the non-simulating criteria, engineering judgement should be used to consider the *performance level* representing the global response of the system.

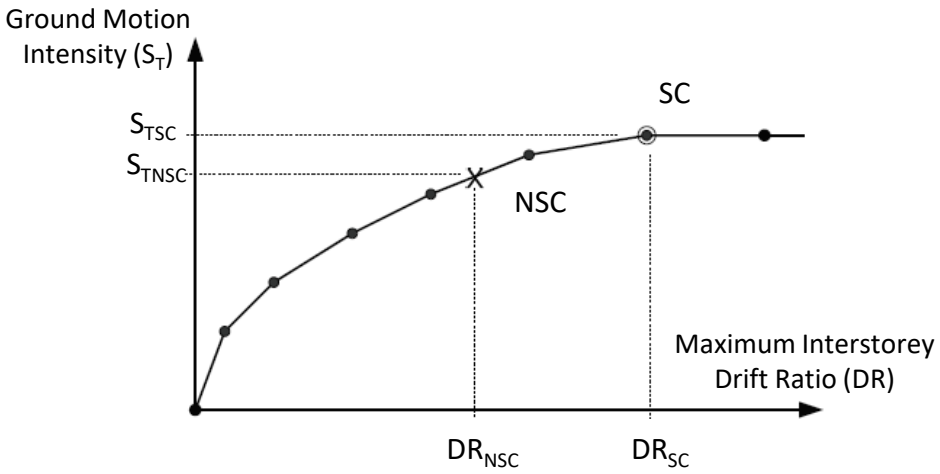

Figure 5-11 *Incremental dynamic analysis* curve showing Simulated Collapse (SC) and Non-Simulated Collapse (NSC) points (FEMA, 2009)

5.4.3 Modelling Software

The software for nonlinear analysis should be capable of performing nonlinear static pushover and nonlinear time history analyses. Moreover, it needs to have the ability of capturing strength and stiffness degradations in the system with highly nonlinear behaviour. Regarding these effects, a significant computational challenge is to accurately capture strain softening (strength degradation after post-peak response). To overcome this challenge and achieve convergence at large inelastic deformations, a robust iterative numerical solution strategy is required. While most modern analysis software can overcome these challenges, effort must be made to investigate the sensitivity of the solution to model parameters and numerical aspects of the computational solution algorithms.

5.5 Nonlinear Analysis (Steps 4 to 6)

Developed models are evaluated by nonlinear static and dynamic analyses to calculate the values of required parameters. As illustrated in the flowchart provided in Figure 5-1, the nonlinear static (pushover) analysis is performed to help validate the models and also to provide statistical data on the system overstrength factor, R_o and period-based ductility, μ_T. The pushover analysis also serves as a preliminary screening process. If the response of the system is satisfactory at this stage (calculated R_o values are equal to or greater than those used in the design), the *archetypes* are sent to the *archetype* detailed screening process, and if not, the design requirements need to be updated. In the detailed screening process, the *archetypes* are evaluated using a target-level ground motion set to divide them into critical and non-critical *archetypes*. The non-critical *archetypes* are directly sent to the performance evaluation step. However, the critical *archetypes* need to be evaluated further using *IDA*.

5.5.1 Nonlinear Static Analysis (*Archetype* Preliminary Screening)

Nonlinear static analysis is used to develop pushover curves for calculating the values of required parameters, i.e., R_o and μ_T. The process in this step is illustrated in Figure 5-12. After developing the *archetype* models, the gravity loads (as described in section 5.4.1.6) are applied and then the models are pushed laterally up to the point corresponding to the *performance level*. The pushover curve, which is defined as base shear versus roof displacement, is obtained in this analysis. Using the pushover curve, $\mu_T$and R_o are calculated for each *archetype* model. The value of $\mu_T$is further used in the performance evaluation process (see Section 5.7.3). The overstrength factor values for each *archetype* ($R_{o,i}$) are used to determine the system overstrength factor (R_o) and compare it to the trial value proposed in the design requirements. If the resultant value is less than the trial value, the design requirements should be modified and the *archetypes* need to be redesigned.

In developing the pushover curve, different lateral load patterns could be used. In the *PBU procedure*, the load pattern consistent with the pattern used in the design of the *archetypes* is suggested. For example, in the *ESF procedure* of the NBC 2020, the design lateral earthquake force V shall be distributed such that a portion, F_t, is concentrated at the top of the building, where F_t is equal to $0.07T_aV$, but does not exceed $0.25V$ and may be considered as zero where the fundamental lateral period, T_a, does not exceed 0.7 s. In addition, the reminder, $V - F_t$, is distributed along the height of the building, including the top level, in accordance with the following formula:

$$F_x = (V - F_t)\mathrm{W}_x h_x / \left(\sum_{i=1}^{n} W_i h_i\right) \tag{5.6}$$

where F_x is the lateral force applied to level x, W_i and W_x are portions of specified dead load that are located at or are assigned to level i or x respectively, h_i and h_x are height, in m, above the base ($i = 0$) to level i, or x respectively. A generic pushover behaviour is illustrated in Figure 5-13. In order to quantify the important points of the behaviour and calculate the overstrength factor and period-based ductility, the pushover curve is idealized by a bilinear curve using maximum base shear (V_{max}), effective yield roof displacement ($\delta_{y,eff}$), and ultimate roof displacement (δ_u). The effective yield roof displacement is calculated by Eq. (5.7),

$$\delta_{y,eff} = C_0 \frac{V_{max}}{W} \left(\frac{g}{4\pi^2}\right) \times \max(T, T_1)^2 \tag{5.7}$$

where, V_{max}/W is the maximum base shear normalized by building weight, g is gravity constant, T is the fundamental period described in section 5.3.3.5 ($C_u T_a$), and T_1 is the fundamental period of the *archetype* model computed using eigenvalue analysis.

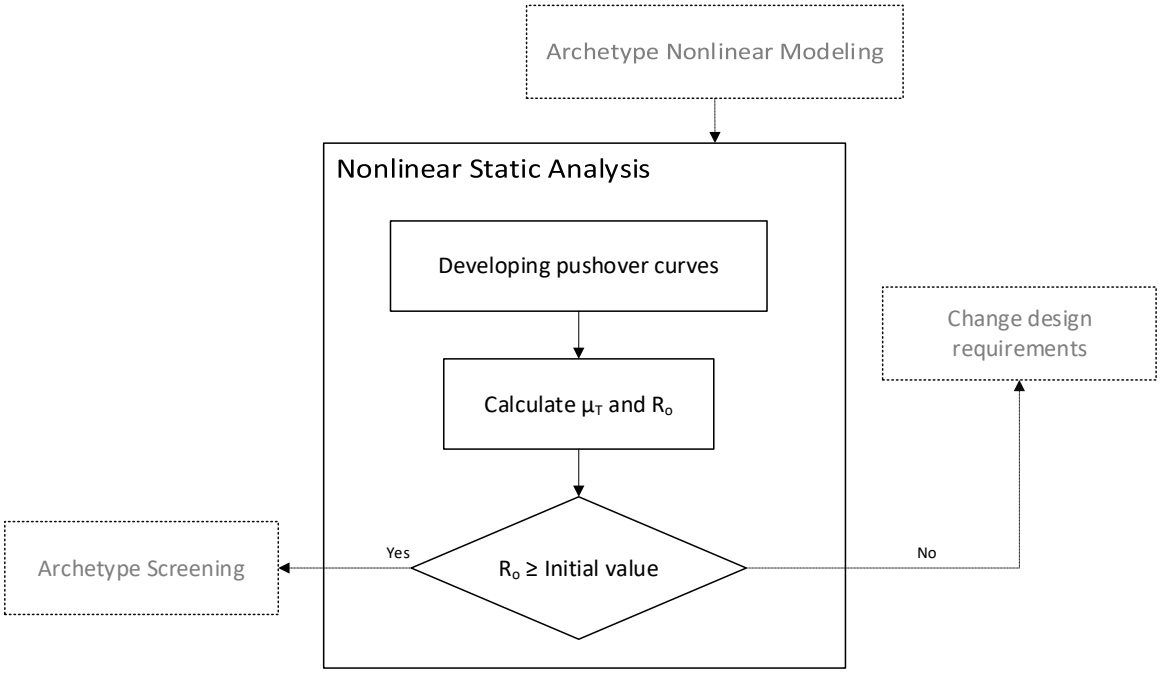

Figure 5-12 Flowchart for pushover analysis and calculating R_o and μ_T

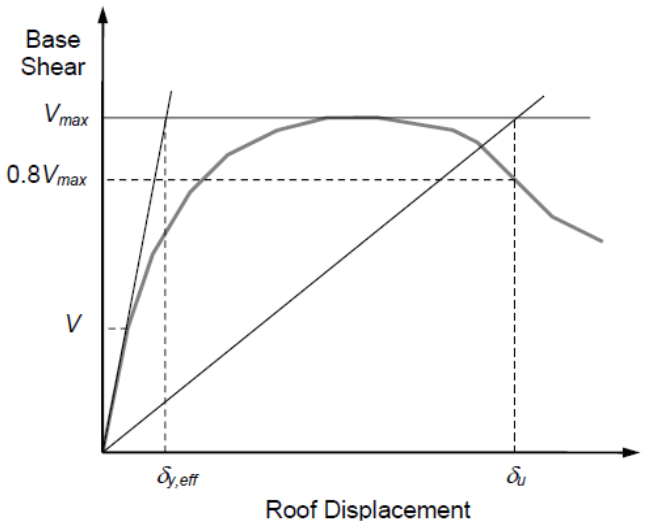

Figure 5-13 Pushover behaviour idealized by a bilinear curve (FEMA, 2009)

The effective yield displacement is intended to represent the analytical period of the model and is used to calculate the ductility ratio to account for the period elongation at the performance point of the model. The term $\max(T, T_1)$ is imposed to ensure that analyses do not over-predict the ductility ratio for cases of the short-period *archetypes* where $T > T_1$. Coefficient C_0 relates fundamental-mode (SDOF) displacement to roof displacement and is calculated by Eq. (5.8). In this equation, m_x is the mass at level x, $\varphi_{1,x}$ ($\varphi_{1,r}$) is the ordinate of the fundamental mode at level x (roof), and N is the number of levels (storeys).

$$C_0 = \varphi_{1,r} \frac{\sum_1^N m_x \varphi_{1,x}}{\sum_1^N m_x \varphi_{1,x}^2} \tag{5.8}$$

The ultimate roof displacement (δ_u) is the performance point up to which the model is laterally pushed. In the *PBU procedure*, the ultimate displacement needs to be quantified using local and global criteria based on the desired performance levels. The global criteria could be defined as a significant drop in lateral strength of the model, where all important deterioration modes are directly simulated into the models or lateral drift limit, as specified in the design requirements. The local criteria are considered where the *performance level* is intended to be conservatively set through the performance of individual components (e.g., hinge rotation limits, stress and strain limits, drop in lateral capacity of components). For example, δ_u for the global collapse point is typically taken as the displacement corresponding to a 20% drop in the maximum base shear ($0.8V_{max}$). In addition, non-simulated collapse points may be considered in calculating this ultimate displacement if they are triggered prior to the ultimate displacement corresponding to a 20% drop in maximum base shear. By calculating the ultimate roof displacement (δ_u), the period-based ductility factor is calculated as Eq. (5.9).

$$\mu_T = \frac{\delta_u}{\delta_{y,eff}} \geq 1.0 \quad (5.9)$$

According to Eq. (5.10), the overstrength factor for a given *archetype* model, R_{oi}, is defined as the ratio of the maximum base shear resistance of each *archetype*, $V_{max,i}$, to its design base shear, V_i. This overstrength factor is calculated for all *archetypes*, and then, by taking an average of the overstrength factor values in each *performance group*, the resultant overstrength factor for the system (R_o) is defined as the smallest average value of all *performance groups*. The calculated system overstrength factor should not be larger than the values suggested by Mitchell et al. (2003), as minimum dependable overstrength. The resultant value should be rounded to the nearest 0.1-unit intervals.

$$R_{oi} = \frac{V_{max,i}}{V_i} \quad (5.10)$$

The cap proposed above is intended to account for the fact that, regardless of the assessed number of *archetypes*, there might be another possible *performance group* that could result in a smaller R_o. The calculated R_o is then compared with the trial value provided in the design requirements. If the resultant value is less than the trial value, then the design requirements need to be modified and the *archetypes* need to be redesigned before going to the next step.

5.5.2 Input Ground Motions

5.5.2.1 Ground Motion Selection

The methodology provided in the *PBU procedure* requires a set of ground motion records that can be used for nonlinear dynamic analysis of buildings and performance evaluation of the proposed system. In this regard, selection criteria including considerations of intensity or amplitude, frequency content, duration, spectral shape and level of the ground motions, which are in turn related to the magnitude and distance of the earthquake events, should be taken into account in developing the ground motion set. Generally, two different approaches could be employed in developing the ground motion set, as part of the proposed *PBU procedure*:

1. Selecting the ground motion set based on earthquake magnitudes, source-to-site distances, without considering the *spectral shape effect* in the selection of ground motions, as recommended in Commentary J of NBC Structural Commentaries (NRC 2015a),
2. Selecting the ground motion set based on mean earthquake magnitude, source-to site distance, and target epsilon obtained using the deaggregation analysis of seismic hazards in the region where the *SFRS* will be located.

The first approach seems more practical than the second one since the *spectral shape effect* is considered by an *SSF*. However, in the second approach where the *SSF* is not required, the procedure requires more work. That is because ground motion selection is affected by the system's behaviour to incorporate the *spectral shape effect*. The effect of spectral shape in Canada is further discussed in Section 5.7.2.

The period range relevant to the vibration of all the *archetypes* should be identified and covered by the selected ground motions. For each *archetype* configuration, the period range is defined by (T_{min}, T_{max}). According to Commentary J of the NBC 2015 (NRC 2015a), the lower-bound T_{min} is taken as the smaller of ($0.15T_1$, $T_{90\%}$), where T_1 is the first-mode period of the structural model of the building and $T_{90\%}$ is the period of the lowest mode that must be included in the dynamic analysis to achieve 90% of the participating mass of the building. The upper-bound T_{max} is taken as the greater of ($2T_1$, 1.5 s). It is important to note that some strong-motion instruments, particularly older models, have inherent limitations in their ability to record long-period vibrations accurately. It is suggested that the record set be considered valid for performance evaluation of tall buildings with elastic fundamental periods up to about four seconds.

According to FEMA P-695, large-magnitude events are preferred over ground motions of smaller magnitude (M < 6.5) events. Large-magnitude events pose the greatest risk of building collapse due to inherently longer durations of strong shaking and larger amounts of energy released. On the other hand, small-magnitude ground motions can cause building damage (typically of a non-structural component damage type) and are not likely to lead to collapse of structures. Moreover, the record set is suggested to include ground motions recorded on either soft rock (Site Class C) or stiff soil (Site Class D) sites. Records on soft soil (Site Class E) or sites susceptible to ground failure (Site Class F) are not recommended. Relatively few strong-motion records are available for Site Class B (rock) sites.

The number of records in the set should be "statistically" sufficient such that the results of performance evaluations adequately describe both the median value and *record-to-record (RTR) uncertainty*. A minimum of five ground motion records for each seismicity level and the total number of records not less than 11 for the whole ground motion set are suggested by the NBC 2015. However, it is recommended that the record set include at least 20 records in the *PBU procedure*. Additionally, to avoid potential event-based bias in the record sets, not more than two records from the same earthquake event should be included. In terms of using the simulated ground motions within the set, the NBC 2015 suggests that recorded ground motions, if available, be preferred over simulated ground motion time histories because recorded ground motions naturally account for the aleatoric uncertainty in actual earthquakes, whereas simulated time histories can only account for uncertainty by assumptions and statistical modelling.

In cases where the *archetype* models are three-dimensional and two components of each ground motion record are required for the time history analysis, it is necessary to provide pairs of orthogonal ground motion components recorded simultaneously at the same station for the same earthquake event. The record set does not have to include the vertical component of the ground motion since this direction of earthquake shaking is not considered of primary importance for performance evaluation, and is not required by the methodology for nonlinear dynamic analysis.

5.5.2.2 Ground Motion Scaling to CLE Spectrum

Where a selected ground motion set is required to be scaled to the CLE spectrum in the *PBU procedure*, the proposed methodology in this section should be used. Records scaling to match the CLE spectrum parallel the ground motion scaling procedure described by Commentary J of the NBC 2015 (NRC 2015a), with the notable exception that the median value of the scaled record set need only match the spectrum at the fundamental period, rather than over the period range described in the NBC. In this regard, the CLE spectrum is defined as a 5%-damped uniform hazard spectrum with a 2% probability of exceedance in 50 years for the building site, as defined in the NBC 2020. Then, each ground motion should be scaled individually such that its response spectrum matches the CLE spectrum, $I_E S(T)$ at the fundamental period, T. For two-dimensional *archetype* models, for which a single component of the record is used, two components of each ground motion are scaled separately as independent ground motions. However, when performing multidirectional analysis, the geometric mean of the spectra of the two horizontal components needs to match the CLE spectrum.

5.5.3 *Archetype* Detailed Screening

The detailed screening process proposed in the *PBU procedure* is intended to make the performance evaluation less laborious by reducing the total number of *archetypes* requiring *IDA*. In this process, the *archetypes* are evaluated by the nonlinear time history analysis using target-level ground motions to divide them into critical and non-critical *archetypes*. The non-critical *archetypes* are deemed to have satisfactory responses and are directly sent to the performance evaluation in step 8 (i.e., requiring only NLTHA rather than *IDA*). However, the critical *archetypes*, are those that are suspected to result in an insufficient margin against meeting the *performance level*. These *archetypes* need to be sent to the detailed evaluation using *IDA*, before concluding on the system performance. Details of the screening process for i^{th} *performance group* (PG_i) are outlined in Figure 5-14.

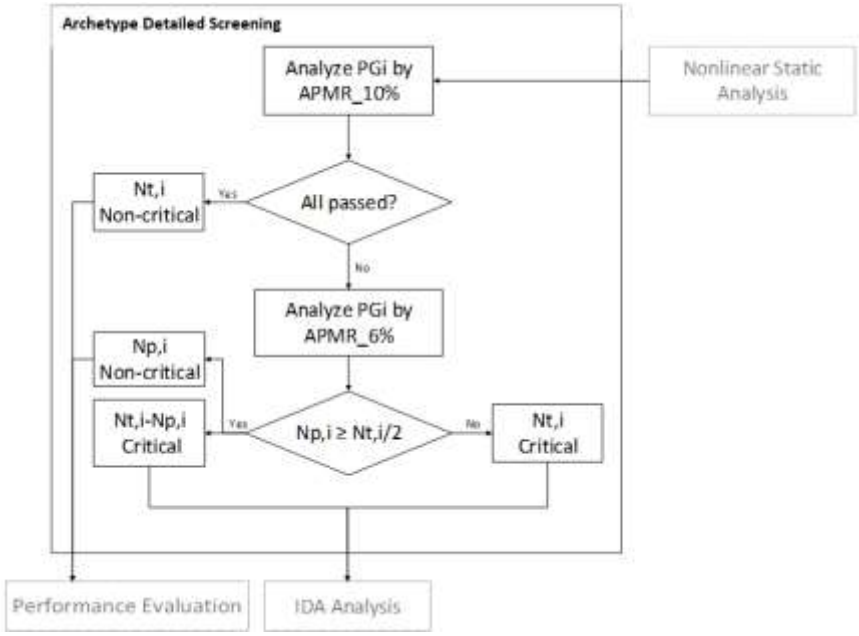

Figure 5-14 Flowchart for *archetype* detailed screening process

In the *PBU procedure*, first, all the *archetypes* within the *performance group* need to be assessed with the NLTHA. The selected ground motion set in Section 5.5.2 used for the NLTHA must be scaled twice. First, it is scaled to the CLE spectrum as described in Section 5.5.2.2. Second, this scaled set of ground motions is scaled again using a scale factor of $APMR_{10\%}$. $APMR_{10\%}$ is the acceptable *APMR* used in the performance evaluation step and is set equal to 2.16, calculated using a 10% probability of exceedance and total uncertainty of $\beta_{TOT} = 0.6$.

By performing the NLTHA, demands are compared to the *performance levels* quantified through both local and global criteria. The *archetype* is considered as passed if half or more than half of the records result in demands within the acceptable range. Then, the number of passing *archetypes* is compared with the total number of *archetypes* within each *performance group*. If the number of passing *archetypes* in a *performance group* ($N_{p,i}$) is equal to the total number of *archetypes* ($N_{t,i}$), the corresponding *performance group* is identified as non-critical and is sent to the performance evaluation step (step 8).

In cases where not all the *archetypes* in the *performance group* are passed, the *archetypes* need to be evaluated using a higher level of ground motions by using a second scale factor, $APMR_{6\%}$. The second scale factor is intended to divide the *archetypes* within a *performance group* into critical and non-critical categories. $APMR_{6\%}$ is the acceptable *APMR* used in the performance evaluation step and is set equal to 2.54, calculated using 6% probability of exceedance and total uncertainty of $\beta_{TOT} = 0.6$. By applying the second scale factor to the CLE ground motions and analyzing the *archetypes*, the number of passing *archetypes* ($N_{p,i}$) is compared to the half number of *archetypes*

in a *performance group* ($N_{t,i}/2$). If $N_{p,i} \geq N_{t,i/2}$, the passing *archetypes* are non-critical and sent to the performance evaluation (step 8). However, the critical *archetypes* are sent to the *IDA* step for further evaluation. Otherwise, if $N_{p,i} < N_{t,i/2}$, the whole *archetypes* within the *performance group* are found to be critical and sent to the *IDA*. More details about the development of the scale factors for detailed screening in the *PBU procedure* are given in Appendix B.

In order to determine the failed or passed *archetypes* in the NLTHA, the probability of performance not met of each *archetype* needs to be calculated. As provided in Eq. (5.11), the probability of performance not met of each *archetype* (P_i) is defined as the number of records exceeding the *acceptance criteria* for the target *performance level* (N_{rf}) divided by the total number of records within the record set (N_{rt}). Using the equation below, the *archetype* is considered as passed if the calculated probability is less than 50%.

$$P_i = \frac{N_{rf}}{N_{rt}} \times 100\ \% \tag{5.11}$$

5.5.4 *Incremental Dynamic Analysis*

As mentioned above, the critical *archetypes* are sent to the *IDA* step to be evaluated in detail. Visualizing the system behaviour through the concept of *IDA* was first developed by Vamvatsikos and Cornell (2002) and then used by FEMA P-695 to evaluate the collapse performance assessment of systems. In the *PBU procedure*, *IDA* is used to evaluate the performance of a system using the target *performance level* defined in the design requirements. The *IDA* process is outlined in Figure 5-15. According to the flowchart, each *archetype* model is incrementally analyzed to determine its median performance intensity, $\hat{S}_{PT}$, and then compared with the CLE design intensity (S_{DT}) by calculating its *PMR*.

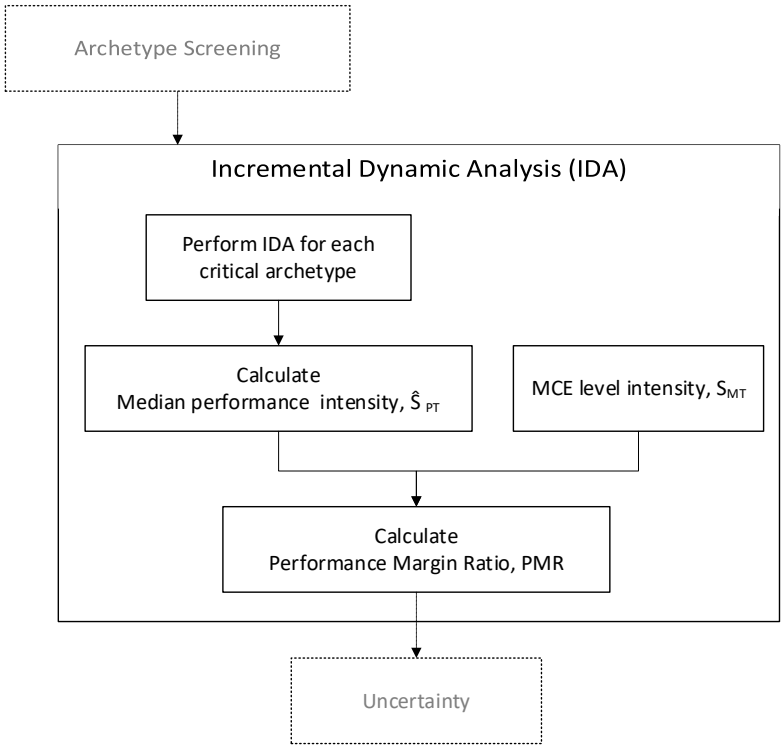

Figure 5-15 Flowchart for performing *IDA* (modified from FEMA P-695)

In the *IDA* process, after applying the factored gravity loads described in Section 5.4.1.6, each critical *archetype* model is analyzed by the set of ground motions selected in Section 5.5.2.1. The ground motions are scaled up incrementally to develop the *IDA* curves and also to determine the performance intensities with acceptable accuracy. An example of the *IDA* curves for a 4-storey RC special moment frame (ATC 2009) is provided in Figure 5-16. In this figure, each *IDA* curve connects points corresponding to the results of one nonlinear dynamic analysis of the model subjected to one ground motion record scaled to increasing spectral intensities. Differences between the lines reflect differences in the response of the same *archetype* model when subjected to different ground motions with different frequency characteristics. As shown in this figure, the *IDA* curves are plotted in terms of the spectral intensity of the ground motions at the fundamental period of the model, S_T, versus the maximum inter-storey drift ratio.

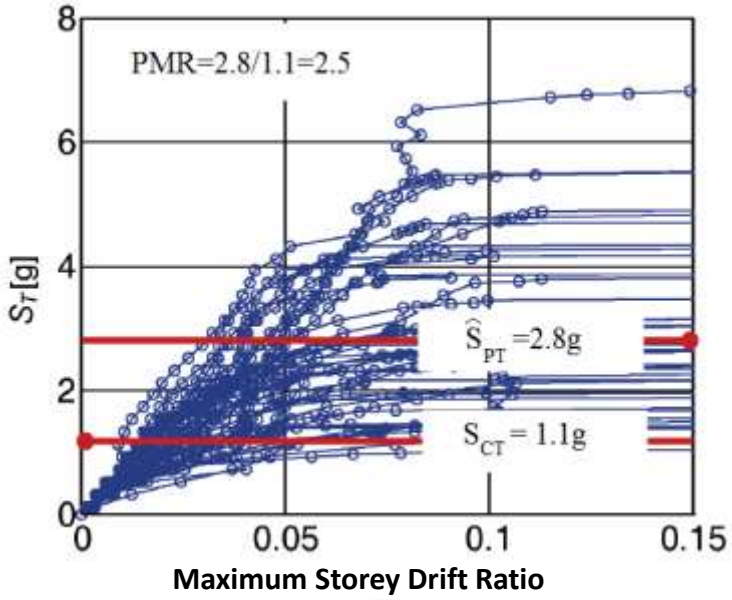

Figure 5-16 *IDA* curves resulted for a single *archetype* model (reproduced from Figure 6-6 of FEMA P695, 2009)

Similar to the screening process, when the system response exceeds the *acceptance criteria*, its corresponding spectral intensity should be identified for each *IDA* curve through global and local performance criteria. The criteria are defined using the target *performance level* specified in the design requirements. For the local (element-based) criteria, maximum rotation of the plastic hinges and also material stress and strain limits could be used. However, the global criteria are defined for overall system response based on the structural and non-structural target *performance levels* through inter-storey drift ratio, tangential stiffness of the *IDA* curve, valid range of modelling, etc. For example, for systems with a target *performance level* of *CP*, the global performance criteria correspond to the global collapse of the model and are defined where the horizontal flat line develops in the *IDA* curve (e.g., 20% tangential stiffness criteria as suggested by Vamvatsikos and Cornell (2002). In this case, other non-simulated criteria need to be considered if they are triggered earlier and govern. Note that the accurate calculation of these *performance levels* strongly depends on the simulated and non-simulated deterioration modes described in Section 5.4.2.

By determining the *performance level* of each *IDA* curve, the median spectral acceleration intensity corresponding to that *performance level* can be obtained as the spectral intensity where half of the ground motions cause the structure to exceed the *acceptance criteria*. The median *performance level* corresponds to a 50% probability in the lognormal collapse fragility curve. Finally, when the median performance intensity of the system is obtained, the *PMR* of each *archetype* is calculated as the ratio of the median performance spectral intensity, $\hat{S}_{PT}$, divided by the CLE spectral intensity, S_{DT}, at the fundamental period. The definition of *PMR* is provided in

Eq. (5.12). Note that the CLE intensity, S_{DT}, is taken directly from the response spectrum for which the model has been designed. The *PMR* of the *archetype* model is used to characterize the performance safety of the structure in Section 5.7.

$$PMR = \frac{\hat{S}_{PT}}{S_{DT}} \tag{5.12}$$

5.5.4.1 Ground Motion Record Scaling in *IDA*

Where the full *IDA* curves are required and the intent is to obtain the median performance intensity with high accuracy, the *archetype* models should be analyzed by each ground motion through a proper record-scaling methodology, such as the hunt-and-fill scaling methodology suggested by Vamvatsikos & Cornell (2002). Since the *IDA* concept required for performance evaluation only requires the identification of median performance intensity, $\hat{S}_{PT}$, *IDA* can be conducted with fewer analyses. In this regard, FEMA P-695 suggests that the median performance intensity can be obtained by first scaling all the records to the CLE spectrum, as described in Section 5.5.2.2, and then increasing the intensity until just over one-half of the scaled ground motion records pass the capacity. In this methodology, the median performance intensity, $\hat{S}_{PT}$, is taken as the lowest performance spectral intensity, S_T, at which one-half of the records exceed the *acceptance criteria* for the target *performance level*. Note that, while the full *IDA* curve is not required in this methodology, a sufficient number of response points should be plotted at increasing intensities to help validate the accuracy of calculating the median performance point of the model and also to observe possible structural resurrections.

5.5.4.2 2D Versus 3D Models

For 2D *archetype* models, two components of each ground motion are applied as independent events to calculate the median performance intensity. In other words, each *archetype* model should be analyzed by all horizontal components of the ground motion set provided. For three-dimensional models, two components of each ground motion are applied simultaneously. To consider all possible conditions, the ground motions are applied twice, once with ground motion records oriented along one principal direction, and then again with the records rotated 90 degrees.

FEMA P-695 indicates that the median intensity resulting from both components of each ground motion in a 3D model is more conservative and, on average, about 20% lower than the corresponding value resulting from a 2D model. To achieve parity with the 2D analyses, an adjustment should be made when calculating the *PMR* using 3D analyses. In this regard, a *PMR* calculated based on median performance intensity, $\hat{S}_{PT}$, obtained from 3D analyses should be multiplied by a factor of 1.2.

5.6 Uncertainty (Step 7)

Different sources of uncertainty affect the performance of a system. In the performance evaluation (step 8) of the *PBU procedure*, these uncertainties are incorporated in determining the system safety factor or *acceptable APMR* described in Section 5.7. A smaller safety factor (or larger *acceptable APMR*) will be used if the performance evaluation process is conducted by a lower total uncertainty (e.g., more robust design requirements, more comprehensive test data, and more detailed nonlinear analysis). FEMA P-695 indicates that common sources of uncertainty, including design requirement uncertainty (β_{DR}), test data uncertainty (β_{TD}), modelling uncertainty (β_{MDL}), and record-to-record uncertainty (β_{RTR}), should be explicitly considered and implemented properly to determine the total uncertainty.

In the *PBU procedure*, it is very important to evaluate all the above sources of uncertainty in the system response, as shown in Figure 5-17. More details about the determination of each source of uncertainty are presented in the following sections.

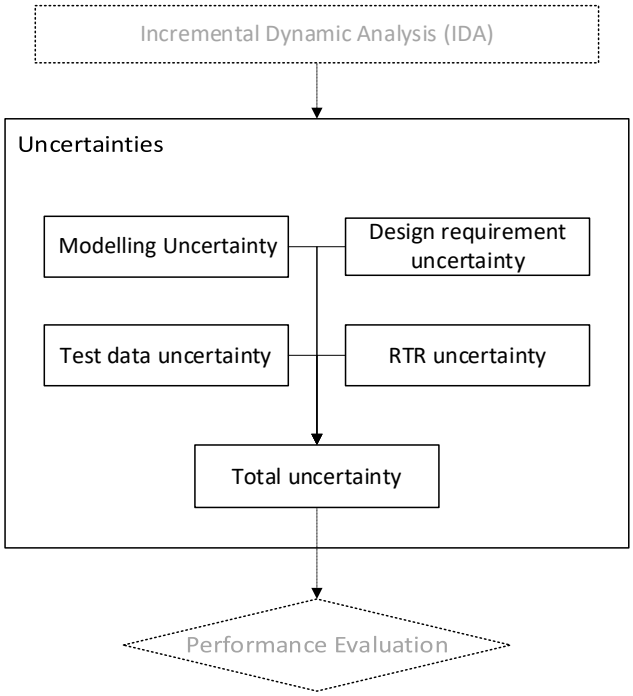

Figure 5-17 Flowchart to consider all sources of uncertainty

5.6.1 Design Requirement Uncertainty

Design requirement uncertainty is related to the completeness and robustness of the design requirements and confidence in the basis of the design requirements. In this regard, the design requirements are rated between (A) Superior and (D) Poor, as shown in Table 5-6. According to

the table, the values of design requirement uncertainty are: (A) Superior, β_{DR} = 0.10; (B) Good, β_{DR} = 0.20; (C) Fair, β_{DR} = 0.35; and (D) Poor, β_{DR} = 0.50.

Table 5-6 Quality rating of the design requirements (ATC 2009)

Completeness and Robustness	Confidence in the Basis of the Design Requirements		
	High	**Medium**	**Low**
High: Extensive safeguards against unanticipated failure modes. All the important design and quality assurance issues are addressed.	(A) Superior β_{DR}=0.10	(B) Good β_{DR}=0.20	(C) Fair β_{DR}=0.35
Medium: Reasonable safeguards against unanticipated failure modes. Most of the important design and quality assurance issues are addressed.	(B) Good β_{DR}=0.20	(C) Fair β_{DR}=0.35	(D) Poor β_{DR}=0.50
Low: Questionable safeguards against unanticipated failure modes. Many important design and quality assurance issues are not addressed.	(C) Fair β_{DR}=0.35	(D) Poor β_{DR}=0.50	---

The highest rating, (A) Superior, applies to systems that include a comprehensive set of design requirements, which provide safeguards against unanticipated failure modes, with a high level of confidence to produce anticipated structural behaviour. As an example, the Superior rating could be considered for the existing code requirements for ductile steel moment frames (NBC 2020 and S16-19) and ductile concrete moment frames (NBC 2020 and CSA A23.3-19) for which detailed experimental results, design, and detailing requirements, and also documented performance in earthquake, are available. On the contrary, the lowest rating, (D) Poor, applies to design requirements that have minimal safeguards against unanticipated failure modes, do not ensure a hierarchy of yielding and failure, and would generally be associated with systems that exhibit behaviour that is difficult to predict. As provided in Table 5-6, the combination of low-quality design requirements in terms of completeness and robustness along with low confidence in the basis of the design requirements is not permitted. In order to determine the rating of the design requirements, two important factors should be considered, as follows.

Completeness and robustness characteristics

Completeness and robustness characteristics of design requirements measure how well the anticipated failure modes are addressed, and how accurately the requirements are implemented in various design stages from fabrication to final construction. Note that simplified design requirements, although conservative, do not necessarily result in a low completeness and robustness rating as long as the conservatism is quantifiable in the context of unanticipated failure modes. Generally, completeness and robustness are rated from High to Low as follows:

- **High:** Design requirements are comprehensive, well vetted, and provide extensive safeguards against unanticipated failure modes. A definite hierarchy of component yielding and failure is established. All the important issues regarding system behaviour have been addressed, resulting in high reliability in the behaviour of the system. There is a high likelihood that the design provisions will be well executed through fabrication, erection, and final construction due to mature construction practices and tightly specified quality assurance requirements.
- **Medium:** Design requirements are partly extensive and provide reasonable safeguards against unanticipated failure modes, but leave some limited potential for the occurrence of such modes. A suggested, but not definite, hierarchy of component yielding and failure are established. While most of the important behavioural issues have been addressed, some have not, which somewhat reduces the reliability of the system. Quality assurance requirements are specified, but do not fully address all the important aspects of fabrication, erection, and final construction.
- **Low:** Design requirements are not extensive and provide questionable safeguards against unanticipated failure modes. A hierarchy of component yielding and failure has been only marginally addressed, and there is a likelihood of the occurrence of unanticipated failure modes. Design requirements do not address all the important behavioural issues, resulting in slightly reliable behaviour of the system. Quality assurance is lacking, written guidance is not provided, and construction practices are not well developed for the type of system and materials.

Confidence in the basis of the design requirements

This factor refers to the degree to which the prescribed design requirements (e.g., material properties, strength criteria, stiffness parameters, and design equations) are representative of actual behaviour and will achieve the intended performance. Generally, the confidence in the basis of the design requirements is rated from High to Low as follows;

- **High:** There is substantiating evidence (experimental data, history of use, similarity with other systems) that the properties, criteria, and equations provided in the design requirements will result in component designs that perform as intended.
- **Medium:** There is some substantiating evidence (experimental data, history of use, similarity with other systems) that the properties, criteria, and equations provided in the design requirements will result in component designs that perform as intended.
- **Low:** There is little substantiating evidence (experimental data, history of use, similarity with other systems) that the properties, criteria, and equations provided in the design requirements will result in component designs that perform as intended.

5.6.2 Test Data Uncertainty

The completeness and robustness of the test data used to define the system as well as confidence in the test results are measured in test data uncertainty. In this uncertainty, not only the quality of the testing program is evaluated, but also how well the tests address key parameters and behavioural issues. Note that, test data uncertainty is closely associated with, but distinct from, modelling uncertainty described in the next section. Test data are rated between (A) Superior and (D) Poor, as shown in Table 5-7. Quantitative values of test data uncertainty are: (A) Superior, β_{TD} = 0.10; (B) Good, β_{TD} = 0.20; (C) Fair, β_{TD} = 0.35; and (D) Poor, β_{TD} = 0.50. As shown in the table, low-quality test data in terms of completeness and robustness with low confidence in the test results is not permitted.

Table 5-7 Quality rating of test data from an experimental investigation program (ATC 2009)

Completeness and Robustness	Confidence in the Test Results		
	High	**Medium**	**Low**
High: Material, component, connection, assembly, and system behaviour well understood and accounted for. All, or nearly all, important testing issues are addressed.	(A) Superior β_{TD}=0.10	(B) Good β_{TD}=0.20	(C) Fair β_{TD}=0.35
Medium: Material, component, connection, assembly, and system behaviour generally understood and accounted for. Most important testing issues addressed.	(B) Good β_{TD}=0.20	(C) Fair β_{TD}=0.35	(D) Poor β_{TD}=0.50
Low: Material, component, connection, assembly, and system behaviour fairly understood and accounted for. Several important testing issues not addressed.	(C) Fair β_{TD}=0.35	(D) Poor β_{TD}=0.50	---

In order to determine the quality rating of the test data, two important factors should be considered.

Completeness and robustness of the test data

Completeness and robustness of a set of test data are rated from high to low based on the degree to which relevant testing issues have been considered in the development of the testing program, and also the extent to which the testing program and other documented experimental evidence quantify the necessary material, component, connection, assembly, and system properties and important behaviour and failure modes.

- **High:** All, or nearly all, important general testing considerations described in Section 5.2.3 are addressed comprehensively in the testing program and other supporting evidence. Experimental evidence is sufficient so that all, or nearly all, important behavioural aspects at all levels (from material to system) are well understood, and the results can be used to quantify all important parameters that affect the design requirements and analytical modelling.
- **Medium:** Most of the important general testing considerations described in Section 5.2.3 are addressed adequately in the testing program and other supporting evidence. Experimental evidence is sufficient so that all, or nearly all, important behavioural aspects at all levels (from material to system) are generally understood, and the results can be used to quantify or deduce most of the important parameters that significantly affect the design requirements and analytical modelling.
- **Low:** some important general testing considerations described in Section 5.2.3 are not addressed adequately in the testing program and other supporting evidence. Experimental evidence is sufficient so that the most important behavioural aspects at all levels (from material to system) are fairly well understood, but the results are not adequate to quantify or deduce, with high confidence, many of the important parameters that significantly affect the design requirements and analytical modelling.

Confidence in the test results

This factor accounts for the reliability and repeatability of the results obtained from the testing program as well as corroboration with available results from other relevant testing programs. Considerations including consistently recording performance to failure for all modes of behaviour and sufficient information to assess uncertainties in the design requirements and analytical models, should also be considered in determining the confidence rating.

- **High:** Reliable experimental information is produced on all important parameters that affect the design requirements and analytical modelling. Comparable tests from other testing programs have produced results that are fully compatible with those from the system-specific

testing program. A sufficient number of tests are performed so that statistical variations in important parameters can be assessed. The test results are fully supported by basic principles of mechanics.

- **Medium:** Moderately reliable experimental information is produced on all important parameters that affect the design requirements and analytical modelling. Comparable tests from other testing programs do not contradict, but do not fully corroborate, the results from the system-specific testing program. A measure of uncertainty in important parameters can be estimated from the test results. The test results are supported by basic principles of mechanics.
- **Low:** Experimental information produced on many of the important parameters that affect the design requirements and analytical modelling is of limited reliability. Comparable tests from other testing programs do not support the results from the system-specific testing program. Insufficient data exist to assess uncertainty in many important parameters. Basic principles of mechanics do not support some of the results of the testing program.

5.6.3 Modelling Uncertainty

The *archetype* models are used to estimate median response of *SFRS* at the performance point. In this regard, the modelling uncertainty is defined to account for the quality of the *archetype* models and to quantify: 1) how well the *archetype* models represent the range of system response at the point corresponding to the *performance level* and associated design parameters; 2) how well the analysis models capture structural performance through both direct simulation and non-simulated deteriorations. According to Table 5-8, the quantitative values of modelling uncertainty are: (A) Superior, β_{MDL} = 0.10; (B) Good, β_{MDL} = 0.20; (C) Fair, β_{MDL} = 0.35; and (D) Poor, β_{MDL} = 0.50. The highest rating, Superior, belongs to cases where the *archetype* models represent the complete range of structural configuration and response at the performance point, with high confidence in the ability of established models to simulate behaviour. As shown in Table 5-7, the combination of low-quality representation of response at the performance point along with low-quality modelling in terms of accuracy and robustness is not permitted.

Table 5-8 Quality rating of *archetype* models (ATC 2009)

Representation of Response at Performance Point	Accuracy and Robustness of Models		
	High	**Medium**	**Low**
High: Models capture the full range of the design space and structural behavioural effects that contribute to the performance point.	(A) Superior β_{MDL}=0.10	(B) Good β_{MDL}=0.20	(C) Fair β_{MDL}=0.35
Medium: Models are generally comprehensive and representative of the design space and behavioural effects that contribute to the collapse points.	(B) Good β_{MDL}=0.20	(C) Fair β_{MDL}=0.35	(D) Poor β_{MDL}=0.50
Low: Significant aspects of the design space and/or seismic behaviour are not captured in the models.	(C) Fair β_{MDL}=0.35	(D) Poor β_{MDL}=0.50	---

In order to determine the quality rating of the *archetype* models, two important factors should be considered.

Representation of response at *performance levels*

This factor refers to how completely and comprehensively the *archetype* models capture the full range of design parameters and associated structural response that is envisioned within the design space. It is rated from high to low as shown below.

- **High:** The set of *archetype* models provides a complete and comprehensive representation of the full range of structural configurations, design parameters and behavioural characteristics that affect structural performance points. They cover the comprehensive *archetype* configurations permitted within the design space, as described in Section 5.3.1. Important general modelling considerations described in Section 5.4.1 are reflected in the *archetype* models.
- **Medium:** The set of *archetype* models provides a reasonably broad and complete representation of the design space. Where the complete design space is not fully represented in the set of models, there is reasonable confidence that the primary structural behaviour affecting the performance points is captured.

- **Low:** The set of *archetype* models does not capture the full range of structural configurations and responses at the performance point due to incomplete defined design space and/or insufficient number of *archetype* configurations. This usually happens when the design space and possible configurations are very large and cannot be represented by a limited number of *archetypes*. Even for well-controlled design criteria (small design space), the number and variety of *archetype* configurations may be insufficient to capture the possible range in response.

Accuracy and robustness of models

This factor is related to the degree to which nonlinear behaviour and deteriorations are directly simulated in the model, or otherwise accounted for in the evaluation. Using non-simulated criteria will lower the accuracy and robustness of a nonlinear model. However, if conservatively applied, the non-simulated check should not necessarily lower the overall quality rating of the assessment procedure. The accuracy and robustness of models are rated from high to low as shown below.

- **High:** Nonlinear models directly simulate all predominate inelastic effects, from the onset of yielding through strength and stiffness degradation causing collapse. Models use either concentrated hinges or distributed finite elements to provide spatial resolution appropriate for the proposed system. Computational solution algorithms are sufficiently robust to accurately track inelastic force redistribution, including cyclic loading and unloading, without convergence problems, up to the performance point.
- **Medium:** Nonlinear models capture most, but not all, nonlinear deterioration and response mechanisms up to the performance point. Models may not be sufficiently robust to track the full extent of deterioration, so that some component-based limit state checks are necessary to assess performance.
- **Low:** Nonlinear models capture the onset of yielding and subsequent strain hardening, but do not simulate degrading response. Onset of degradation is primarily evaluated using non-simulated component limit state checks. Overall uncertainty in response quantities is increased due to the inability to capture the effects of deterioration and redistribution.

5.6.4 *Record-to-Record Uncertainty*

Record-to-record uncertainty, β_{RTR}, is related to variability in the response of the *archetypes* to different ground motion records. This kind of variability could be seen in the *IDA* curves provided in Figure 5-16. This variability in the response is a function of; 1) variation in frequency content and also dynamic characteristics of various records, and 2) variability in the hazard characterization as reflected in the ground motion set. Therefore, it strongly depends on the record set provided, and an accurate calculation would require performance data from a large number of

archetypes. As the record set is not provided in this *PBU procedure*, the *record-to-record uncertainty* cannot be represented by a single value. Therefore, it is suggested that the *record-to-record uncertainty* be conservatively determined from the *IDA* results of the critical *archetypes*. Note that the precise calculation of the *record-to-record uncertainty* does not significantly affect the resultant collapse margin ratios, when combined with other sources of uncertainties (ATC 2009).

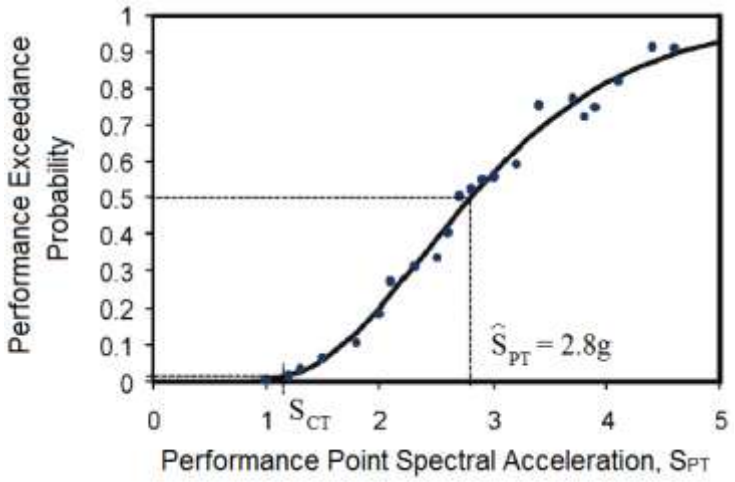

Figure 5-18 Fragility curve resulting from performance data points (reproduced from Figure 6-7 of FEMA P-695, 2009)

After performing the *IDA* on the critical *archetypes* and developing their *IDA* curves, the spectral intensity corresponding to the *performance level* of the *SFRS* is obtained for each *IDA* curve and is defined as *performance level* spectral intensity. It is suggested that the *record-to-record uncertainty* be calculated from the resulting *performance level* spectral intensities for each critical *archetype*. In this regard, fragility curve points are plotted using a cumulative distribution function (CDF) of *performance level* spectral intensities to find their probability of exceedance. The *record-to-record uncertainty* (β_{RTR}) is defined as the standard deviation of a lognormal distribution curve fitted to the points.

5.6.5 Total Uncertainty

The total uncertainty, β_{TOT}, is obtained by combining the design requirement uncertainty, β_{DR}, test data uncertainty, β_{TD}, modelling uncertainty, β_{MDL}, and record-to-record uncertainty, β_{RTR}, using the square root of the sum of the square (SRSS) method, as provided in Eq. (5.13). In this equation, it is assumed that all the uncertainties are independent random variables yielding lognormal distributions. This total uncertainty is further used in determining the *acceptable APMR*.

$$\beta_{TOT} = \sqrt{\beta_{RTR}^2 + \beta_{DR}^2 + \beta_{TD}^2 + \beta_{MDL}^2} \quad (5.13)$$

Given the total uncertainty and the median performance point obtained from *IDA*, the fragility curve can be plotted, as shown in Figure 5-19. Generally speaking, larger uncertainty results in a flatter fragility curve. Given a median intensity, larger uncertainty results in a larger probability of exceedance at the CLE intensity, S_{DT}. Figure 5-19 compares two different β_{TOT} values for a specific *archetype* model.

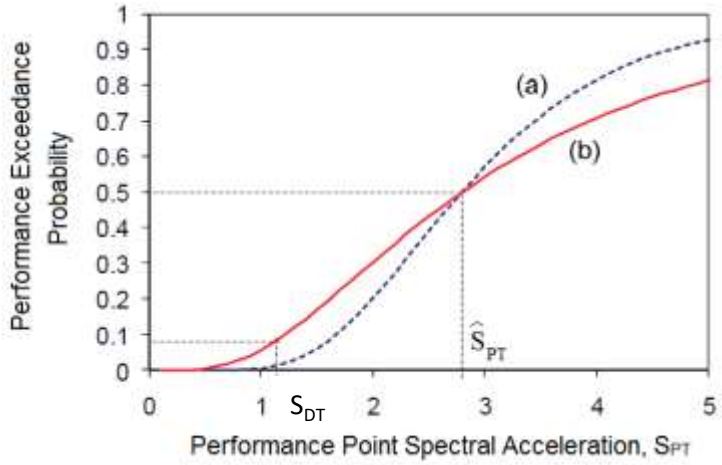

Figure 5-19 Two system fragility curves with the same median value, but different total uncertainty values (ATC 2009)

5.7 Performance Evaluation (Step 8)

This section describes the process for evaluating the seismic performance of the proposed *SFRS* and assessing the acceptability of the trial R_d and R_o values suggested in the design requirements using the results of nonlinear static and nonlinear dynamic analyses. The trial values are evaluated in terms of the acceptability of the *APMR* values calculated either from *IDA* or a detailed screening process, as described in Sections 5.7.2 and 5.7.3. The acceptability is measured by comparing the calculated *PMR* values, after adjusting for the *spectral shape effect*, to the acceptable values that depend on the uncertainties described in Section 5.6. If the *APMR* values are within the acceptable range, it means that the trial values of R_d and R_o and design requirements are satisfactory, and the results should be documented for peer review (step 9). Otherwise, the design requirements need to be modified, and then the system needs to be re-evaluated by repeating the evaluation process. In general, it is expected that more than one iteration of the evaluation process will be required to determine optimal (and acceptable) values of R_d and R_o for the system of interest. The performance evaluation procedure is outlined in Figure 5-20.

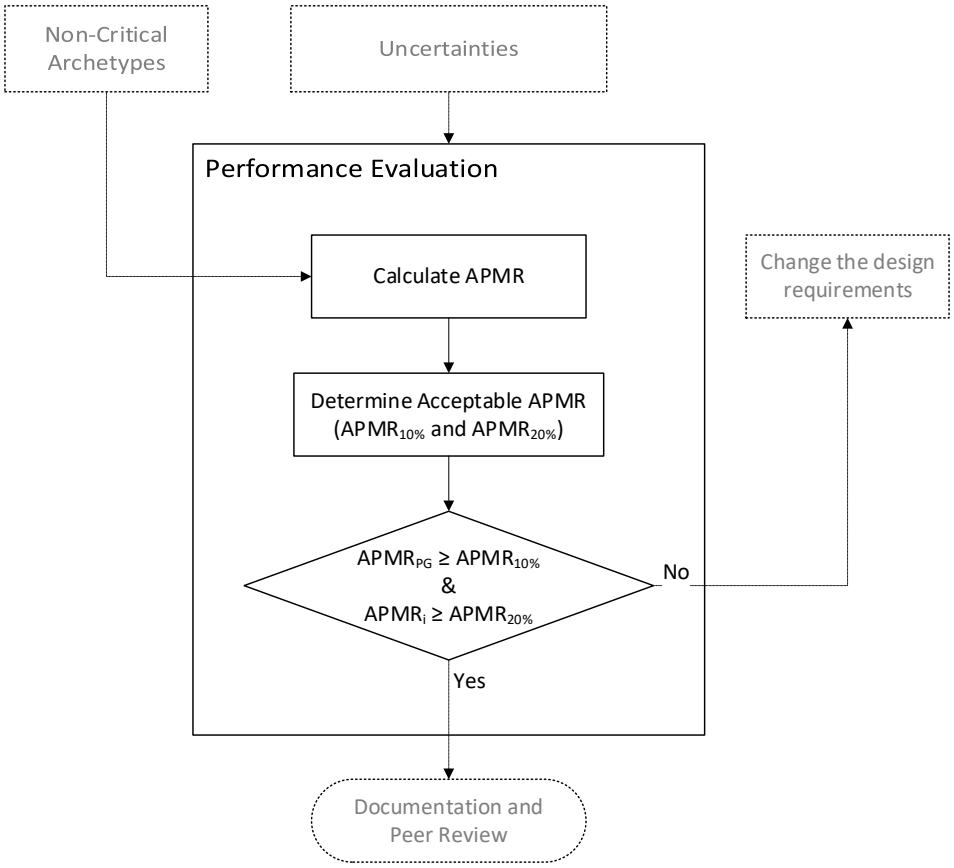

Figure 5-20 Flowchart for the performance evaluation procedure

5.7.1 Performance Evaluation Using Target *Performance Levels*

To evaluate the seismic performance of a system and adjust its R_d and R_o, demands resulting from analyses and *performance levels* should be compared in all *archetypes* and *performance groups* using a suitable safety factor. In this regard, the general scheme presented by the FEMA P-695 methodology for performance evaluation of systems is followed. However, rather than focusing on collapse like the FEMA P-695 does, different *performance levels* are considered in the *PBU procedure*.

Performance of the system in the corresponding *archetype* configuration is acceptable when CLE spectral intensity at the fundamental period (S_{DT}) represents an exceedance probability lower than the predefined acceptable exceedance probability (e.g., 10%), as shown in Figure 5-21. In other words, *APMR*, which is defined as median performance spectral intensity divided by CLE spectral intensity ($\hat{S}_{PT}/S_{DT}$) and then adjusted for *spectral shape effects*, should be more than the *acceptable APMR* of 10% ($APMR_{10\%}$). $APMR_{10\%}$ represents the system safety factor accounting for both the uncertainty and level of confidence and indicates the acceptable margin between the CLE spectral intensity (S_{DT}) and the spectral intensity having an exceedance probability of 50%

($\hat{S}_{PT}$), as illustrated in Figure 5-21(b). The adjustment for *spectral shape effects* is further discussed in Section 5.7.3.

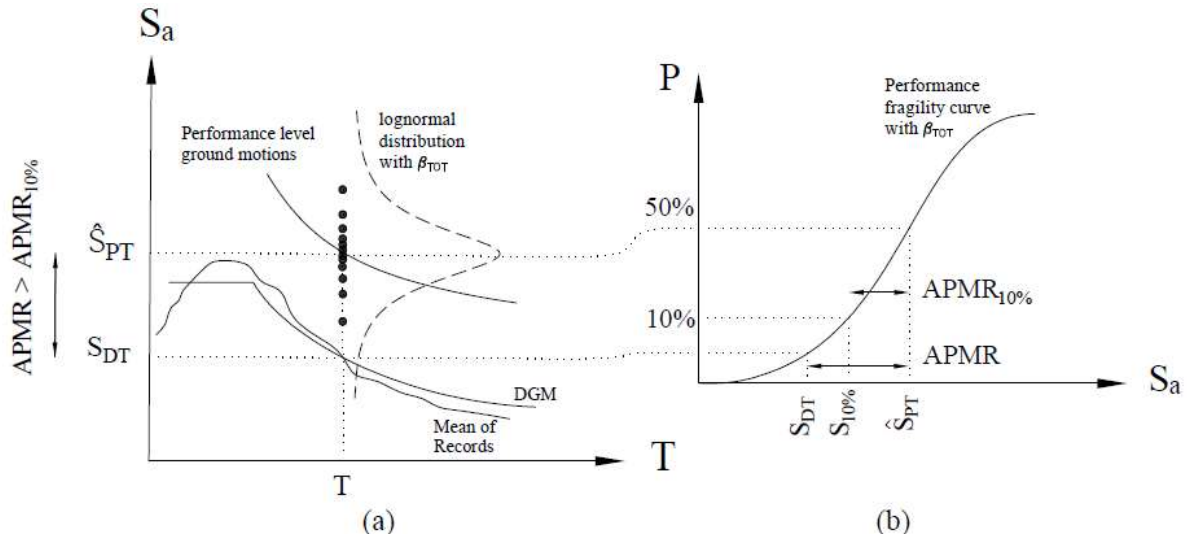

Figure 5-21 General scheme for seismic performance evaluation of systems using *IDA* results in *PBU procedure*; a) *performance level* spectral intensities obtained from *IDA*, b) fragility curve developed for an *archetype* (Fazileh, et al., 2023)

The calculation of $\hat{S}_{PT}$ highly depends on the *performance levels* considered for the system for the specified *seismic hazard level*. As presented earlier in Section 5.4.2, the *SFRS* performance is quantified through local and global criteria and needs to be selected based on the desired performance objectives in different *importance categories*. Table 5-9 provides suggested *performance levels* for different *importance categories* defined in the NBC 2020. As explained earlier, the *performance levels* are quantified through local and global criteria and are used to calculate the median *performance level* spectral intensity ($\hat{S}_{PT}$) in each *importance category*. The *APMR* values are then calculated and compared with $APMR_{10\%}$ by assuming an acceptable conditional exceedance probability of 10% for all *importance categories* (see Table 5-9).

Table 5-9 *Performance levels* for different *importance categories* in the NBC 2020

Importance category	Importance factor, I_E	Proposed *Performance Level*
Low	0.8	*CP*
Normal	1.0	*LS-CP*
High	1.3	*IO-LS*
Post-disaster	1.5	*IO*

The performance-based procedure described above is different from the risk-based methodology suggested by FEMA P-695 and NIST GCR 12-917-20 (NIST 2012) in terms of the *performance level* and acceptable safety factor. For more details, the general schemes for these two procedures are depicted in Figure 5-22 using spectral coordinates. In Figure 5-22, the *APMR* and its equivalent in FEMA P-695 (Adjusted Collapse Margin Ratio, ACMR) are expressed in terms of the spectral displacement ratio using the equal displacement rule. *APMR* in the *PBU procedure* is defined as the ratio of *performance level* spectral displacement (SD_{PT}) to CLE spectral displacement (SD_{DT}), adjusted for *spectral shape effect*. The *APMR* is compared with the *acceptable APMR* having an exceedance probability of 10% ($ACMR_{10\%}$). The ACMR in FEMA P-695 is defined as the ratio of median collapse spectral displacement (SD_{CT}) and MCE_R spectral displacement (SD_{MT}), adjusted for *spectral shape effect*. The ACMR is compared with the acceptable ACMR having an exceedance probability of *Y%* ($ACMR_{Y\%}$).

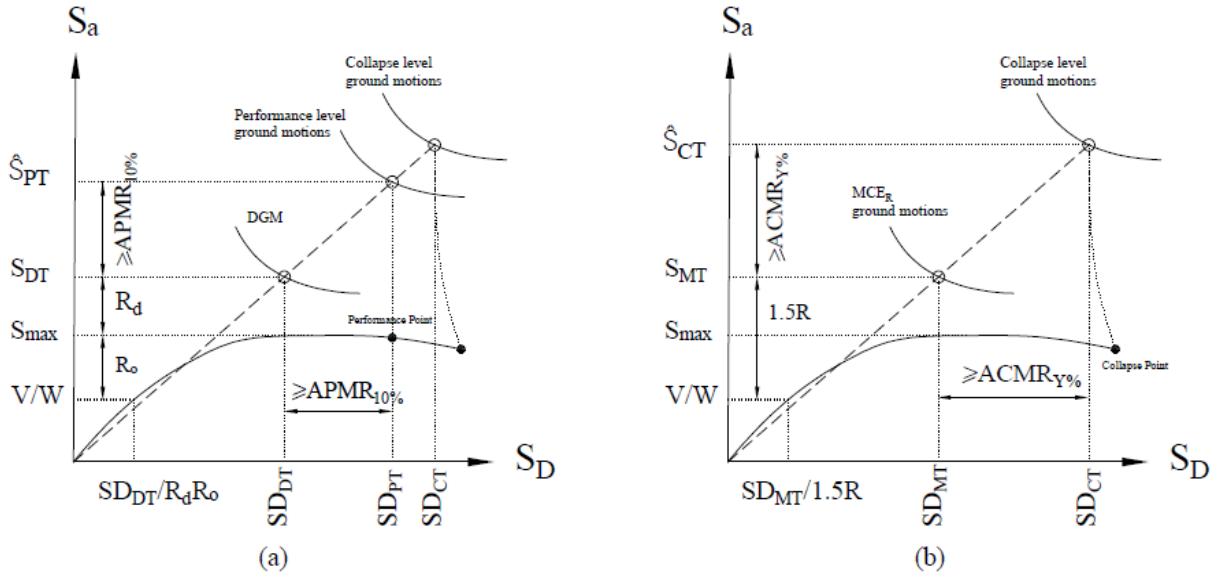

Figure 5-22 Performance evaluation of a system: a) performance-based approach in the *PBU procedure*, b) risk-based approach in NIST GCR 12-917-20 (NIST 2012)

In the *PBU procedure* illustrated in Figure 5-22 (a), the safety factor ($APMR_{10\%}$) is constant for all *importance categories* and different objectives are met by defining a suitable *performance level*. However, in the risk-based approach shown in Figure 5-22 (b), the global capacity of a system is considered as the *performance level* and is kept constant in all *importance categories* (or risk categories as defined by FEMA P-695 and ASCE/SEI 7 (ASCE 2017). In this methodology, the safety factor (or acceptable *ACMR*) is not constant and is calculated based on the desired conditional probability of collapse (*Y%*) in each *importance category*. Using code-based importance factors (I_E), NIST GCR 12-917-20 (NIST 2012) has calculated the required conditional probabilities of collapse (*Y%*) as 20%, 10%, 5%, and 2.5% for risk categories I, II, III, and IV, respectively.

5.7.2 *Performance Margin Ratio* for Evaluation of Performance Groups

As discussed in Section 5.3.2, *archetype* configurations are assembled into multiple *performance groups* to provide a basis for statistical assessment of minimum and average properties of the system. In this regard, the results for each *performance group* are averaged over critical and non-critical *archetypes*. The critical *archetypes* have accurate *PMR* values calculated in the *IDA* process. However, the *IDA* process is not conducted for the non-critical *archetypes*, and therefore, their *PMR* values are not calculated. To make the statistical process possible within each *performance group*, the minimum value of the scale factors used in the screening process ($PMR_{10\%}$ and/or $PMR_{6\%}$) could be used as a conservative estimation for the *PMR* of the non-critical *archetypes*. After determining the *PMR* values for critical and non-critical *archetypes*, they are adjusted using *spectral shape factor* to obtain *APMR* values, as described in Section 5.7.3, and then averaged in each *performance group*.

5.7.3 *Adjusted Performance Margin Ratio*

The *PMR* can be significantly influenced by the frequency content (spectral shape) of the ground motion record set. Recent studies have found that potential ground motions in the west of the U.S. and Canada, which are used for performance evaluation, have a distinct spectral shape. These ground motions are peaked at the period of interest (i.e., around 1.0 second), but drop off rapidly at longer and shorter periods. Since the ground motion intensities used in the *PBU procedure* are defined based on the spectral acceleration at the fundamental period, the performance evaluation results would be conservative for structures having sufficient ductility to elongate their periods. This means that the actual *PMR* values of these structures are higher than the calculated values.

The most direct approach to account for this *spectral shape factor* is to select a unique set of ground motions that have the appropriate shape for each site, *seismic hazard level*, and structural period of interest, as described in Section 5.5.2.1. Alternatively, simplified *SSF* may be used to adjust the

calculated *PMR* values. According to FEMA P-695, the *SSF* is calculated for each *archetype* using Eq. (5.14), where, $\bar{\varepsilon}_0(T)$ represents the target epsilon value for the site, and *hazard level* of the building at the fundamental period, $\bar{\varepsilon}_r(T)$ represents the mean epsilon values for a predetermined record set selected at the fundamental period, and β_1 represents the sensitivity of a particular structure to changes in the epsilon value and is calculated as Eq. (5.15).

$$SSF_i = \exp\left(\beta_1[\bar{\varepsilon}_0(\mathrm{T}) - \bar{\varepsilon}_r(\mathrm{T})]\right) \tag{5.14}$$

$$\beta_1 = 0.14(\mu_T - 1)^{0.42} \tag{5.15}$$

After applying *SSF*, the *PMR* values calculated (or assumed) for each *archetype* i are adjusted by Eq. (5.16) to obtain the *APMR*.

$$APMR_i = SSF_i \times PMR_i \tag{5.16}$$

It should be noted that, since *SSFs* are a function of structural behaviour and seismic design level, the governing *performance group* with *APMR* may not be the same as the governing *performance group* with *PMR* before the adjustment.

5.7.4 Acceptable *Adjusted Performance Margin Ratio*

In order to evaluate the seismic performance of the proposed system, an acceptably low, yet reasonable, probability of exceedance needs to be established. In the *PBU procedure*, it is suggested that the probability of exceedance due to CLE ground motions, with a 2% probability of exceedance in 50 years, be limited to 10%. On average, each *performance group* needs to meet this probability of exceedance. However, it is possible that some individual *archetypes* (i.e., outliers) exceed this value. A limit of twice the value, or 20%, is suggested as a criterion for evaluating the acceptability of potential "outliers" within a *performance group*.

Using the 10% and 20% conditional exceedance probabilities, *acceptable APMR* values ($APMR_{10\%}$ and $APMR_{20\%}$) should be obtained as shown in Table 5-10. According to the table, lower values of acceptable probability of exceedance and higher levels of total uncertainty result in higher required values of *acceptable APMR*. The values in Table 5-10 are calculated based on the lognormal distribution of *performance level* spectral intensities with a median value of $\hat{S}_{PT}$ and a logarithmic standard deviation equal to the total system uncertainty, β_{TOT}, calculated in Section 5.6.5.

Using the calculated acceptable *APMRs*, the acceptable performance results when, for each *performance group*, the *APMR* meets the following two criteria:

- The average value of the *APMR* for each *performance group* exceeds $APMR_{10\%}$:

$$\overline{APMR_i} \geq APMR_{10\%} \quad (5.17)$$

- The individual values of the *APMR* for each *archetype* within a *performance group* exceeds $APMR_{20\%}$:

$$APMR_i \geq APMR_{20\%} \quad (5.18)$$

Table 5-10 Acceptable values of *adjusted performance margin ratios*

Total System Uncertainty	Probability of Exceedance			Total System Uncertainty	Probability of Exceedance		
	6% ($APMR_{6\%}$)	10% ($APMR_{10\%}$)	20% ($APMR_{20\%}$)		6% ($APMR_{6\%}$)	10% ($APMR_{10\%}$)	20% ($APMR_{20\%}$)
0.275	1.53	1.42	1.26	0.625	2.64	2.23	1.69
0.3	1.59	1.47	1.29	0.65	2.75	2.3	1.73
0.325	1.66	1.52	1.31	0.675	2.86	2.38	1.76
0.35	1.72	1.57	1.34	0.7	2.97	2.45	1.80
0.375	1.79	1.62	1.37	0.725	3.09	2.53	1.84
0.4	1.86	1.67	1.4	0.75	3.21	2.61	1.88
0.425	1.94	1.72	1.43	0.775	3.34	2.7	1.92
0.45	2.01	1.78	1.46	0.8	3.47	2.79	1.96
0.475	2.09	1.84	1.49	0.825	3.61	2.88	2.00
0.5	2.18	1.90	1.52	0.85	3.75	2.97	2.04
0.525	2.26	1.96	1.56	0.875	3.90	3.07	2.09
0.55	2.35	2.02	1.59	0.9	4.05	3.17	2.13
0.575	2.44	2.09	1.62	0.925	4.21	3.27	2.18
0.6	2.54	2.16	1.66	0.95	4.38	3.38	2.22

5.8 Documentation and Peer Review (Step 9)

5.8.1 Recommended Qualifications, Expertise and Responsibilities for Development Team

5.8.1.1 Development Team

The development team is a group of researchers evaluating an existing *SFRS* or introducing a new *SFRS*, who need to have certain qualifications, experience and expertise, including the ability to: 1) adequately test materials, components and assemblies; 2) develop comprehensive design and construction requirements; 3) develop *archetype* designs; 4) select a ground motion set; and 5) analyze *archetype* models. The development team needs to be expert users of NBC requirements, material-specific reference standards and their commentaries. Additionally, the development team needs to have experience and expertise to interpret test data and develop sophisticated nonlinear models capable of simulating the *SFRS* response. The development team is responsible for

following the *PBU procedure*, documenting the results, and getting the approval of the peer review panel.

5.8.1.2 Sponsor

The sponsor is a person or organization that has proposed a new *SFRS* and will benefit from its use. The sponsor is responsible for assembling the development team, selecting an independent review panel under the supervision of the Standing Committee on Earthquake Design (SC-ED), and finally submitting the proposed *SFRS* for approval and use.

5.8.1.3 Testing Laboratories

The testing laboratories used in performance evaluation of the proposed *SFRS* need to have the capability to perform material, component, connection, assembly, and system tests as required. The testing laboratories should comply with national or international accreditation criteria. Testing laboratories that are not accredited may still be used for an experimental investigation program, subject to the approval of the peer review panel.

5.8.2 Documentation of Development and Results

The results at each step of the performance evaluation need to be documented thoroughly for: 1) review by and the required approval of a peer review panel; 2) review by and the required approval of an authority having jurisdiction over its eventual use; and ultimately 3) use in design and construction. It is recommended that the documentation include at least the following information.

- System information, including but not limited to: intended application and expected performance objective, limitation on *SFRS* use, typical horizontal and vertical geometric configurations, etc.
- Clear and complete design requirements providing sufficient information to quantify strength limit states, proportion and detail the components, analyze the predicted response, and confirm satisfactory behaviour regarding the target *performance level*.
- Summary of test data and other supporting evidence from an experimental investigation program validating material properties and component behaviour, calibrating nonlinear analysis models, and establishing performance *acceptance criteria*.
- Description of *archetype* configurations and extent of the design space.
- Identification of the *performance groups*, applicable seismicity level, and gravity load intensities.

- Information on *archetype* models, including: model configurations, nonlinear modelling parameters, analysis software, model calibration, etc.
- Description of local and global criteria for determining performance points in *archetype* models.
- Details of the selected ground motion set.
- Summary of nonlinear modelling results, demand parameters, and response quantities.
- Description of quality ratings for design requirements, test data, and nonlinear models.
- Summary of performance evaluation results, derived quantities, and *acceptance criteria*.
- Proposed *seismic force modification factors*, i.e., R_d and R_o.

5.8.3 Peer Review Panel

Since the performance evaluation process is primarily done in a research environment, it is essential that details of each step be reviewed by an independent peer review panel. The review should include, but not be limited to, system information, design requirements, testing program and results, selected *archetype* configurations and design, ground motion set, modelling and nonlinear analysis, selection of performance point criteria, and final selection of the proposed R_d and R_o.

The peer review panel is responsible for reporting their expert opinion on the work performed by the development team, their findings, recommendations, and conclusions. If there are any areas where the peer review panel was not satisfied, that information should be made available as part of the peer review documentation and, if possible, reflected in the total uncertainty used in calculating the *acceptance criteria*, and also in determining the final values of the proposed R_d and R_o.

It is recommended that the peer review panel consist of individuals who are familiar with the process of the *PBU procedure* and have sufficient knowledge and experience in material, component and assembly testing, engineering design and construction, seismic hazard and selection of ground motion, and simulation of structural nonlinear behaviour. If a unique computer code is developed by the development team, the peer review panel should be capable of performing independent analyses of the proposed *SFRS* using other analysis platforms.

The peer review panel members need to be selected by the sponsor under supervision of the SC-ED of the NBC. Alternatively, the sponsor can submit funding to the SC-ED, which then uses the funding to implement an independent peer review process.

5.8.4 Submission

It is expected that the sponsor will wish to submit the proposed *SFRS* to an authority for approval and use. In some cases, the proposed *SFRS* could be submitted to the SC-ED, but this committee would normally only accept *SFRSs* similar to *SFRSs* that are already listed in the standard. If a proposed *SFRS* is intended for a single project application, then documentation could be submitted, along with drawings and calculations for the single application, to the authority having jurisdiction over the site where the *SFRS* is being proposed for use.

6 Example Applications

To evaluate the efficiency of the proposed *PBU procedure*, a comprehensive and systematic application study was initiated covering three different materials, namely, concrete, wood, and steel. The application study is performed through a joint collaboration between the Seismic Resilience Team (SRT) of the NRC and several teams from different universities, including:

- University of Ottawa, investigating the reinforced concrete moment-resisting (CMF) systems at two different ductility levels, i.e., conventional construction (CC-CMF) and ductile (D-CMF) systems, see Section 6.1,
- University of Ottawa, investigating the light-frame wood shear wall systems, see Section 6.2,
- University of British Columbia (UBC), investigating the conventional construction RC shear wall systems, see Section 6.3, and
- University of Polytechnique Montréal and McMaster University, jointly investigating the moderately ductile steel concentrically braced frame systems, see Section 6.4.

The detailed procedures for applying the *PBU procedure* to evaluate the current code-specified *seismic force modification factors* (R_d and R_o) for the above-selected *SFRSs* are presented in the following sections. The results of the research outcome are also discussed.

6.1 Reinforced Concrete Moment-resisting Systems

The NBC 2020 provides more than 40 *SFRSs* having different ductility levels to mitigate effects of strong ground motions in Canada. The CC-CMF system is one of the *SFRSs* with the lowest ductility levels and features minimum seismic design requirements. The D-CMF system, on the other hand, has one of the highest ductility levels with maximum seismic design requirements. The ductility-related factor (R_d) and overstrength-related factor (R_o) are set as R_d =1.5 and R_o=1.3 for CC-CMF and R_d=4.0 and R_o=1.7 for D-CMF, which have remained unchanged since the NBC 2005. The seismic performance of these two ductility-level systems is not clearly specified in the NBC and is thus of major concern. Few studies have been conducted to systematically evaluate the seismic performance of the reinforced concrete moment-resisting frames designed with the NBC. For example, a research study was carried out by Fazileh et al. (2022) on the CC-CMF systems based on the FEMA P-695 methodology. The results indicate that the CC-CMF system, which was designed for the Normal *importance category* for the Ottawa and Vancouver seismicity

levels, is able to meet an acceptable margin ratio against the Life Safety *performance level*. However, the conclusion was made upon a limited number of *archetypes* and seismic areas due to the laborious *IDA* step in the FEMA P-695 methodology. Noh and Tesfamariam (2018) performed a collapse risk assessment of both ductile and moderately ductile reinforced concrete frames. However, only four *archetypes* were developed for each ductility category. In this study, the CC-CMF and D-CMF systems were evaluated using the *PBU procedure* to first assess the accuracy of the different steps devised in the procedure, especially the detailed screening step and, second, to evaluate the seismic response of the system and its margin against different *performance levels*.

A total number of 36 reinforced concrete (RC) moment frame *archetypes* were developed covering a wide range of structural configurations (i.e., bay span lengths, number of storeys, seismic categories, and irregularities). These *archetypes* consisted of two different levels of ductility, including 21 CC-CMF *archetypes* and 15 D-CMF *archetypes*. While the primary objective of this investigation was to examine the efficiency of the *PBU procedure*, a quantitative seismic performance assessment of both CC-CMF and D-CMF systems at different *performance levels*, e.g., *IO*, *LS*, and *CP*, was also performed as a secondary objective.

To fulfill the primary objective of this study, the seismic performance evaluation of both CC-CMF and D-CMF *archetypes* was conducted via two different approaches:

1) following the *PBU procedure* ***without*** using its screening feature and directly running full *IDA* on all *archetypes*, and

2) following the *PBU procedure* ***with*** the use of its screening feature to decide on the required analysis procedure for a given *archetype* (i.e., NLTHA or *IDA*).

It is noteworthy that running full *IDA* on all *archetypes* is expected to yield the most accurate results. However, the number of *IDA* runs can grow rapidly with an increase in the number of *archetypes*. The screening feature of the *PBU procedure* has been developed with this challenge in mind, in order to save some *archetypes* (i.e., non-critical) from unnecessary full *IDA* runs.

6.1.1 *Archetype* Development

A six-storey building, as documented in the Canadian concrete design handbook (CAC 2006) is used as the reference building for *archetype* development. As shown in Figure 6-1, all frames in the X-direction have variable span lengths of 5.7 m to 8.0 m. The building's height is 4.5 m for the first storey and 3.5 m for the other storeys. The unfactored gravity loads for this building include dead load (partitions: 1.0 kPa, roofing: 1.0 kPa, mechanical equipment over the 5.7-m span: 1.6 kPa), live loads (4.8 kPa at the first floor and 2.4 kPa at other floors), and snow loads (2.3 kPa at the roof). The distributed gravity loads are applied over the floors and transferred to the frame

beams in the X-direction through the secondary beams aligned in the Y-direction. Therefore, frames in the X-direction carry the major portion of the gravity loads and are selected as the basis for developing the required *archetypes* for seismic performance assessment of both CC-CMF and D-CMF systems.

All *archetypes* developed for both systems are listed in Table 6-1. These *archetypes* are designed per the design requirements in the NBC 2015 (NRC 2015b) and CSA A23.3-14 (CSA 2014b). The *archetype* IDs provided in the table are defined with several key configuration parameters, such as gravity load level, seismic category (SC), geometric variation, and system irregularity. More details about these parameters are provided in the following subsections.

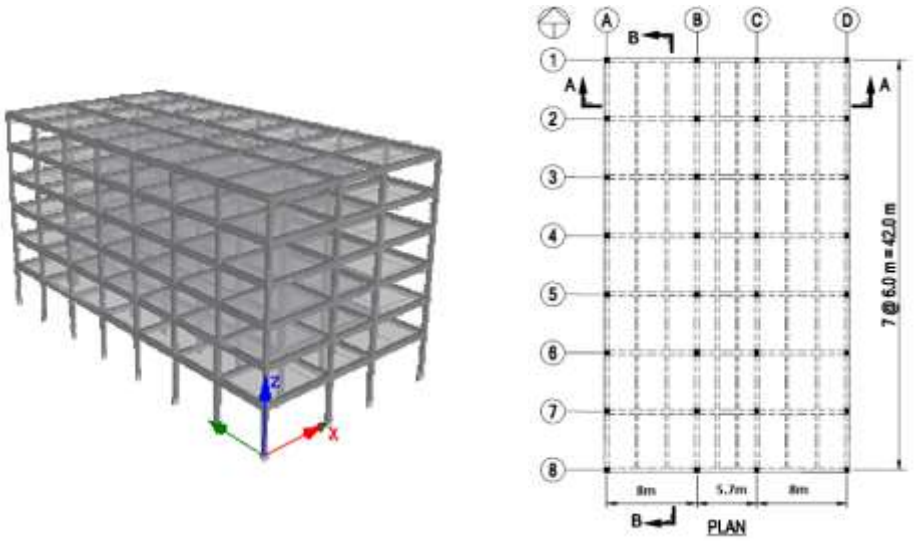

Figure 6-1 Three-dimensional and plan views of the reference building

Table 6-1 CC-CMF and D-CMF *archetypes* developed for performance evaluation

PG #	Bay Length (m)	Gravity Load Level	SC	Irregularity Type	Period Domain	T (sec)	Storeys	Total Height (m)	*Archetype* ID	
									Conv.	Duct.
1	5.7-8	High	3	Regular	Long	0.54	2	8	C-2S3H	
						0.86	4	15	C-4S3H	
						1.14	6	22	C-6S3H	
2	5.7-8	High	4	Regular	Long	0.54	2	8	C-2S4H	D-2S4H
						0.86	4	15	C-4S4H	
						1.14	6	22		D-6S4H
						1.89	12	43		D-12S4H
						2.75	20	71		D-20S4H
3	5.7-8	Low	3	Regular	Long	0.54	2	8	C-2S3L	
						0.86	4	15	C-4S3L	
						1.14	6	22	C-6S3L	
4	5.7-8	Low	4	Regular	Long	0.54	2	8	C-2S4L	D-2S4L
						0.86	4	15	C-4S4L	
						1.14	6	22		D-6S4L
						1.89	12	43		D-12S4L
5	5.5	High	3	Regular	Long	1.14	6	22	C-6S3HB5	
6	5.5	High	4		Long	0.54	2	8	C-2S4HB5	
						1.89	12	43		D-12S4HB5
7	8	High	3	Regular	Long	1.14	6	22	C-6S3HB8	
8	8	High	4		Long	0.54	2	8	C-2S4HB8	
						1.89	12	43		D-12S4HB8
9	5.7-8	High	3/4	Soft Storey	Long	0.61	2	8		D-2S4HS
						0.90	4	16	C-4S3HS	
						1.18[1]	6	23[1]	C-6S3HS	D-6S4HS
						1.94	12	44.5		D-12S4HS
				Weak Storey	Long	0.86	4	15	C-4S3HW	
						1.14	6	22	C-6S3HW	
10	5.7-8	High	3/4	Vertical	Long	0.54	2	8	C-2S3HV	D-2S4HV
						0.86	4	15	C-4S3HV	
						1.14	6	22	C-6S3HV	D-6S4HV
						1.89	12	43		D-12S4HV

6.1.1.1 Gravity Load Level

The gravity load level represents the gravity-to-seismic-load ratio that could significantly affect the seismic response of the system. As presented in Section 5.3.1.3, two gravity levels, i.e., high and low, resulting from different framing layouts could effectively incorporate the upper and lower bounds of the system's response. Therefore, the space frame selected from the X-direction interior frames of the reference building is used to represent the high gravity load level with a gravity-to-seismic-load ratio of 1.0, as shown in Figure 6-2(a). To account for the low gravity load level, the framing layout of the reference building is modified by decreasing the floor plan dimensions to 21.7 m × 24 m. Then the lateral resisting frame at the perimeter as shown in Figure 6-2(b) is considered the low-gravity frame with a gravity-to-seismic-load ratio of 0.25. As shown in Table 6-1, "H" and "L" included in the *archetype* ID represent the high and low gravity load levels, respectively.

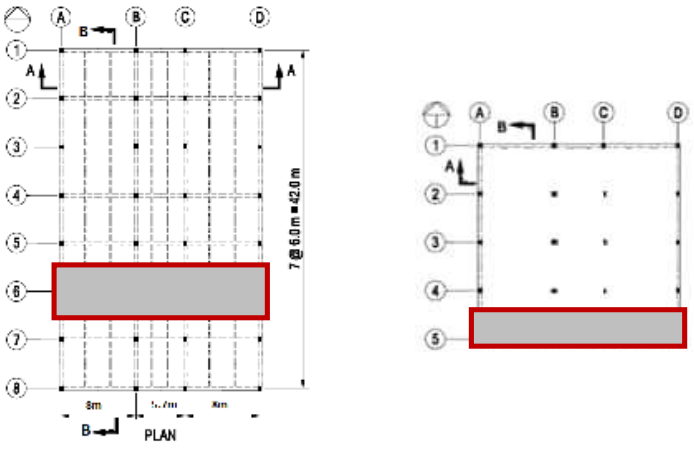

(a) Space frame (b) Perimeter frame

Figure 6-2 High and low gravity levels considered, using different framing layouts

6.1.1.2 Seismic Level

The seismic areas in Canada are divided into four different seismic categories based on the design ground motion spectral acceleration values at the periods of 0.2 sec and 1.0 sec, as shown in Table 5-3. As suggested in Section 5.3.1.6, it is sufficient to evaluate the *SFRS* for the highest seismic level permitted. Therefore, High (SC4) shown in Table 5-3 is used to develop the D-CMF *archetypes*. However, both High (SC4) and Moderately High (SC3) are considered for the CC-CMF *archetypes* to cover all possible configurations due to the height limits indicated in the NBC for CC-CMF systems with different seismic categories.

Based on Table C-3 of the NBC 2015, Ucluelet and Squamish are selected as the seismic sites to represent the upper bound spectra of SC4 and SC3, respectively. As shown in Table 6-1, "S4" and "S3" included in the *archetype* ID represent the High (SC4) and Moderately High (SC3) seismic categories, respectively.

6.1.1.3 Geometric Variation

As discussed in Section 5.3.1.1, different configurations of the RC moment frames within the code-permitted range are required in the performance evaluation process. Therefore, in addition to the original layout of the reference building, the frame is further modified to have equal span lengths as shown in Figure 6-3. Given the maximum heights indicated in the NBC for different seismic categories, the number of storeys is also modified to create frames with different heights and fundamental periods. A two-storey frame with a total height of 8.0 m is selected as the shortest frame considered in this study, applicable to both SC3 and SC4 for CC-CMF and D-CMF. The

NBC limits the application of the CC-CMF *archetypes* to 10.0 m and 20.0 m in SC4 and SC3, respectively. So, the two-storey (8.0 m) and four-storey (15.0 m) frames are the tallest frames allowed in these seismic categories. The number of storeys was further increased to four (15 m) and six (22 m) to study the behaviour of the CC-CMF beyond the specified height limits, as shown in Figure 6-4. Note that the NBC does not provide any height limits for D-CMF, therefore *archetypes* with different numbers of storeys up to 20 (71m) were defined for this ductility level. The empirical fundamental periods of models with different numbers of storeys and heights according to the NBC vary from 0.54 to 1.14 sec for CC-CMF and 0.54 to 2.75 sec for D-CMF *archetypes*.

As shown in Table 6-1, the last digits "5" and "8" of the *archetype* ID represent frames with equal span lengths of 5 m and 8 m, respectively. The number of storeys is indicated right after the dash sign in the *archetype* ID.

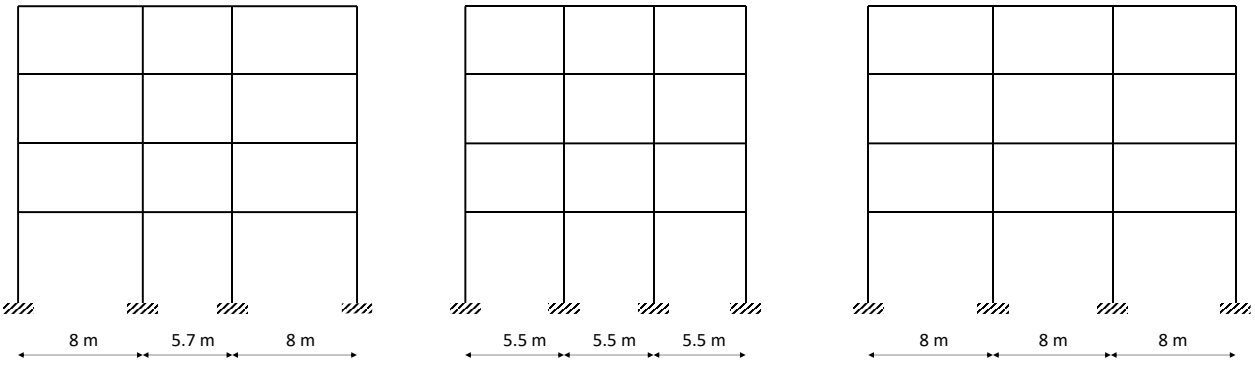

Figure 6-3 Different bay lengths considered in the study

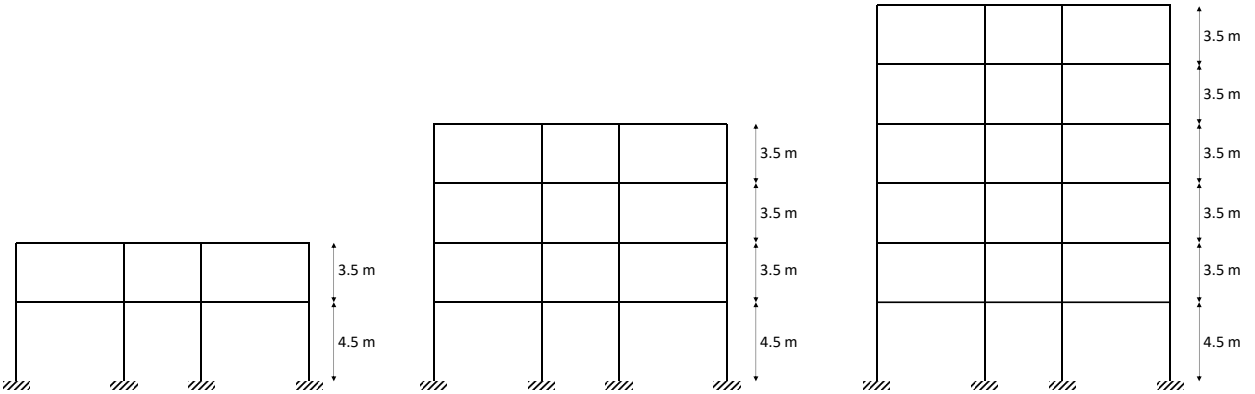

Figure 6-4 Different number of storeys considered in the study

6.1.1.4 System Irregularity

According to Section 5.3.1.2, three out of six vertical irregularities in the NBC 2015 are considered, including vertical stiffness irregularity (soft storey), discontinuity in capacity irregularity (weak storey), and vertical geometric irregularity.

The weak storey irregularity is defined by the NBC where the storey shear strength is less than that in the storey above. Since all the frames in this study comply with the NBC, reducing the storey capacity to less than that required for the design is not possible. Therefore, the irregularity is created by increasing the capacity of the second-storey columns (such as 4S3HW and 6S3HW), while keeping the cross-sections the same as in the regular models. The ratio of first-storey-to-second-storey capacities is decreased to about 80% using this approach. Note that the weak storey irregularity is only considered for the CC-CMF *archetypes*.

To create models with vertical geometric irregularity, the storey dimension is decreased gradually by reducing the number of bay spans in the upper storeys, as shown in Figure 6-5. As per the NBC, this type of irregularity is triggered when the horizontal dimensions of the *SFRS* in any storey are more than 130% of that in an adjacent storey.

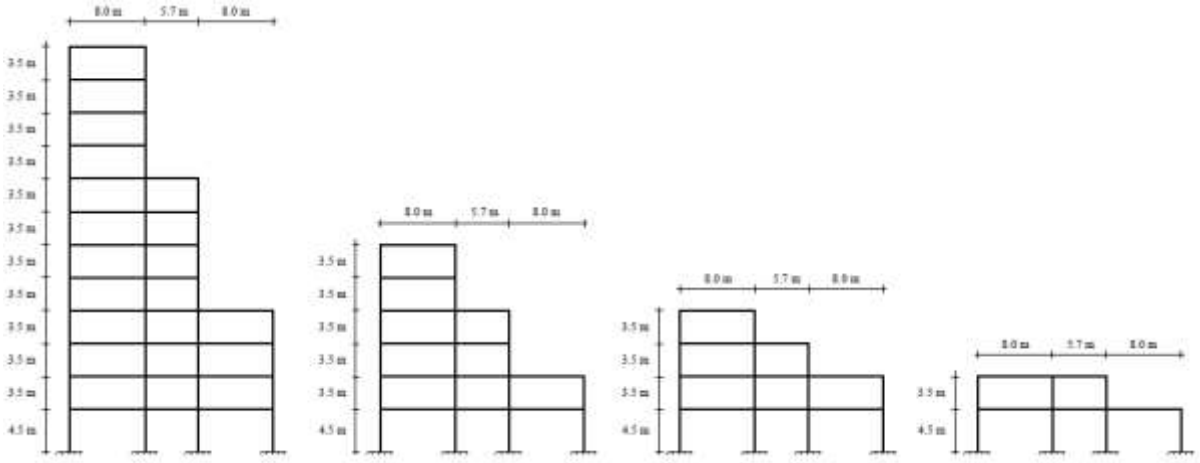

Figure 6-5 Vertical geometric irregularity in two-, four-, and six-storey frames

6.1.2 *Archetype* Modelling

According to Section 5.4, the lumped plasticity modelling approach (uniaxial spring hinge model), as suggested by FEMA P-695 and NIST GCR 17-917-46, is used in this study to model the responses of the *archetypes* developed with the OpenSees software (McKenna et al. 2010), as illustrated in Figure 6-6. In each numerical model, the beams and columns of the frame are modelled using the "elasticBeamColumn" elements, and the section nonlinearity is simulated through lumped springs attached to the ends of the elements. The nonlinear response of each spring

is described by the "MModIMKPeakOriented" uniaxial material model, referred to as IMK hereinafter. In addition, the P-Δ effects due to the gravity loads of the *SFRS* and the weights transferring from the interior gravity frames are taken into account by including leaning columns as shown in Figure 6-6.

The parameters in the IMK model were calculated using empirical equations calibrated from experimental data (Haselton and Deierlein 2007, ATC 2009, 2017a). The model is expected to simulate the degradations associated with flexural and flexural-shear failure modes as the experimental database used for the calibration including elements having both types of behaviour (Liel 2008). To account for all sources of the flexibility before yielding, including shear, flexure and bond-slip, the effective elastic stiffness of the frame members was also calculated by the empirical equations and assigned to the end springs. The flexibility of the elastic elements (beams and columns) was therefore adjusted to preserve the lateral stiffness of the members.

The beam-column connections were modelled using Joint2D elements with the "ModIMKPinching" uniaxial material model to account for the finite joint size as well as the elastic and inelastic responses of the joint. The nonlinear behaviour of the joints was calculated and assigned as recommended by (Liel 2008).

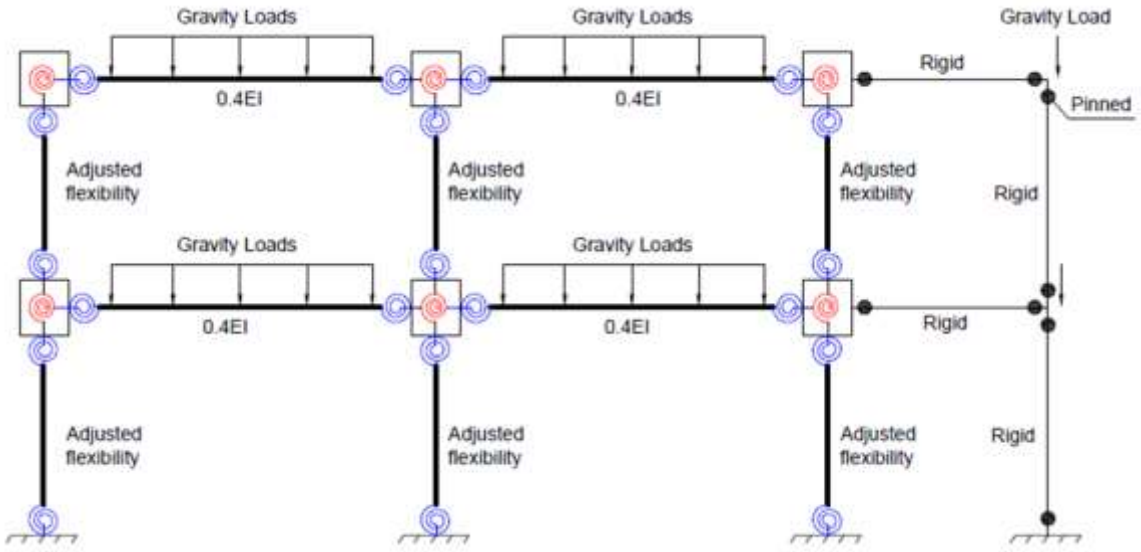

Figure 6-6 Nonlinear frame model in OpenSees

The above modelling approach was verified against three experimental studies: specimen BG6 by Saatcioglu and Grira (Saatcioglu and Grira 1999) and specimens U3 and U4 by Saatcioglu and Ozcebe (Saatcioglu and Ozcebe 1989). The specimens were modelled and analyzed for lateral displacement-controlled quasi-static loading protocols. The IMK backbone curve assigned to the models (black dashed line) and cyclic results (red dashed line) are provided in Figure 6-7. The

results show that the modelling approach has acceptable accuracy in estimating initial stiffness, yielding, strain hardening, cyclic and in-cycle deteriorations, etc.

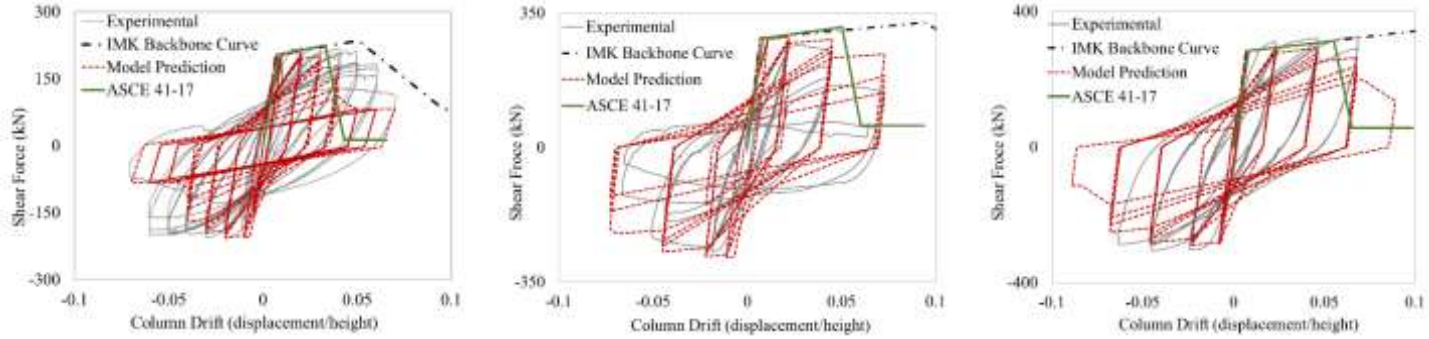

(a) (b) (c)

Figure 6-7 Verification examples: a) specimen BG-6, b) specimen U3, and c) specimen U4

6.1.3 Nonlinear Analysis

6.1.3.1 Performance Criteria

Commentary J of the NBC 2015 defines the *performance objective* of buildings with the Normal *importance category* as somewhere between *LS* and *CP*. The *LS* was conservatively selected in this study for the performance evaluation of the CC-CMF and D-CMF systems, for which performance objectives were quantified through different local and global performance criteria. Other *performance levels*, such as *IO* and *CP*, were also assessed for comparison.

As one of the global performance criteria for both static pushover and time history analyses in the following sections, drift ratios of 1.0%, 2.5%, and 4.0% were selected for the *IO*, *LS*, and *CP* performance objectives, respectively. The 1.0% and 2.5% drift ratios were selected as per design requirements in the NBC 2020 for Post-disaster and Normal importance buildings, respectively. The 4.0% drift is considered the onset of strength degradation in the CC-CMF *archetypes* based on experimental observations by Khosravi (Khosravi 2021). On the other hand, no global drift limit was used for the D-CMF *archetypes*.

ASCE 41 (ASCE 2017b) defines backbone curves for nonlinear responses of different structural components and recommends plastic hinge rotation limits at different *performance levels*. The hinge rotation limits corresponding to the *performance levels* of *IO*, *LS* and *CP* were selected for beams, columns, and joints as the local performance criteria for both nonlinear static and dynamic analyses. For example, the ASCE 41 backbone curves were also developed for the verification specimens in Section 6.1.2, as shown in Figure 6-7 (solid green line). According to the figure, the capping rotations, which are defined as plastic rotations with significant loss of lateral force

capacity, are close to the 20% drop in lateral capacity of the specimens calculated by the IMK model (dashed red line). Moreover, other nonlinear factors, including initial stiffness and yield rotations are close to those of the IMK model.

6.1.3.2 Pushover Analysis

Following the *PBU procedure* as described in Figure 5-1, the pushover analysis was first performed for all developed *archetypes* to calculate the required parameters of R_o and μ_T as well as assess the nonlinear behaviour of the *archetypes* before further time history analyses.

The pushover analysis results are provided in Table 6-2, along with the fundamental periods of the *archetypes* computed using eigenvalue analysis, T_1. As presented in Section 5.5.1, R_o for each *archetype* was calculated as the maximum base shear from the pushover analysis (V_{max}) divided by the design base shear (V_d). The average of the R_o values of the *archetypes* within each *PG* was calculated, and the system's overstrength value was taken as the minimum of the average values of all *PG*s, i.e., R_o=1.55 for CC-CMF and R_o=1.71 for D-CMF. The calculated overstrength value is 20% larger than the NBC recommended value (i.e., 1.3) for CC-CMF and is almost the same as that recommended for D-CMF in the NBC, i.e., 1.7.

To calculate the period-based ductility factor, the ultimate roof displacement δ_u for each *performance level* was defined as the roof displacement where the first local criterion (i.e., ASCE 41 hinge rotation limit) was met, while not exceeding the roof displacement corresponding to the inter-storey drift ratio of 4.0% (i.e., the global criterion for CC-CMF only). The effective roof displacement ($\delta_{y,eff}$) was calculated based on Eq. (5.7). The calculated μ_T values for LS are provided in Table 6-2. The period-based ductility factors for other *performance levels* were also computed and used later for the performance evaluation.

Table 6-2 Overstrength factors and period-based ductility factors for *LS*

PG #	Conventional Model	T_1 (sec)	$\mu_{T\text{-}LS} = \delta_{u\text{-}LS}/\delta_{y,eff}$ (m)	$R_o = V_{max}/V_d$ (kN)	Ductile Model	T_1 (sec)	$\mu_{T\text{-}LS} = \delta_{u\text{-}LS}/\delta_{y,eff}$ (m)	$R_o = V_{max}/V_d$ (kN)
1	C-2S3H	0.73	3.82 = 0.27/0.07	1.79 = 887/495				
	C-4S3H	1.12	3.00 = 0.36/0.12	1.66 = 1177/711				
	C-6S3H	1.42	2.28 = 0.35/0.16	1.57 = 1332/850				
Average:				**1.67**				
2	C-2S4H	0.49	3.27 = 0.27/0.08	1.67 = 2451/1,466	D-2S4H	0.64	4.23 = 0.26/0.06	2.65 = 1027/388
	C-4S4H	0.58	2.61 = 0.33/0.12	1.79 = 5378/3,011	D-6S4H	1.15	5.08 = 0.58/0.12	2.20 = 1579/717
					D-12S4H	1.67	5.75 = 0.84/0.15	1.85 = 1950/1055
					D-20S4H	2.27	5.96 = 1.35/0.23	1.62 = 3046/1880
Average:				**1.73**				**2.08**
3	C-2S3L	0.85	3.51 = 0.28/0.08	1.54 = 2120/1369				
	C-4S3L	1.07	2.79 = 0.31/0.11	1.62 = 3291/2035				
	C-6S3L	1.40	2.24 = 0.36/0.16	1.64 = 4033/2454				
Average:				**1.60**				
4	C-2S4L	0.46	3.73 = 0.27/0.07	1.76 = 7302/4158	D-2S4L	0.64	5.86 = 0.25/0.04	1.76 = 1890/1072
	C-4S4L	0.48	3.26 = 0.31/0.10	1.82 = 15656/8612	D-6S4L	1.14	6.23 = 0.55/0.09	1.68 = 3479/2069
					D-12S4L	1.69	5.60 = 0.76/0.14	1.69 = 4980/2943
Average:				**1.79**				**1.71**
5	C-6S3HB5	1.48	2.53 = 0.40/0.16	1.55 = 973/629				
Average:				**1.55**				
6	C-2S4HB5	0.50	3.38 = 0.28/0.08	1.71 = 1904/1112	D-12S4HB5	1.71	5.67 = 0.87/0.15	1.71 = 1486/871
Average:				**1.71**				**1.71**
7	C-6S3HB8	1.37	2.11 = 0.33/0.16	1.66 = 1575/949				
Average:				**1.66**				
8	C-2S4HB8	0.49	3.85 = 0.30/0.08	1.72 = 2817/1641	D-12S4HB5	1.74	6.60 = 1.04/0.16	1.83 = 2263/1237
Average:				**1.72**				**1.83**
9	4S3HS	1.29	2.63 = 0.39/0.15	1.62 = 1110/683	D-2S4HS	0.78	3.75 = 0.32/0.09	2.72 = 1051/386
	6S3HS	1.52	2.32 = 0.41/0.18	1.66 = 1395/842	D-6S4HS	1.29	4.02 = 0.57/0.14	2.17 = 1611/743
	4S3HW	1.12	3.28 = 0.39/0.12	1.67 = 1184/711	D-12S4HS	1.80	4.71 = 0.76/0.16	1.85 = 1901/1030
	6S3HW	1.42	2.70 = 0.42/0.16	1.56 = 1329/850				
Average:				**1.63**				**2.25**
10	2S3HV	0.71	3.81 = 0.29/0.08	1.90 = 776/409	D-2S4HV	0.60	4.35 = 0.29/0.07	3.08 = 991/322
	4S3HV	1.02	4.81 = 0.53/0.11	1.65 = 691/419	D-6S4HV	1.13	6.81 = 0.66/0.10	1.86 = 964/517
	6S3HV	1.36	3.39 = 0.51/0.15	1.50 = 838/558	D-12S4HV	1.60	7.44 = 1.13/0.15	1.59 = 1348/848
Average:				**1.68**				**2.18**

6.1.3.3 Screening

The static pushover analyses were followed by the detailed screening process as described in Section 5.5.3. The far-fault record set (44 records) suggested in FEMA P-695 was used for the time history analysis in this application example.

According to the flowchart for screening shown in Figure 5-14, the *archetypes* in each *PG* were first analyzed by ground motions scaled by 2.16, and the number of records resulting in demands within the acceptable range (Rec_p) for *LS* are provided in Table 6-3. The acceptable range was defined based on the local and global *LS* performance criteria, as presented in Section 6.1.3.1. By comparing the number of records in the acceptable range with the total number of records for each *archetype*, it can be noted that all the CC-CMF *archetypes* in *PG* #1, #3, #5, and #10 passed the

screening for the first scale factor. Therefore, these *PG*s were identified as non-critical (NC) *PG*s, and no *IDA* analysis was required. All D-CMF *archetypes*, on the other hand, failed the screening for the first scale factor.

The *PG*s that failed the screening for the first scale factor were further analyzed with ground motions scaled by 2.54. As shown in Table 6-3, the number of passing *archetypes* (N_p) in *PG* #9 is 3, which is larger than half of the number of *archetypes* in this *PG*, i.e., $N_t/2 = 2$. Therefore, only the failed *archetype* C-6S3HS in *PG* #9 was considered NC for further *IDA* evaluation. Since all the other critical (C) CC-CMF *PG*s identified from the screening for the first scale factor also failed the screening for the second scale factor, they were sent to the *IDA*. The results provided for D-CMF show that all the *archetypes* failed to satisfy the screening criteria and thus required further *IDA*. Compared with FEMA P-695, which requires *IDA* for all *archetypes*, the *PBU procedure* screened 13 CC-CMF *archetypes* out from *IDA*.

Table 6-3 Detailed *archetype* screening results for *LS*

PG	Conventional *Archetypes*				Ductile *Archetypes*			
	Model	$APMR_{10\%}$ (2.16×DGM) Rec_p	$APMR_{6\%}$ (2.54×DGM) Rec_p	Status	Model	$APMR_{10\%}$ (2.16×DGM) Rec_p	$APMR_{6\%}$ (2.54×DGM) Rec_p	Status
1	C-2S3H C-4S3H C-6S3H	40 (Pass) 39 (Pass) 32 (Pass)		NC				
2	C-2S4H C-4S4H	15 (Fail) 21 (Fail)	17 (Fail) 13 (Fail)	C	D-2S4H D-6S4H D-12S4H D-20S4H	16 (Fail) 6 (Fail) 2 (Fail) 1 (Fail)	9 (Fail) 1 (Fail) 0 (Fail) 0 (Fail)	C
3	C-2S3L C-4S3L C-6S3L	37 (Pass) 28 (Pass) 23 (Pass)		NC				
4	C-2S4L C-4S4L	22 (Pass) 4 (Fail)	15 (Fail) 3 (Fail)	C C	D-2S4L D-6S4L D-12S4L	5 (Fail) 2 (Fail) 0 (Fail)	2 (Fail) 0 (Fail) 0 (Fail)	C
5	C-6S3HB5	25 (Pass)		NC				
6	C-2S4HB5	19 (Fail)	12 (Fail)	C	D-12S4HB5	2 (Fail)	1 (Fail)	C
7	C-6S3HB8	21 (Fail)	12 (Fail)	C				
8	C-2S4HB8	21 (Fail)	16 (Fail)	C	D-12S4HB5	2 (Fail)	1 (Fail)	C
9	C-4S3HS C-6S3HS C-4S3HW C-6S3HW	36 (Pass) 20 (Fail) 38 (Pass) 32 (Pass)	31 (Pass) 16 (Fail) 32 (Pass) 24 (Pass)	NC[1]	D-2S4HS D-6S4HS D-12S4HS	14 (Fail) 6 (Fail) 1 (Fail)	6 (Fail) 4 (Fail) 0 (Fail)	C
10	C-2S3HV C-4S3HV C-6S3HV	37 (Pass) 26 (Pass) 24 (Pass)		NC	D-2S4HV D-6S4HV D-12S4HV	10 (Fail) 0 (Fail) 5 (Fail)	5 (Fail) 0 (Fail) 2 (Fail)	C

[1] *IDA* analysis is only required for C-6S3HS

6.1.3.4 IDA

The identified critical *archetypes* were then sent to the *IDA* to develop the full *IDA* curves and compute the *PMR* values. For each of the 44 ground motion records, the spectral intensity was

scaled up until the predicted structural response exceeded the local and/or global *LS* performance criteria, as described in Section 6.1.3.1. For each ground motion record, the intensity at which the first performance criterion met was recorded. Then the median intensity at the *LS performance level* ($\hat{S}_{PT-LS}$) was determined for the *archetype*. As shown in Table 6-4, the *PMRs* for *LS* (PMR_{LS}) were calculated as $\hat{S}_{PT-LS}/S_{DT}$, where S_{DT} is the spectral acceleration of the design ground motion. It should be noted that the PMR_{LS} value for an NC *archetype* was conservatively assumed to be equal to the scale factor used in the screening process, either 2.16 or 2.54, from which the *archetype* was identified as passed.

Table 6-4 Performance evaluation results for *LS*

PG	Conventional *Archetypes*				Ductile *Archetypes*			
	Model	PMR_{LS}	*SSF*	*APMR* (*LS* > Acceptable)	Model	PMR_{LS}	*SSF*	$APMR_{LS}$
1	C-2S3H	2.16	1.12	2.42 > 1.66 : OK				
	C-4S3H	2.16	1.15	2.48 > 1.66 : OK				
	C-6S3H	2.16	1.16	2.51 > 1.66 : OK				
Average				**2.47 > 2.16 : OK**				
2	C-2S4H	1.98	1.19	2.36 > 1.62 : OK	D-2S4H	1.97	1.25	2.47 > 1.52 : OK
	C-4S4H	2.03	1.17	2.38 > 1.62 : OK	D-6S4H	1.25	1.38	1.73 > 1.52 : OK
					D-12S4H	1.11	1.50	1.66 > 1.52 : OK
					D-20S4H	0.96	1.51	1.45 < 1.52 : NG
Average				**2.37 > 2.09 : OK**				**1.83 < 1.90 : NG**
3	C-2S3L	2.16	1.13	2.44 > 1.66 : OK				
	C-4S3L	2.16	1.14	2.46 > 1.66 : OK				
	C-6S3L	2.16	1.15	2.48 > 1.66 : OK				
Average				**2.46** > 2.16 : OK				
4	C-2S4L	1.75	1.21	2.12 > 1.62 : OK	D-2S4L	1.49	1.30	1.94 > 1.52 : OK
	C-4S4L	1.69	1.19	2.01 > 1.62 : OK	D-6S4L	1.06	1.43	1.52 = 1.52 : OK
					D-12S4L	0.92	1.49	1.37 < 1.52 : NG
Average				**2.06 ≈ 2.09 : OK**[1]				**1.61 < 1.90 : NG**
5	C-6S3HB5	2.16	1.18	2.55 > 1.66 : OK				
Average				**2.55 > 2.16 : OK**				
6	C-2S4HB5	1.88	1.20	2.25 > 1.62 : OK	D-12S4HB5	1.21	1.49	1.81 > 1.52 : OK
Average				**2.25 > 2.09 : OK**				**1.81 < 1.90 : NG**
7	C-6S3HB8	1.93	1.14	2.21 > 1.56 : OK				
Average				**2.21 > 1.96 : OK**				
8	C-2S4HB8	1.99	1.21	2.42 > 1.62 : OK	D-12S4HB5	1.23	1.54	1.89 > 1.52 : OK
Average				**2.42 > 2.09 : OK**				**1.89 < 1.90 : NG**
9	C-4S3HS	2.54	1.16	2.95 > 1.66 : OK	D-2S4HS	1.60	1.25	2.01 > 1.52 : OK
	C-6S3HS	2.28	1.17	2.67 > 1.59 : OK	D-6S4HS	1.18	1.36	1.60 > 1.52 : OK
	C-4S3HW	2.54	1.16	2.95 > 1.66 : OK	D-12S4HS	1.10	1.44	1.58 > 1.52 : OK
	C-6S3HW	2.54	1.18	3.00 > 1.66 : OK				
Average				**2.89 > 2.16 : OK**				**1.73 < 1.90 : NG**
10	C-2S3HV	2.16	1.12	2.42 > 1.66 : OK	D-2S4HV	1.69	1.25	2.11 > 1.52 : OK
	C-4S3HV	2.16	1.19	2.57 > 1.66 : OK	D-6S4HV	1.32	1.43	1.88 > 1.52 : OK
	C-6S3HV	2.16	1.20	2.59 > 1.66 : OK	D-12S4HV	1.25	1.58	1.98 > 1.52 : OK
Average				**2.53 > 2.16 : OK**				**1.99** > 1.90 : OK

[1]The $APMR_{LS}$ was considered acceptable because the difference between the calculated and acceptable values is less than 1.4%. It can be noted that the status of the archetype and performance group were flagged as "OK" if the above criteria were satisfied. Otherwise, the archetype and performance group were flagged as "NG".

6.1.4 Performance Evaluation

According to Section 5.7, the performance evaluation involves a comparison of the computed *PMR* value with the corresponding *acceptable APMR*. The *acceptable APMRs* for each *archetype* and each *PG* are determined based on the total uncertainty, β_{TOT}, and the conditional exceedance probabilities of 10% and 20%, respectively. Before the comparison, the computed *PMRs* need to be adjusted by the *SSF* to calculate the *APMRs*. The *APMRs* are compared with the acceptable *APMRs* for each *archetype* as well as the average of each *PG*.

6.1.4.1 Uncertainty Sources

According to Section 5.6, β_{TOT} was determined with the following assumptions for different uncertainty sources:

- Design requirement uncertainty, β_{DR}: The gravity and seismic design requirements available in CSA A23.3-14 and the NBC 2015 were used in this study, which reflect many years of development and include lessons learned from a number of major earthquakes. Therefore, the design requirement uncertainty was categorized as (A) Superior with an uncertainty value of $\beta_{DR} = 0.1$.
- Test data uncertainty, β_{TD}: The code design requirements as well as the nonlinear models used in this application study relied on the existing test data of beams and columns reported in the Pacific Earthquake Engineering Research Center's Structural Performance Database developed by Berry, Parrish, and Eberhard (Berry et al. 2004). The database covers a wide range of column design configurations and contains both monotonic and cyclic loading protocols. However, limited test data is available for collapse and post-peak behaviour of the elements. Therefore, the test data uncertainty was categorized as (B) Good with an uncertainty value of $\beta_{TD} = 0.2$.
- Modelling uncertainty, β_{MDL}: Although the modelling approach used in this application study can accurately simulate the global inelastic behaviour of the moment frame components, there is still room for improved modelling by considering the P-M-M interaction, incorporating non-simulated responses for CC-CMF *archetypes*, etc. Therefore, the modelling uncertainty was categorized as (B) Good with $\beta_{MDL} = 0.2$ for D-CMF and (C) Fair with $\beta_{MDL} = 0.35$ for CC-CMF.
- *Record-to-record uncertainty*, β_{RTR}: Since the record set suggested by FEMA P-695 was used, β_{RTR} was calculated as $\beta_{RTR} = 0.1 + 0.1\mu_T \leq 0.4$.

According to Eq. (5.13), the total uncertainty was computed and then used to determine the *acceptable APMRs* as shown in Table 6-4.

6.1.4.2 Adjusted Performance Margin Ratios

According to Section 5.7.3, the calculated *PMRs* were adjusted to incorporate the *spectral shape effects* by applying the *SSF*. In this study, the *SSF* was estimated based on the relationship between the *SSF* and the values of structural period and period-based ductility, as derived in FEMA P-695. The *SSF* values for both CC-CMF and D-CMF are provided in Table 6-4.

6.1.4.3 Evaluation Results

It can be noted from Table 6-4 that all the CC-CMF *archetypes* and their *PG*s represent adequate *APMRs* and the system passes the performance evaluation requirements for *LS*, while some of the D-CMF and *PG*s do not show adequate *APMRs* and the system does not pass the requirements for *LS*. Note that the average *APMR* in *PG* #4 of CC-CMF is only 2% less than the acceptable value, while the individual *archetypes* represent at least 24% larger *APMRs*, so the *PG* is considered as passed. The conservative response for the CC-CMF could be attributed to the evolving seismic design requirements over time in CSA A23.3 towards more stringency for conventional construction, which are expected to be required for a system with higher ductility levels;

In addition to *LS*, the *APMRs* with respect to other *performance levels*, such as *IO* and *CP*, were also calculated for both CC-CMF and D-CMF *archetypes* by following the same procedure as presented above. More details can be found in the final report #A1-018030 (Fazileh et al. 2023b). Table 6-5 and Figure 6-5 provide the *APMR* values for different *performance levels*. It can be noted that the CC-CMF *archetypes* represent higher margin ratios than D-CMF systems in all *performance levels*. The CC-CMF *archetypes* failed to achieve *IO,* but exhibited a considerable margin for *CP*. Although they failed to achieve *IO* and *LS*, the D-CMF *archetypes* could achieve *CP*. It could be concluded that the existing design requirements for the RC moment frames result in a *performance level* between *LS* and *CP*.

Table 6-5 *IDA* results for CC-CMF *archetypes*

PG	Model	*APMR*				Acceptable *APMR*
		IO	*LS*	*CP*	Global collapse	
1	C-2S3H	1.66	4.04	4.52	4.52	1.62
	C-4S3H	1.39	3.76	4.14	4.14	1.62
	C-6S3H	0.96	3.25	3.69	3.69	1.59
	PG	1.33	3.68	4.12	4.12	2.09
2	C-2S4H	1.05	2.36	2.63	2.68	1.62
	C-4S4H	0.96	2.38	2.59	2.78	1.62
	PG	1.01	2.37	2.61	2.73	2.09
3	C-2S3L	1.61	3.90	4.37	4.37	1.62
	C-4S3L	1.39	2.76	3.35	3.56	1.62
	C-6S3L	1.16	2.28	2.58	3.20	1.59
	PG	1.39	2.98	3.43	3.71	2.09
4	C-2S4L	1.00	2.12	2.14	2.14	1.62
	C-4S4L	1.15	2.01	2.18	2.46	1.62
	PG	1.07	2.06	2.16	2.30	2.09
5	C-6S3HB5	1.40	3.64	3.18	3.18	1.62
	PG	1.40	3.64	3.18	3.18	2.09
6	C-2S4HB5	1.09	2.25	2.34	2.34	1.62
	PG	1.09	2.25	2.34	2.34	2.09
7	C-6S3HB8	0.99	2.21	2.54	2.90	1.56
	PG	0.99	2.21	2.54	2.90	1.96
8	C-2S4HB8	1.00	2.42	2.55	2.55	1.62
	PG	1.00	2.42	2.55	2.55	2.09
9	C-4S3HS	1.32	3.98	3.71	3.71	1.59
	C-6S3HS	1.11	2.67	3.02	3.02	1.59
	C-4S3HW	1.40	3.85	4.26	4.26	1.62
	C-6S3HW	0.96	3.22	3.63	3.63	1.62
	PG	1.20	3.43	3.65	3.65	2.09
10	C-2S3HV	1.62	3.86	3.85	3.85	1.62
	C-4S3HV	1.24	2.98	3.10	3.15	1.62
	C-6S3HV	1.08	2.52	3.05	3.05	1.62
	PG	1.31	3.12	3.33	3.35	2.09

Table 6-6 *IDA* results for D-CMF *archetypes*

PG	Model	*APMR*				Acceptable *APMR*
		IO	*LS*	*CP*	Global collapse	
1	D-2S4H	0.75	2.47	3.15	3.16	1.52
	D-6S4H	0.60	1.73	2.86	3.43	1.52
	D-12S4H	0.67	1.66	2.51	3.24	1.52
	D-20S4H	0.60	1.45	2.33	2.70	1.52
	PG	0.65	1.83	2.71	3.13	1.9
2	D-2S4L	0.71	1.94	2.83	3.82	1.52
	D-6S4L	0.48	1.52	2.46	3.39	1.52
	D-12S4L	0.54	1.37	2.13	2.69	1.52
	PG	0.58	1.61	2.47	3.30	1.9
3	D-12S4HB5	0.71	1.81	2.50	3.24	1.52
	PG	0.71	1.81	2.50	3.24	1.9
4	D-12S4HB8	0.67	1.89	2.74	3.36	1.52
	PG	0.67	1.89	2.74	3.36	1.9
5	D-2S4HS	0.76	2.01	2.79	2.99	1.52
	D-6S4HS	0.56	1.60	2.80	3.00	1.52
	D-12S4HS	0.61	1.58	2.40	2.95	1.52
	PG	0.64	1.73	2.66	2.98	1.9
6	D-2S4HV	0.73	2.11	2.27	2.27	1.52
	D-6S4HV	0.74	1.88	2.82	3.51	1.52
	D-12S4HV	0.90	1.98	2.82	3.70	1.52
	PG	0.79	1.99	2.64	3.16	1.9

6.1.5 Iteration: Adjustment of R_d

As presented above, the use of the code-specified values for the seismic design of conventional construction RC moment frames (i.e., $R_d = 1.5$ and R_o = 1.3) resulted in an acceptable *PMR* for the *performance level* of *LS* and a considerable margin against the objective of *CP*. The results indicate the potential of using a higher value of $R_d R_o$ for the seismic design of the system. As shown in Table 6-5, the lower margin ratios for the *archetypes* came from those designed with a low gravity load level and a high seismic load level (SC4). Therefore, *PG* 4 with the lowest margin ratio is considered the critical *performance group* and selected in this section. Specifically, a new set of R_d and R_o values, i.e., R_d = 2.0 and R_o = 1.3, is assumed to evaluate its potential applicability for future seismic design.

With the above assumption of R_d and R_o, the two *archetypes* in *PG* 4 are redesigned as per CSA A23.3-14 for further performance evaluation. A larger R_d implies a higher ductility of the system, which could require more stringent seismic design requirements to obtain the expected ductility. To also account for the influence of the design detailing on the seismic performance, the following two design cases representing different ductility levels are considered:

- Case 1: Seismic design requirements as per Section 21.8 of CSA A23.3-14. This case represents the current design practice for conventional construction RC moment frames.
- Case 2: Seismic design requirements as per Section 21.7 of CSA A23.3-14 for moderately ductile RC moment frames. This case represents more stringent design detailing than Case 1.

With the newly designed *archetypes*, the same modelling approaches and performance criteria as described in Sections 6.1.2 and 6.1.3.1 are used for the following nonlinear analyses and performance assessments.

6.1.5.1 Pushover

Pushover analysis was first performed, and the computed R_o and μ_T factors for different *performance levels* are provided in Table 6-7. It can be noted that the computed R_o of the two *archetypes* were both greater than 1.3 specified in the current NBC. In addition, larger values of R_o and μ_T were obtained for Case 2 *archetypes,* which implied the benefits of higher detailing requirements for both peak strength and ductility.

Table 6-7 Pushover analysis results for $R_d = 2.0$

Design Case	Model	Period	Overstrength					Period-based ductility		
		T (sec)	V_{max}	V_d	R_o (Model)	R_o (Code)	Status	μ_{T-IO}	μ_{T-LS}	μ_{T-CP}
Case 1	C-2S4L	0.46	5532	3119	1.77	1.30	OK	1.13	2.64	3.23
	C-4S4L	0.54	11108	6294	1.76	1.30	OK	1.31	2.36	2.92
Case 2	C-2S4L	0.46	5687	3119	1.82	1.30	OK	1.53	2.73	3.32
	C-4S4L	0.54	11529	6294	1.83	1.30	OK	1.44	2.56	3.17

Where, V_{max} is the maximum base shear predicted from the OpenSees model; μ_{T-IO}, μ_{T-LS}, and μ_{T-CP} are period-based ductility with respect to *IO*, *LS*, and *CP performance levels*. The *archetype* was flagged as "OK" if the computed R_o was no less than 1.3 as specified in the code.

6.1.5.2 *Archetype* Screening

Following the same procedure as presented in Section 6.1.3.3, the screening results for the redesigned *archetypes* are shown in Table 6-8. It can be noted that no greater than 10 ground motions passed the two screening factors (i.e., 2.16 and 2.54) for the two *archetypes* of both design

cases. Therefore, the *performance group* and the two *archetypes* are both identified as critical, and the *IDA* procedure is required for both design cases.

Table 6-8 Screening results for *PG* 4 designed with $R_d = 2.0$

Design Cases	Model	Rec_t	2.16×DGM		2.54×DGM	
			Rec_p	Status	Rec_p	Status
Case 1	C-2S4L	44	9	Fail	1	Fail
	C-4S4L	44	10	Fail	9	Fail
Case 2	C-2S4L	44	10	Fail	3	Fail
	C-4S4L	44	8	Fail	7	Fail

6.1.5.3 *IDA* and Performance Evaluation

Based on the *IDA*, the *APMR* for each *performance level* is calculated and compared to the acceptable *APMR* as shown in Table 6-9. For the individual *archetype* assessment of Case 1, both C-2S4L and C-4S4L could achieve the *performance level* for *CP*. However, only C-2S4L achieved *LS*. For the average *PG* assessment of Case 1, only *CP* can be achieved. Therefore, compared with those designed with $R_d = 1.5$, the conventional construction moment frames designed using $R_d = 2.0$ and the current design requirements tend to be more vulnerable to earthquake loads.

For the individual *archetype* assessment of Case 2, both *archetypes* had an acceptable margin for *LS* and *CP*. However, in terms of the average *performance group* assessment, only *CP* could be achieved. Compared with Case 1, the design detailing requirements for moderately ductile frames tended to increase the *APMR*s. However, such improvement was not significant enough to alter the major conclusions from the results of Case 1.

Table 6-9 Performance evaluation results for *PG* 4 designed with $R_d = 2.0$

Design Case	Model	*APMR*			Acceptable *APMR*	Status		
		IO	*LS*	*CP*		*IO*	*LS*	*CP*
Case 1	C-2S4L	1.17	1.70	2.09	1.62	NG	OK	OK
	C-4S4L	0.97	1.76	2.28	1.62	NG	OK	OK
Performance Group		1.07	1.73	2.18	2.09	NG	NG	OK
Case 2	C-2S4L	1.17	1.80	2.17	1.62	NG	OK	OK
	C-4S4L	0.98	1.78	2.27	1.62	NG	OK	OK
Performance Group		1.08	1.79	2.22	2.09	NG	NG	OK

6.1.6 Influence of Ground Motion Set

Both the screening and *IDA* procedures of the *PBU procedure* require a set of ground motion records to be used for nonlinear time history analysis of *archetypes*. The set of ground motion records could influence the calculated probability P_i in the screening process and the calculated *PMR* of each *archetype* from *IDA*. In addition, it could also significantly affect the parameters in the evaluation process, including the *record-to-record uncertainty* (β_{RTR}) and the *SSF*, which is used to adjust the calculated *PMR* for *APMR*.

Two sets of ground motions are compared: Set-1 is selected from the far-field ground motion records provided in FEMA P-695, and Set-2 is selected from the PEER NGA database (https://ngawest2.berkeley.edu/). The records in Set-2 are selected to represent three sources of potential damaging earthquakes (i.e., shallow crustal earthquakes, deep in-slab earthquakes, and interface earthquakes) in western Canada.

6.1.6.1 Fixed Ground Motion Set in FEMA P-695 (Set-1)

FEMA P-695 suggests a fixed set of ground motion records to be used for quantification of the seismic performance of building systems designed with the seismic provisions of ASCE/SEI 7 in the U.S. It includes 44 far-field strong ground motions selected to cover various source types, site conditions in California and other western United States locations. More details about the ground motions can be found in the FEMA P-695 document. It should be noted that this set of ground motions has been used in the above sections for both CC-CMF and D-CMF *archetypes*.

As suggested in Section 5.5.2.1, since the ground motions were selected without considering the *spectral shape effects*, the calculated structural response based on this fixed ground motion set needs to be modified through the *SSF* as below:

$$SSF = \exp\left(\beta_1[\bar{\varepsilon}_0(T) - \bar{\varepsilon}_r(T)]\right) \tag{6.1}$$

where $\bar{\varepsilon}_0(T)$ and $\bar{\varepsilon}_r(T)$ are mean epsilon values at the structural period T of the site from deaggregation analysis and the general set of selected records, respectively;

As proposed by Haselton et al. (2007) (Haselton and Deierlein 2007), the factor β_1 in Eq. (6.1) can be obtained from a linear regression analysis of Eq. (6.2) to represent the sensitivity of median performance spectral intensity ($S_{PT}(T)$) at the structural period T to the ε value of each motion record, $\varepsilon_r(T)$.

$$\mu_{LN(S_{PT}(T))} = \beta_0 + \beta_1\varepsilon_r(T) \tag{6.2}$$

where $\mu_{LN(S_{PT}(T))}$ is the mean value of the logarithmic mean of $S_{PT}(T)$.

Considering the significant effort required for calculating *SSF* based on Eq. (6.1), FEMA P-695 provides simplifications of each term on the right-hand side of Eq. (6.1). Based on analyses of many different RC frame buildings, FEMA P-695 suggests the following equation to calculate β_1:

$$\beta_1 = 0.14(\mu_T - 1)^{0.42} \tag{6.3}$$

where μ_T is the period-based ductility defined in Eq. (5.9).

The parameter $\bar{\varepsilon}_0(T)$ in Eq. (6.1) is dependent on the site and *seismic hazard level* of interest. Based on data from the United States Geological Survey (USGS), the $\bar{\varepsilon}_0(T)$ values at a structural period of 1.0 s for different seismic design categories (SDCs) are used as the target ε values for *SSF*. This is because most building structures have periods close to 1.0 s.

With the 44 far-field ground motions in FEMA P-695, the following simplified equation can be used to estimate $\bar{\varepsilon}_r(T)$ in Eq. (6.1):

$$\varepsilon_r(T) = 0.6(1.5 - T) \tag{6.4}$$

Based on Eqs. (6.3) and (6.4), the *SSF* becomes a function of structural period T and μ_T and the values are provided in FEMA P-695.

In addition to *SSF* for *APMR*, the *record-to-record uncertainty* (β_{RTR}) is also dependent on the selected ground motion set. β_{RTR} is defined as the lognormal standard deviation associated with uncertainty in the response of an *archetype* structure due to differences in frequency content and other characteristics of ground motion records. For 44 far-field ground motions in FEMA P-695, the following equation can be used:

$$\beta_{RTR} = 0.1 + 0.1\mu_T \leq 0.4 \tag{6.5}$$

Then the total uncertainty β_{TOT} can be determined according to Eq. (5.13). The total uncertainty value can be used to determine the acceptable *APMR*, which is a function of β_{TOT} and the values of acceptable performance probability, i.e., 10% for $APMR_{10\%}$ and 20% for $APMR_{20\%}$, as presented in Table 9-4 or Table 9-5 of FEMA P-695.

6.1.6.2 New Ground Motion Set for Western Canada (Set-2)

As presented in Section 6.1.1, all *archetypes* developed for both CC-CMF and D-CMF are assumed to be located at the sites in western Canada. To ensure the selected ground motions are representative of the expected ground motions of the sites, 44 ground motions from the PEER NGA database were selected to cover three earthquake sources in western Canada: shallow crustal, in-slab, and interface. More details about the selected ground motions can be found in Appendex C. The ground motion set is referred to as Set-2 in this study. The selected ground motions are

illustrated in Figure 6-8, where they are scaled at the structural period of 0.5 s for one of the developed *archetypes* (C-2S4H) in Table 6-1.

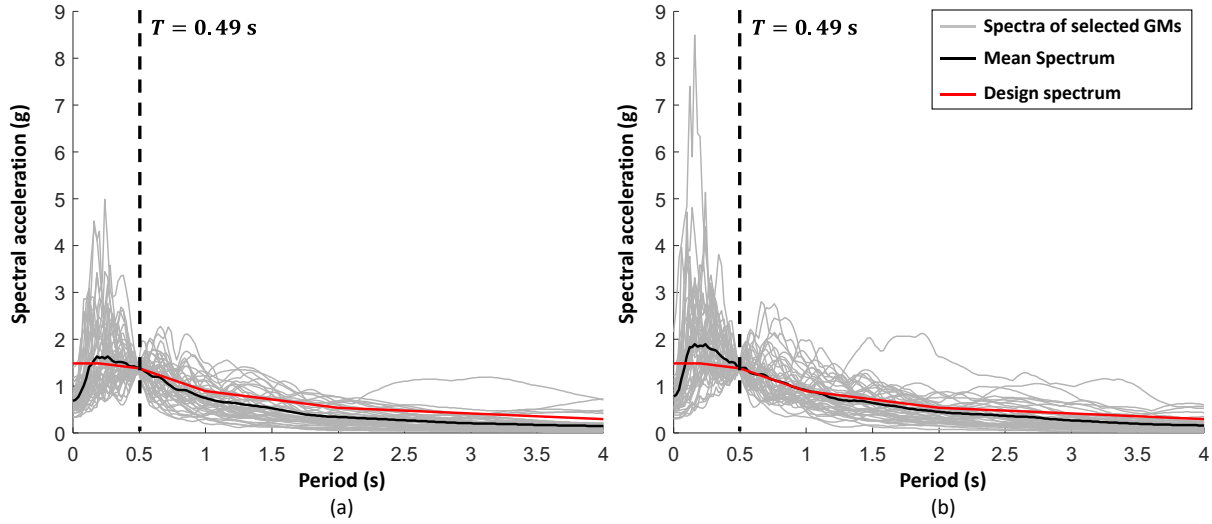

Figure 6-8 Spectral accelerations of the scaled (a) Set-1 (b) Set-2 ground motions at the structural period of *archetype* C-2S4H

As presented in Section 6.1.1, the *archetypes* of the *SFRSs* considered in this study were designed for the cities of Ucluelet and Squamish, which are close to the city of Vancouver. Therefore, the *spectral shape effect* should be minor. To confirm this hypothesis, the *SSF* of each *archetype* was calculated based on Eq. (6.1). Instead of using the simplifications in Eqs. (6.3) to (6.4) for the fixed ground motion set in FEMA P-695, the parameters $\bar{\varepsilon}_{\text{record}}(T)$, β_1, and $\bar{\varepsilon}_0(T)$ required for calculating *SSF* in Eq. (6.1) for the new ground motion set were determined as follows:

- $\bar{\varepsilon}_r(T)$: the ε value of each selected ground motion in Set-2 for the *archetypes* in this study was calculated from an assumed attenuation equation of the ground motion. As mentioned in FEMA P-695, consistent results can be obtained from the use of different attenuation equations. Therefore, the empirical attenuation relationship proposed by Abrahamson and Silva (1997) was used in this study.
- β_1: based on Eq. (6.2), β_1 is obtained from a linear regression analysis with the calculated $S_{PT}(T)$ for each *archetype* and the ε value of each selected ground motion at the period of the *archetype*.
- $\bar{\varepsilon}_0(T)$: based on the deaggregation analysis conducted by Halchuk & Adams (2004), the mean ε values for Vancouver and Victoria, which are close to the cities investigated in this study (i.e., Squamish and Ucluelet), are found to be 1.40 and 1.90, respectively, at the period of 1.0 s. These values were assumed in this study for calculating the *SSFs*.

To consider the influence of the ground motion Set-2 on the *record-to-record uncertainty*, β_{RTR} was calculated directly from the *IDA* of each *archetype* instead of using the simplified equation (i.e., Eq. (6.5)), which is only applicable to Set-1 ground motion records. Table 6-10 lists the β_{RTR} values for developed *archetypes* with respect to *CP* based on the ground motion Set-1 and Set-2.

Table 6-10 β_{RTR} values for ground motion Set-1 and Set-2 (*CP*)

PG	*Archetype* ID (CC-CMF)	β_{RTR} Set-1	β_{RTR} Set-2	*Archetype* ID (D-CMF)	β_{RTR} Set-1	β_{RTR} Set-2
1	C-2S3H	0.4	0.35			
	C-4S3H	0.4	0.36			
	C-6S3H	0.37	0.31			
2	C-2S4H	0.40	0.32	D-2S4H	0.40	0.39
	C-4S4H	0.40	0.44	D-6S4H	0.40	0.45
				D-12S4H	0.40	0.42
				D-20S4H	0.40	0.61
3	C-2S3L	0.40	0.33			
	C-4S3L	0.40	0.31			
	C-6S3L	0.35	0.40			
4	C-2S4L	0.40	0.36	D-2S4L	0.40	0.43
	C-4S4L	0.40	0.35	D-6S4L	0.40	0.43
				D-12S4L	0.40	0.34
5	C-6S3HB5	0.38	0.36			
6	C-2S4HB5	0.40	0.39	D-12S4HB5	0.40	0.38
7	C-6S3HB8	0.33	0.24			
8	C-2S4HB8	0.40	0.36	D-12S4HB8	0.40	0.38
9	C-4S3HS	0.36	0.34	D-2S4HS	0.40	0.45
	C-6S3HS	0.36	0.30	D-6S4HS	0.40	0.48
	C-4S3HW	0.40	0.37	D-12S4HS	0.40	0.43
	C-6S3HW	0.40	0.31			
10	C-2S3HV	0.40	0.28	D-2S4HV	0.40	0.44
	C-4S3HV	0.40	0.37	D-6S4HV	0.40	0.34
	C-6S3HV	0.40	0.36	D-12S4HV	0.40	0.39

6.1.6.3 Results

As indicated in Section 6.1.3.2, all *archetypes* passed the preliminary screening process after the nonlinear pushover analyses. This study mainly focuses on the influence of the ground motion set on the detailed screening, *IDA*, and performance evaluation processes in the *PBU procedure*.

Detailed screening. Table 6-11 compares the detailed screening results using the two ground motion sets. It can be noted that more than half of the CC-CMF *archetypes* (i.e., 13 out of 21) were screened out from the *IDA* when ground motion Set-1 was used for the detailed screening process.

The benefit of the screening process to improve evaluation efficiency became less significant when ground motion Set-2 was used for CC-CMF. Specifically, *IDA* was required for five *archetypes* in addition to the eight *archetypes* identified as critical for ground motion Set-1. For D-CMF *archetypes*, the use of ground motion Set-2 also tended to reduce the number of records having acceptable results. It was found that all D-CMF *archetypes* required *IDA* since they all failed the screening of both scale factors ($APMR_{10\%}$ and $APMR_{6\%}$) regardless of the ground motion sets.

Table 6-11 Screening results of CC-CMF and D-CMF *archetypes*

PG	*Archetype* ID (CC-CMF)	*IDA* requirement Set-1	*IDA* requirement Set-2	*Archetype* ID (D-CMF)	*IDA* requirement Set-1	*IDA* requirement Set-2
1	C-2S3H					
	C-4S3H					
	C-6S3H					
2	C-2S4H	Y	Y	D-2S4H	Y	Y
	C-4S4H	Y	Y	D-6S4H	Y	Y
				D-12S4H	Y	Y
				D-20S4H	Y	Y
3	C-2S3L		Y			
	C-4S3L		Y			
	C-6S3L		Y			
4	C-2S4L	Y	Y	D-2S4L	Y	Y
	C-4S4L	Y	Y	D-6S4L	Y	Y
				D-12S4L	Y	Y
5	C-6S3HB5		Y			
6	C-2S4HB5	Y	Y	D-12S4HB5	Y	Y
7	C-6S3HB8	Y	Y			
8	C-2S4HB8	Y	Y	D-12S4HB8	Y	Y
9	C-4S3HS		Y	D-2S4HS	Y	Y
	C-6S3HS	Y	Y	D-6S4HS	Y	Y
	C-4S3HW			D-12S4HS	Y	Y
	C-6S3HW		Y			
10	C-2S3HV			D-2S4HV	Y	Y
	C-4S3HV		Y	D-6S4HV	Y	Y
	C-6S3HV		Y	D-12S4HV	Y	Y

Note: "Y" indicates that *IDA* is required for the *archetype* evaluation.

***IDA* and performance evaluation.** Table 6-12 shows the calculated *PMR* values from *IDA* for the *LS* performance of CC-CMF. It can be noted that the use of the two ground motion sets leads to similar *PMR* values. However, since the ground motion Set-2 was selected for the sites where the *archetypes* were designed, the *SSF* factors are closer to 1.0 in comparison with the *SSF* values for ground motion Set-1. For example, the calculated *SSF* factor of *archetype* C-2S4HB8 is 1.20

for Set-1, which is about 20% greater than that of Set-2 (i.e., 1.01). With larger *SSF* factors, the computed *APMR* values based on ground motion Set-1 are larger than the values using ground motion Set-2. Meanwhile, the acceptable *APMR* values for Set-1 are also found to be larger than those for Set-2, as shown in Table 6-12. This is because the ground motion Set-1 has a higher *record-to-record uncertainty* than that of the ground motion Set-2. The average ratios of *APMR* to acceptable *APMR*, referred to as $\overline{APMR/AAPMR}$ in Table 6-12, for CC-CMF using Set-1 and Set-2 are 1.69 and 1.44, respectively. The slightly lower $\overline{APMR/AAPMR}$ for Set-2 does not alter the conclusion made from Set-1 that the CC-CMF *archetypes* can achieve *LS* performance. The *APMR* and the acceptable *APMR* values were also calculated for *IO* and *CP performance levels*. Consistent conclusions were made from the two ground motion sets that the CC-CMF system in the NBC has an acceptable safety margin against *LS* and *CP*.

Similar trends can be observed from D-CMF *archetypes*, as shown in Table 6-13. The table shows the results for *CP performance level*. The $\overline{APMR/AAPMR}$ of the *archetypes* for Set-1 and Set-2 are 1.63 and 1.53, respectively, which indicates an acceptable margin of the D-CMF system in the NBC against *CP*. The *APMR* values for *IO* and *LS* were also computed and compared with the acceptable *APMR*s. It was found that the *performance levels* of both *IO* and *LS* could not be achieved regardless of the ground motion set used for the performance assessment.

Table 6-12 *IDA* results of CC-CMF *archetypes* for *LS*

PG	*Archetype* ID	*SSF*		*PMR*		*APMR*		*AAPMR*		Status	
		Set-1	Set-2	Set-1	Set-2	Set-1	Set-2	Set-1	Set-2	Set-1	Set-2
1	C-2S3H	1.12	1.06	3.60	2.67	4.03	2.84	1.62	1.43	OK	OK
	C-4S3H	1.15	1.03	3.26	2.64	3.75	2.71	1.62	1.44	OK	OK
	C-6S3H	1.16	1.00	2.81	2.19	3.26	2.19	1.59	1.44	OK	OK
	PG (mean)					3.68	2.58	2.09	1.74	OK	OK
2	C-2S4H	1.19	1.07	1.98	1.95	2.36	2.08	1.62	1.43	OK	OK
	C-4S4H	1.17	1.09	2.03	1.81	2.38	1.97	1.62	1.44	OK	OK
	PG (mean)					2.37	2.03	2.09	1.74	OK	OK
3	C-2S3L	1.13	1.08	3.44	2.24	3.89	2.41	1.62	1.43	OK	OK
	C-4S3L	1.14	1.07	2.42	1.99	2.76	2.12	1.62	1.44	OK	OK
	C-6S3L	1.15	1.11	1.98	2.23	2.28	2.46	1.59	1.45	OK	OK
	PG (mean)					2.97	2.33	2.09	1.75	OK	OK
4	C-2S4L	1.21	1.06	1.75	1.71	2.12	1.82	1.62	1.44	OK	OK
	C-4S4L	1.19	1.04	1.69	1.58	2.01	1.64	1.62	1.46	OK	OK
	PG (mean)					2.06	1.73	2.09	1.76	OK*	OK*
5	C-6S3HB5	1.18	1.08	3.09	2.23	3.65	2.42	1.62	1.50	OK	OK
6	C-2S4HB5	1.20	1.11	1.88	1.94	2.26	2.15	1.62	1.44	OK	OK
7	C-6S3HB8	1.14	1.08	1.93	1.68	2.20	1.82	1.56	1.46	OK	OK
8	C-2S4HB8	1.21	1.01	1.99	1.87	2.41	1.88	1.62	1.43	OK	OK
9	C-4S3HS	1.16	1.00	3.43	2.25	3.98	2.26	1.59	1.44	OK	OK
	C-6S3HS	1.17	1.13	2.28	1.76	2.67	1.99	1.59	1.44	OK	OK
	C-4S3HW	1.16	1.04	3.31	2.70	3.84	2.81	1.62	1.44	OK	OK
	C-6S3HW	1.18	1.01	2.73	2.08	3.22	2.10	1.62	1.44	OK	OK

	PG (mean)					3.43	2.29	2.09	1.74	OK	OK
10	C-2S3HV	1.12	1.05	3.45	2.45	3.86	2.57	1.62	1.43	OK	OK
	C-4S3HV	1.19	1.10	2.50	2.03	2.98	2.24	1.62	1.44	OK	OK
	C-6S3HV	1.20	1.06	2.10	2.18	2.52	2.30	1.62	1.57	OK	OK
	PG (mean)					3.12	2.37	2.09	1.81	OK	OK

Table 6-13 *IDA* results of D-CMF *archetypes* for *CP*

PG	*Archetype* ID	*SSF*		*PMR*		*APMR*		*AAPMR*		Status	
		Set-1	Set-2	Set-1	Set-2	Set-1	Set-2	Set-1	Set-2	Set-1	Set-2
1	D-2S4H	1.36	1.12	2.32	1.97	3.16	2.21	1.52	1.52	OK	OK
	D-6S4H	1.51	1.12	1.90	1.92	2.87	2.15	1.52	1.58	OK	OK
	D-12S4H	1.61	1.37	1.56	2.18	2.51	2.99	1.52	1.55	OK	OK
	D-20S4H	1.61	1.70	1.45	2.00	2.33	3.40	1.52	1.75	OK	OK
	PG (mean)					2.72	2.69	1.90	2.05	OK	OK
2	D-2S4L	1.37	1.13	2.07	1.66	2.84	1.88	1.52	1.56	OK	OK
	D-6S4L	1.50	1.16	1.64	1.73	2.46	2.01	1.52	1.56	OK	OK
	D-12S4L	1.61	1.30	1.32	1.96	2.13	2.55	1.52	1.47	OK	OK
	PG (mean)					2.47	2.14	1.90	1.92	OK	OK
3	D-12S4HB5	1.61	1.33	1.55	2.11	2.50	2.81	1.52	1.51	OK	OK
4	D-12S4HB8	1.61	1.39	1.70	2.43	2.74	3.38	1.52	1.51	OK	OK
5	D-2S4HS	1.35	1.18	2.07	1.96	2.79	2.31	1.52	1.58	OK	OK
	D-6S4HS	1.45	1.17	1.93	1.92	2.80	2.25	1.52	1.61	OK	OK
	D-12S4HS	1.58	1.41	1.52	2.01	2.40	2.83	1.52	1.56	OK	OK
	PG (mean)					2.66	2.46	1.90	2.02	OK	OK
6	D-2S4HV	1.32	1.07	1.72	1.54	2.27	1.65	1.52	1.57	OK	OK
	D-6S4HV	1.47	1.19	1.92	1.80	2.82	2.14	1.52	1.47	OK	OK
	D-12S4HV	1.61	1.27	1.75	2.07	2.82	2.63	1.52	1.43	OK	OK
	PG (mean)					2.64	2.14	1.90	1.84	OK	OK

6.1.7 Summary Observations

The *PBU procedure* is used in this section to evaluate the seismic performance of CC-CMF and D-CMF in the NBC. The objective of this application is twofold: 1) to assess the details provided in the *PBU procedure*, and 2) to evaluate the adequacy of R_d and R_o in the NBC and other seismic design requirements in Canada. Based on the design and modelling of 36 *archetypes* binned into 10 *PG*s, the following findings are summarized:

- The *PBU procedure* can quantify the seismic performance of concrete moment-resisting frames for the target *performance level* having specific performance objectives. The *performance levels* need to be quantified through local and global performance criteria, which are highly system-dependent and need to be carefully defined based on the structural characteristics at different ductility levels.
- A comparison of the results between the detailed screening and the full *IDA* highlights the accuracy of the detailed screening in identifying the critical and non-critical *archetypes*.

The effectiveness of the detailed screening in the *PBU procedure* to reduce the number of *archetypes* for *IDA* is dependent on the ductility of the moment-resisting frame systems. For example, the detailed screening for CC-CMF reduces the number of *archetypes* for *IDA* by more than 60%. However, it is ineffective for the D-CMF *archetypes* as this ductility level cannot achieve *LS* for which the screening is carried out.

- The CC-CMF system evaluated in this section provided a sufficient margin ratio against the *LS performance level*, while the D-CMF system can only achieve the *CP performance level*. For both ductility levels, *archetypes* designed for high seismic categories and low gravity levels have a higher probability of exceedance values from *CP*.
- The R_o is calculated as 1.55 for CC-CMF (20% higher than the value in the NBC) and $R_o = 1.71$ for D-CMF (1% higher than the value in the NBC).
- Based on the current seismic design detailing in CSA A23.3-14, the increase of R_d tends to reduce the *PMR* against *LS* and *CP* for CC-CMF. However, further studies are required to comprehend the conclusion and quantify R_d and R_o.
- Based on the developed *archetypes* in this section, it is found that the efficiency of the *PBU* screening process in terms of reducing the number of *archetypes* for *IDA* is dependent on the selected ground motion records. However, after a systematic consideration of the *spectral shape effect* and various sources of uncertainties, the *PBU procedure* is found to be insensitive to the selected ground motions for seismic performance evaluation.

6.2 Light-frame Wood Shear Wall System

This section presents the application of the *PBU procedure* for determining and evaluating R_o and R_d of selected light-frame wood shear walls, as defined in the NBC 2020. The study includes an assessment of 2D light-frame wood shear wall buildings, based on the design of 16 *archetypes*.

6.2.1 *Archetype* Development

This study is based on the following design assumptions and *archetype* configurations:

- Design codes and standards are the NBC 2020 and CSA O86 2019 (CSA 2019);
- *Importance category* is Normal;
- Seismicity regions are assumed consistent for all *SFRSs*, and they include one location in Montreal (SC-3) and one in Vancouver (SC-4);
- 20% increase in base shear will be considered for buildings with more than four storeys when the mechanic-based method is used to determine the fundamental period of the building;
- Torsional moment is considered in the design, including accidental eccentricity;

- Design of shear walls is based on the worst-case scenario of diaphragm relative rigidity (rigid or flexible) and, as such, is based on the envelope approach;
- Force distribution between shear wall segments is based on their relative stiffness.

It should be noted that the 20% increase in the base shear for buildings with five storeys or higher was proposed when the mid-rise provisions were introduced into the British Columbia Building Code (BCBC) in order to reduce the risk of a soft storey by restricting the seismic design force levels. It is not clear whether this increase in base shear was based on analysis (e.g., FEMA P-695), or simply to ensure conservatism in the design until more research is available. It is therefore proposed that analysis with and without the 20% increase in the base shear be conducted for at least one *archetype* to establish the validity of this approach.

Although torsional effects, including accidental torsion, will be included in the analysis procedure, it is agreed to use a symmetric plan for all *archetypes*. Since the *IDA* will be conducted on a single shear line, having a building with significant torsional sensitivity may lead to an overly conservative design. Therefore, the plan of the building was kept symmetric in both orthogonal directions to minimize such conservatism in the design.

In order to investigate the current height limits in the NBC 2020, the analysis is expected to consider several storey heights and different numbers of storeys. The *archetypes* will therefore consist of three different storey levels for the Montreal location (e.g., three-, six- and eight-storey buildings), where the eight-storey building is expected to reach the total building height of 30 m, and two different building levels for the Vancouver site (e.g., three- and six-storey), with the six-storey building reaching a total building height of 20 m.

With the above assumptions, seven different *performance groups* have been considered in the seismic performance evaluation, as shown in Table 6-7, which demonstrates the selected *PG*s for this study. The table also provides the number of *archetypes* in each *PG*, the number of storeys, and the abbreviations used for individual building *archetypes*. The abbreviation includes the seismicity level through the city name (VAN or MONT), followed by the number of storeys (e.g., 3, 5, 8), presence of gravity loads (G), diaphragm flexibility (i.e., F, R) and the type of irregularity considered (e.g., weak, GILD). More details about the *archetype* development can be found in the NRC report A1-018030 (Fazileh et al. 2023b).

Table 6-14 *Performance groups* and building *archetypes* information

Performance Group	Number of *Archetypes*	Seismicity Level	Gravity Load	Number of Storeys	Remarks	Building Name	*Archetype* Name
PG 1	2	High (Vancouver)	No	3	Basic *Archetype*	Vancouver 3	VAN3
			No	6	Basic *Archetype*	Vancouver 6	VAN6
PG 2	3	Moderate (Montreal)	No	3	Basic *Archetype*	Montreal 3	MONT3
			No	5	Basic *Archetype*	Montreal 5	MONT5
			No	8	Basic *Archetype*	Montreal 8	MONT8
PG 3	2	High (Vancouver)	Yes	3	-	Vancouver 3	VAN3G
			Yes	6	-	Vancouver 6	VAN6G
PG 4	3	Moderate (Montreal)	Yes	3	-	Montreal 3	MONT3G
			Yes	5	-	Montreal 5	MONT5G
			Yes	8	-	Montreal 8	MONT8G
PG 5	2	High	No	6	Irregular Type 6	Vancouver 6	VAN6Weak
		Moderate	No	3	Irregular Type 9	Montreal 3	MONT3GILD
PG 6	2	High	No	6	W/O 1.2 factor	Vancouver 6	VAN6W/O1.2
		Moderate	No	8	W/O 1.2 factor	Montreal 8	MONT8W/O1.2
PG 7	2	High (Vancouver)	No	6	Rigid Diaphragm	Vancouver 6	VAN6R
			No	6	Flexible Diaphragm	Vancouver 6	VAN6F

6.2.2 *Archetype* Modelling

In order to evaluate the seismic performance of the building *archetypes* through nonlinear static and dynamic analyses, the models of the building *archetypes* are developed based on established modelling procedures for light-frame wood shear walls subjected to lateral seismic loads. For this purpose, the OpenSees platform (McKenna et al. 2010) is used, as illustrated in Figure 6-9. In this configuration, each shearwall segment is modelled using rigid elements (e.g., elasticBeamColumn of the OpenSees library) connected to each other through pin connections. This modelling technique is similar to that of the CUREE Caltech project (Porter et al. 2002). The shear behaviour of the shear wall is implemented using a shear spring (zero-length element) located at the mid-height of the shearwall segment. Tie-downs rods, representing the hold-downs, are modelled to incorporate the cumulative effects of displacements along the height of the buildings. This is done by modelling zero-length spring elements at the base of each storey.

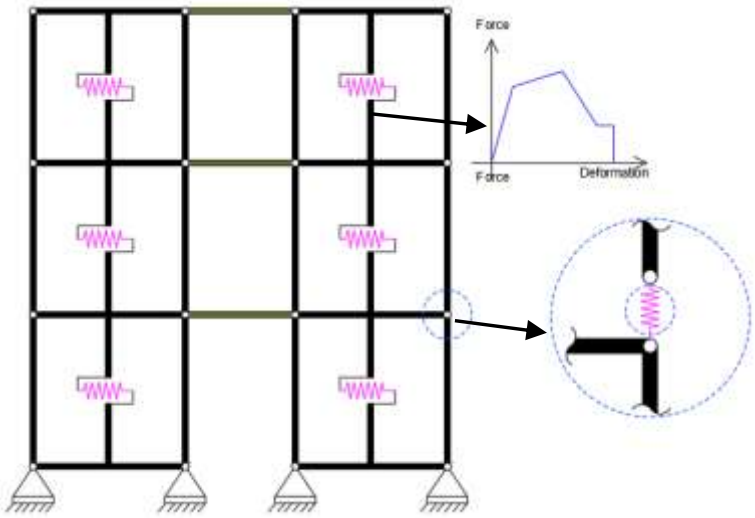

Figure 6-9 OpenSees model of a light-frame wood shear wall

In both pushover and dynamic time history analyses, the nonlinear force-displacement (F-D) behaviour of the shear walls is simulated through a multi-linear curve. Pinching4 material behaviour found in the OpenSees library is used for both the pushover and nonlinear dynamic analyses. It should be noted that the hysteretic behaviour of the Pinching4 material can model the strength and stiffness degradation as well as the pinching behaviour which are important characteristics of light-frame wood shear walls. Figure 6-10 shows the backbone curve as well as a schematic view of the hysteretic behaviour of the Pinching4 material.

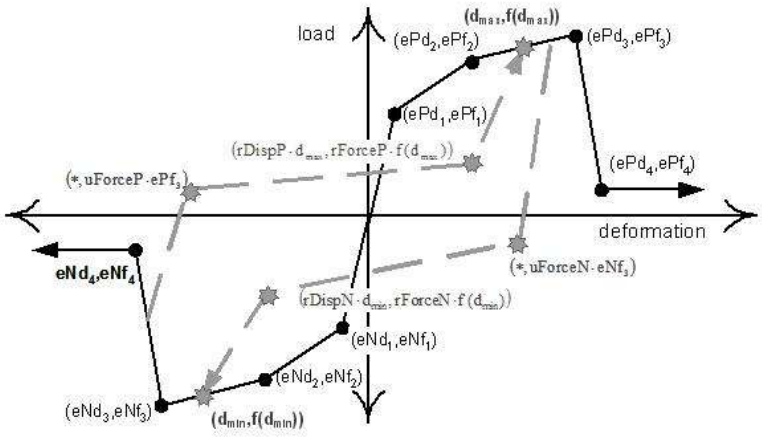

Figure 6-10 Pinching4 F-D curve used in the OpenSees model for nonlinear static and dynamic analyses (McKenna 2011)

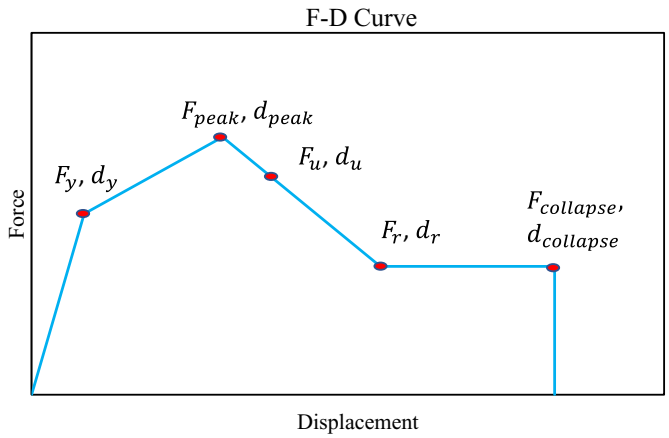

Figure 6-11 Coordinate of an F-D curve

The coordinates of the F-D curve of the Pinching4 material model are shown in Figure 6-11. In the figure, F_y and d_y are the yield force and the yield displacement of the shear wall, respectively. F_{peak} and d_{peak} are the maximum resistance of the shear wall and its corresponding displacement, respectively. F_{ult} and d_{ult} are the points corresponding to a 20% decrease in peak resistance. F_r and d_r are residual force and displacements, respectively. $F_{collapse}$ and $d_{collapse}$ are points representing the final point of the F-D curve, and they correspond to the collapse of the shear wall. NIST GCR 17-917-45 (ATC 2017b) recommends that $d_{collapse}$ be 1.5 d_{ult} and, as such, this value is adopted in the current study. The coordinates of the F-D curve can be determined using the regression formulas proposed by Line et al. based on available test results on full-scale shear walls (Line et al. 2008).

Figure 6-12 shows an example of a calibrated Pinching4 material to a shear wall test in the literature (Line et al. 2008). It should be noted that a similar methodology has been used to develop the material parameters for all designed shear walls in this study.

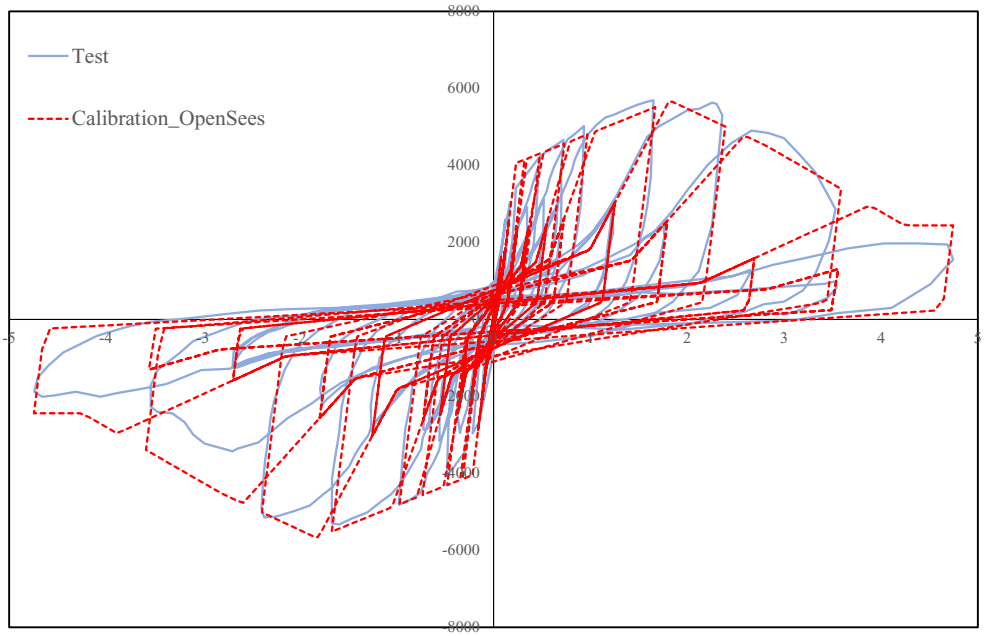

Figure 6-12 Calibration of the Pinching4 material against a tested shear wall (Specimen E1, (Line et al. 2008)**)**

The behaviour of the rod-in-the-tie-down system is modelled using an elastic material, but with different stiffnesses in tension and compression (see Figure 6-13). Maintaining elastic behaviour in the hold-down follows the requirements outlined in the CSA O86-19. *K* is the tie-down tensile stiffness which equals *EA/h*. *E* is the elastic modulus of the rod tie-down material (i.e., steel), taken equal to 200,000 MPa. *A* is the rod's cross-sectional area, and *h* is the length of the rod, which is equal to the storey height. A high stiffness value, equal to 20 times the tension stiffness *K*, is considered for the rod springs in compression, simulating the contact behaviour of the vertical end studs and the shearwall bottom plate.

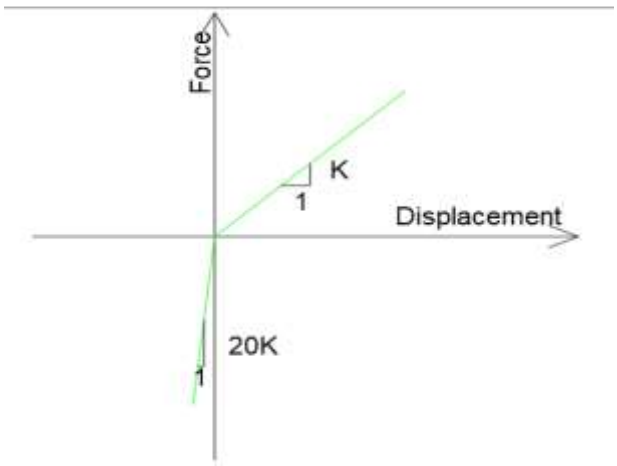

Figure 6-13 Elastic material used for modelling rod tie-downs

6.2.3 Nonlinear Analysis

6.2.3.1 Performance Criteria

In this study, the inter-storey drift ratio was used as the performance criterion. Specifically, the roof displacements correspond to interstorey drift ratio levels of 1%, 2.5%, and 4.5% and were used for *performance levels* of *IO*, *LS*, and *CP*, respectively, as shown in Figure 6-14.

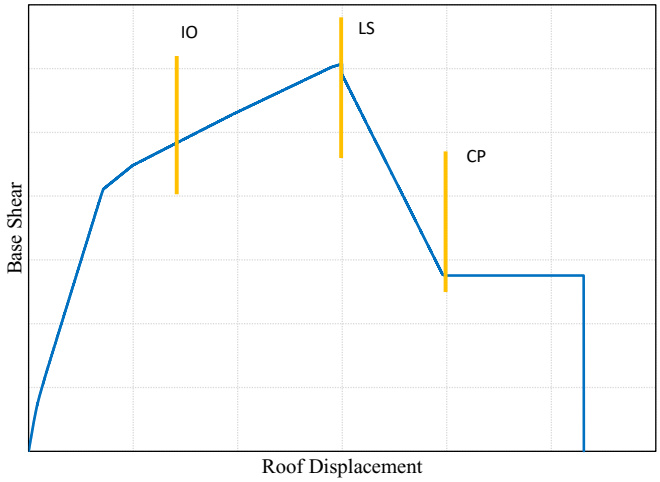

Figure 6-14 Roof displacements corresponding to different *performance levels*

6.2.3.2 Pushover Analysis

The pushover analysis for all building *archetypes* was conducted in OpenSees, and the base-shear versus roof-displacement curves were developed. For each building *archetype*, one shear line was selected to be representative of the whole building. The selected shear line is loaded with

increasing lateral force until the failure point. The lateral load pattern over the height of the building in the pushover analysis corresponds to the lateral load distribution in the design step.

Based on the *PBU procedure*, the value of R_o was found to be 2.16 that is taken as the minimum average of the calculated R_o values of each *performance group,* as summarized in Table 6-15.

Table 6-15 Overstrength-related factor values for all *PG*s

Performance Group	Number of *Archetypes*	Number of Storeys	*Archetype*	R_o
PG 1	2	3	VAN3	2.26
		6	VAN6	2.29
			Average	**2.28**
PG 2	3	3	MONT3	2.31
		5	MONT5	2.13
		8	MONT8	2.10
			Average	**2.18**
PG 3	2	3	VAN3G	2.26
		6	VAN6G	2.16
			Average	**2.21**
PG 4	3	3	MONT3G	2.31
		5	MONT5G	2.13
		8	MONT8G	2.18
			Average	**2.21**
PG 5	2	6	VAN6Weak	2.23
		3	MONT3GILD	2.08
			Average	**2.16**
PG 6	2	6	VAN6W/O1.2	2.36
		8	MONT8W/O1.2	2.18
			Average	**2.27**
PG 7	2	6	VAN6R	2.28
		6	VAN6F	2.32
			Average	**2.30**

Based on Eq. (5.9), μ_T values for all *archetypes* at different *performance levels* were calculated, as shown in Table 6-16.

Table 6-16 Period-based ductility values of the *archetypes*

Performance Group	*Archetype*	T_a (sec)	T_1 (sec)	C_0	V_{max} (kN)	W (kN)	$\delta_{y\text{-}eff}$ (mm)	δ_{IO} (mm)	δ_{LS} (mm)	δ_{CP} (mm)	$\mu_{T\text{-}IO}$	$\mu_{T\text{-}LS}$	$\mu_{T\text{-}CP}$
PG 1	VAN3	0.527	0.582	1.243	163.890	404.880	42.344	75.725	179.442	228.664	1.788	4.238	5.400
	VAN6	0.820	0.887	1.309	159.981	408.490	100.228	129.727	307.410	321.692	1.294	3.067	3.210
PG 2	MONT3	0.527	0.843	1.228	99.638	425.120	50.824	80.214	190.080	236.462	1.578	3.740	4.653
	MONT5	0.821	1.260	1.260	82.546	377.390	108.697	137.889	326.752	338.572	1.269	3.006	3.115
	MONT8	1.256	1.960	1.313	163.553	1072.520	191.078	253.557	600.846	649.382	1.327	3.145	3.399
PG 3	VAN3G	0.527	0.620	1.261	121.447	303.760	48.151	63.229	149.832	199.372	1.313	3.112	4.141
	VAN6G	0.700	0.830	1.357	139.276	329.000	98.330	125.486	297.360	310.400	1.276	3.024	3.157
PG 4	MONT3G	0.527	0.780	1.233	85.857	317.170	50.453	64.356	152.502	198.322	1.276	3.023	3.931
	MONT5G	0.821	1.240	1.284	109.878	515.550	104.581	132.209	313.292	316.972	1.264	2.996	3.031
	MONT8G	1.256	2.050	1.320	128.174	804.380	219.641	265.089	628.172	636.794	1.207	2.860	2.899
PG 5	VAN6Weak	0.830	0.852	1.343	215.330	609.120	85.650	119.135	282.310	296.400	1.391	3.296	3.461
	MONT3GILD	0.527	0.830	1.235	108.822	493.550	46.604	66.397	157.340	203.460	1.425	3.376	4.366
PG 6	VAN6W/O1.2	0.940	0.896	1.344	157.549	609.120	76.344	95.532	226.380	262.922	1.251	2.965	3.444
	MONT8W/O1.2	1.256	2.138	1.313	122.648	1076.160	169.987	219.803	520.860	520.924	1.293	3.064	3.065
PG 7	VAN6R	0.941	0.928	1.363	169.870	490.000	103.992	127.229	301.490	320.492	1.223	2.899	3.082
	VAN6F	0.941	0.937	1.336	129.640	408.230	93.378	125.697	297.860	317.600	1.346	3.190	3.401

T_a: Design period; T_1: First-mode period from Eigenvalue analysis

6.2.3.3 Selected Ground Motions

The selected ground motion records should represent the geological condition and *seismic hazard level* that is consistent with the seismicity of the region where the building is constructed (e.g., fault mechanism, crustal or subduction earthquakes, etc.). In this study, two sets of ground motions were prepared by NRC for the Vancouver and Montreal locations. The number of ground motion records for the performance evaluation of the Vancouver *archetypes* is 44. These records are representative of different source mechanisms, i.e., crustal, in-slab, and interface earthquakes. The total number of ground motions for the Montreal site is 32, and they were chosen from crustal earthquakes that have *seismic hazard levels* consistent with the seismicity of the region. More details about the selection and scaling of ground motions can be found in Appendix C.

6.2.3.4 Screening

In this study, the maximum acceptable interstorey drift ratio of 2.5% according to the NBC 2020 for buildings designed for the *LS performance level* was used for the detailed screening. Based on the screening procedure described in Section 5.5.3, the screening results are summarized in Table 6-17. It can be noted that for the intensity level corresponding to a 10% probability of exceedance, $APMR_{10\%}$, more than half of the *archetypes* and most of the *PG*s failed except *PG* 4, in which all *archetypes* passed this level of shaking. Therefore, *PG* 4 is considered non-critical. The passed *archetypes* from different *PG*s are further analyzed using a scale factor corresponding to the

acceptable $APMR_{6\%}$. All previously passed *archetypes* failed to meet the performance criteria except one *archetype* (MONT8), which is on the verge of failure criterion (e.g., 16/32 ground motion records resulted in the interstorey drift ratio exceeding 2.5%). Therefore, only six out of seven *PG*s (excluding PG 4) require *IDA* for further evaluation.

Table 6-17 Results of detailed *archetype* screening

Performance Group	*Archetype*	SF=1.0 CLE	Np,i / Nt,i	SF=2.16 $APMR_{10\%}$	Np,i / Nt,i	SF=2.54 $APMR_{6\%}$	Np,i / Nt,i	*Archetype* Status
***PG* 1**	VAN3	Pass	42/44	Fail	9/44	-	-	Critical
	VAN6	Pass	43/44	Fail	19/44	-	-	Critical
***PG* 2**	MONT3	Pass	32/32	Fail	13/32	-	-	Critical
	MONT5	Pass	32/32	Pass	21/32	Fail	11/32	Critical
	MONT8	Pass	32/32	Pass	24/32	Pass	16/32	Critical
***PG* 3**	VAN3G	Pass	40/44	Fail	7/44	-	-	Critical
	VAN6G	Pass	43/44	Pass	25/44	Fail	-	Critical
***PG* 4**	MONT3G	Pass	32/32	Pass	17/32			Non-Critical
	MONT5G	Pass	32/32	Pass	20/32			Non-Critical
	MONT8G	Pass	32/32	Pass	20/32			Non-Critical
***PG* 5**	VAN6Weak	Pass	41/44	Fail	20/44	-	-	Critical
	MONT3GILD	Pass	32/32	Fail	11/32	-	-	Critical
***PG* 6**	VAN6W/O1.2	Pass	36/44	Fail	6/22	-	-	Critical
	MONT8W/O1.2	Pass	32/32	Pass	19/32	Fail	15/32	Critical
***PG* 7**	VAN6R	Pass	40/44	Fail	12/44	-	-	Critical
	VAN6F	Pass	40/44	Fail	14/44	-	-	Critical

6.2.3.5 IDA

All failed *archetypes* in this study were analyzed under incrementally increasing intensity of the ground motions until a specific *performance level* is exceeded. After finalizing all *IDA* analyses, the median intensity that passes a specific *performance level* ($\hat{S}_{PT}$) can be determined. To calculate the *PMR* corresponding to the *performance level* of interest of each *archetype*, the $\hat{S}_{PT}$ is divided by the CLE intensity (S_{DT}) at the design period of that *archetype*. Table 6-18 shows the calculated *PMR* values of all *archetypes* in this study.

Table 6-18 *Performance margin ratios* of all *archetypes*

PG	*Archetype*	*PMR*			β_{RTR}		
		IO	***LS***	***CP***	***IO***	***LS***	***CP***
***PG* 1**	VAN3	0.786	1.573	1.760	0.299	0.350	0.370
	VAN6	0.894	1.774	2.029	0.270	0.421	0.490
	Average	**0.840**	**1.674**	**1.894**	**0.285**	**0.385**	**0.430**
***PG* 2**	MONT3	0.786	1.538	1.782	0.322	0.300	0.350
	MONT5	0.770	1.697	1.828	0.383	0.350	0.350
	MONT8	0.817	2.055	2.275	0.067	0.474	0.547
	Average	**0.791**	**1.764**	**1.962**	**0.257**	**0.375**	**0.416**
***PG* 3**	VAN3G	0.792	1.529	1.699	0.313	0.400	0.400
	VAN6G	0.903	1.681	1.872	0.269	0.451	0.512
	Average	**0.848**	**1.605**	**1.786**	**0.291**	**0.425**	**0.456**
***PG* 4**	MONT3G	0.945	1.595	1.670	0.312	0.300	0.300
	MONT5G	0.860	1.567	1.697	0.320	0.380	0.350
	MONT8G	0.807	2.044	2.341	0.264	0.394	0.441
	Average	**0.871**	**1.735**	**1.903**	**0.299**	**0.358**	**0.364**
***PG* 5**	VAN6Weak	0.797	1.506	1.664	0.268	0.477	0.524
	MONT3GILD	0.791	1.313	1.501	0.316	0.320	0.320
	Average	**0.794**	**1.410**	**1.583**	**0.292**	**0.398**	**0.422**
***PG* 6**	VAN6W/O1.2	0.746	1.404	1.539	0.273	0.481	0.500
	MONT8W/O1.2	0.774	1.916	2.192	0.229	0.460	0.539
	Average	**0.760**	**1.660**	**1.866**	**0.251**	**0.470**	**0.519**
***PG* 7**	VAN6R	0.906	1.931	2.190	0.296	0.396	0.462
	VAN6F	0.791	1.627	1.814	0.251	0.458	0.566
	Average	**0.849**	**1.779**	**2.002**	**0.273**	**0.427**	**0.514**

6.2.4 Performance Evaluation

6.2.4.1 Uncertainty Sources

Based on Section 5.6 in this document, the total uncertainty for each *archetype* was calculated, as shown in Table 6-19. According to Section 5.6.4, β_{RTR} values were obtained for different *performance levels* based on *IDA* results, as shown in Table 6-18. For other uncertainty terms, a constant value of 0.2 is assumed. This value refers to a "good" condition, according to Sections 5.6.1 to 5.6.3. Based on Table 5-10 and the calculated total uncertainty values, the corresponding acceptable $APMR_{10\%}$ and $APMR_{20\%}$ can be obtained and then compared with the *APMR,* as presented in the following section.

Table 6-19 *Archetype* performance evaluation

		APMR			β_{TOT}				*APMR*				
PG	***Archetype***	***IO***	***LS***	***CP***	***IO***	***LS***	***CP***	***IO 20%***	***IO 10%***	***LS 20%***	***LS 10%***	***CP 20%***	***CP 10%***
	VAN3	0.83	1.74	1.97	0.458	0.492	0.507	1.47		1.51		1.53	
***PG* 1**	VAN6	0.93	1.93	2.21	0.439	0.545	0.600	1.45		1.58		1.66	
	Average	**0.88**	**1.83**	**2.09**	**0.448**	**0.518**	**0.552**		**1.78**		**1.94**		**2.02**
	MONT3	0.79	1.55	1.79	0.473	0.458	0.492	1.49		1.47		1.51	
***PG* 2**	MONT5	0.78	1.76	1.90	0.516	0.492	0.492	1.54		1.51		1.51	
	MONT8	0.82	2.08	2.31	0.353	0.587	0.647	1.34		1.64		1.72	
	Average	**0.80**	**1.80**	**2.00**	**0.431**	**0.510**	**0.541**		**1.79**		**1.92**		**1.99**
	VAN3G	0.82	1.66	1.88	0.467	0.529	0.529	1.48		1.56		1.45	
***PG* 3**	VAN6G	0.94	1.83	2.05	0.439	0.568	0.618	1.45		1.61		1.56	
	Average	**0.88**	**1.75**	**1.96**	**0.453**	**0.549**	**0.573**		**1.78**		**2.02**		**1.86**
	MONT3G	0.98	1.74	1.82	0.466	0.458	0.458	1.49		1.47		1.47	
***PG* 4**	MONT5G	0.87	1.62	1.76	0.471	0.514	0.492	1.48		1.54		1.51	
	MONT8G	0.81	2.07	2.37	0.436	0.525	0.561	1.44		1.56		1.60	
	Average	**0.89**	**1.81**	**1.98**	**0.457**	**0.498**	**0.502**		**1.80**		**1.90**		**1.90**
	VAN6Weak	0.83	1.63	1.80	0.438	0.589	0.628	1.45		1.64		1.70	
***PG* 5**	MONT3GILD	0.79	1.32	1.51	0.469	0.472	0.472	1.48		1.49		1.49	
	Average	**0.81**	**1.47**	**1.66**	**0.453**	**0.528**	**0.546**		**1.79**		**1.97**		**2.01**
	VAN6W/O1.2	0.77	1.49	1.65	0.441	0.593	0.608	1.45		1.65		1.67	
***PG* 6**	MONT8W/O1.2	0.78	1.94	2.22	0.415	0.576	0.640	1.42		1.62		1.70	
	Average	**0.77**	**1.72**	**1.93**	**0.428**	**0.584**	**0.624**		**1.73**		**2.11**		**2.23**
	VAN6R	0.93	2.04	2.32	0.456	0.526	0.578	1.47		1.56		1.62	
***PG* 7**	VAN6F	0.81	1.73	1.93	0.428	0.574	0.663	1.43		1.62		1.75	
	Average	**0.87**	**1.89**	**2.13**	**0.441**	**0.550**	**0.620**		**1.76**		**2.02**		**2.20**

6.2.4.2 Adjusted Performance Margin Ratios

The *PMRs* calculated in Section 6.2.3.5 were adjusted so as to consider the *spectral shape effect*. As suggested in the *PBU procedure* (Section 5.7.3), the *spectral shape effect* was taken into account by an *SSF* which can be calculated according to Eq. (5.14). The calculated *SSFs* for different *performance levels* are given in Table 6-20.

Table 6-20 *SSF* values

Performance Group	*Archetype*	T_a (sec)	T_1 (sec)	$\bar{\varepsilon}_0(T_a)$	$\bar{\varepsilon}_r(T_a)$	$\beta_{1\text{-IO}}$	$\beta_{1\text{-LS}}$	$\beta_{1\text{-CP}}$	SSF_{IO}	SSF_{LS}	SSF_{CP}
PG 1	VAN3	0.527	0.582	1.520	1.082	0.127	0.229	0.261	1.057	1.106	1.121
	VAN6	0.820	0.887	1.472	1.032	0.084	0.190	0.195	1.038	1.087	1.090
PG 2	MONT3	0.527	0.843	0.460	0.434	0.111	0.214	0.241	1.003	1.006	1.006
	MONT5	0.821	1.260	0.421	0.230	0.081	0.188	0.192	1.016	1.036	1.037
	MONT8	1.256	1.960	0.355	0.287	0.088	0.193	0.202	1.006	1.013	1.014
PG 3	VAN3G	0.527	0.620	1.520	1.082	0.086	0.192	0.226	1.038	1.088	1.104
	VAN6G	0.700	0.830	1.472	1.014	0.082	0.188	0.193	1.038	1.090	1.093
PG 4	MONT3G	0.527	0.780	0.460	0.434	0.081	0.188	0.220	1.002	1.005	1.006
	MONT5G	0.821	1.240	0.421	0.230	0.080	0.187	0.189	1.015	1.036	1.037
	MONT8G	1.256	2.050	0.355	0.287	0.072	0.182	0.183	1.005	1.012	1.012
PG 5	VAN6Weak	0.830	0.852	1.424	1.039	0.094	0.198	0.204	1.037	1.079	1.082
	MONT3GILD	0.527	0.830	0.460	0.434	0.098	0.201	0.233	1.003	1.005	1.006
PG 6	VAN6W/O1.2	0.940	0.896	1.424	1.089	0.078	0.186	0.204	1.027	1.064	1.071
	MONT8W/O1.2	1.256	2.138	0.355	0.287	0.084	0.190	0.190	1.006	1.013	1.013
PG 7	VAN6R	0.941	0.928	1.400	1.089	0.075	0.183	0.190	1.023	1.059	1.061
	VAN6F	0.941	0.937	1.400	1.089	0.090	0.195	0.202	1.028	1.062	1.065

T_a: Design period; T_1: First-mode period from Eigenvalue analysis; $\bar{\varepsilon}_0$ is the target epsilon of the building site; $\bar{\varepsilon}_r$ is the mean epsilon of the selected ground motions; $\beta_{1\text{-X}}$ and $SSF_{IO\text{-X}}$ are the regression constant and *spectral shape factor* corresponding to the *performance level* of X, where X can be *IO*, *LS*, and *CP*.

6.2.4.3 Evaluation Results

The *APMR* values of all *archetypes* are compared with the acceptable *APMR* values, as shown in Table 6-19. It can be noted that most *archetypes* can achieve *LS*, but their average *APMR* values for the *PG*s are all found to be less than the acceptable *APMR* values. As for the *CP performance level*, *PG*s 1 to 4 are found to have adequate performance margins against *CP*. *PG*s 5 to 6, however, fail to satisfy Eq. (5.17) for the *performance groups*. Therefore, the study indicates that the designed *archetypes* based on the current design code cannot achieve *CP performance level*.

6.2.5 Summary Observations

The objective of this research is to gain insight into the applicability of the *PBU procedure* by investigating the behaviour of light-frame wood shear walls. Sixteen *archetypes* for two different locations, Vancouver and Montreal, representing SC3 and SC4 seismic categories in the NBC, have been designed according to the NBC 2020 and CSA-O86:19 requirements, and their seismic

performances have been evaluated using nonlinear static (pushover) analysis, nonlinear time history analysis, and *IDA*. Based on the assumptions for the *archetype* development, modelling, and performance evaluation, the current R_d and R_o and design requirements for light-frame wood shear walls are found to be sufficient to achieve the *CP performance level* only for the regular studied *archetypes*.

6.3 Conventional Construction Reinforced Concrete Shear Wall System

This section presents the findings of a study that focused on the seismic performance assessment of the Conventional Construction Concrete Shear Wall system in Canada. This system is one of the 44 *SFRSs* specified by the NBC 2020 to ensure building structure safety. The study used the *PBU procedure* and systematically evaluated several *archetype* configurations, analyzing the impact of height, seismicity, irregularity, and gravity load levels on R_d and R_o. Seven performance groups and 18 *archetypes* were developed for nonlinear static (pushover) and dynamic analyses (time history and *IDA*). Sample results are presented in this section, and the results indicate that the CSA A23.3-19 and NBC 2020 requirements for the Conventional Construction Concrete Shear Wall system represent the lower bound of values for R_d and R_o. This study provides valuable insight into the seismic performance of this type of *SFRS* and highlights the need for ongoing evaluation to ensure building safety in seismic regions.

6.3.1 Archetype Development

This section presents the design of a five-story RC structure in Montreal, assuming site class C. The corresponding R_d and R_o are defined as 1.5 and 1.3, respectively, according to the NBC 2020. The required design and detailing provisions of CSA A23.3-19 associated with the corresponding R_d and R_o are in Table 11.1 of the 4th edition of the Concrete Design Handbook (CAC 2015). Based on the table, shear walls in conventional construction systems must have a factored resistance greater than or equal to factored loads. Also, the factored shear resistance must exceed shear corresponding to the factored flexural resistance or shear corresponding to $R_d R_o$ = 1.3.

The layout of the *archetypes* is developed with an industry partner (Glotman Simpson Consulting Engineers) to ensure that it represents the typical practice in Canada. The structural wall configuration in Figure 6-9 has a centrally located elevator core shear wall. This plan configuration is chosen to be as symmetrical as possible to minimize the plan irregularities.

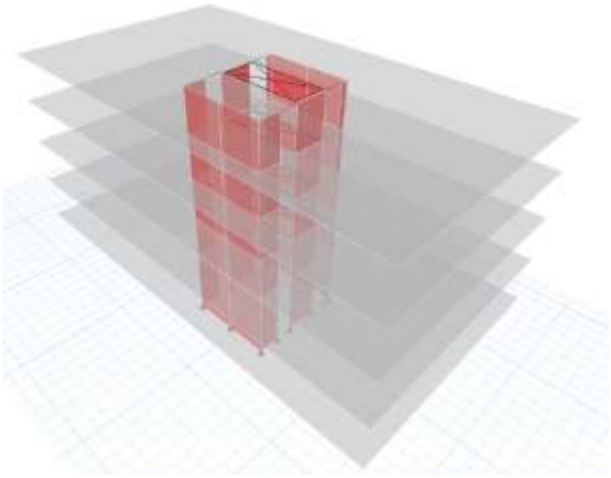

Figure 6-15 3D view of the five-storey building

As shown in Figure 6-16, the thickness of the cantilever walls and coupled walls are 305 mm and 457.2 mm, respectively. Each floor has a 457-mm slab with concrete strength of 35 MPa. It should be mentioned that a rigid body diaphragm is assigned to all floors. All walls are 4,572 mm tall on the first floor and 2,946 mm on the other floors.

All developed *archetypes* and defined *performance groups* are presented in Table 6-21.

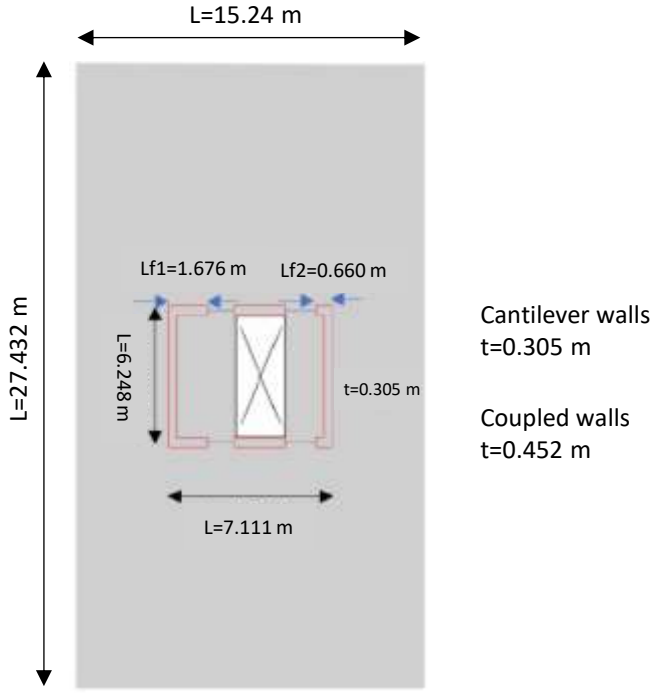

Figure 6-16 Plan view of the five-storey building

Table 6-21 Proposed *archetypes* and *performance groups*

PG	Regularity	Seismicity	Axial Load	No of *Archetypes*	*Archetype* Label	No of Storeys	Description
1	Regular	SC4	High	3	A14 A18 A22	9 7 5	-
2	Regular	SC4	Low	3	A16 A20 A24	9 7 5	-
3	Regular	SC3	High	3	A2 A6 A10	12 9 5	-
4	Regular	SC3	Low	3	A4 A8 A12	12 9 6	-
5	Irregular	SC4	High Low	2	A13 A15	9 9	GILD GILD
6	Irregular	SC3	High Low	2	A1 A3	12 12	Podium Podium
7	Irregular	SC3	High Low	2	A5 A7	9 9	GILD GILD

6.3.1.1 Gravity Load Level

There are two categories for the applied axial load on each wall. The axial load applied to a wall plays a key role in the response. Therefore, the axial load ratios on the RC shear walls varying from low (5%) to high (25%) are considered for *archetype* development in this study.

6.3.1.2 Seismicity Level

Two different seismic categories shown in Figure 6-17 are considered in this study. Garment District in Montreal and Burnaby in British Columbia are considered seismic category 3 (SC-3) and 4 (SC-4), respectively.

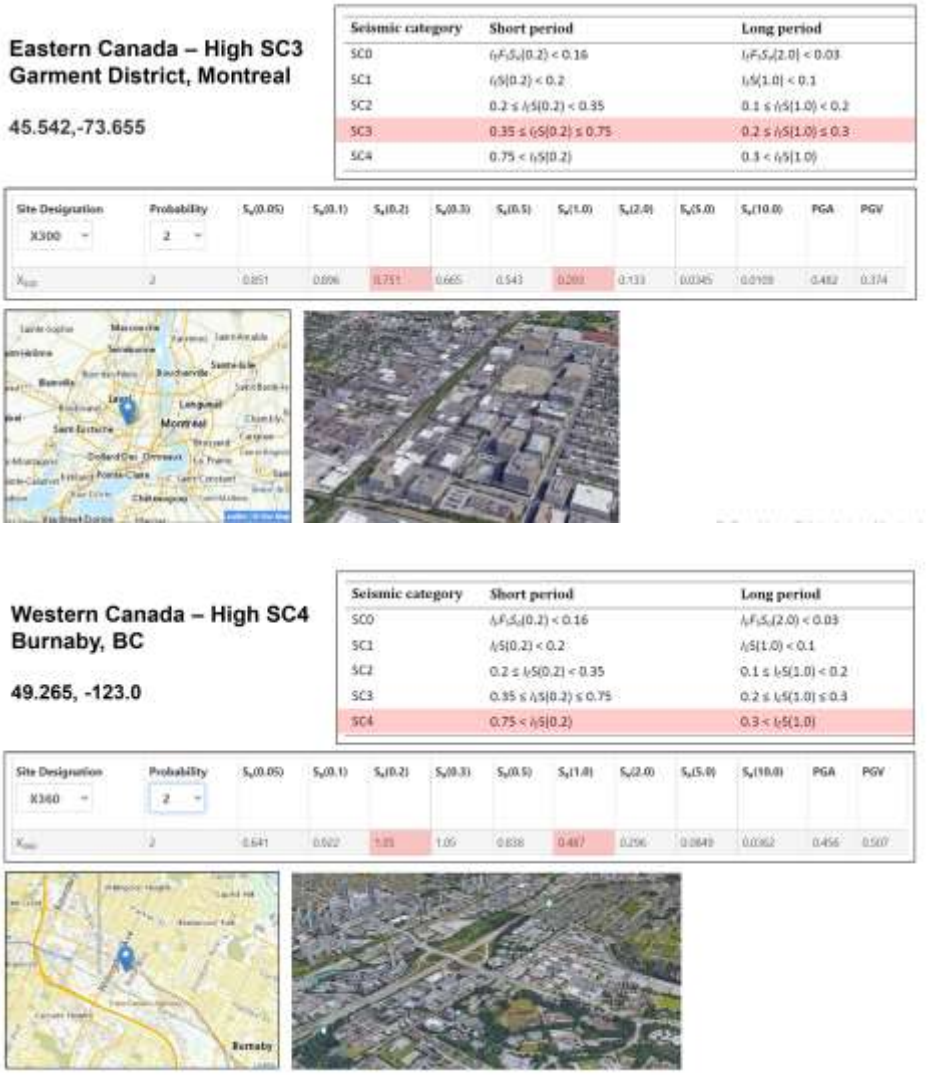

Figure 6-17 Seismic categories used in this study

6.3.1.3 Geometric Variation

Height is considered a variable that affects wall flexibility. Taller walls are more flexible than shorter ones. The height of the *archetypes* is limited to 40 metres in SC-3 and 30 metres in SC-4. Therefore, the proposed *archetypes*, as shown in Figure 6-18, are five-storey, seven-storey, and twelve-storey buildings in SC-3 and five-storey, seven-storey, and nine-storey buildings in SC-4.

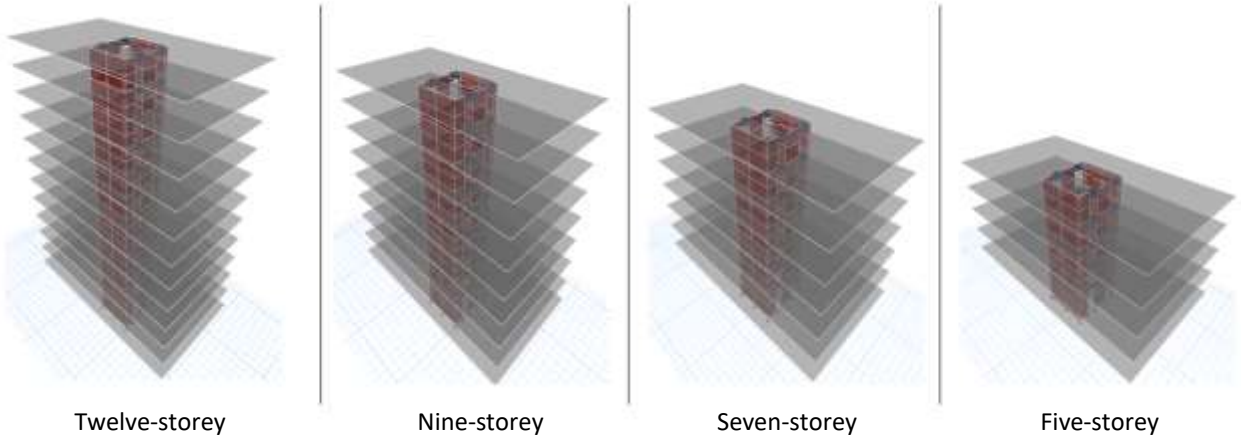

Figure 6-18 3D view of regular *archetypes*

6.3.1.4 System Irregularity

The NBC 2020 considers nine types of irregularities. Two types of them are investigated in this project. Irregularity type 2 (mass irregularity) is considered for *archetypes* 1 and 3 by assuming two podium levels, as shown in Figure 6-13. Also, irregularity type 9 (Gravity-Induced Lateral Demand (GILD)) is modelled in *archetypes* 5, 7, 13, and 15. A 3D and plan views of those *archetypes* are shown in Figure 6-14. According to the definition of GILD in the NBC, if the alpha value calculated from Eq. (6.6) exceeds 0.1, GILD, irregularity exists on the *SFRS*.

$$\alpha = \frac{\text{overturning moment demand due to gravity loads alone}}{\text{overturning moment resistance at the base of the wall}} \tag{6.6}$$

The slabs and columns layout is designed in a way that gravity loads can provide an overturning moment of about 10 percent of wall flexural resistance.

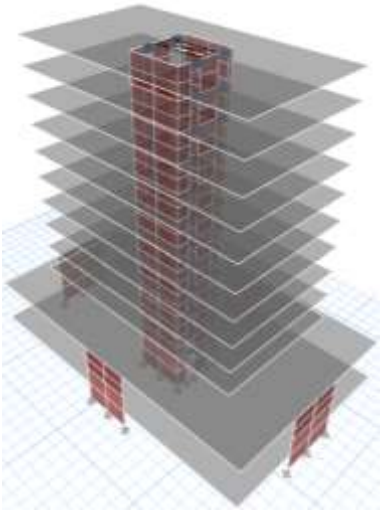

Figure 6-19 3D view of *archetypes* 1 and 3

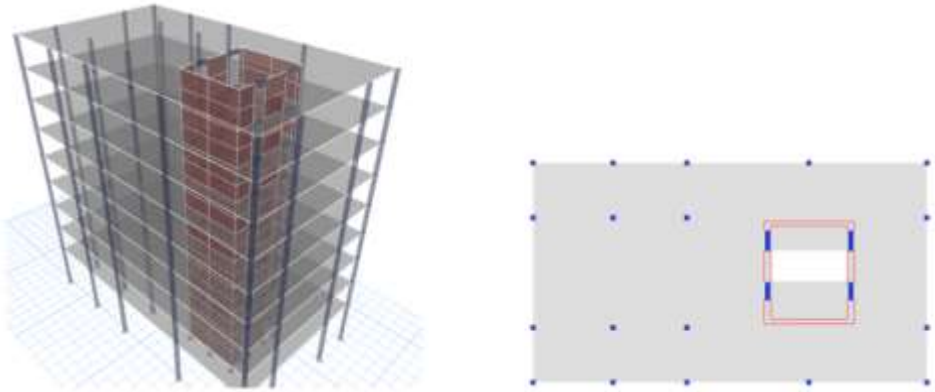

Figure 6-20 *Archetypes* with GILD irregularity: (left): 3D view, (right): plan view

6.3.2 *Archetype* Modelling

To model the developed *archetypes*, a framework was developed to use the automation capability of OpenSessPy (Zhu et al. 2018) to conduct the modelling, perform static and dynamic analyses, and postprocess the result data. The modelling approach in OpenSeesPy is described in this section.

Figure 6-21 presents the analytical modelling in OpenSeesPy. The fibre-type beam-column element, the linear elastic beam-column element, and the truss element are used to model the shear wall, leaning column, and links between the wall and leaning column, respectively.

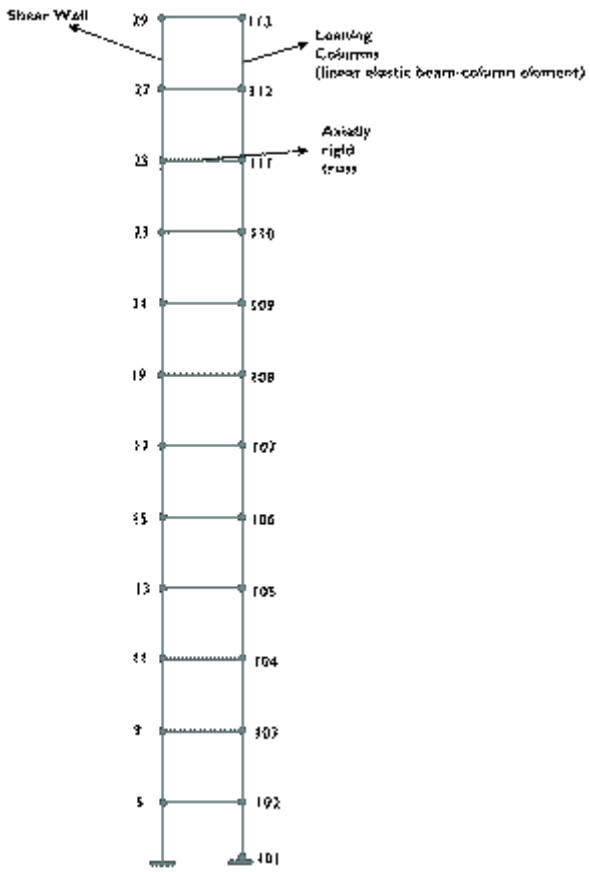

Figure 6-21 2D modelling of shear wall and leaning column in OpenSeesPy (Zhu et al. 2018)

As shown in Figure 6-22, the green and blue areas show the tributary area of the wall and leaning column, respectively. The axial force applied to the wall and the leaning column in the nonlinear model is based on these tributary areas. To prevent the contribution of the leaning columns in lateral resistance of the shear wall, low stiffness rotational springs are modelled using the "ZeroLength" element in OpenSeesPy and assigned to both ends of the leaning columns at each storey level.

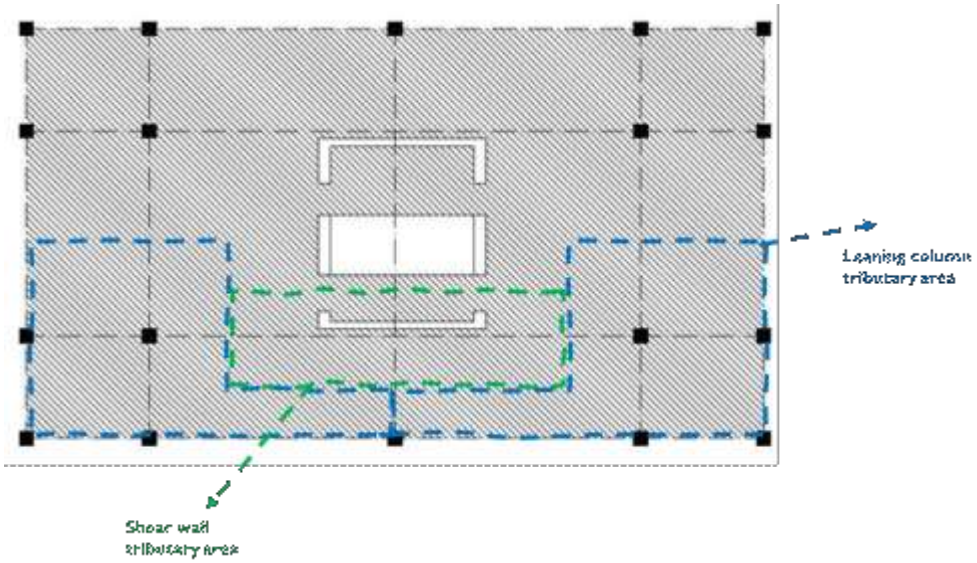

Figure 6-22 Tributary area of the shear wall and leaning column

6.3.2.1 Flexural Response

The cantilever wall has a C-shaped section, as shown in Figure 5-16. Modelling the C-shaped and I-shaped sections is possible in OpenSeesPy, while the latter is more effortless and unchallenging. Also, only the perpendicular distance between each fibre and the bending axis essentially affects the wall's behaviour. Therefore, the wall section is modelled as an I-shaped section with several steel and concrete fibres, as illustrated in Figure 6-23.

There are several modelling approaches for RC shear walls in the literature. Although using a fibre-based modelling approach will consider the shear and axial-flexure behaviour independently, it can reasonably estimate slender shear wall behaviour dominated by flexure (Kolozvari 2013). Also, this modelling approach is more numerically robust and less computationally demanding than modelling approaches that can consider the interaction of the shear-flexure behaviour of the wall (Pugh 2012). Therefore, the fibre-type beam-column element is used in this study to model the RC shear walls.

All longitudinal rebars, concrete in boundaries, and concrete in the web are defined using steel material ("Steel02" material in OpenSeesPy), confined concrete ("Concrete02" material in OpenSeesPy), and unconfined concrete ("concrete02" material in OpenSeesPy), respectively.

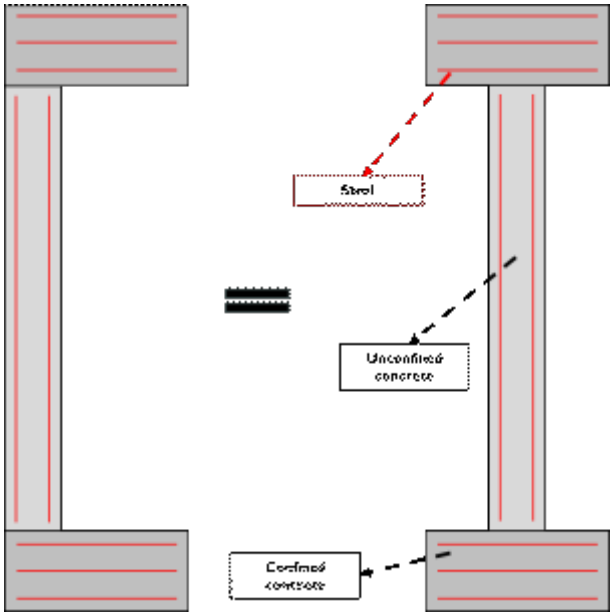

Figure 6-23 Wall section configuration implemented in OpenSeesPy

6.3.2.2 Shear Response

A linear stress-strain relationship is assumed for the shear response of the shear wall and aggregated with the axial-flexural response of the wall using the "Section aggregator" command in OpenSeesPy, as shown in Figure 6-24. The terms in the formula are shear stiffness modifier (C_{GA}), concrete elastic shear modulus ($G = 0.4E$), and effective flanged wall area assumed as A_{web}. A sensitivity analysis is performed to find out the effect of different shear stiffness modifiers on the shear wall behaviour. It is concluded that the shear wall behaviour is not sensitive to this parameter. The shear stiffness modifier is assumed as 0.5 based on the PEER TBI recommendation (PEER 2017).

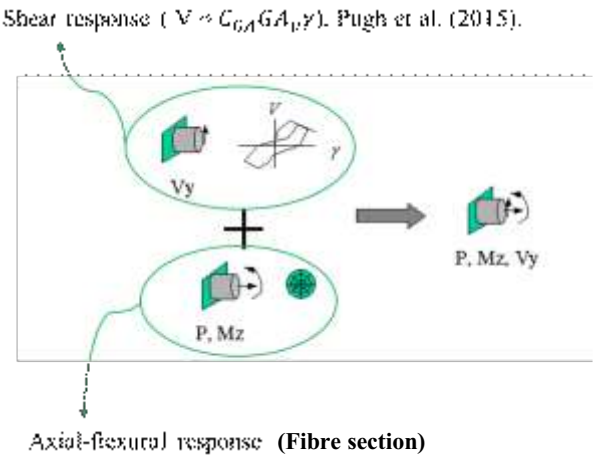

Figure 6-24 Section aggregator command in OpenSees (McKenna 2011)

6.3.2.3 Material Regularization

Material regularization is required to prevent damage localization in shear wall modelling using fibre-type beam-column elements. But, material regularization is not applicable for shear walls without softening behaviour before failure (Pugh 2012). The section analysis on shear wall *archetype* A12 (shown in Figure 6-25) has a hardening response prior to failure due to steel rupture; therefore, material regularization is not required for this *archetype*. However, the other walls may have a softening response because of a lower longitudinal reinforcement ratio or higher axial load demand.

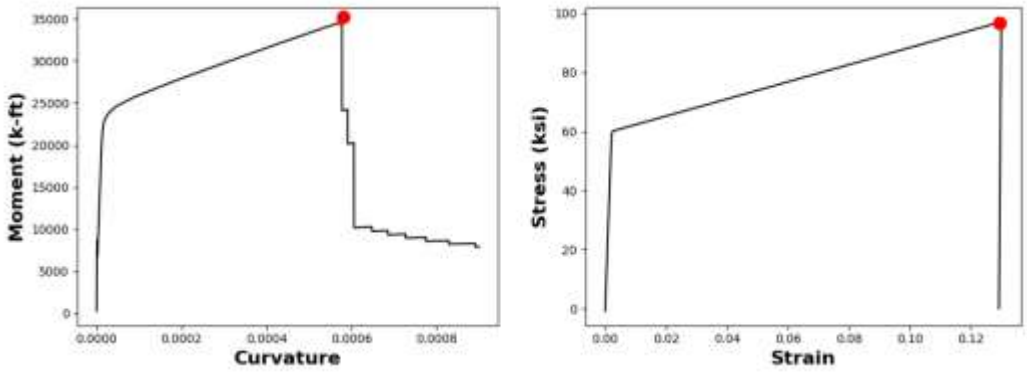

Figure 6-25 Section analysis of A12 at the base: Left) Moment-curvature, Right) Boundary steel fibre in tension

6.3.2.4 Model Validation

To validate the proposed nonlinear model and calibrate the model parameters, the cyclic response of specimen RW-A15-P10-S78, as tested by Tran and Wallace (Tran and Wallace 2015), is

simulated under the same displacement protocol. Both the specimen and its hysteresis behaviour are illustrated in Figure 6-26. In the hysteresis plot, the blue and red lines represent the experimental and numerical results, respectively. The numerical model not only can capture the loading and unloading stiffness, but also capture the strength prior to a drift of 2%. Although the model is not able to capture the strength degradation adequately, it can reasonably present the wall behaviour since all *archetypes* in this study have hardening behaviour before failure.

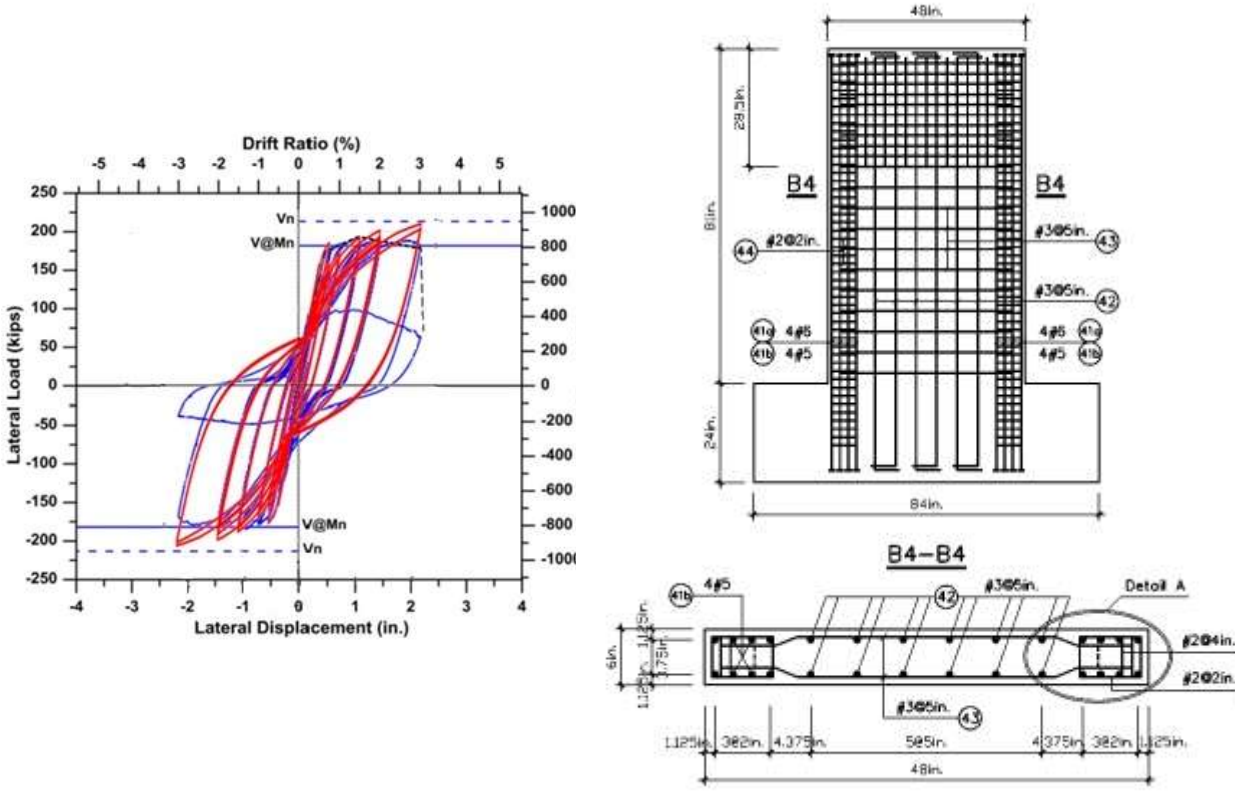

Figure 6-26 Verification and calibration: left) The analytical and experimental hysteresis of the specimen; right) Specimen RW-A15-P10-S78 tested by Tran and Wallace (Tran and Wallace 2015)

6.3.3 Nonlinear Analysis

6.3.3.1 Performance Criteria

In both static and dynamic analyses, the capacity of the *archetypes* needs to be calculated based on the desired *performance level* of the system quantified through different local and global performance criteria. The performance criteria used in this study cover two *performance levels* of *LS* and *CP* to find out the *performance margin ratio* of the system against each one.

As one of the global performance criteria in both static (pushover) analysis and dynamic analyses (limited time history analysis in the detailed screening and *IDA*), drift ratios of 2.5% and 4.0% were selected for the *LS* and *CP performance levels'* objectives, respectively. According to ASCE 7 Chapter 16 (ASCE 2017a), peak transient storey drift ratios can be as high as double the values specified in ASCE 7 Table 12.12-1. This table suggests a limit of 2.0% for buildings, five storeys or more above the base, in both Risk Categories I and II. A drift ratio of 4.0% was chosen as it is double the recommended value of 2.0%. Non-convergence in time history analysis representing instability was considered as a global criterion at *CP* for the dynamic analyses. It is noted that facing numerical problems and non-convergence issues are very common in nonlinear time history analysis. To find the storey mechanism out of the other types of numerical problems, an algorithm was devised inside the framework to change the analysis parameters (algorithms and tests) and time steps to deal with the non-convergence issue.

The local criteria are defined based on limitations for steel rebar strain. The strain limits for rebars are set to 0.02 (ten times the yield strain) and 0.1 (the tensile rupture strain with consideration of low-cycle fatigue is 0.05, while without consideration of this effect, it is 0.13) for *LS* and *CP*, respectively.

6.3.3.2 Pushover Analysis

The pushover analysis was conducted for all *archetypes* to calculate the required R_o as well as to assess the nonlinear behaviour of the models before going to the laborious time history analyses. All pushover curves for each *PG* are presented in Figure 6-27.

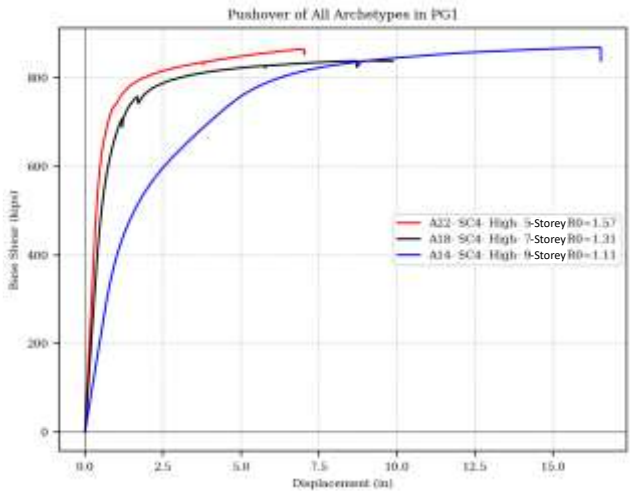

(a)

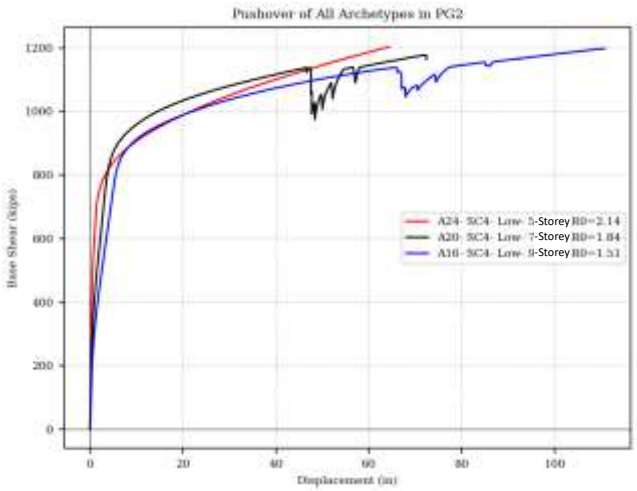

(b)

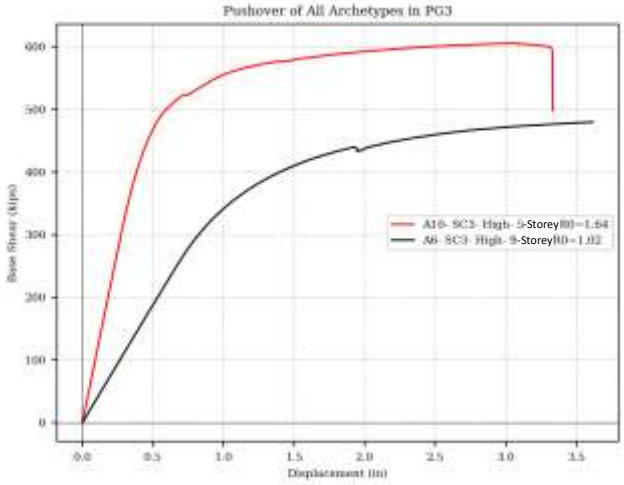

(c)

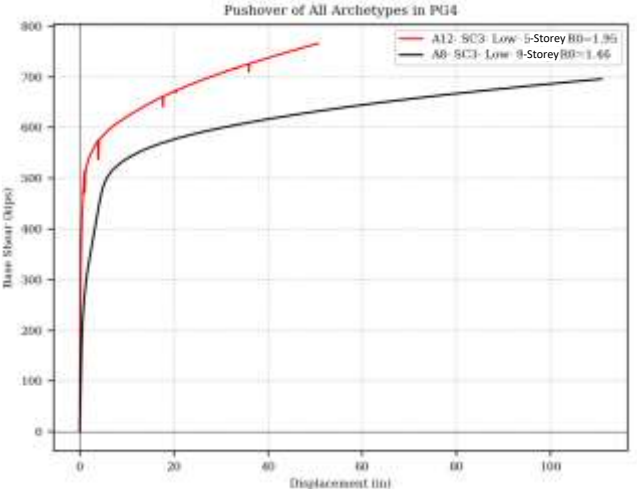

(d)

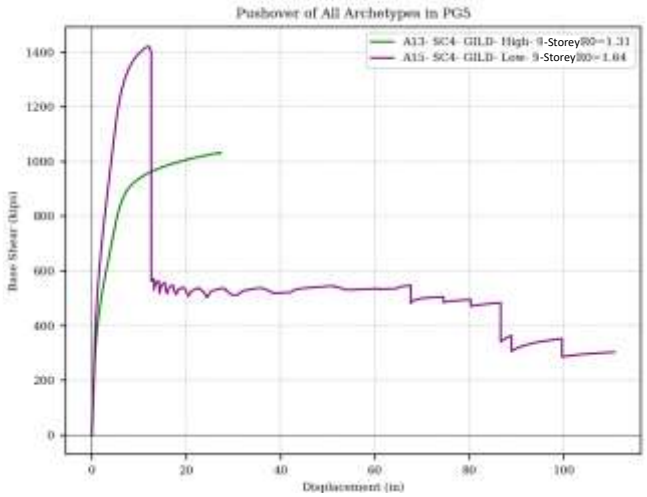

(e)

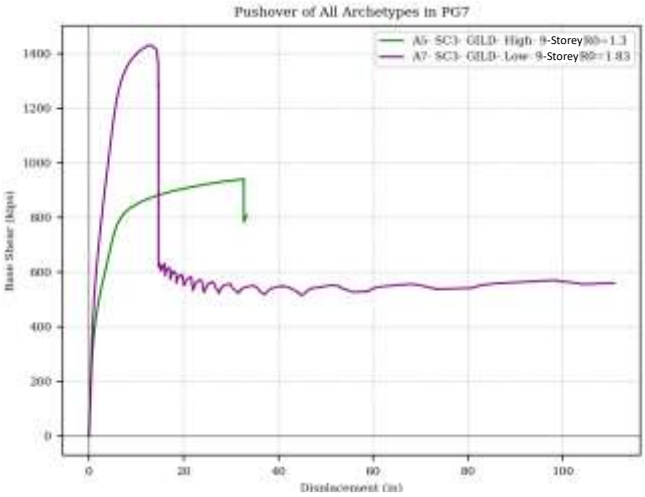

(f)

Figure 6-27 Pushover curves for all *archetypes*; a) *PG*1. b) *PG*2, c) *PG*3, d) *PG*4, e) *PG*5, f) *PG*7

As shown in Table 6-22, the R_o value for each *archetype* is calculated and presented. In addition, the calculated R_o values for each *PG* are averaged and shown in the last column of the table. The minimum average R_o value of different *PG*s is 1.33. The code-prescribed R_o value of 1.3 is less than the calculated R_o value in this study.

Table 6-22 Pushover analysis results

PG	***Archetype* Label**	**Ro**	**Avg (Ro)**
1	A14 A18 A22	1.15 1.31 1.57	1.33
2	A16 A20 A24	1.51 1.84 2.14	1.83
3	A2 A6 A10	UR 1.02 1.64	1.33
4	A4 A8 A12	1.00 1.46 1.95	1.47
5	A13 A15	1.31 1.64	1.48
6	A1 A3	UR UR	UR
7	A5 A7	1.3 1.83	1.57

UR : Under Review

6.3.3.3 Selected Ground Motions

To implement the *PBU procedure*, a collection of ground motion records is necessary to carry out nonlinear dynamic analysis of buildings and assess the effectiveness of the proposed system. The selection criteria for these records should factor in various aspects such as intensity, amplitude, frequency content, duration, spectral shape, and ground motion level. These parameters are linked to the magnitude and distance of the earthquake events and should be carefully considered when developing the ground motion set.

This study includes two distinct ground motion sets, specifically designed for Montreal and Vancouver, respectively. More details about the selected ground motions are given in Appendix C.

For *IDA*, it is necessary to scale the ground motion records individually to match the design spectrum ordinate at the fundamental design period (imperial period from the NBC equation, or the

value from the model, whichever governed the design) of the *archetype* first, then run the *IDA*. The ground motion records have been individually scaled to match the design spectrum ordinate at the fundamental design period of *archetype* A4, A8, and A12, which are 0.93 sec, 0.59 sec, and 0.25 sec, respectively.

6.3.3.4 Screening

The screening results of *PG*4's *archetypes* A4, A8, and A12 are presented in this section. As shown in Figure 6-28 to Figure 6-30, the *archetypes* A4 and A8 successfully passed the initial *archetype* screening by demonstrating inter-storey drift and rebar tensile strain values below 2.5% and 0.1, respectively. Conversely, *archetype* A12 did not pass this initial screening, as more than half of the ground motion records resulted in rebar strains exceeding 0.1. As per the *PBU* methodology, it is necessary to amplify the ground motions and subsequently perform a time history analysis for the *archetypes* A4 and A8 that passed the first screening. In the second screening process, although these *archetype"* inter-storey drifts remained acceptable, they failed to meet the local performance criteria. Consequently, all the *archetypes* in *PG*4 are required to undergo *IDA*.

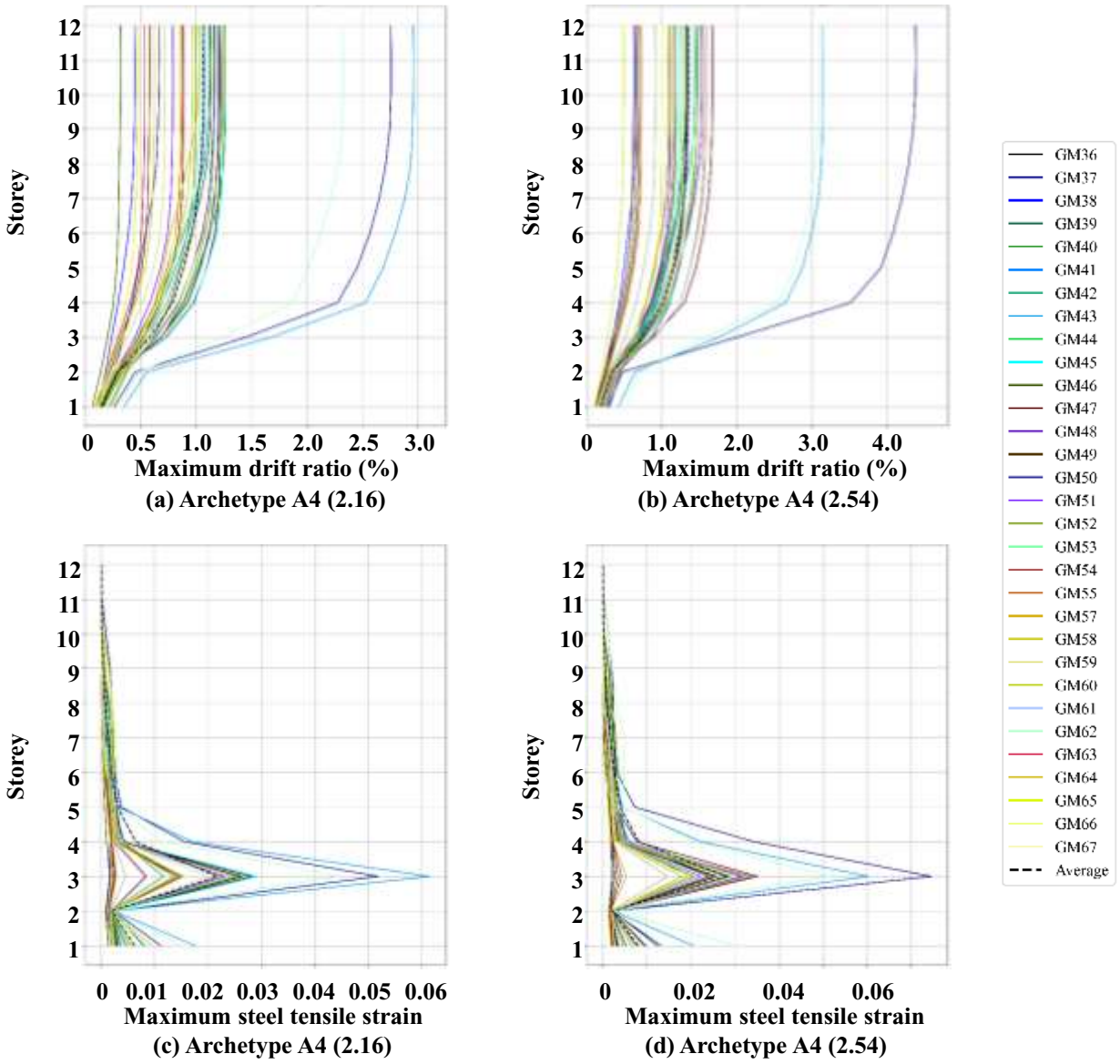

Figure 6-28 *Archetype* screening for A4: a) Maximum inter-storey drift under the first scale factor, b) Maximum inter-storey drift under the second scale factor, c) Maximum rebar tensile strain under the first scale factor, d) Maximum rebar tensile strain under the second scale factor

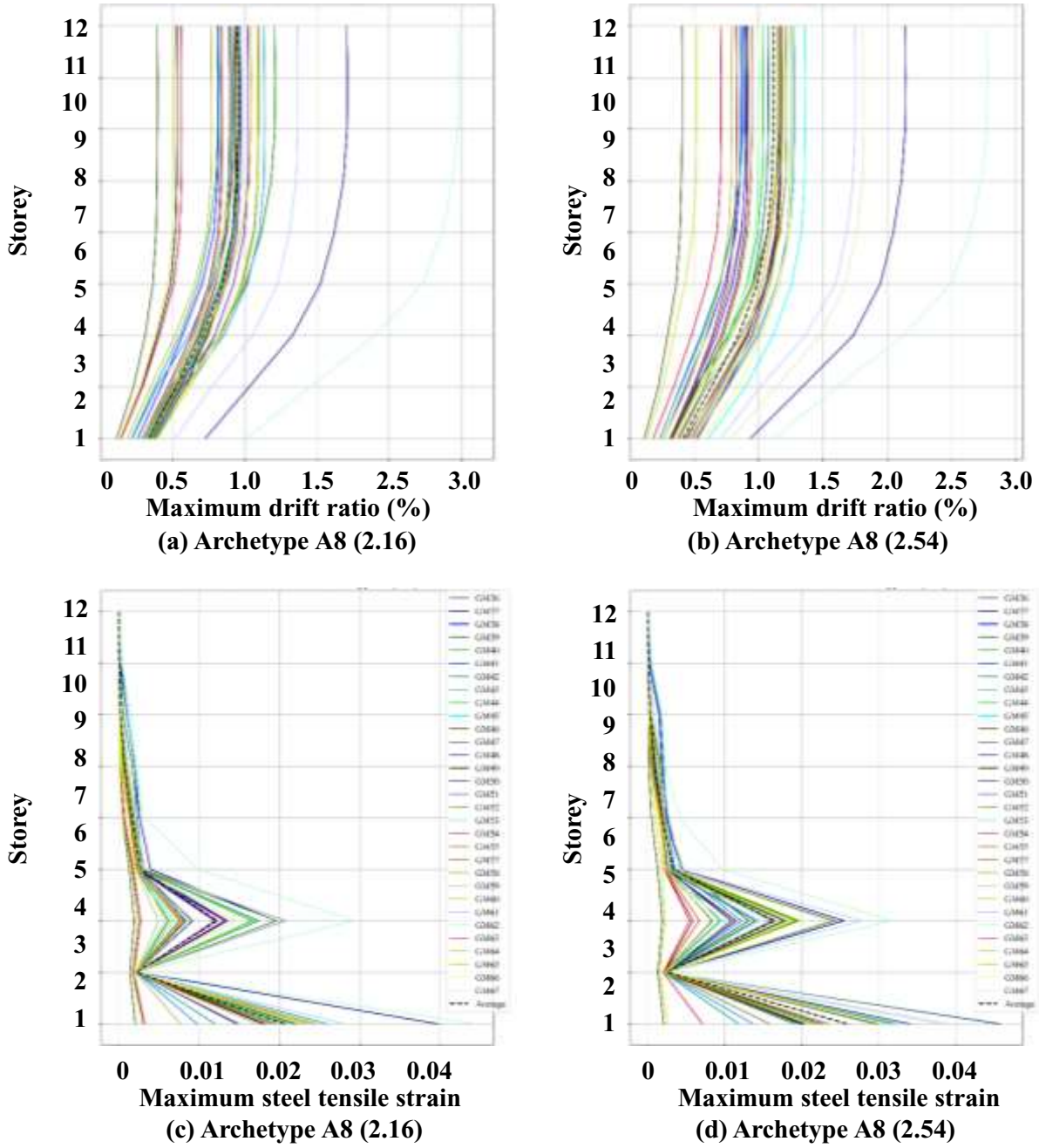

Figure 6-29 *Archetype* screening for A8: a) Maximum inter-storey drift under the first scale factor, b) Maximum inter-storey drift under the second scale factor, c) Maximum rebar tensile strain under the first scale factor, d) Maximum rebar tensile strain under the second scale factor

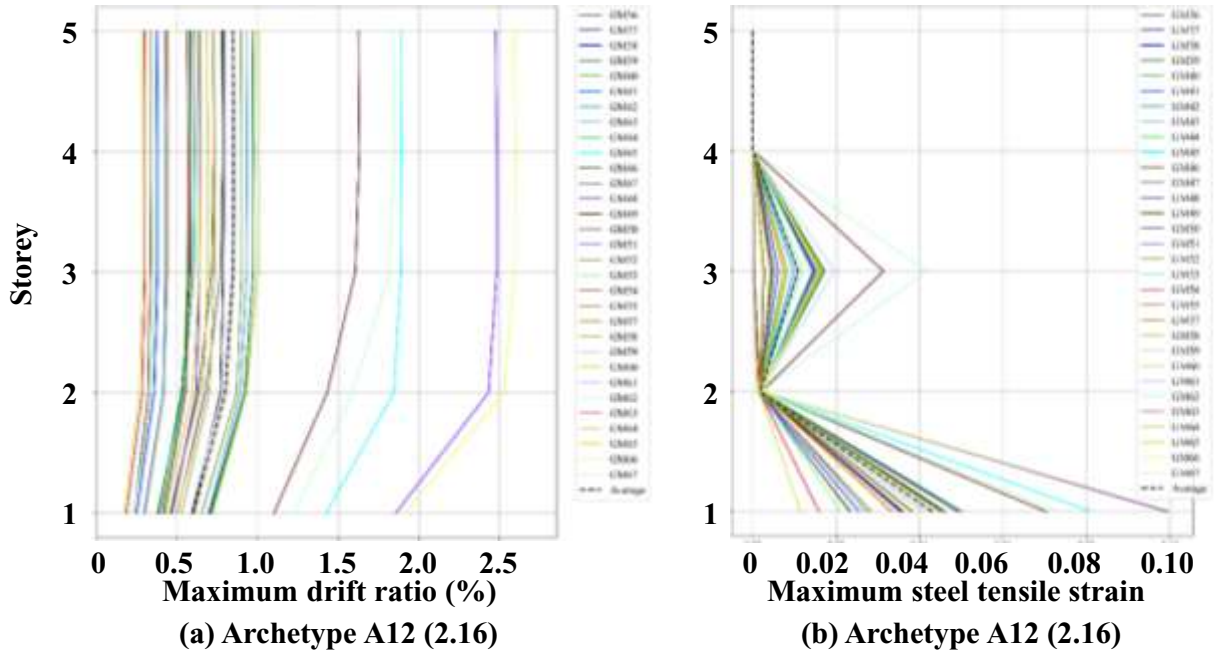

(a) Archetype A12 (2.16) **(b) Archetype A12 (2.16)**

Figure 6-30 *Archetype* screening for A12: a) Maximum inter-storey drift under the first scale factor, b) Maximum inter-storey drift under the second scale factor

6.3.3.5 IDA

IDA was conducted for all *archetype* models to develop the *IDA* curves. Then, using different local and global performance criteria, the median *performance level* spectral intensity ($\hat{S}_{PT}$) was calculated for each *archetype*. An illustration of the *IDA* curves and calculated *PMR* values for *Archetypes* A4, A8, and A12, which are part of *PG* 4, are presented in Figure 6-31 and Table 6-23.

Table 6-23 *PMR* of *archetype*s A4, A8, and A12 (*PG* 4)

Archetype	Performance Level	Performance Criteria		Collapse Mechanism (Local/Global)	Resultant *PMR*
		Rebar Strain	Inter-storey Drift (%)		
A4	*LS*	0.02	2.5	Local	2.1
	CP	0.1	4	Global	7.1
A8	*LS*	0.02	2.5	Local	2.2
	CP	0.1	4	Global	6.6
A12	*LS*	0.02	2.5	Local	1.3
	CP	0.1	4	Global	5.0

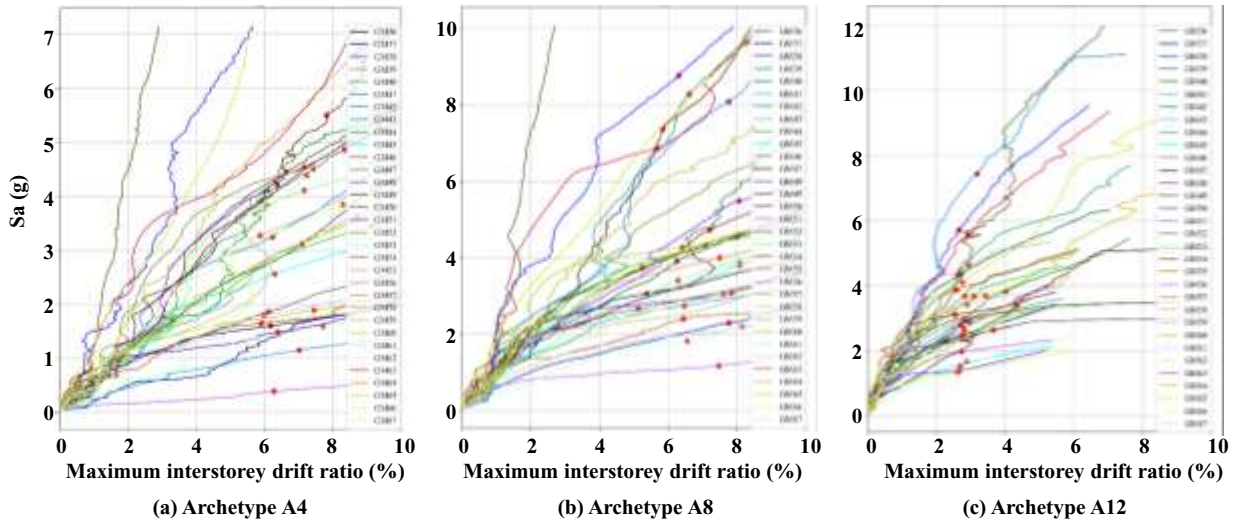

Figure 6-31 *IDA* curves for a) A4, b) A8, and c) A12

6.3.4 Performance Evaluation

6.3.4.1 Uncertainty Sources

According to Section 5.6, it is crucial to explicitly consider and properly propagate different sources of uncertainty to determine the total uncertainty associated with the system. In this study, the design requirements (β_{DR}), test data (β_{TD}), and modelling (β_{MDL}) uncertainties are assumed to be good (equal to 0.2). To determine the *record-to-record uncertainty* (β_{RTR},i) for each individual *archetype*, performance point intensities obtained in the *IDA* process are used.

6.3.4.2 Adjusted Performance Margin Ratios

The calculated *PMR*s in Section 6.3.3.5 were adjusted by *SSF* to obtain the *APMR*. In this study, the *SSF* in Eq. (6.1) is calculated based on the simplified function in FEMA P-695 for β_1 (i.e., Eq. (6.3)). $\bar{\varepsilon}_0(T)$ in Eq. (6.1) are assumed for Vancouver and Montreal, as shown in Figure 6-32. For computing the mean epsilon value for a selected ground motion set at the period of interest *T*, $\bar{\varepsilon}_r(T)$, ground motion prediction equations developed by Boore & Atkinson (2008) and Abrahamson et al. (2016) are used for crustal earthquake ground motions and subduction-zone earthquake ground motions (i.e., in-slab and interface), respectively. The calculated *APMR*s for *PG*s 2 and 4 are illustrated in Table 6-24 and Table 6-25.

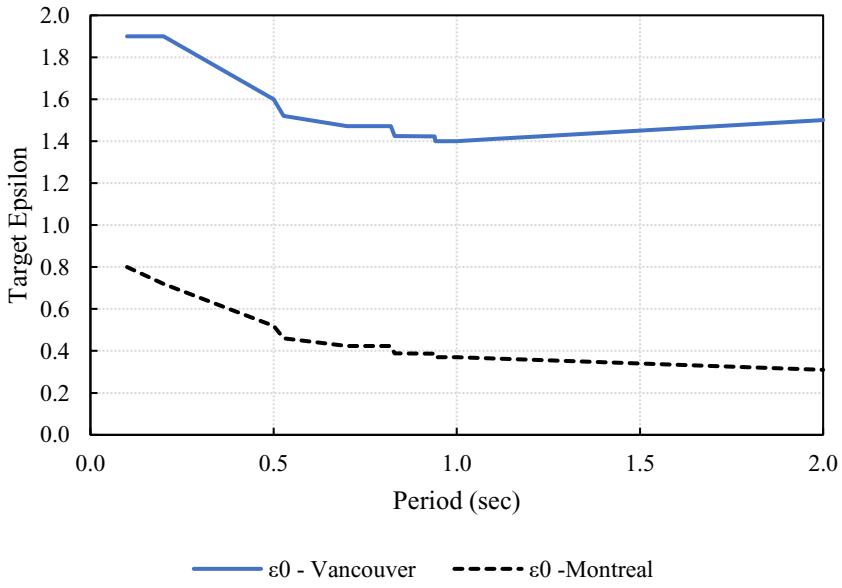

Figure 6-32 Target epsilon values for Vancouver and Montreal

Table 6-24 *SSF* of *archetypes* in PG 2 and PG 4

Performance Group	Abbreviation	SSF_{LS}	SSF_{CP}
PG 1	A22	1.1	1.1
	A18	1.1	1.1
	A14	1.1	1.1
PG 2	A24	1.3	1.3
	A20	1.2	1.2
	A16	1.1	1.1
PG 3	A6	1.0	1.0
	A10	1.0	1.0
PG 4	A12	1.1	1.1
	A8	1.0	1.0
	A4	1.0	1.0

Table 6-25 *PMR*s of *archetypes* in PG 1 to PG 4

PG	Archetype	PMR		APMR		Acceptable Performance Margin Ratios			
		LS	CP	LS	CP	APMR20% LS	APMR10% LS	APMR20% CP	APMR10% CP
PG1	A22	0.4	1.5	0.4	1.7	1.7		1.7	
	A18	0.5	1.3	0.6	1.5	1.7		1.8	
	A14	0.5	1.3	0.6	1.4	1.8		2.0	
	Average	**0.5**	**1.3**	**0.5**	**1.5**		**2.2**		**2.5**
PG2	A24	0.9	4.4	1.1	5.9	1.5		1.5	
	A20	1.4	4.7	1.7	5.6	1.5		1.7	
	A16	1.7	4.8	1.9	5.4	1.6		1.7	
	Average	**1.4**	**4.6**	**1.6**	**5.6**		**1.9**		**2.1**
PG3	A6	0.5	1.4	0.5	1.5	1.7		1.8	
	A10	0.5	1.2	0.6	1.2	1.6		1.7	
	Average	**0.5**	**1.3**	**0.5**	**1.3**		**2.1**		**2.3**
PG4	A12	1.3	5.0	1.4	5.6	1.4		1.6	
	A8	2.2	6.6	2.3	6.7	1.5		1.6	
	A4	2.1	7.1	2.2	7.2	1.6		1.7	
	Average	**1.9**	**6.2**	**1.9**	**6.5**		**1.8**		**2.1**

6.3.4.3 Evaluation Results

It can be seen from Table 6-25 that all *archetypes* in *PG*s 2 and 4 have sufficient margin against the *performance level* of *CP*. For *LS*, only *PG* 4 has the acceptable margin, while *PG* 2 fails to meet both individual and average performance criteria as specified in Section 5.7.4.

6.3.5 Summary Observations

Based on the *archetypes* developed in this study, the calculated *APMR* values for Life Safety *performance level* are not close to the acceptable values, indicating that the use of the rebar tensile strain of 0.02 (ten times the yield strain) seems to be too restrictive. Additionally, the *APMR* values for *CP performance level* are smaller than the acceptable values for *PG* 1 and *PG* 3, suggesting that this conventional concrete shear wall system has insufficient margin against collapse too. However, *PG* 2 and *PG* 4 for *CP performance level* are much greater than the acceptable values for *PG* 1 and *PG* 3, suggesting that this conventional concrete shear wall system has a sufficient margin against collapse.

6.4 Moderately Ductile Steel Concentrically Braced Frame System

In this section, the values of the R_d and R_o factors that are specified in the NBC 2020 for moderately ductile (Type MD) steel concentrically braced frames (CBFs) are evaluated using the *PBU procedure*. As specified in the procedure, *archetypes* were developed and categorized into several *performance groups*, depending on the site (seismic category), bracing configuration, building usage, number of storeys (total height of the structure), and irregularity conditions. The *archetypes* were designed in accordance with the provisions of the NBC 2020 and the CSA S16-19 standard. Detailed numerical models that are capable of simulating nonlinear responses including buckling and low-cycle fatigue fracture of bracing members, as well as flexural yielding and buckling of beams and columns, were developed. R_o was evaluated for each *archetype* using nonlinear static (pushover) analysis. The seismic performance of the *archetypes* was then evaluated using site representative ground motion ensembles. According to the procedure, this performance evaluation was performed in two phases: 1) a screening phase to determine whether the *archetypes* satisfy the *immediate occupancy*, *life safety*, and *CP* performance criteria; 2) for the *archetypes* not satisfying the performance criteria, a second phase in which *IDA* was performed, with a focus on both global and local seismic response parameters.

For the Type MD CBF system, the procedure was validated for three different building types:

1. Low-rise (2- and 3-storey) office buildings;
2. Mid-rise (4- to 14-storey) office buildings;
3. Mid-rise (6- to 10-storey) storage buildings;

As presented in the following section, 14 *performance groups* with 54 different *archetypes* are designed, modelled, and evaluated following the *PBU procedure*.

6.4.1 *Archetype* Development

As described in Table 6-26, 14 *performance groups* that included a total of 54 *archetypes* of steel concentrically braced frame structures were defined for this study. The grouping parameters included: 1) braced frame configuration, 2) design gravity load level, 3) design seismic load level, 4) building size and occupancy, 5) vertical irregularity condition, and 6) numbers of storeys.

Table 6-26 *Performance groups*

Conf.	Design load levels		Building size and Occupancy	Irregularity	Number of storeys	No. of *archetypes*	*PG*
	Gravity	Seismic					

IV	Low	SC3	Low-rise office	R	2, 3	2	*PG*1
			Mid-rise office	R	4, 6, 8, 10, 12, 14	6	*PG*2
				I	4, 6, 10, 14	4	*PG*3
		SC4	Low-rise office	R	2, 3	2	*PG*4
			Mid-rise office	R	4, 6, 8, 10, 12, 14	6	*PG*5
				I	4, 6, 10, 14	4	*PG*6
2X	Low	SC3	Mid-rise office	R	4, 6, 8, 10, 12, 14	6	*PG*7
				I	4, 6, 10, 14	4	*PG*8
		SC4	Mid-rise office	R	4, 6, 8, 10, 12, 14	6	*PG*9
				I	4, 6, 10, 14	4	*PG*10
	High	SC3	Mid-rise storage	R	4, 6, 10	3	*PG*11
		SC4	Mid-rise storage	R	4, 6, 10	3	*PG*12
1X	Low	SC3	Low-rise office	R	2, 3	2	*PG*13
		SC4	Low-rise office	R	2, 3	2	*PG*14

Three braced frame configurations were investigated in this study: 1) inverted V-bracing (IV), two-storey X-bracing (2X), and one-storey X-bracing (1X). Those braced frame configurations are illustrated in Figure 6-33 for a 4-storey building. As discussed later, IV and 2X braced frames were used for the mid-rise office and mid-rise storage buildings. One-storey X-bracing was used only in the low-rise office buildings, together with IV-braced frames. For some of the buildings, different bracing configurations were used in the two building orthogonal directions.

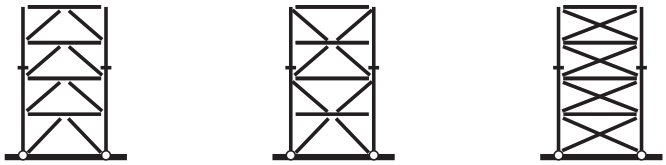

Figure 6-33 Inverted V-bracing (IV), two-storey X-bracing (2X), and one-storey X-bracing (1X) configurations for a 4-storey building

6.4.1.1 Gravity Load Level

As indicated in Table 6-26, two different levels of gravity loads have been considered for the buildings: low gravity loads corresponding to an office occupancy and a high gravity loading condition due to a storage occupancy.

6.4.1.2 Seismicity Level

Two seismic load conditions are considered for all building types: 1) moderate seismic conditions, for which the design spectral ordinates at periods of 0.2 s and 1.0 s are close to the upper limit for Seismic Category SC3, and 2) high seismic conditions, for which the design spectral ordinates at periods of 0.2 s and 1.0 s fall within the range for Seismic Category SC4. Two different sites were selected for the two seismic conditions: a site located in Montreal, QC, for the moderate seismic loading condition, and a site located in Vancouver, BC, for the high seismic loading condition. More details about the sites are given in Appendix C.

6.4.1.3 Building Plan and Frame Selection

Three different building sizes and occupancies commonly encountered in Canada for steel building structures were considered in this study, namely: 1) low-rise office buildings, 2) mid-rise office buildings, and 3) mid-rise storage buildings.

Low-rise office buildings

The low-rise office buildings are characterized by a large footprint, and buildings with 2 and 3 storeys were examined. The height of the first storey is 4.8 m, whereas a 4.0 m storey height is used for the upper levels. The plan view and braced frame elevation of the buildings are illustrated in Figure 6-34 for Montreal (SC3). In these buildings, the roof structure consists of 38-mm-deep bare steel deck panels placed on equally spaced open-web steel joists. The floor structure is a 65-mm-thick concrete slab acting compositely with 76-mm-deep steel deck panels (total slab thickness = 141 mm) supported on composite W-shape beams supported by the columns or composite W-shape girders spanning between the columns. On the building perimeter, the exterior walls are supported on the foundation wall at the grade level. At the upper levels, the exterior walls rest on the floor slab that extends 400 mm outside the exterior column centre lines.

As shown, the floor plan comprises a core area that covers the 7 interior bays in the N-S direction of the 9.3-m-wide E-W central bay. The remaining floor area is used for office space. The core area includes services such as washrooms, meeting rooms, corridors, elevators, and stairways. That area is designed for an occupancy live load of 4.8 kPa. The office space on the floor is designed for an occupancy live load of 2.4 kPa.

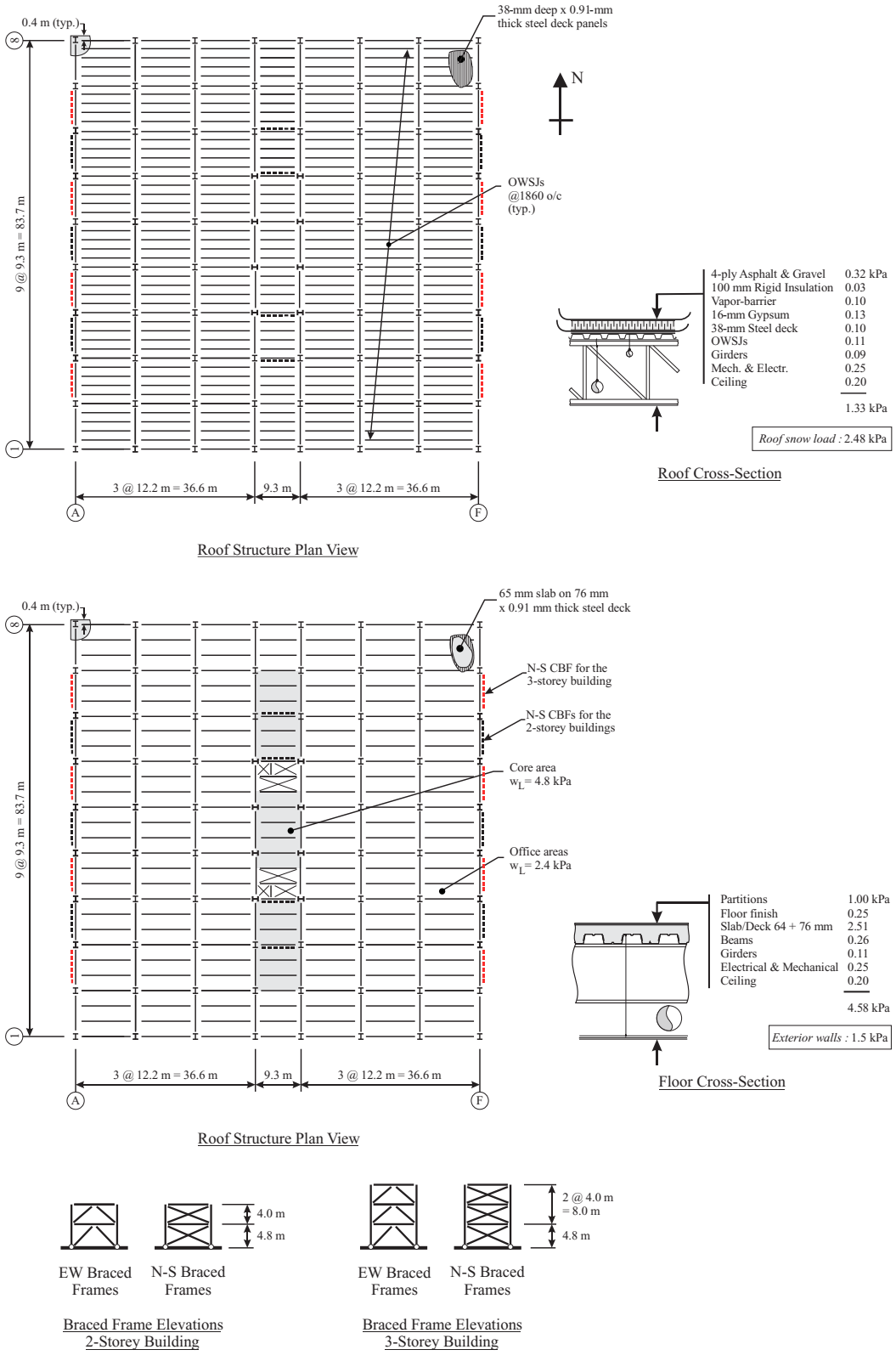

Figure 6-34 Low-rise office buildings in Montreal (SC3)

As indicated in Figure 6-34, the number of braced bays in the low-rise office buildings varies depending on the location (Montreal *vs* Burnaby) and the number of storeys. In addition, two different bracing configurations are used: IV-bracing located in the 9.3-m-wide central bay in the E-W direction as this configuration allows for building occupants to circulate along the 9.3-m-wide central bay, and single-storey X-braced frames located along the East and West exterior column lines in the N-S direction. For the latter, the type of X-bracing also depends on the building location: tension-compression (TC) bracing for Burnaby (SC4) and tension-only (TO) bracing for Montreal (SC3). Bracing configurations and types are summarized in Table 6-27.

Table 6-27 Number and configuration of the braced frames in the low-rise office buildings

Number of Storeys	Seismic Category	Direction	Bracing Configuration	Number of Braced Frames
2	SC3	EW	IV	4
2	SC3	NS	1X (TO)	6
3	SC3	EW	IV	4
3	SC3	NS	1X (TO)	8
2	SC4	EW	IV	6
2	SC4	NS	1X (TC)	8
3	SC4	EW	IV	6
3	SC4	NS	1X (TC)	8

Mid-rise office buildings

The mid-rise office buildings are characterized by a smaller footprint compared to that of the low-rise office buildings. Building structures having from 4 to 14 storeys were examined. The structure plan view for these buildings is illustrated in Figure 6-35. For these buildings, two vertical irregularity conditions were examined. For the regular building cases (R), the first storey height is 4.8 m, whereas the storey height for the other storeys is 4.0 m (see Fig. 4-7). For the irregular building cases (I), the first storey height is increased to 6.6 m whereas the other storey height remained equal to 4.0 m.

The roof structure of the mid-rise office buildings differs from that of the low-rise office buildings, as it is constructed with a 65 mm concrete slab acting compositely with a 51 mm deep steel deck (total slab thickness = 116 mm). The deck-slab assembly is supported on W-shaped steel beams that are supported on W-shaped girders or the columns. The usage of the floor area is the same as in the low-rise office buildings.

As shown in Figure 6-35, IV braced frames are used in the core area along the E-W direction whereas two-storey X braced frames are used along the exterior walls in the N-S direction. The layout of the braced frames in the mid-rise buildings are summarized in Table 6-28.

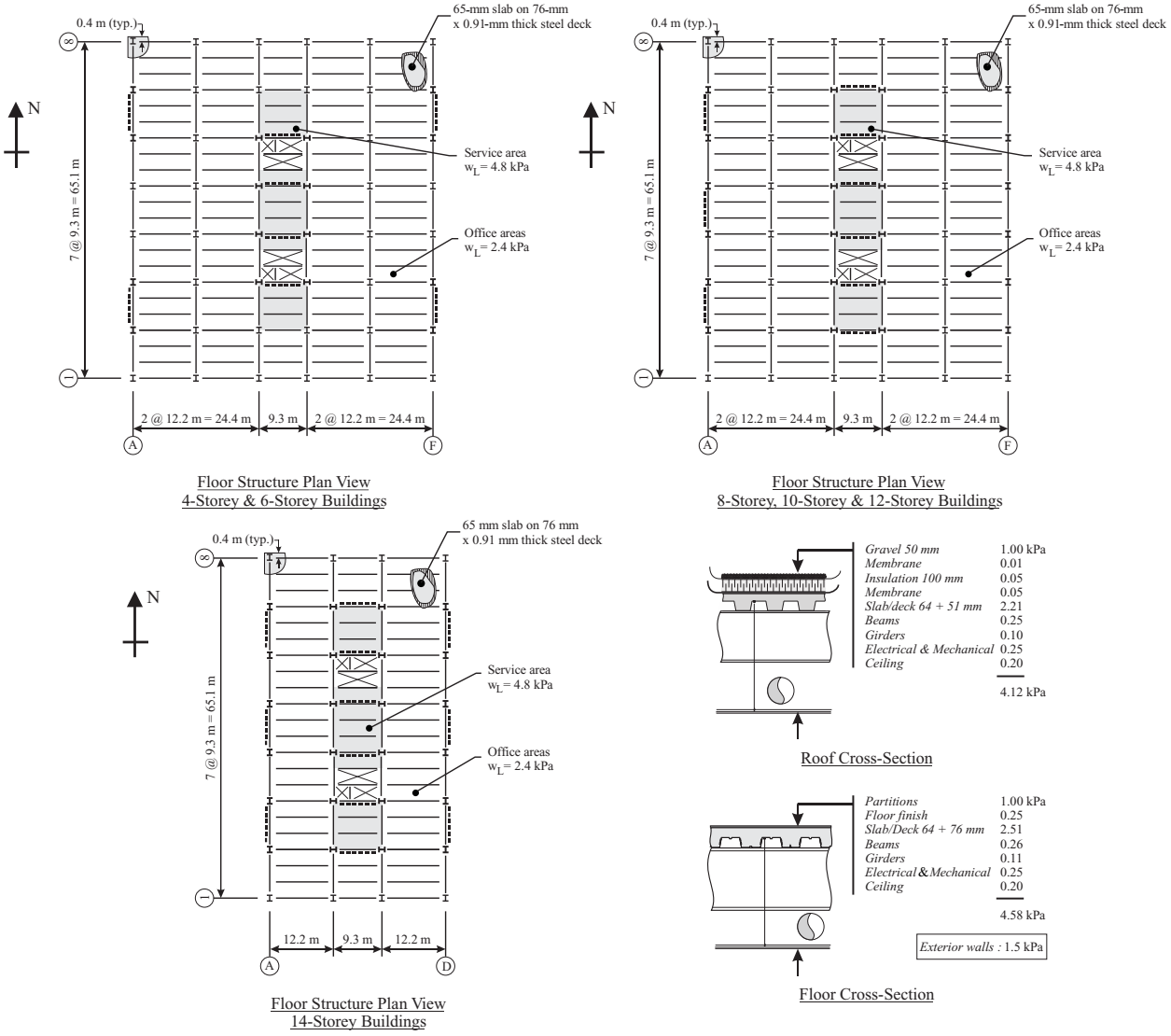

Figure 6-35 Plan view of the mid-rise office buildings

Table 6-28 Layout of braced frames in mid-rise office buildings

No. of storeys	Irregularity condition	Seismic category	Direction	Conf.	No. of building spans	No. of braced frames
4	R	SC3	EW	IV	5	4
4	R	SC3	NS	2X	7	4
4	R	SC4	EW	IV	5	4
4	R	SC4	NS	2X	7	4
4	I	SC3	EW	IV	5	4
4	I	SC3	NS	2X	7	4
4	I	SC4	EW	IV	5	4
4	I	SC4	NS	2X	7	4
6	R	SC3	EW	IV	5	4
6	R	SC3	NS	2X	7	4
6	R	SC4	EW	IV	5	4
6	R	SC4	NS	2X	7	4
6	I	SC3	EW	IV	5	4
6	I	SC3	NS	2X	7	4
6	I	SC4	EW	IV	5	4
6	I	SC4	NS	2X	7	4
8	R	SC3	EW	IV	5	4
8	R	SC3	NS	2X	7	4
8	R	SC4	EW	IV	5	6
8	R	SC4	NS	2X	7	6
10	R	SC3	EW	IV	5	4
10	R	SC3	NS	2X	7	4
10	R	SC4	EW	IV	5	6
10	R	SC4	NS	2X	7	6
10	I	SC3	EW	IV	5	4
10	I	SC3	NS	2X	7	4
10	I	SC4	EW	IV	5	6
10	I	SC4	NS	2X	7	6
12	R	SC3	EW	IV	5	4
12	R	SC3	NS	2X	7	4
12	R	SC4	EW	IV	5	6
12	R	SC4	NS	2X	7	6
14	R	SC3	EW	IV	5	4
14	R	SC3	NS	2X	7	4
14	R	SC4	EW	IV	3	6
14	R	SC4	NS	2X	7	6
14	I	SC3	EW	IV	5	4
14	I	SC3	NS	2X	7	4
14	I	SC4	EW	IV	3	6
14	I	SC4	NS	2X	7	6

Storage buildings

As shown in Figure 6-36, the mid-rise storage buildings considered in this study have a square footprint with columns spaced 9 m o/c in both orthogonal directions. Buildings having 4, 6, 8, and 10 storeys were examined. The braced frame elevations of these buildings are identical to those shown in Figure 6-36. The storey height distribution is identical to the low-rise or regular mid-rise office buildings, i.e., 4.8 m for the first level and 4.0 m for the upper levels. The roof and floor structures are the same as those of the mid-rise office buildings. The usage of the building floor area is only for storage designed for an occupancy live load of 7.6 kPa. Two-storey X (2X) braced frames placed along the exterior walls are used in both the EW and NS directions. Due to the similarities along both directions, only the EW direction is analyzed for the storage buildings. The number of braced bays for each location is illustrated in Figure 6-36 and described in Table 6-29.

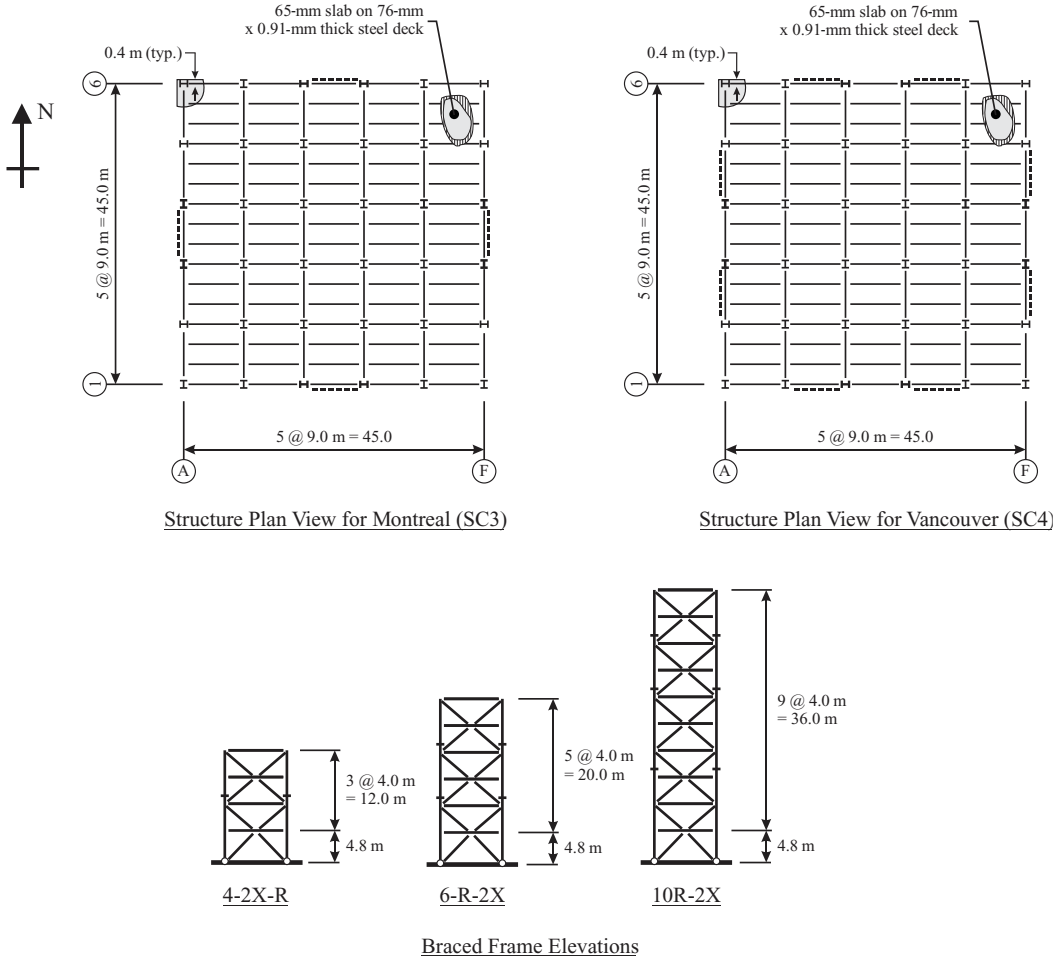

Figure 6-36 Structure plan views and braced frame elevations for the mid-rise storage buildings

Table 6-29 Layout of braced frames in storage buildings

No. of storeys	Seismic category	Direction	Conf.	No. of building spans	No. of braced frames
4	SC3	EW	2X	5	2
4	SC3	NS	2X	5	2
6	SC3	EW	2X	5	2
6	SC3	NS	2X	5	2
10	SC3	EW	2X	5	2
10	SC3	NS	2X	5	2
4	SC4	EW	2X	5	4
4	SC4	NS	2X	5	4
6	SC4	EW	2X	5	4
6	SC4	NS	2X	5	4
10	SC4	EW	2X	5	4
10	SC4	NS	2X	5	4

6.4.2 *Archetype* Modelling

The nonlinear static (pushover) analyses and NLTHA were conducted using the Open System for Earthquake Engineering Simulation, OpenSees. The numerical model included one of the braced frames of the *archetype* buildings along the direction being examined, together with two leaning columns to account for global P-delta effects due to gravity loads carried by the portion of the building laterally stabilized by the braced frame studied. Gravity columns of the building structures were not included in the models. Although the braced frames studied are planar, three-dimensional models were used to reproduce the out-of-plane buckling response of the bracing members and columns.

6.4.2.1 Modelling of Bracing Members and Gusset Plate Assemblies

For the bracing members, the modelling approach proposed by Karamanci & Lignos (2014) was used. This modelling approach allows for simulating the strength loss of the brace member due to the low-cycle fatigue in addition to the global buckling phenomenon and material nonlinearity. This low-cycle fatigue failure response was simulated using the fatigue material model proposed by Uriz et al. (2008), which is available in OpenSees. This material model is based on a linear strain accumulation rule in accordance with the Coffin-Manson relationship (Manson 1965) in the logarithmic domain. The parameters for this model, calibrated to a number of past experimental results of steel braces by Karamanci & Lignos (2014), were adopted. The following modelling details and parameters have been proposed for steel braces with HSS modelled with displacement-based beam-column elements: 1) 8 elements along the brace length; 2) Gauss-Lobatto integration scheme with 5 integration points; 3) the number of fibres along the width of the cross-section =

10; 4) the number of fibres through the thickness = 4; 5) Menegotto-pinto steel material parameters, b = 0.001, R_0 = 22.0, cR_1 = 0.925, cR_2 = 0.25, a_1 = 0.03, a_2 = 22, a_3 = 0.020, a_4 = 22; 6) fatigue material parameters, ε_o = Eq. 6.1 shown below, and m = -0.300; and 7) global geometric imperfection with the maximum amplitude of 0.3% of the brace effective length. Fibre discretization of the brace member cross-section is illustrated in Figure 6-37.

$$\varepsilon_0 = 0.291 \cdot \left(\frac{kL}{r}\right)^{-0.484} \cdot \left(\frac{w}{t}\right)^{-0.613} \cdot \left(\frac{E}{F_y}\right)^{0.303} \tag{6.7}$$

where kL/r is the brace global slenderness ratio with kL being the effective length of the brace, taken as the o/c length between "$2t_g$" plastic hinges in the gusset plates, and r is the moment of gyration with respect to the buckling axis, E and F_y are Young's modulus and the yield stress of the steel brace, respectively, and w/t is the local slenderness ratio of the HSS cross section determined per AISC 360-10 (ANSI/AISC 2016b). Note that brace fracture was considered only in the nonlinear time history analyses and was not considered in the nonlinear static (pushover) analyses.

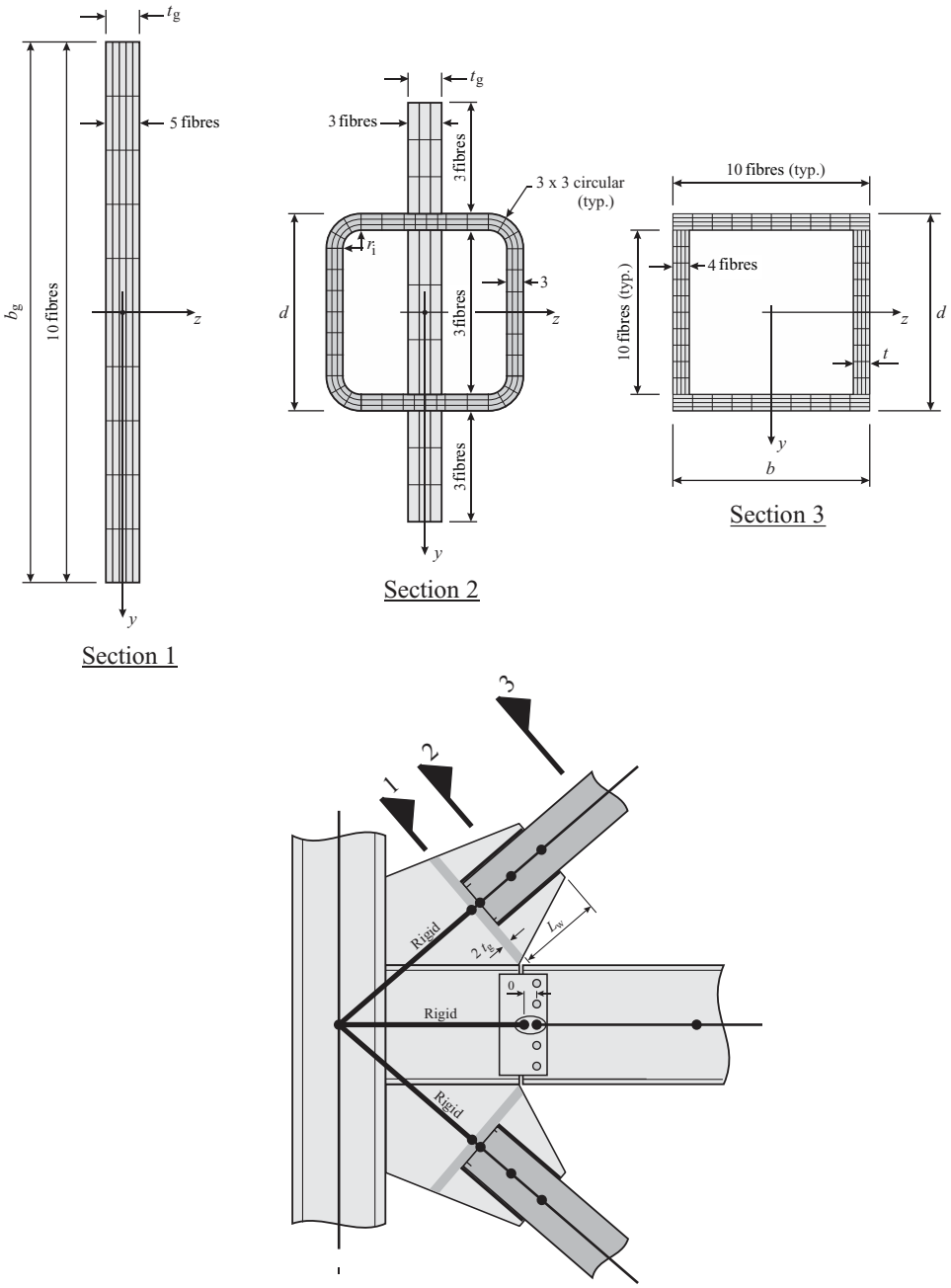

Figure 6-37 Discretization of the cross-section of the bracing members and gusset plate assemblies

Given that the modelling approach and the associated parameters proposed by Karamanci and Lignos (2014) to simulate brace low-cycle fatigue fracture response are directly adopted in this study, no model validation for this model is required. Nonetheless, the fracture simulation response was investigated for a representative experimental result, which was also used by Karamanci and Lignos (2014) in order to validate our model implementation. Specimen no. HSS1-1 tested by Fell

et al. (2009) was used for this purpose. The specimen was fabricated from ASTM A500, gr. B, HSS 101x101x6.4. For model validation, the geometrical dimensions and the yield stress as reported by Fell et al. were used in the model. The comparison of brace axial force–axial displacement relationships between the test results and the simulation is shown in Figure 6-38. Although the simulation slightly underpredicts the drift at which fracture occurs, this result confirms the capacity of the model for predicting load-deformation response and brace fracture.

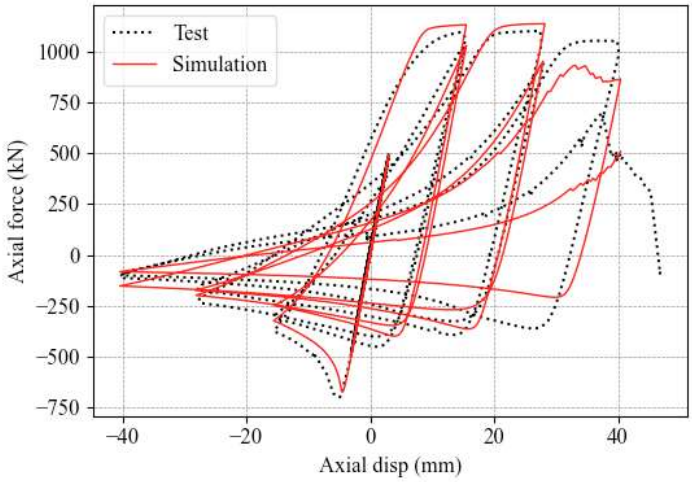

Figure 6-38 Simulation of the cyclic inelastic response of Specimen HSS1-1 from Fell et al. (2009)

The gusset plates can be modelled using zero-length rotational spring elements exhibiting nonlinear rotational response, as used by Karamanci and Lignos (2014) in their frame simulations. Alternatively, they can be modelled using force-based nonlinear beam-column elements with fibre discretization to better represent the interaction between axial and flexural stress responses. In this study, the second approach was adopted. The adopted model is illustrated in Figure 6-37. As shown in Figure 6-37, the "2 t_g" hinge zone was modelled using ten fibres across the width and five fibres across the gusset plate thickness. Over the weld length L_w, fibre discretization was used for both the HSS and gusset plates. In this case, the brace model included circular fibres to represent the HSS rounded corners.

6.4.2.2 Modelling of Beams and Columns

Modelling of the beams and the columns was similar to the brace modelling except that low-cycle fatigue failure was not simulated and force-based nonlinear beam-column elements were employed instead of displacement-base elements. The Steel02 material was used with F_y = 385 MPa, R_o = 30, cR_1 = 0.925, cR_2 = 0.15, b = 0.002, a_1 = a_3 = 0.4, and a_2 = a_4 = 22. Residual stresses in accordance with (Galambos and Ketter (1959) were assigned to the material. In each storey, five

elements were used with five integration points and Gauss-Lobatto integration scheme. Column bases were assumed to be fixed to represent the fixity restraint provided by the anchor rods. Splice connections were also assumed to be continuous for in-plane and out-of-plane flexure.

6.4.2.3 Modelling of P-Delta Columns

P-delta columns were modelled using the co-rotational truss elements to reproduce geometric nonlinearities. At every storey along the column height, the nodes of the P-delta columns and braced frame columns were assigned the same displacements along the X-directions.

6.4.2.4 Other Modelling Assumptions

Co-rotational geometric transformation was used to accurately reproduce member buckling as well as P-delta effects on the response. In the model, 2% Rayleigh damping was used in the first two modes for buildings up to 4 storeys and in the first and third modes for taller buildings. The damping stiffness was obtained using the mass proportional factor and committed stiffness proportional factor. Horizontal masses were assigned at the nodes of the P-delta columns.

6.4.3 Nonlinear Analysis

6.4.3.1 Performance Criteria

In both static and dynamic analyses, the capacity of the *archetypes* needs to be calculated based on the desired *performance level* of the system quantified through different local and global performance criteria. Regardless of the desired *performance levels* for the steel braced frames, which is assumed to be between *LS* and *CP* in the NBC 2020 (Devall 2003, NRC 2022), the performance criteria used in this study cover all three *performance level*s of *IO*, *LS*, and *CP* to find out the margin ratio of the system against each one. The selected global and local performance criteria are further discussed in the following paragraphs.

Table 6-30 summarizes the adopted global and local performance criteria. As one of the global performance criteria in both static (pushover) analysis and dynamic analyses (response history analysis in the screening and *IDA*), drift ratios of 1.0%, 2.5%, and 4.0% were selected for *IO*, *LS*, and *CP performance levels*, respectively. The 1.0% and 2.5% drift ratios were selected as per the NBC 2020 seismic design requirements for post-disaster buildings (with interpreted *performance level* of *IO*) and normal importance buildings (with interpreted *performance level* of *LS*), respectively. The 4.0% drift limit for the *CP performance level* is in agreement with the drift limit of 3.0% to 4.5% suggested by PEER/TBI (PEER 2017). While facing numerical problems and non-convergence issues are very common in nonlinear time history analysis, such issues did not occur in the analyses within the drift range specified above, as discussed later. Other global criteria such as 20% loss in the base shear strength or flat line formation in the *IDA* curve Vamvatsikos

and Cornell (2002) could be adopted. However, these are not considered in this study since they were found to be not critical.

The local criteria are defined based on limitations for plastic axial deformations of the braces. In this study, the plastic deformation limits calculated from Table C3.4 of AISC 342-22 (AISC 2022) were used as local criteria for static and dynamic analyses (see Table 6-30). These deformation limits have been developed based on various experimental studies. For other structural members such as beams and columns as well as connections, deformation limits are not considered since their failures are prevented in the design and appropriate detailing. In Table 6-30, Δ_c is the axial deformation at expected buckling strength, Δ_T is the axial deformation at expected tensile yield strength, and n_c and n_T are parameters for compression and tension, respectively, both of which are functions of both local and global slenderness and steel material grade.

Table 6-30 Global and local performance criteria

	IO	*LS*	*CP*
Max. storey drift ratio	1.0 %	2.5 %	4.0 %
Max. brace compressive plastic deformation	$\min(1.5\Delta_C, 0.7n_C\Delta_C)$	$0.7n_C\Delta_C$	$n_C\Delta_C$
Max. brace tensile plastic deformation	$\min(1.5\Delta_T, 0.7n_T\Delta_T)$	$0.7n_T\Delta_T$	$n_T\Delta_T$

6.4.3.2 Selected Ground Motions

An ensemble of site-representative ground motion records was created for each location, Burnaby and Montreal. For each site, the ground motions were selected based on the magnitude-distance scenarios dominating the seismic hazard. For Vancouver, a total of 44 ground motion records were selected: 11 from crustal earthquakes and 33 from subduction-zone earthquakes. Out of the 33 ground motions, 11 were from deep in-slab earthquakes and 22 were from interface subduction earthquakes. For Montreal, a total of 32 ground motions all from crustal earthquakes were selected. More details about the selected ground motion records are given in Appendix C.

6.4.3.3 Pushover Analysis

The pushover analysis was conducted for all *archetypes* to calculate the required parameters (R_o and μ_T) as well as to assess the nonlinear behaviour of the models before going to the laborious time history analyses.

All of the obtained parameters R_o and μ_T are summarized in Table 6-31. It can be noted that R_o was found to be greater than the NBC value of 1.3 in all *archetype* models. It ranges from 1.7 to 2.3. The results indicate that the current R_o value for the moderately ductile steel braced frames specified in the NBC 2020 is on the conservative side and has a relatively great margin against the

actual overstrength. The period-based ductility values calculated based on each *performance level* limit ($\mu_{T,IO}$, $\mu_{T,LS}$, and $\mu_{T,CP}$) are going to be used in the performance evaluation at the end of the *PBU* methodology, especially for calculating the *SSF*. As given in Table 6-31, some period-based ductility values are less than 1.0. Those are going to be replaced with 1.0 since the *SSF* cannot be calculated with those values less than 1.0

Table 6-31 Pushover analysis results

PG	Model	Overstrength Calculations					Ductility Calculations						
		V_{max} (kN)	V_d (kN)	R_o	R_o (Code)	Status	$\delta_{u\text{-}IO}$ (mm)	$\delta_{u\text{-}LS}$ (mm)	$\delta_{u\text{-}CP}$ (mm)	$\delta_{y,eff}$ (mm)	$\mu_{T\text{-}IO}$	$\mu_{T\text{-}LS}$	$\mu_{T\text{-}CP}$
1	L2R-IV-3	3310	1590	2.1	1.3	Pass	23	60	87	19	1.3	3.2	4.7
	L3R-IV-3	4117	2135	1.9	1.3	Pass	41	89	108	30	1.4	3.0	3.7
					PG:	Pass							
2	M4R-IV-3	2477	1252	2.0	1.3	Pass	47	86	116	31	1.5	2.8	3.7
	M6R-IV-3	2526	1320	1.9	1.3	Pass	82	163	193	49	1.7	3.3	3.9
	M8R-IV-3	2264	1203	1.9	1.3	Pass	102	153	208	59	1.7	2.6	3.5
	M10R-IV-3	2305	1204	1.9	1.3	Pass	148	246	270	68	2.2	3.6	4.0
	M12R-IV-3	2532	1433	1.8	1.3	Pass	185	265	297	101	1.8	2.6	2.9
	M14R-IV-3	2999	1669	1.8	1.3	Pass	249	372	403	141	1.8	2.6	2.9
					PG:	Pass							
3	M4I-IV-3	2382	1164	2.0	1.3	Pass	58	132	154	32	1.8	4.1	4.8
	M6I-IV-3	2591	1306	2.0	1.3	Pass	82	168	200	58	1.4	2.9	3.5
	M10I-IV-3	2070	1198	1.7	1.3	Pass	143	215	247	75	1.9	2.9	3.3
	M14I-IV-3	2997	1671	1.8	1.3	Pass	254	365	393	150	1.7	2.4	2.6
					PG:	Pass							
4	L2R-IV-4	3417	1608	2.1	1.3	Pass	23	68	92	29	0.8	2.3	3.1
	L3R-IV-4	4136	2411	1.7	1.3	Pass	44	91	110	47	0.9	1.9	2.4
					PG:	Pass							
5	M4R-IV-4	4458	2441	1.8	1.3	Pass	63	89	121	58	1.1	1.5	2.1
	M6R-IV-4	4600	2617	1.8	1.3	Pass	96	151	195	83	1.1	1.8	2.3
	M8R-IV-4	3814	2083	1.8	1.3	Pass	125	176	205	152	0.8	1.2	1.3
	M10R-IV-4	3972	2197	1.8	1.3	Pass	169	217	265	200	0.8	1.1	1.3
	M12R-IV-4	3882	2192	1.8	1.3	Pass	218	316	350	217	1.0	1.5	1.6
	M14R-IV-4	2914	1532	1.9	1.3	Pass	234	333	375	343	0.7	1.0	1.1
					PG:	Pass							
6	M4I-IV-4	4580	2416	1.9	1.3	Pass	68	100	160	72	0.9	1.4	2.2
	M6I-IV-4	4616	2634	1.8	1.3	Pass	102	205	262	104	1.0	2.0	2.5
	M10I-IV-4	4004	2196	1.8	1.3	Pass	174	223	273	220	0.8	1.0	1.2
	M14I-IV-4	2948	1531	1.9	1.3	Pass	249	369	406	370	0.7	1.0	1.1
					PG:	Pass							

Table 6-31 Pushover analysis results (continued)

PG	Model	Overstrength Calculations					Ductility Calculations						
		V_{max} (kN)	V_d (kN)	R_o	R_o (Code)	Status	$\delta_{u\text{-}IO}$ (mm)	$\delta_{u\text{-}LS}$ (mm)	$\delta_{u\text{-}CP}$ (mm)	$\delta_{y,eff}$ (mm)	$\mu_{T\text{-}IO}$	$\mu_{T\text{-}LS}$	$\mu_{T\text{-}CP}$
7	M4R-2X-3	2705	1252	2.2	1.3	Pass	50	82	95	35	1.4	2.3	2.7
	M6R-2X-3	2753	1301	2.1	1.3	Pass	86	152	185	54	1.6	2.8	3.4
	M8R-2X-3	2686	1203	2.2	1.3	Pass	112	205	234	71	1.6	2.9	3.3
	M10R-2X-3	2610	1196	2.2	1.3	Pass	169	249	279	87	1.9	2.9	3.2
	M12R-2X-3	2855	1433	2.0	1.3	Pass	218	294	330	116	1.9	2.5	2.9
	M14R-2X-3	3251	1669	1.9	1.3	Pass	285	401	423	135	2.1	3.0	3.1
					PG:	Pass							
8	M4I-2X-3	2663	1159	2.3	1.3	Pass	61	111	142	42	1.5	2.7	3.4
	M6I-2X-3	2790	1274	2.2	1.3	Pass	90	157	189	63	1.4	2.5	3.0
	M10I-2X-3	2567	1198	2.1	1.3	Pass	168	283	340	84	2.0	3.4	4.0
	M14I-2X-3	3262	1671	2.0	1.3	Pass	300	412	438	166	1.8	2.5	2.6
					PG:	Pass							
9	M4R-2X-4	4318	2349	1.8	1.3	Pass	77	101	119	57	1.4	1.8	2.1
	M6R-2X-4	4424	2544	1.7	1.3	Pass	105	168	204	88	1.2	1.9	2.3
	M8R-2X-4	4565	2052	2.2	1.3	Pass	151	247	276	184	0.8	1.3	1.5
	M10R-2X-4	3897	2075	1.9	1.3	Pass	197	252	276	199	1.0	1.3	1.4
	M12R-2X-4	4172	2161	1.9	1.3	Pass	267	366	452	238	1.1	1.5	1.9
	M14R-2X-4	3264	1495	2.2	1.3	Pass	283	409	452	390	0.7	1.0	1.2
					PG:	Pass							
10	M4I-2X-4	4493	2330	1.9	1.3	Pass	67	99	118	71	0.9	1.4	1.7
	M6I-2X-4	4709	2565	1.8	1.3	Pass	125	158	178	107	1.2	1.5	1.7
	M10I-2X-4	3927	2090	1.9	1.3	Pass	192	249	275	219	0.9	1.1	1.3
	M14I-2X-4	3251	1504	2.2	1.3	Pass	295	413	465	416	0.7	1.0	1.1
					PG:	Pass							

Table 6-31 Pushover analysis results (continued)

PG	Model	Overstrength Calculations					Ductility Calculations						
		V_{max} (kN)	V_d (kN)	R_o	R_o (Code)	Status	$\delta_{u\text{-}IO}$ (mm)	$\delta_{u\text{-}LS}$ (mm)	$\delta_{u\text{-}CP}$ (mm)	$\delta_{y,eff}$ (mm)	$\mu_{T\text{-}IO}$	$\mu_{T\text{-}LS}$	$\mu_{T\text{-}CP}$
11	S4R-2X-3	4568	2397	1.9	1.3	Pass	60	99	125	33	1.8	3.0	3.8
	S6R-2X-3	5017	2511	2.0	1.3	Pass	108	137	155	52	2.1	2.6	3.0
	S10R-2X-3	4574	2505	1.8	1.3	Pass	193	253	278	72	2.7	3.5	3.9
					PG:	Pass							
12	S4R-2X-4	4656	2506	1.9	1.3	Pass	65	100	125	67	1.0	1.5	1.9
	S6R-2X-4	5523	2750	2.0	1.3	Pass	117	221	304	116	1.0	1.9	2.6
	S10R-2X-4	5937	3154	1.9	1.3	Pass	219	262	292	198	1.1	1.3	1.5
					PG:	Pass							
13	L2R-1XC-3	1900	1060	1.8	1.3	Pass	20	77	100	16	1.2	4.7	6.2
	L2R-1XH-3	1865	1060	1.8	1.3	Pass	20	56	66	16	1.2	3.5	4.2
	L3R-1XC-3	1856	1067	1.7	1.3	Pass	19	87	108	29	0.7	3.0	3.7
	L3R-1XH-3	1814	1067	1.7	1.3	Pass	19	74	83	28	0.7	2.6	2.9
					PG:	Pass							
14	L2R-1XC-4	2673	1206	2.2	1.3	Pass	38	57	70	29	1.3	1.9	2.4
	L2R-1XH-4	2524	1206	2.1	1.3	Pass	34	51	61	28	1.2	1.8	2.2
	L3R-1XC-4	4103	1784	2.3	1.3	Pass	59	121	159	62	1.0	2.0	2.6
	L3R-1XH-4	3903	1784	2.2	1.3	Pass	49	101	138	59	0.8	1.7	2.4
					PG:	Pass							

6.4.3.4 Screening

Following the screening procedure as presented in Section 5.5.3, individual ground motions (GMs) of each ground motion set selected for the western (i.e., 44 GMs) and the eastern (i.e., 32 GMs) Canada design sites were first scaled to have the spectral acceleration equal to the CLE ground motion intensity at the design fundamental period. Then, the ground motions were further scaled up by a factor of 2.16, which corresponds to the acceptable *adjusted PMR* calculated using a 10% conditional exceedance probability and a total uncertainty of $\beta_{TOT} = 0.6$. With these scaled ground motions, NLTHA was performed.

Table 6-32 summarizes the screening results. For each *archetype*, the total number of ground motions (i.e., Rec_t) and the number of ground motions under which the structural response passed the *acceptance criteria* (i.e., Rec_p) are shown. Given that the objective of the NBC 2020 is *structural safety*, *performance level* limits for *LS* are considered as the *acceptance criteria*. The nonlinear time history analyses suggest that, in all *archetypes*, the *acceptance criteria* were not satisfied under almost all ground motions. The *archetype* is considered as passed if half or more than half of the records result in demands within the acceptable range; thus all the *archetypes* did not pass in this study. Although there is another step in the screening process in which the ground motions are further scaled up to 2.54 times the DGM, this step was not performed since the

acceptance criteria were not satisfied even at the ground motion intensity corresponding to a scale factor of 2.16. Consequently, all the *archetypes* are considered "critical"; thus *IDA* will be conducted for all of them.

Table 6-32 Screening results

PG	Model	Rec_t	$APMR_{10\%}$ (2.16)		
			Rec_p	Status	
1	L2R-IV-3	32	0	Fail	Critical
	L3R-IV-3	32	0	Fail	
2	M4R-IV-3	32	0	Fail	Critical
	M6R-IV-3	32	0	Fail	
	M8R-IV-3	32	0	Fail	
	M10R-IV-3	32	0	Fail	
	M12R-IV-3	32	0	Fail	
	M14R-IV-3	32	1	Fail	
3	M4I-IV-3	32	0	Fail	Critical
	M6I-IV-3	32	0	Fail	
	M10I-IV-3	32	0	Fail	
	M14I-IV-3	32	0	Fail	
4	L2R-IV-4	44	0	Fail	Critical
	L3R-IV-4	44	0	Fail	
5	M4R-IV-4	44	1	Fail	Critical
	M6R-IV-4	44	0	Fail	
	M8R-IV-4	44	0	Fail	
	M10R-IV-4	44	0	Fail	
	M12R-IV-4	44	0	Fail	
	M14R-IV-4	44	0	Fail	
6	M4I-IV-4	44	0	Fail	Critical
	M6I-IV-4	44	0	Fail	
	M10I-IV-4	44	0	Fail	
	M14I-IV-4	44	0	Fail	

Table 6-32 Screening results (continued)

PG	Model	Rec_t	$APMR_{10\%}$ (2.16)		
			Rec_p	Status	
7	M4R-2X-3	32	0	Fail	Critical
	M6R-2X-3	32	0	Fail	
	M8R-2X-3	32	0	Fail	
	M10R-2X-3	32	0	Fail	
	M12R-2X-3	32	0	Fail	
	M14R-2X-3	32	0	Fail	
8	M4I-2X-3	32	0	Fail	Critical
	M6I-2X-3	32	0	Fail	
	M10I-2X-3	32	0	Fail	
	M14I-2X-3	32	0	Fail	
9	M4R-2X-4	44	0	Fail	Critical
	M6R-2X-4	44	0	Fail	
	M8R-2X-4	44	0	Fail	
	M10R-2X-4	44	0	Fail	
	M12R-2X-4	44	1	Fail	
	M14R-2X-4	44	1	Fail	
10	M4I-2X-4	44	0	Fail	Critical
	M6I-2X-4	44	0	Fail	
	M10I-2X-4	44	0	Fail	
	M14I-2X-4	44	1	Fail	
11	S4R-2X-3	32	0	Fail	Critical
	S6R-2X-3	32	0	Fail	
	S10R-2X-3	32	0	Fail	
12	S4R-2X-4	44	0	Fail	Critical
	S6R-2X-4	44	0	Fail	
	S10R-2X-4	44	0	Fail	
13	L2R-1XC-3	32	0	Fail	Critical
	L2R-1XH-3	32	0	Fail	
	L3R-1XC-3	32	0	Fail	
	L3R-1XH-3	32	0	Fail	
14	L2R-1XC-4	44	0	Fail	Critical
	L2R-1XH-4	44	0	Fail	
	L3R-1XC-4	44	0	Fail	
	L3R-1XH-4	44	1	Fail	

6.4.3.5 IDA

IDA was conducted for 58 *archetype* models. Then, using different local and global performance criteria, as discussed in Section 6.4.3.1, the median *performance level* spectral intensity ($\hat{S}_{PT}$) was calculated for each *archetype* for each *performance level*.

6.4.4 Performance Evaluation

6.4.4.1 Uncertainty Sources

The acceptable *APMR*, which will be compared with the *APMR* obtained from *IDA*s, requires information on uncertainties that affect the performance of a system. The sources of uncertainties considered for this purpose are 1) design requirement uncertainty (β_{DR}), 2) test data uncertainty (β_{TD}), 3) modelling uncertainty (β_{MDL}), and 4) *record-to-record uncertainty* (β_{RTR}). The square root of the sum of squares (SRSSs) of the four uncertainties is considered the total uncertainty (β_{TOT}) and is used to determine the acceptable *APMR*.

In this study, the quality of the first three uncertainties is considered to be "good" based on the descriptions for judging the quality of each uncertainty in the *PBU* methodology. This quality category corresponds to the uncertainty of 0.2 (i.e., $\beta_{DR} = \beta_{TD} = \beta_{MDL} = 0.2$). Regarding the *record-to-record uncertainty*, the dispersion of the log-normal function of the fragility curve presented in the previous section (i.e., β_{ln}) is considered equal to β_{RTR}.

6.4.4.2 Adjusted Performance Margin Ratios

The calculated *PMR*s in Section 6.4.3.5 were adjusted by the *SSF* to obtain the *APMR*. In this study, the *SSF* in Eq. (6.1) is calculated based on the simplified function in FEMA P-695 for β_1 (i.e., Eq. (6.3)). $\bar{\varepsilon}_0(T)$ in Eq. (6.1) are approximately assumed to be 1.8 and 1.0 for western and eastern Canada, respectively. For the computation of the mean epsilon value for a selected ground motion set at the period of interest T, $\bar{\varepsilon}_r(T)$, ground motion prediction equations developed by Boore & Atkinson (2008) and Abrahamson et al. (2016) are used for crustal earthquake ground motions and subduction-zone earthquake ground motions (i.e., in-slab and interface), respectively. The calculated *SSF* and *APMRs* are shown in Table 6-33.

Table 6-33 Performance evaluation

PG	Model	*SSF*			*APMR*			Acceptable *APMR* (*LS*, *CP*)		Status* (*LS*, *CP*)
		IO	*LS*	*CP*	*IO*	*LS*	*CP*	$APMR_{10\%}$	$APMR_{20\%}$	
1	L2R-IV-3	1.04	1.11	1.14	0.49	1.00	1.31	1.69, 1.71	1.41, 1.42	NG, NG
	L3R-IV-3	1.05	1.10	1.11	0.51	1.12	1.49			NG, OK
				Avg.	0.50	1.06	1.40			NG, NG
2	M4R-IV-3	1.06	1.10	1.12	0.43	0.85	1.08	2.00, 1.96	1.58, 1.56	NG, NG
	M6R-IV-3	1.04	1.06	1.07	0.41	0.75	0.96			NG, NG
	M8R-IV-3	1.02	1.02	1.03	0.40	0.82	1.13			NG, NG
	M10R-IV-3	1.02	1.02	1.02	0.40	0.79	0.99			NG, NG
	M12R-IV-3	1.00	1.00	1.00	0.39	0.67	0.99			NG, NG
	M14R-IV-3	1.00	1.00	1.00	0.38	0.70	0.97			NG, NG
				Avg.	0.40	0.76	1.02			NG, NG
3	M4I-IV-3	1.05	1.09	1.10	0.42	0.99	1.17	1.97, 1.94	1.57, 1.55	NG, NG
	M6I-IV-3	1.03	1.05	1.06	0.39	0.73	0.93			NG, NG
	M10I-IV-3	1.02	1.02	1.02	0.40	0.80	1.01			NG, NG
	M14I-IV-3	1.00	1.00	1.00	0.38	0.67	0.91			NG, NG
				Avg.	0.40	0.80	1.00			NG, NG
4	L2R-IV-4	1.00	1.25	1.31	0.45	1.00	1.40	1.67, 1.68	1.40, 1.40	NG, OK
	L3R-IV-4	1.00	1.20	1.23	0.45	1.13	1.38			NG, NG
				Avg.	0.45	1.07	1.39			NG, NG
5	M4R-IV-4	1.06	1.14	1.19	0.44	0.79	1.01	1.84, 1.85	1.49, 1.49	NG, NG
	M6R-IV-4	1.08	1.16	1.21	0.41	0.75	0.96			NG, NG
	M8R-IV-4	1.00	1.07	1.10	0.34	0.66	0.83			NG, NG
	M10R-IV-4	1.00	1.05	1.10	0.32	0.55	0.70			NG, NG
	M12R-IV-4	1.01	1.11	1.13	0.29	0.46	0.57			NG, NG
	M14R-IV-4	1.00	1.00	1.06	0.28	0.50	0.68			NG, NG
				Avg.	0.35	0.62	0.79			NG, NG
6	M4I-IV-4	1.00	1.12	1.20	0.44	0.80	1.02	1.84, 1.82	1.49, 1.48	NG, NG
	M6I-IV-4	1.00	1.18	1.22	0.37	0.71	0.92			NG, NG
	M10I-IV-4	1.00	1.03	1.09	0.33	0.51	0.70			NG, NG
	M14I-IV-4	1.00	1.00	1.06	0.29	0.50	0.65			NG, NG
				Avg.	0.36	0.63	0.82			NG, NG

Table 6-33 Performance evaluation (continued)

PG	Model	*SSF*			*APMR*			Acceptable *APMR* (*LS, CP*)		Status* (*LS, CP*)
		IO	*LS*	*CP*	*IO*	*LS*	*CP*	$APMR_{10\%}$	$APMR_{20\%}$	
7	M4R-2X-3	1.05	1.09	1.10	0.43	0.76	0.96	1.94, 1.96	1.55, 1.56	NG, NG
	M6R-2X-3	1.03	1.06	1.06	0.44	0.81	0.98			NG, NG
	M8R-2X-3	1.01	1.02	1.02	0.38	0.79	0.99			NG, NG
	M10R-2X-3	1.01	1.02	1.02	0.42	0.86	1.10			NG, NG
	M12R-2X-3	1.00	1.00	1.00	0.41	0.71	0.88			NG, NG
	M14R-2X-3	1.00	1.00	1.00	0.37	0.65	0.77			NG, NG
				Avg.	0.41	0.76	0.95			NG, NG
8	M4I-2X-3	1.04	1.07	1.08	0.48	0.96	1.16	1.90, 1.95	1.52, 1.55	NG, NG
	M6I-2X-3	1.03	1.04	1.05	0.42	0.79	0.99			NG, NG
	M10I-2X-3	1.02	1.02	1.03	0.42	0.79	0.94			NG, NG
	M14I-2X-3	1.00	1.00	1.00	0.39	0.64	0.75			NG, NG
				Avg.	0.43	0.79	0.96			NG, NG
9	M4R-2X-4	1.12	1.17	1.19	0.47	0.77	0.94	1.80, 1.81	1.47, 1.48	NG, NG
	M6R-2X-4	1.09	1.18	1.21	0.42	0.77	0.93			NG, NG
	M8R-2X-4	1.00	1.10	1.12	0.37	0.68	0.82			NG, NG
	M10R-2X-4	1.00	1.09	1.11	0.30	0.50	0.59			NG, NG
	M12R-2X-4	1.06	1.12	1.15	0.32	0.53	0.65			NG, NG
	M14R-2X-4	1.00	1.04	1.07	0.28	0.56	0.70			NG, NG
				Avg.	0.36	0.64	0.77			NG, NG
10	M4I-2X-4	1.00	1.12	1.15	0.42	0.76	0.97	1.79, 1.79	1.46, 1.47	NG, NG
	M6I-2X-4	1.08	1.13	1.15	0.42	0.69	0.82			NG, NG
	M10I-2X-4	1.00	1.07	1.09	0.30	0.48	0.58			NG, NG
	M14I-2X-4	1.00	1.00	1.06	0.28	0.54	0.68			NG, NG
				Avg.	0.35	0.62	0.76			NG, NG
11	S4R-2X-3	1.07	1.11	1.12	0.47	0.87	1.07	1.82, 1.85	1.48, 1.50	NG, NG
	S6R-2X-3	1.04	1.05	1.06	0.39	0.69	0.81			NG, NG
	S10R-2X-3	1.02	1.02	1.02	0.45	0.68	0.82			NG, NG
				Avg.	0.43	0.75	0.90			NG, NG
12	S4R-2X-4	1.00	1.14	1.18	0.43	0.94	1.16	1.73, 1.75	1.44, 1.45	NG, NG
	S6R-2X-4	1.02	1.17	1.22	0.44	0.97	1.14			NG, NG
	S10R-2X-4	1.06	1.10	1.11	0.34	0.62	0.71			NG, NG
				Avg.	0.40	0.84	1.00			NG, NG
13	L2R-1XC-3	1.02	1.09	1.10	0.27	0.82	0.96	1.70, 1.68	1.42, 1.41	NG, NG
	L2R-1XH-3	1.03	1.07	1.08	0.27	0.69	0.81			NG, NG
	L3R-1XC-3	1.00	1.10	1.12	0.18	0.62	0.68			NG, NG
	L3R-1XH-3	1.00	1.09	1.10	0.18	0.49	0.57			NG, NG
				Avg.	0.23	0.66	0.76			NG, NG
14	L2R-1XC-4	1.12	1.20	1.24	0.74	1.28	1.47	1.67, 1.69	1.40, 1.41	NG, OK
	L2R-1XH-4	1.10	1.19	1.23	0.65	1.11	1.36			NG, NG
	L3R-1XC-4	1.00	1.20	1.25	0.57	1.42	1.65			NG, OK
	L3R-1XH-4	1.00	1.17	1.23	0.50	1.28	1.53			NG, OK
				Avg.	0.61	1.27	1.50			NG, NG

*For each *archetype*, "Pass" if $APMR > APMR_{20\%}$, and "Fail" if not. For the average of each *performance group*, "Pass" if the average *APMR*s > $APMR_{10\%}$, and "Fail" if not.

6.4.4.3 Evaluation Results

It can be noted from Table 6-33 that all the *archetypes* and the *performance groups* failed to pass the criteria specified in the *PBU* methodology. This indicates that the moderately ductile steel braced frames designed in accordance with the NBC 2020 do not satisfy the design objective quantified by this *PBU* methodology, thus the *life safety performance level* is not met. Given that there was a sufficient safety margin in the R_o value as demonstrated in the pushover analysis section, this issue is mainly attributed to the overestimation of R_d (R_d = 3.0), which represents the system ductility. While this is outside the scope of this study, the R_o and R_d values for the steel brace frames will need to be further investigated and refined with the *PBU* methodology such that the objective in the NBC can be properly achieved.

6.4.5 Summary Observations

A total of 14 *performance groups* (including 54 *archetypes*) were developed based on the site (seismic category 3 or 4), bracing configuration, building usage, number of storeys (total height of the structure), and irregularity conditions. The *archetypes* were designed in accordance with the provisions of the NBC 2020 and the CSA S16-19 standard. Detailed numerical models that are capable of simulating nonlinear responses including buckling and low-cycle fatigue fracture of bracing members, as well as flexural yielding and buckling of beams and columns, were developed. The findings obtained from the nonlinear incremental static (pushover) analysis, the *archetype* screening process using nonlinear response history analysis, and *IDA* are summarized as follows:

- The static pushover analysis results suggest that the Type MD CBFs possess overstrength R_o greater than the code-specified value of 1.3. The calculated R_o values range from 1.7 to 2.3. This indicates that the current overstrength factor specified for Type MD CBFs is conservative.
- *IDA* results showed that the *PMRs* were less than 1.0 for many *archetypes*, even for the *CP performance level*, indicating that the Type MD CBFs are likely to exceed *CP* limits even under design-level ground motions.
- Comparing the *APMRs* with the acceptable *APMR*s, none of the Type MD CBF *archetypes* investigated in this study satisfied the acceptance level of *APMR*s, even for the *CP performance level*. The average *APMR*s in each *performance group* are up to three times smaller than the acceptable values. This suggests that the current ductility-related force modification factor R_d may need to be revisited and reassessed thoroughly such that MD-CBFs can achieve the intended *performance level* in the NBC.

While the seismic performance of the Type MD CBFs was systematically investigated in this study, further detailed investigation of the response of the individual *archetypes* is needed to identify the

technical reasons that caused the inadequate seismic performance observed in this study. Moreover, the seismic response of the Type MD CBFs is highly sensitive to the fracture response of the bracing members, and it is expected that the performance evaluation results presented in this report were greatly influenced by the reliability of the fracture model. Detailed analysis of the numerical simulations of each *archetype* has been initiated. Results of these additional investigations of the seismic responses of the Type MD CBF *archetypes* examined in this report will be used to revisit the R_d and R_o values currently specified for the Type MD CBFs in the NBC.

7 References

Abrahamson, N., Gregor, N., and Addo, K. 2016. BC hydro ground motion prediction equations for subduction earthquakes. Earthquake Spectra, **32**(1): 23–44.

Abrahamson, N., and Silva, W. 1997. Empirical response spectral attenuation relations for shallow crustal earthquakes. Seismological Research Letters, **68**(1): 94–127.

AISC. 2022. Seismic provisions for evaluation and retrofit of existing structural steel buildings. American Institute of Steel Construction, Chicago, IL.

American Society of Civil Engineers (ASCE). 2017. Minimum Design Loads for Buildings and Other Structures, ASCE Standard ASCE/SEI 7-16. American Society of Civil Engineers, Reston, Virginia.

Ancheta, T., Darragh, R., Stewart, J., Seyhan, E., Silva, W., Chiou, B., Wooddell, K., Graves, R., Kottke, A., Boore, D., Kishida, T., and Donahue, J. 2014. NGA-West2 database. Earthquake Spectra, **30**(3): 989–1005.

ANSI/AISC. 2016a. Seismic provisions for structural steel buildings (ANSI/AISC 314-16). Chicago, Illinois.

ANSI/AISC. 2016b. Specification for structural steel buildings (ANSI/AISC 360-16). American Institute of Steel Construction, Chicago, IL.

ASCE. 2017a. Minimum design loads and associated criteria for buildings and other structures (ASCE/SEI 7-16). Reston, Virginia.

ASCE. 2017b. Seismic Evaluation and Retrofit of Existing Building (ASCE 41-17). American Society of Civil Engineers, Reston, Virginia.

ASTM E2126-19. 2019. Standard Test Methods for Cyclic (Reversed) Load Test for Shear Resistance of Vertical Elements of the Lateral Force Resisting Systems for Buildings. West Conshohocken, PA.

ATC. 2007. Interim testing protocols for determining the seismic performance characteristics of structural and nonstructural components (FEMA 461). Redwood City, California.

ATC. 2009. Quantification of building seismic performance factors (FEMA P695). Redwood City, CA.

ATC. 2012. Assessing seismic performance of buildings with configuration irregularities: calibrating current standards and practices (FEMA P-2012). Redwood City, California.

ATC. 2017a. Guidelines for nonlinear structural analysis for design of buildings (NIST GCR 17-917-46v1)). Redwood City, CA.

ATC. 2017b. Recommended modeling parameters and acceptance criteria for nonlinear analysis in support of seismic evaluation, retrofit, and design (NIST GCR 17-917-45). Redwood City, CA.

AWC. 2016. Manual for engineering wood construction. Leesburg, VA.

Berry, M., Parrish, M., and Eberhard, M. 2004. PEER structural performance database. Berkeley, California.

Boore, D.M., and Atkinson, G.M. 2008. Ground motion prediction equations for the average horizontal component of pga, pgv, and 5%-damped psa at spectral periods between 0.01 s and 10.0 s. Earthquake Spectra, **24**(1): 99–138.

Bozorgnia, Y., Abrahamson, N.A., Ahdi, S.K., Ancheta, T.D., Al Atik, L., Archuleta, R.J., Atkinson, G.M., Boore, D.M., Campbell, K.W., Chiou, B., Contreras, V., Darragh, R.B., Derakhshan, S., Donahue, J., Gregor, N., Gulerce, Z., Idriss, I., Chen, J., Kishida, T., Kottke, A.R., Kuehn, N., Kwak, D., Kwok, A., Lin, P., Macedo, J., Mazzoni, S., Midorikawa, S., Muin, S., Parker, G.A., Rezaeian, S., Si, H., Silva, W.J., Stewart, J.P., Walling, M., Wooddell, K., and Youngs, R.R. 2021. NGA-subduction research program. Earthquake Spectra, **38**(2): 783–798.

CAC. 2006. Concrete design handbook. *In* 3rd Editio. Cement Association of Canada, Ottawa, ON.

CAC. 2015. Concrete design handbook. *In* 4th Edition. Cement Association of Canada, Ottawa, ON.

CSA. 2014a. Design of Steel Structures (CSA S16–14). Canadian Standards Association (CSA), Mississauga, Ontario, Canada.

CSA. 2014b. Design of concrete structures (CSA-A23.3–14). Mississauga, ON, Canada.

CSA. 2019. Engineering design in wood (CSA O86-19). Canadian Standards Association Group, Toronto, ON, Canada.

CSA 23.3:19. 2019. Design of Concerete Structures. *In* 4th editio. Canadian Standards Association, Ottawa, ON.

CSA S16:19. 2019. Design of Steel Structures. Canadian Standards Association, Ottawa, ON.

Deierlein, G.G., Reinhorn, A.M., and Willford, M.R. 2010. Nonlinear structural analysis for seismic design: a guide for practicing engineers. Gaithersburg, MD.

Devall, R.H. 2003. Background information for some of the proposed earthquake design provisions for the 2005 edition of the national building code of canada. Canadian Journal of Civil Engineering, **30**(2): 279–286.

Fajfar, P. 2017. Analysis in seismic provisions for buildings: past, present and future. Bulletin of Earthquake Engineering, **16**: 2567–2608.

Fazileh, F., Fathi-Fazl, R., Dolati, A., Ventura, C.E., Saatcioglu, M., Lau, D., Yang, T., Sadeghian, V., and Erochko, J. 2023a. Methodology for determination of seismic force modification factors in Canada: performance-based unified procedure. Earthquake Spectra, **39**(1): 218–241.

Fazileh, F., Fathi-Fazl, R., and Huang, X. 2023b. Performance-based unified procedure for determination of seismic force modification factors Rd, Ro in NBC (Final report #A1-018030). Ottawa, ON, Canada.

Fell, B. V, Kanvinde, A.M., and Deierlein, G.G. 2009. Experimental investigation of inelastic cyclic buckling and fracture of steel braces. Journal of Structural Engineering, ASCE, **135**(1).

Fzaileh, F., Khosravi, S., Dolati, A., Fathi-Fazl, R., and Saatcioglu, M. 2022. Seismic performance assessment of conventional construction concrete moment-resisting frame buildings in Canada using the FEMA P695 methodology. Canadian Journal of Civil Engineering, **49**(9): 1508–1517.

Galambos, T. V, and Ketter, R.L. 1959. Columns under combined bending and thrust. ASCE Journal of the Engineering Mechanics Division, **85**(2).

Halchuk, S., and Adams, J. 2004. Deaggregation of seismic hazard for selected Canadian cities. *In* 13th World Conference on Earthquake Engineering. Vancouver, Canada.

Haselton, C.B., and Deierlein, G.G. 2007. Assessment seismic collapse safety of modern reinforced concrete moment frame build-ings. Stanford, CA.

Ibarra, L.F., Medina, R.A., and Krawinkler, H. 2005. Hysteretic models that incorporate strength and stiffness deterioration. Earthquake Engineering and Structural Dynamics, **34**(12): 1489–1511. doi:10.1002/eqe.495.

IBC. 2015. Preparing Canada for an earthquake: a national conversation report. Vancouver, B.C.

ICBO. 1927. Uniform Building Code. *In* 1927th edition. International Conference of Building Officials, Long Beach, CA.

ICC. 2009. Acceptance criteria for prefabricated wood shear panels (ICC-ES AC130). Brea, California.

Karamanci, E., and Lignos, D.G. 2014. Computational approach for collapse assessment of concentrically braced frames in seismic regions. Journal of Structural Engineering, ASCE, **140**(8).

Khosravi, S. 2021. Seismic retrofit of reinforced concrete frame buildings with tension only braces. University of Ottawa.

Kolozvari, K.I. 2013. Analytical modeling of cyclic shear-flexure interaction in reinforced concrete structural walls. Ph.D. dissertation, University of California, Los Angeles, CA.

Krawinkler, H., Gupta, A., Medina, R., and Luco, N. 2000. Loading histories for seismic performance testing of SMRF components and assemblies. Stanford, California.

Krawinkler, H., Parisi, F., Ibarra, L., Ayoub, A., and Medina, R. 2001. Development of a testing protocol for woodframe structures. Stanford, CA.

Liel, A.B. 2008. Assessing the collapse risk of california's existing reinforced concrete frame structures: metrics for seismic safety decisions. Ph.D. dissertation, Stanford University, Stanford, California.

Line, P., Waltz, N., and Skaggs, T. 2008. Seismic equivalence parameters for engineered wood frame wood structural panel shear walls. Wood Design Focus, **18**(2): 13–19.

Manson, S.S. 1965. A complex subject - some simple approximations. Experimental Mechanics, **5**(7): 193–226.

Mazzoni, S. 2021. NGA subduction database preliminary ground motion suite. Los Angeles, CA.

McKenna, F. 2011. OpenSees: A framework for earthquake engineering simulation. Computing in Science and Engineering, **13**(4): 58–66. doi:10.1109/MCSE.2011.66.

McKenna, F., Scott, M.H., and Fenves, G.L. 2010. Nonlinear finite-element analysis software architecture using object composition. Journal of Computing in Civil Engineering, **24**(1): 95–107.

Mitchell, D., Karacabeyli E., Paultre, P., Saatcioglu M., and Anderson D.L. 2003. Seismic force modification factors for the proposed 2005 edition of the national building code of Canada. Canadian Journal of Civil Engineering, **30**: 308–327.

NEHRP Consultants Joint Venture. 2012. Soil-structure interaction for building structures.

NIST. 2010. Evaluation of the FEMA P-695 methodology for quantification of building seismic performance factors (NIST GCR 10-917-8). Gaithersburg, Maryland.

NIST. 2012. Tentative framework for development of advanced seismic design criteria for new buildings (NIST GCR 12-917-20). Gaithersburg, Maryland.

Noh, N.M., and Tesfamariam, S. 2018. Seismic collapse risk assessment of code-conforming RC moment resisting frame buildings designed with 2014 Canadian Standard Association Standard A23.3. Frontiers in Built Environment, **4**(53).

NRC. 1970. National Building Code of Canada. National Research Council Canada, Ottawa, ON.

NRC. 1975. National Building Code of Canada. National Research Council, Ottawa, ON.

NRC. 1977. National Building Code of Canada. National Research Council Canada, Ottawa, ON.

NRC. 1980. National Building Code of Canada. National Research Council Canada, Ottawa, ON.

NRC. 1985. National Building Code of Canada. National Research Council Canada, Ottawa, ON.

NRC. 1990. National Building Code of Canada. National Research Council Canada, Ottawa, ON.

NRC. 1995. National Building Code of Canada. National Research Council Canada, Ottawa, ON.

NRC. 2005. National Building Code of Canada. National Research Council of Canada, Ottawa, ON.

NRC. 2015a. User's guide – NBC 2015 structural commentaries (part 4 of division B). Ottawa, ON.

NRC. 2015b. National Building Code of Canada. National Research Council of Canada, Ottawa, ON.

NRC. 2022. National building code of Canada. National Research Council Canada, Ottawa. ON.

PEER. 2017. Tall building initiative: guidelines for performance based seismic design of tall buildings. Berkeley, CA.

Porter, K.A., Beck, J.L., Seligson, H.A., Scawthorn, C.R., Tobin, L.T., Young, R., and Boyd, T. 2002. Improving loss estimation for woodframe buildings volume 1: report. Richmond, CA.

Porter, M.L. 1987. Sequential Phased Displacement (SPD) Procedure for TCCMAR Testing. *In* Proceedings of the Third Meeting of the Joint Technical Coordinating Committee on Masonry Research, U.S. - Japan Coordinated Earthquake Research Program. Tomamu, Japan.

Pugh, J.S. 2012. Numerical simulation of walls and seismic design recommendations for walled buildings. Ph.D. dissertation, University of Washington, Seattle, WA.

Saatcioglu, M., and Grira, M. 1999. Confinement of reinforced concrete columns with welded reinforcement grids. ACI Structural Journal, **96**(1): 29–39.

Saatcioglu, M., and Ozcebe, G. 1989. Response of reinforced concrete columns to simulated seismic loading. ACI Structural Journal, **86**(1): 3–12.

SDI. 2015. Diaphragm design manual. Glenshaw, PA.

Technical Committee ISO/TC 165. 2010. Timber Structures: Static and Cyclic Lateral Load Test Methods for Shear Walls.

Technical Committee : ISO/TC 165 Timber structures. 2003. Timber structures — Joints made with mechanical fasteners — Quasi-static reversed-cyclic test method.

Tran, T.A., and Wallace, J.W. 2015. Cyclic testing of moderate-aspect-ratio reinforced concrete structural walls. ACI Structural Journal, **112**(6): 653–666.

Uriz, P., Filipou, F.C., and Mahin, S.A. 2008. Model for cyclic inelastic buckling of steel braces. Journal of Structural Engineering, ASCE, **134**(4): 619–628.

Vamvatsikos, D., and Cornell, C.A. 2002. Incremental dynamic analysis. Earthquake Engineering and Structural Dynamics, **31**(3): 491–514.

Zhu, M., Mckenna, F., and Scott, M.H. 2018. OpenSeesPy: Python library for the OpenSees finite element framework. Software X, **7**: 6–11.

Appendix A: Seismic Modification Factors in the NBC

A.1 NBC 2005 to 2020

Since the NBC 2005, although the dynamic analysis approach became the default analysis method and was enforced to be used for structures with certain irregularities, the *equivalent static force procedure* was still permitted to be used for certain conditions. Except for the changes made for the seismic hazards and the upper and lower bounds of the design base shear for specific *SFRSs*, the equation developed in the NBC 2005 is consistently used in the NBC 2005 to the current NBC (i.e., NBC 2020) to calculate the minimum design base shear (V):

$$V = S(T_a)M_v I_E W/(R_d R_o) \quad \text{(A.1)}$$

where,

$S(T_a)$ = 5%-damped design spectral response acceleration, expressed as a ratio to gravitational acceleration, for a period of T_a; T_a is the fundamental lateral period of vibration of the building in the direction under consideration;
M_v = factor to account for higher mode effects on base shear, as defined in Sentence 4.1.8.11.(6) in the NBC 2020;
I_E = earthquake importance factor of the structure, as described in Sentence 4.1.8.5.(1) in the NBC 2020;
W = building weight equal to the summation of the dead load, except that the minimum partition load need not exceed 0.5 kPa, 25% of the design snow load, 60% of the storage load for areas used for storage, and the full contents of any tanks as described in the NBC 2020;
R_d = ductility-related *seismic force modification factor*;
R_o = overstrength-related *seismic force modification factor*.

A comprehensive review of the evolution of coefficients and factors accounting for the effect of overstrength and ductility capacity of structural systems in the NBC can be found in the Final Project Report (No. A1-018030) for the development of the *PBU procedure*. The *seismic force modification factors* used in different editions of the NBC discussed in Chapter 1 are listed in the following table.

Table A.1. ***Seismic force modification factors*** **as per the NBC 2020**

Type of *SFRS*	R_d	R_o
Steel Structures Designed and Detailed According to CSA S16		
Ductile moment-resisting frames	5.0	1.5
Moderately ductile moment-resisting frames	3.5	1.5
Limited ductility moment-resisting frames	2.0	1.3
Moderately ductile truss moment-resisting frames	3.5	1.6
Moderately ductile concentrically braced frames		
Tension-compression braces	3.0	1.3
Tension-only braces	3.0	1.3
Limited ductility concentrically braced frames		
Tension-compression braces	2.0	1.3
Tension-only braces	2.0	1.3
Ductile buckling-restrained braced frames	4.0	1.2
Ductile eccentrically braced frames	4.0	1.5
Ductile plate walls	5.0	1.6
Moderately ductile plate walls	3.5	1.3
Limited ductility plate walls	2.0	1.3
Conventional construction of moment-resisting frames, braced frames, or plate walls		
Assembly occupancies	1.5	1.3
Other occupancies	1.5	1.3
Other steel *SFRS*(s) not defined above	1.0	1.0
Concrete Structures Designed and Detailed According to CSA A23.3		
Ductile moment-resisting frames	4.0	1.7
Moderately ductile moment-resisting frames	2.5	1.4
Ductile coupled walls	4.0	1.7
Moderately ductile coupled walls	2.5	1.4
Ductile partially coupled walls	3.5	1.7
Moderately ductile partially coupled walls	2.0	1.4
Ductile shear walls	3.5	1.6
Moderately ductile shear walls	2.0	1.4
Conventional construction		
Moment-resisting frames	1.5	1.3
Shear walls	1.5	1.3
Two-way slabs without beams	1.3	1.3
Tilt-up construction		
Moderately ductile walls and frames	2	1.3
Limited ductility walls and frames	1.5	1.3
Conventional walls and frames	1.3	1.3

Other concrete *SFRS*(s) not listed above	1.0	1.0
Masonry Structures Designed and Detailed According to CSA S304		
Ductile shear walls	3.0	1.5
Moderately ductile shear walls	2.0	1.5
Conventional construction		
Shear walls	1.5	1.5
Moment-resisting frames	1.5	1.5
Unreinforced masonry	1.0	1.0
Other masonry *SFRS*(s) not listed above	1.0	1.0
Timber Structures Designed and Detailed According to CSA O86		
Shear walls		
Nailed shear walls: wood-based panel	3.0	1.7
Shear walls: wood-based and gypsum panels in combination	2.0	1.7
Moderately ductile cross-laminated timber shear walls: platform-type construction	2.5	1.5
Limited ductility cross-laminated timber shear walls: platform-type construction	1.0	1.3
Braced or moment-resisting frames with ductile connections		
Moderately ductile	2.0	1.5
Limited ductility	1.5	1.5
Other wood- or gypsum-based *SFRS*(s) not listed above	1.0	1.0
Cold-Formed Steel Structures Designed and Detailed According to CSA S136		
Shear walls		
Screw-connected shear walls – wood-based panels	2.5	1.7
Screw-connected shear walls – wood-based and gypsum panels in combination	1.5	1.7
Diagonal strap concentrically braced walls		
Limited ductility	1.9	1.3
Conventional construction	1.2	1.3
Other cold-frame *SFRS*(s) not defined above	1.0	1.0

A.2 NBC 1990 to 1995

Compared with the earlier editions of the NBC, the NBC 1990 made significant changes to the design base shear equation. One of the major changes was the replacement of the coefficient K with a single *seismic force modification factor*, R, and the inclusion of a calibration factor, U, to maintain the minimum design base shear at the same level of protection for buildings with "good" to "excellent" capability of resisting seismic loads consistent with the R factors used. The minimum design base shear was determined as follows.

$$V = U \cdot (v \cdot S \cdot I \cdot F \cdot W)/R \tag{A.2}$$

where $U = 0.6$ and it has been interpreted as an explicit representation of overstrength. In comparison to the two factors, R_d and R_o, used in the NBC 2005 to the NBC 2020, a single factor R is used to reflect the capability of a structure to dissipate energy through inelastic behaviour. The value of the R factor ranges from 1.0 to 4.0 for systems with different levels of ductility. These values were directly linked to different CSA structural design standards for reinforced concrete, steel, timber, and masonry structures with conforming seismic detailing requirements for each *SFRS*.

The NBC 1995 followed the same equation, i.e., Eq. (A.2), for calculating the minimum design base shear (V). However, several updates were made to the table of the modification factor R for different types of *SFRSs*. For example, a number of new *SFRSs*, such as nominally ductile and ordinary steel plate walls, ductile coupled walls, and reinforced masonry walls with nominal ductility, were included in the NBC 1995.

Table A.2. *Seismic force modification factor* R as per the NBC 1995

Case	Type of Lateral-load-resisting System	*R*
Steel Structures Designed and Detailed According to CSA S16		
1	ductile moment-resisting frame	**4.0**
2	ductile eccentrically braced frame	**4.0**
3	ductile steel plate shear wall	**4.0**
4	ductile braced frame	**3.0**
5	moment-resisting frame with nominal ductility	**3.0**
6	nominally ductile steel plate shear wall	**3.0**
7	braced frame with nominal ductility	**2.0**
8	ordinary steel plate shear wall	**2.0**
9	other lateral-load-resisting systems not defined in cases 1 to 8	**1.5**
Reinforced Concrete Structures Designed and Detailed According to CSA A23.3		
10	ductile moment-resisting frame	**4.0**
11	ductile coupled wall	**4.0**
12	other ductile wall systems	**3.5**
13	moment-resisting frame with nominal ductility	**2.0**
14	wall with nominal ductility	**2.0**
15	other lateral-load-resisting systems not defined in cases 10 to 14	**1.5**
Timber Structures Designed and Detailed According to CSA O86		
16	nailed shear panel with plywood, waferboard or OSB	**3.0**
17	concentrically braced heavy timber frame with ductile connections	**2.0**
18	moment-resisting wood frame with ductile connections	**2.0**
19	other systems not included in 16 to 18	**1.5**
Masonry Structures Designed and Detailed According to CSA S304.1		
20	reinforced masonry with nominal ductility	**2.0**
21	reinforced masonry	**1.5**
22	unreinforced masonry	**1.0**
23	other lateral-load-resisting systems not defined in cases 1 to 22	**1.0**

Table A.3. *Seismic force modification factor* R as per the NBC 1990

Case	Type of Lateral load-resisting System	*R*
Steel Structures Designed and Detailed According to CAN/CSA-S16.1 -M		
1	ductile moment-resisting space frame	**4.0**
2	ductile eccentrically braced frame	**3.5**
3	ductile braced frame	**3.0**
4	moment-resisting space frame with nominal ductility	**3.0**
5	braced frame with nominal ductility	**2.0**
6	other lateral-force-resisting systems not defined in Cases 1 to 5	**1.5**
Reinforced Concrete Structures Designed and Detailed According to CAN3-A23.3-M		
7	ductile moment-resisting space frame	**4.0**
8	ductile flexural wall	**3.5**
9	moment-resisting space frame with nominal ductility	**2.0**
10	wall with nominal ductility	**2.0**
11	other lateral-force-resisting systems not defined in Cases 7 to 10	**1.5**
Timber Structures Designed and Detailed According to CAN/CSA-O86.1-M		
12	nailed shear panel with plywood, waferboard or strandboard	**3.0**
13	concentrically braced heavy timber space frame with ductile connections	**2.0**
14	moment-resisting wood space frame with ductile connections	**2.0**
15	other systems not included in 12 to 14	**1.5**
Masonry Structures Designed and Detailed According to CAN3-S304-M		
16	reinforced masonry	**1.5**
17	unreinforced masonry	**1.0**
18	other lateral-load-resisting systems not defined in cases 1 to 17	**1.0**

A.3 NBC 1970 to 1985

The NBC 1970 calculated the minimum design base shear as follows.

$$V = \frac{1}{4} R \cdot K \cdot C \cdot I \cdot F \cdot W \tag{A.3}$$

where,

R = Earthquake factor and is equal to the seismic zone number except for Zone 3, where R is equal to 4;

K = Type of construction factor;

C = structural flexibility factor with a value of 0.1 for all one- and two-storey buildings and a value of $0.05/\sqrt[3]{T}$ for all other buildings, where T is the fundamental period of structure;

I = importance factor with a value of 1.3 for all buildings designed for post-disaster services and schools and a value of 1.0 for all other buildings;

F = foundation factor with a value of 1.5 for the structure founded on soils having low dynamic shear modulus, such as highly compressible soils, and a value of 1.0 for other soils; and

W = total building weight equal to the dead load including the following: 25% of the design snow load; for areas used for storage, the full design live load multiplied by the live load reduction factor; and the full contents of any tanks.

The type of construction factor K was introduced in the NBC 1970 as a judgment factor to reflect experience in design and construction. It was intended to account for the energy-absorbing capacity of the structural system by damping and inelastic actions. Types of construction that are recognized to have performed well in earthquakes are assigned lower values of K.

The factor K was also used in the NBC 1975 (NRC 1975) to calculate the minimum design base shear as follows.

$$V = A \cdot S \cdot K \cdot I \cdot F \cdot W \tag{A.4}$$

where A is the horizontal design ground motion acceleration with values of 0, 0.02, 0.04, and 0.08 for seismic zones 0, 1, 2, and 3, respectively; S is the seismic response factor that is similar to the flexibility factor C in Eq. (A.3); Compared with the term $RC/4$ in the NBC 1970, the term AS was calibrated to be 20% less. I and W have the same values as those in the NBC 1970; F is the same as in the NBC 1970 except for the inclusion of an intermediate foundation factor of $F = 1.3$ for soft soils or compact coarse-grained, firm and stiff fine-grained soils with a depth greater than 50

ft. The type of construction factor K remained the same except for some updates for existing and newly included systems.

Eq. (A.4) was unchanged in the NBC 1977 (NRC 1977) and the NBC 1980 (NRC 1980). In addition, the same K values were used in the NBC 1985 regardless of the changes of the seismic base shear equation to account for the new seismic zoning maps, as shown below.

$$V = v \cdot S \cdot K \cdot I \cdot F \cdot W \quad \text{(A.5)}$$

Where v is the zonal velocity factor and is obtained from Chapter 1 of Supplement to the NBC 1985; S is the seismic response factor, the value of which is dependent on the structural period T and the seismic zone; K, I, F, and W remained the same. As presented in the following sub-section, K is comparable to the R factor in the later editions of the NBC.

Table A.4. Summary of coefficient *K* in the NBC 1970 to 1985

Type of Arrangement of Resisting Elements	***K*** **NBC 1970**	***K*** **NBC 1975 to 1985**
Ductile moment-resisting space frame resisting 100% of required force	0.67	0.70
Dual system of ductile moment-resisting space frame and ductile flexural walls (frame must be designed to resist at least 25% of total base shear)	0.80	0.70
Dual system of ductile moment-resisting space frame and shear walls or steel bracing (frame must be designed to resist at least 25% of total base shear, and walls or bracing must be designed to resist 100% of base shear)		0.80
Other framing systems not defined above	1.00	
Ductile flexural walls and ductile framing systems not defined above		1.00
Systems without space frames (box systems)	1.33	
Dual system with ductile space frame with masonry infill (infilled wall system must be designed to resist 100% of base shear and frame; without infill, must be designed to resist at least 25% of total base shear)		1.30
Systems not defined above with continuous reinforced concrete, structural steel, or reinforced masonry shear walls		1.30
Other structural systems not defined above	2.00	
Unreinforced masonry		2.00

A.4 NBC 1965

It was understood from the observation of several strong ground shakings that the level of demand and damage that occur in different buildings are different. Therefore, starting from the NBC 1965, minimum base shear demand for design of new structures included more sophisticated parameters to account for the condition of the foundation, importance of the building according to its occupancy type, site seismicity, and construction type of the building.

The NBC 1965 introduced a number of new factors in the calculation of the minimum design base shear (V):

$$V = R \cdot C \cdot I \cdot F \cdot S \cdot W \tag{A.6}$$

where,

R = Earthquake factor and is equal to the seismic zone number except in Zone 3, where R is equal to 4 [Supplement No. 1 of the NBC 1965 provided R values for 582 locations across Canada];

C = Coefficient reflecting the type of construction (see Table A-5);

I = Earthquake importance factor, which has the value 1.3 for buildings in which large assemblies of people or that are essentially important for public well-being, such as hospitals and power stations, and has the value 1.0 for all other buildings;

F = Foundation factor reflecting foundation conditions, which has the value 1.5 for buildings founded on highly compressible soil, and the value 1.0 for other soil conditions;

S = Coefficient reflecting the number of storeys of the building and is defined by

$$S = \frac{0.25}{9 + N} \tag{A.7}$$

where N is the total number of storeys; and

W = Building weight equal to the total of the design load due to materials of construction incorporated in the build, the design load resulting from the use of the building for storage, and the design load due to the weight of service equipment and machinery.

Table A-5: *C* values for different types of construction in the NBC 1965

Type of construction	C value
Buildings framed in steel or reinforced concrete, with moment-resisting connections, with floors and roof sufficiently strong and stiff to distribute lateral forces among structural elements of varying flexibility, and in which the frame alone is able to carry 50% of the design shears or in which shear walls are adequately reinforced to carry design shear forces in a ductile fashion	0.75
Other types of building	1.25

Appendix B: Scale Factor for Nonlinear Analysis in Detailed Screening Process

The FEMA P-695 methodology, to avoid any over-conservatism in the performance evaluation, permits individual and average results within each *performance group* to be assessed using 20% and 10% acceptable conditional probabilities, respectively. By using this statistical approach in the *PBU procedure*, a problem arises for the specific cases where one or more *archetypes* in a *performance group* pass the detailed screening process (using the ground motions scaled by $APMR_{10\%}$), while other *archetypes* do not pass. If *IDA* is performed for only the *archetypes* flagged as failed, rather than all the *archetypes*, then taking the average of *APMR* in the *performance group* would result in an unrealistic value. This is because *IDA* is conducted with a 20% acceptable probability of exceedance for individual *archetypes*, while the initial NLTHA in the *PBU procedure* is conducted using a scale factor corresponding to a 10% acceptable probability of exceedance ($APMR_{10\%}$).

To overcome this issue, a second scale factor ($APMR_{Z\%}$, larger than $APMR_{10\%}=2.16$) was proposed to be used in the detailed screening. The second scale factor ($APMR_{Z\%}$) can be obtained from Eq. (B.1) based on a required conditional probability of exceedance for passing *archetypes* (*Z%*) through the detailed screening, to ensure an acceptable conditional probability of exceedance for the average of the response in the *IDA* (10%). As provided in this equation, the $APMR_{Z\%}$ depends on the number of *archetypes* within each *performance group* and is a function of acceptable conditional exceedance probabilities considered for individual (20%) and average (10%) responses. It is conservatively assumed that the passed *archetypes* using the second scale factor will result in $APMR_{Z\%}$ and the failed *archetypes* will result in $APMR_{20\%}$.

$$\frac{N_p \times APMR_{Z\%} + (N_t - N_p) \times APMR_{20\%}}{N_t} \geq APMR_{10\%} \qquad \text{(B.1)}$$

In order to identify the appropriate value of $APMR_{Z\%}$, a case study was performed by varying the total number of *archetypes*, as well as the passing number of *archetypes* within a *performance group*. Table B-1 shows the required conditional probability of exceedance values (*Z%*) for each combination of N_p and N_t, calculated from Eq. (B.1) based on 10% and 20% acceptable conditional probabilities of exceedance for average and individual *archetype* assessments in the performance evaluation. To calculate the values of this table, $APMR_{Z\%}$ was first calculated using $APMR_{10\%}$ and $APMR_{20\%}$ of 2.16 and 1.66, respectively (obtained from Table B-2 using $\beta_{TOT}=0.6$). Then, the *Z%* exceedance probability was obtained using the cumulative density function for lognormal distribution having total uncertainty of $\beta_{TOT}=0.6$. The colours of this table are defined as;

- Dark grey colour represents the required probabilities of exceedance for different *performance groups* in which more than half of the *archetypes* fail the detailed screening;
- Moderate grey colour represents cases where the number of *archetypes* passing the detailed screening are at least half of the total *archetypes*; and
- Light grey colour represents cases where much less than half of the *archetypes* fail the detailed screening.

The required probability of exceedance for the second scale factor is conservatively calculated by taking the average of all the moderate, grey-coloured cells (5.2%, 7.1%, 5.2%, 6.5%, 5.2%, and 6.1%) which equals ~6%. An acceptable *APMR* of 6% ($APMR_{Z\%}=APMR_{6\%}$) is equal to 2.54, using a 6% conditional probability of exceedance and a total uncertainty of $\beta_{TOT}=0.6$ (see Table 5-10). The $APMR_{6\%}$ is therefore proposed as the second scale factor required in the detailed screening process in the *PBU procedure*.

Table B-1. Case study for required $APMR_{Z\%}$ and ($Z\%$) for calculating the second scale factor in the detailed screening process

		Number of archetypes in a PG passing screening (N_p)						
		1	2	3	4	5	6	7
Total number of archetypes in a PG (N_t)	1	2.16 (10%)						
	2	2.66 (5.2%)	2.16 (10%)					
	3	3.16 (2.8%)	2.41 (7.1%)	2.16 (10%)				
	4	3.66 (1.6%)	2.66 (5.2%)	2.33 (7.9%)	2.16 (10%)			
	5	4.16 (0.9%)	2.91 (3.7%)	2.49 (6.5%)	2.29 (8.4%)	2.16 (10%)		
	6	4.66 (0.5%)	3.16 (2.8%)	2.66 (5.2%)	2.41 (7.1%)	2.26 (8.6%)	2.16 (10%)	
	7	5.16 (0.3%)	3.41 (2.0%)	2.83 (4.2%)	2.54 (6.1%)	2.36 (7.7%)	2.24 (8.9%)	2.16 (10%)

It should be noted that the first and second scaling factors (i.e., 2.16 and 2.54 for the $\beta_{TOT}=0.6$) can be replaced for any other total uncertainty estimate for any specific *SFRS*. For example, for an *SFRS* with more robust design requirements, more comprehensive test data, and more detailed nonlinear analysis, a lower total uncertainty value can be assumed to find the corresponding $APMR_{10\%}$ and $APMR_{6\%}$ values from Table B-2 to scale up the ground motions for the detailed screening. The total uncertainty of 0.6 is suggested in the screening step of the *PBU procedure* as a reasonable first assumption, which is consistent with the assumptions in SEI-ASCE 7 for the calculation of risk-targeted hazards.

Table B-2. Acceptable values of *adjusted performance margin ratios*

Total System Uncertainty	Probability of Exceedance			Total System Uncertainty	Probability of Exceedance		
	6% ($APMR_{6\%}$)	10% ($APMR_{10\%}$)	20% ($APMR_{20\%}$)		6% ($APMR_{6\%}$)	10% ($APMR_{10\%}$)	20% ($APMR_{20\%}$)
0.275	1.53	1.42	1.26	0.625	2.64	2.23	1.69
0.3	1.59	1.47	1.29	0.65	2.75	2.3	1.73
0.325	1.66	1.52	1.31	0.675	2.86	2.38	1.76
0.35	1.72	1.57	1.34	0.7	2.97	2.45	1.80
0.375	1.79	1.62	1.37	0.725	3.09	2.53	1.84
0.4	1.86	1.67	1.4	0.75	3.21	2.61	1.88
0.425	1.94	1.72	1.43	0.775	3.34	2.7	1.92
0.45	2.01	1.78	1.46	0.8	3.47	2.79	1.96
0.475	2.09	1.84	1.49	0.825	3.61	2.88	2.00
0.5	2.18	1.90	1.52	0.85	3.75	2.97	2.04
0.525	2.26	1.96	1.56	0.875	3.90	3.07	2.09
0.55	2.35	2.02	1.59	0.9	4.05	3.17	2.13
0.575	2.44	2.09	1.62	0.925	4.21	3.27	2.18
0.6	2.54	2.16	1.66	0.95	4.38	3.38	2.22

A worst-case scenario example of a *performance group* with four *archetypes* using the detailed screening is provided in Table B-3. As shown in this example, using NLTHA scaled by $APMR_{10\%}$ and $APMR_{6\%}$ (scale factors of 2.16 and 2.54, respectively), *archetypes* 1 and 2 are assumed as passed, while *archetypes* 3 and 4 are assumed as failed. Based on the proposed detailed screening in the *PBU procedure*, only *archetypes* 3 and 4 need to be assessed using *IDA* with a 20% exceedance probability. Assuming these two *archetypes* pass the *IDA*, the whole *performance group* will pass the performance evaluation.

For this example, it is also assumed that the *IDA* is performed for all four *archetypes*, and the calculated *APMR* values are provided in the last column of Table B-3. It is assumed that the two *archetypes* passing the detailed screening have slightly better performance than the $APMR_{6\%}$ (i.e., *APMR* of 2.6 > 2.54), while the two *archetypes* failing the detailed screening would marginally

pass the *IDA* (*APMR* of 1.7 > 1.66). Based on the *PBU procedure*, this *performance group* is deemed to have an acceptable response. It is noteworthy that the average value of *APMR* from *IDA* is calculated to be 2.20, which is slightly larger than the threshold of 2.16 for a 10% conditional probability of exceedance. This example is considered to be a worst-case scenario, because exactly half of the *archetypes* failed the detailed screening and only half of them passed it. In cases where more than half of the *archetypes* pass the detailed screening, the average *APMR* will surely be larger than the threshold of 2.16. This demonstrates that the recommended second scaling factor can successfully identify the critical *archetypes* in the detailed screening process, which are therefore required to be further assessed by the *IDA* procedure.

Table B-3. Example for detailed screening procedure

	Archetype No.	Detailed Screening ($APMR_{10\%}$=2.16)	Detailed Screening ($APMR_{6\%}$=2.54)		*APMR* (from *IDA*)	
Performance Group	1	Pass	Pass	Non-critical	2.6	Pass
	2	Pass	Pass	Non-critical	2.6	Pass
	3	Fail	Fail	Critical	1.7	Pass
	4	Fail	Fail	Critical	1.7	Pass
				Average	2.2	Pass

Appendix C: Ground Motions for Nonlinear Time History Analysis and *IDA*

This appendix includes more details about the selection and scaling of ground motion records for nonlinear dynamic analyses (time history analysis and *IDA*), as presented in Section 6: Example Applications. Two sets of ground motion records were developed for the building sites in Vancouver (western Canada) and Montreal (eastern Canada), respectively. Site designations X_{300} and X_{360} (i.e., with average shear wave velocities $V_{s,30}$ equal to 300 m/s and 360 m/s) were adopted for the two sites, respectively, to obtain the design spectrum ordinates targeted for the two seismic loading conditions.

The characteristics of the selected sites are given in Table C-1. The UHS ordinates with a 2%-in-50-years probability of exceedance, as obtained from the Earthquakes Canada website, are given in Table C-2. The UHS ordinates for the two sites and the resulting design spectra are plotted in Figure C-1.

Table C-1. Characteristics of the selected sites

Seismic Loading Condition	Location	Coordinates	$V_{s,30}$ (m/s)	S_s (kPa)	S_r (kPa)
SC3	Montreal, QC eastern Canada	45.542°N -73.655°W	300	2.6	0.4
SC4	Burnaby, BC western Canada	49.265°N -123.0°W	360	2.3	0.2

Table C-2. 2%-50 years UHS data for the SC3 and SC4 sites

T (s)	UHS ordinates, S_a (g)	
	SC3	SC4
0.0 (PGA)	0.482	0.456
0.05	0.851	0.641
0.1	0.896	0.922
0.2	0.751	1.05
0.3	0.665	1.05
0.5	0.543	0.838
1.0	0.293	0.487
2.0	0.133	0.296
4.0	0.0479[1]	0.1151[1]
5.0	0.0345	0.0849
10.0	0.0109	0.0362

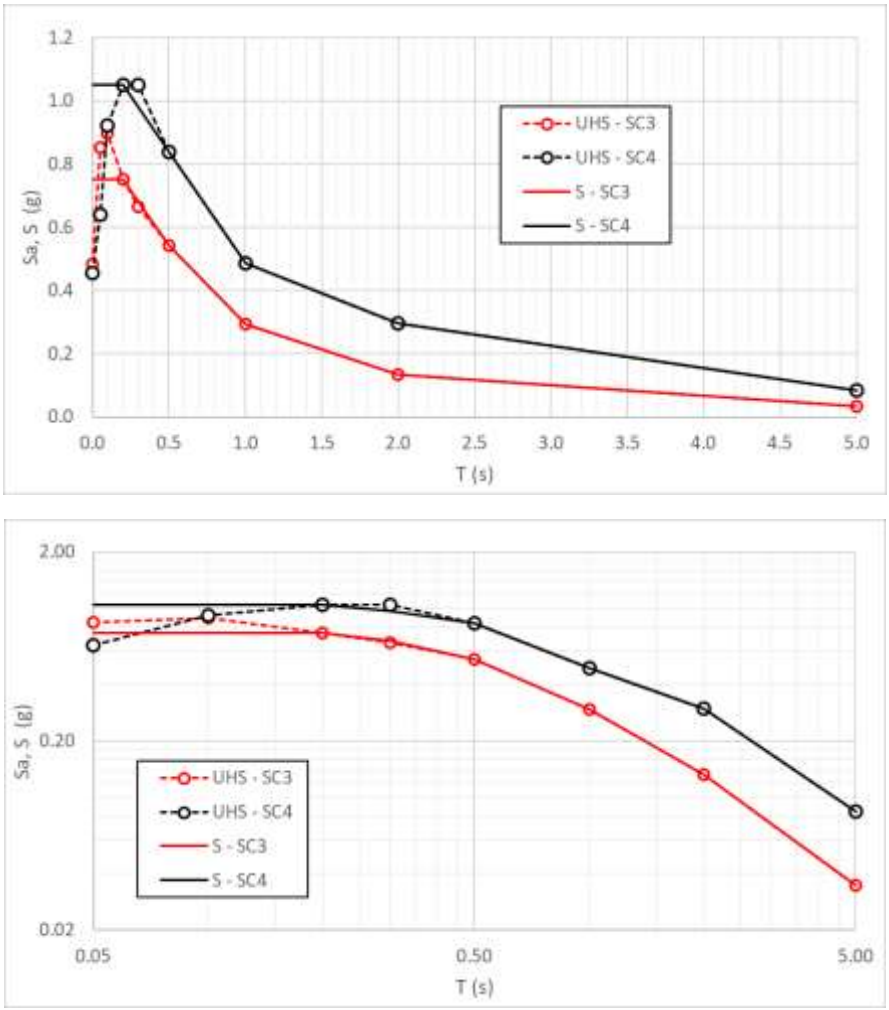

Figure C-1. UHS ordinates and design spectra for the two selected sites: linear scale (top); log-log scale (bottom)

Selected Ground Motions for Vancouver

Ground motions were selected and scaled to uniform hazard spectrum (UHS) in accordance with Canada's 6th-generation seismic hazard model (Open File 8630) to be used in the NBC 2020 for a site in Vancouver using V_{s30} = 360 m/sec. The seismicity in southwestern British Columbia is dominated by the subduction of the oceanic Juan de Fuca plate beneath the continental North America plate occurring about 100 km west of southern Vancouver Island in what is called the Cascadia Subduction Zone. UHS deaggregation results show significant interface contribution from magnitude 8.5+ earthquakes at distances of 100 to 150 km for the period of 1 second and greater. Contribution of shallow crustal earthquakes with magnitude 6.5 to 7.5 earthquake at distances of 0 to 25 km to UHS is observed from peak ground acceleration (PGA) up to $T = 1$

second. In addition, a large in-slab contribution of magnitude 6.5 to 7.5 earthquakes at distances of 40 to 80 km from PGA up to $T = 1$ second is observed. According to the deaggregation results, the period range of scaling $T_R = 0$ to 4 seconds is separated into two sections:

- Short-period range: $T_{R_short} = 0$ to 1.0 seconds including shallow crustal and deep in-slab sources.
- Long-period range: $T_{R_long} = 1.0$ to 4.0 seconds (subduction interface source).

As shown in Figure C-2, two suites of 22 records are linearly scaled to the target UHS over the period range of scaling (T_{RS}) as followings:

- Suite 1 is matched to the target spectrum over T_{RS_short} comprised of 11 shallow crustal and 11 deep in-slab records.
- Suite 2 is matched to the target spectrum over T_{RS_long} between 1.0 and 4.0 seconds, comprised of 22 subduction interface records.

The PEER NGA West-2 database (Ancheta et al. 2014) was used for the crustal records, and the PEER preliminary NGA-sub database (Bozorgnia et al. 2021, Mazzoni 2021) provided the subduction in-slab and interface records. Tables C-3, C-4, and C-5 summarizes the parameters of the selected shallow crustal, in-slab, and subduction interface records, respectively.

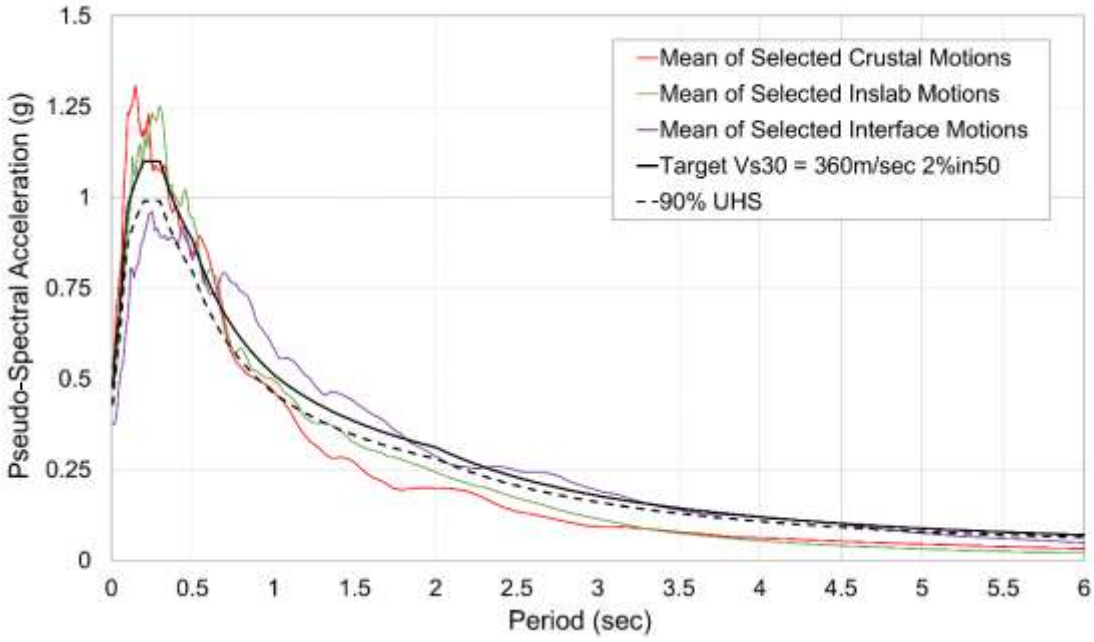

Figure C-2. Comparison of mean of selected and linearly scaled motion records with site UHS – crustal and in-slab records in period range $T_{RS_long} = 0\ s - 1$ s and interface subduction in period range $T_{RS_long} = 1\ s - 4\ s$

Table C-3. Selected crustal records

Magnitude	R_{jb} (km)	V_{s30} (m/s)	Fault type	Year	Earthquake name	Station
6.93	14	672	Reverse Oblique	1989	Loma Prieta	San Jose - Santa Teresa Hills
6.93	12	714	Reverse Oblique	1989	Loma Prieta	UCSC
6.69	14	398	Reverse	1994	Northridge-01	LA - UCLA Grounds
7.62	33	665	Reverse Oblique	1999	Chi-Chi_ Taiwan	ILA067
7.62	26	705	Reverse Oblique	1999	Chi-Chi_ Taiwan	TCU045
7.62	35	520	Reverse Oblique	1999	Chi-Chi_ Taiwan	TCU047
7.01	17	355	Reverse	1992	Cape Mendocino	Fortuna Fire Station
6.52	5	411	Reverse	2003	San Simeon_ CA	Templeton - 1-storey Hospital
6.80	25	640	Reverse	2007	Chuetsu-oki_ Japan	Tokamachi Chitosecho
6.90	16	826	Reverse	2008	Iwate_ Japan	IWT010
6.90	5	399	Reverse	2008	Iwate_ Japan	MYGH02

Note: R_{jb} is the Joyner-Boore distance defined as the closest distance to the surface projection of the fault, V_{s30} is the average shear-wave velocity from the surface to a depth of 30 m.

Table C-4. Selected in-slab records

Magnitude	R_{hyp} (km)	V_{s30} (m/s)	Year	Earthquake name	Station
7.60	64	N/A	2001	El Salvador	QC
6.83	72	758	2001	Geiyo	EHM006
6.83	56	561	2001	Geiyo	EHM008
6.70	48	399	1949	Olympia	OLY0
6.80	50	437	2001	Nisqually	PCFR
6.80	47	399	2001	Nisqually	2130
6.51	93	586	1992	38, Costa Rica	2894
6.83	44	396	2001	Geiyo	973
7.02	51	816	2006	Pingtung.Doublet1	KAU042
7.02	41	494	2006	Pingtung.Doublet1	KAU082
6.80	67	463	2001	Nisqually	1422

Note: R_{hyp} is the hypocentral distance.

Table C-5. Selected subduction interface records

Magnitude	R_{rup} (km)	V_{s30} (m/s)	Year	Earthquake name	Station
8.29	87	605	2015	Coquimbo	GO04
8.29	99	283	2003	Tokachi-oki	HKD078
8.29	77	189	2003	Tokachi-oki	HKD085
8.29	111	381	2003	Tokachi-oki	HKD094
8.29	90	458	2003	Tokachi-oki	HKD095
8.29	125	568	2003	Tokachi-oki	HKD105
8.29	65	342	2003	Tokachi-oki	HKD109
8.81	35	332	2010	El Maule	CCSP-97
8.81	35	340	2010	El Maule	Constitucion

8.80	50	528	2010	El Maule	Hualane
8.81	79	370	2010	El Maule	Matanzas
8.20	48	743	2014	Iquique	HMBCXH
8.80	117	622	2010	El Maule	ANTU
9.12	60	259	2011	Tohoku	FKS012
9.12	60	259	2011	Tohoku	FKS012
9.12	137	168	2011	Tohoku	FKS020
9.12	119	308	2011	Tohoku	IWT011
9.12	144	427	2011	Tohoku	MYG005
9.12	111	205	2011	Tohoku	MYG006
9.12	81	205	2011	Tohoku	MYG010
9.12	99	279	2011	Tohoku	MYG015
9.12	123	310	2011	Tohoku	TCG005

Note: R_{rup} is the rupture distance.

Selected Ground Motions for Montreal

For Montreal, there are 32 ground motion records all selected from crustal earthquakes and scaled to UHS. Specifically, the ground motion set includes ten ground motion records selected from earthquakes with average magnitude and rupture distance of 5.92 and 18 km, respectively. These ten ground motions were scaled to UHS for the period range of 0.15 s to 1.0 s, as shown in Figure C-3(a). The rest of the 22 ground motion records were selected from stronger earthquakes with average magnitude and rupture distance of 7.11 and 31.1 km, respectively. These stronger earthquakes were scaled to UHS for the period range of 1.0 s to 6.0 s, as shown in Figure C-3(b). More details about the selected 32 ground motions are shown in Table C-6.

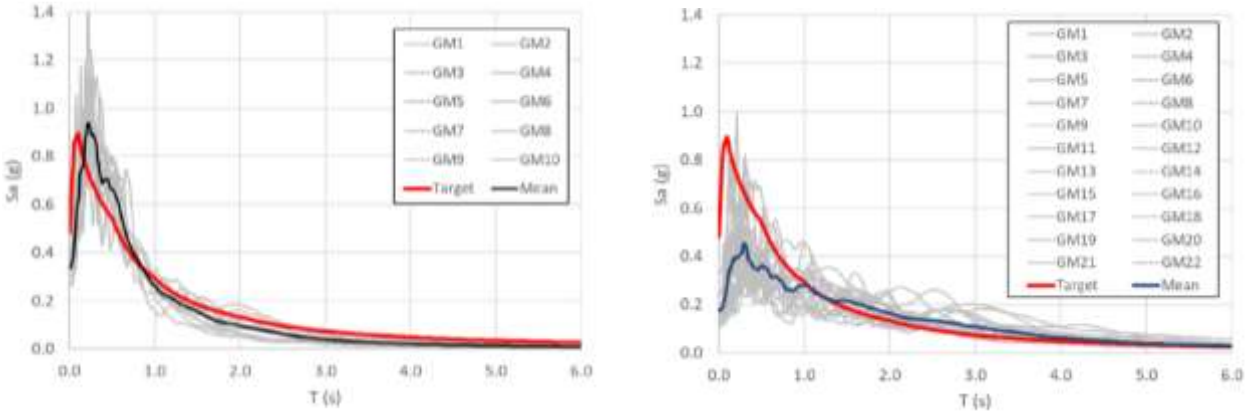

Figure C-3. Comparison of mean of selected and linearly scaled motion records with site UHS (a) in period range 0.15 s to 1.0 s and (b) in period range 1.0 s to 6.0 s

Table C-6. Selected ground motions for Montreal

Magnitude	R_{jb} (km)	V_{s30} (m/s)	Year	Earthquake name	Station
7.28	27	368	1992	Landers	Springs Fire Sta #36
7.01	17	388	1992	Cape Mendocino	Ferndale Fire Sta
5.27	23	271	1987	Whittier Narrows 01	Buena Park, La Palm
5.90	26	329	1981	Taiwan SMART1(5)	SMART1 O09
5.90	26	307	1981	Taiwan SMART1(5)	SMART1 M02
7.13	42	383	1999	Hector Mine	Amboy
7.62	41	423	1999	Chi-Chi, Taiwan	TCU033
7.62	10	259	1999	Chi-Chi, Taiwan	CHY101
7.51	14	282	1999	Koaceli, Turkey	Duzce
7.28	27	345	1992	Landers	Northridge 17645 Saticoy St
7.28	69	383	1992	Landers	Amboy
7.01	40	337	1992	Cape Mendocino	Eureka - Myrtle & West
6.93	24	268	1989	Loma Prieta	Sunnyvale - Colton Ave.
6.93	8	348	1989	Loma Prieta	Saratoga - W Valley Coll.
6.93	8	381	1989	Loma Prieta	Saratoga - Aloha Ave.
6.93	31	425	1989	Loma Prieta	Palo Alto SLAC Lab
6.93	28	282	1989	Loma Prieta	Holister South & Pine
6.93	12	350	1989	Loma Prieta	Gilroy Array #3
6.93	35	238	1989	Loma Prieta	Dumbarton Bridge West End FF
6.93	24	240	1989	Loma Prieta	Agnews State Hospital
5.99	25	303	1987	Whittier Narrows 01	LB - Rancho Los Cerritos
5.99	20	321	1987	Whittier Narrows 01	Burbank N Buena Vista
7.30	55	288	1986	Taiwan SMART1(45)	Smart1 O04
7.30	56	276	1986	Taiwan SMART1(45)	Smart1 I01
7.30	56	309	1986	Taiwan SMART1(45)	Smart1 C00
6.19	6	316	1986	Chalfant Valley 02	Zack Brothers Ranch
5.77	6	316	1986	Chalfant Valley 01	Zack Brothers Ranch
6.19	13	350	1984	Morgan Hill	Gilroy Array #3
5.91	3	382	1980	Mammoth Lakes 03	Convict Creek
6.06	1	382	1980	Mammoth Lakes 01	Convict Creek
6.53	22	242	1979	Imperial Valley 06	Delta
6.50	27	219	1954	Northern California 03	Ferndale City Hall

NRC.CANADA.CA • INFO@NRC-CNRC.GC.CA • 877-672-2672 •